Deintensification of radiotherapy for HPV positive oropharyngeal squamous cell carcinoma through biological response-based adaptation

Dr Sarah Jane Hargreaves

MBBS MRCP(UK) FRCR

A thesis submitted to the University of Cardiff for the degree of Doctor of Medicine, MD

Volume 1 of 1

MD November 2022

For Ben and for our boys, Rufus and Caspar

Author's Declaration

I declare as sole author of this thesis that the work presented here represents my personal research conducted whilst a clinical fellow at Velindre University NHS Trust between November 2017 and January 2021. The work produced in close collaboration with or by other colleagues is acknowledged within the text.

Sarah Hargreaves

November 2022

Summary

Human Papillomavirus associated Oropharyngeal Squamous Cell Carcinoma (HPV positive OPSCC) tends to affect younger and fitter patients and has a superior prognosis compared to the HPV negative OPSCC. Treatment of OPSCC can be surgical and/or non-surgical, and both modalities are associated with high levels of toxicity in the acute and chronic setting. Given the improved survival in a younger and healthier population of patients, contemporaneous HPV positive OPSCC research has largely focused on methods of de-intensifying treatment whilst retaining high cure rates with the aim of reducing the rate of long-term toxicity.

As part of my thesis, I wrote a study protocol for a novel PET-based adaptive radiotherapy trial, PEARL. This is a phase 2 feasibility study for HPV positive OPSCC patients. It aims to look at the dosimetric advantages of adapting radiotherapy plans based upon primary tumour response after 2 weeks of concurrent chemoradiotherapy seen on Fluorodeoxyglucose Positron Emission Tomography CT (FDG PET-CT) scans. In my thesis I show the dosimetric impact of adaptation in a pilot study and the re-working of the initial planning method to improve the adaptive planning process. In addition, I look at whether Proton Beam Therapy - based radiotherapy offers an additional dosimetric advantage in this cohort of patients. Finally, I investigate whether more can be done to refine the Planning Target Volume (PTV) margins implemented for set-up error by exploring the relationship between the position of the hyoid bone and primary tumour volume as seen on verification imaging.

Table of Contents

Table of Contents

Figures

Acknowledgements

The work presented in this thesis involved valuable contributions, and the support of many individuals within Velindre University NHS Trust as well as those outside of the work environment. I would like to express my thanks to all those involved:

First and foremost, I would like to thank my main supervisors Professor Mererid Evans and Professor John Staffurth. Both devoted a huge amount of time and energy to their detailed reviews of my work, provided wise guidance, and displayed never-ending support and encouragement.

To my associate supervisors Dr Thomas Rackley and Professor Emiliano Spezi. Thank you for your time and effort in refining the PEARL protocol, implementing ATLAAS, and working with me to ensure the PEARL study is the best it can be.

To Professor Chris Marshall, Director of PETIC, for your friendly welcome and limitless support which has helped PEARL run so smoothly.

To Dr Nachi Palaniappan and Dr Richard Webster for welcoming me into the Velindre Head and Neck crew and always being available for clinical advice.

To Owain Woodley, VMAT head and neck planner, who worked with me on refining the PEARL pilot study and spent so much of his non-existent time teaching me the ins and outs of VMAT head and neck planning. Thank you also to Jamil Lambert, IMPT planner at The Rutherford Cancer Centre in Newport, for teaching me the broad strokes of IMPT planning and producing high quality modelled adaptive IMPT plans.

To Dr Philip Wheeler, Clinical Scientist, and Salvatore Berenato, Research Fellow, for working with me on the Head and Neck EdgeVCC project, helping me interpret the automated planning data and on-going work regarding the Dose Volume Histogram analysis for the PEARL patients.

To Rhydian Maggs, Physicist, for working with me on the structure of the PEARL RTTQA process and how to securely transfer anonymised data internationally between Wales and England!

To Steffan Jones, Senior imaging radiographer, for the patient lists, teaching me the ways of XVI transfer, and reviewing my hyoid chapter.

To Dr Nicholas Morley, Consultant Nuclear Medical Expert for assistance with manually contouring avid volumes and discussions on the Hopkins Criteria.

To my Bristol and Bath Head and Neck crew: Dr Matthew Beasley, Dr Emma De Winton, Dr Georgina Casswell and Dr Pippa Lewis for your much valued support in the MDT, clinic, and much needed recruitment of PEARL patients!

To Dr Zoe Hudson for all your sage thesis-related advice on our walks home from work.

To my fellow research fellows in the academic offices at Velindre: Elin, Sahar and Emma for all the chats and distractions when things were difficult. Emma, thank you too for your NTCP modelling prowess!

To my sister-in-law Kate, for her last-minute MS Word expertise. Thank you, Mike and Fran for your lovely big dining room table and allowing me to cover it in paper when I come to stay.
To Vicky for helping whenever we need you.

To my mum and dad for always being there for me, and for all the child-care!

Finally, to my husband Ben, for his constant support, provision of tea and never wavering belief that I will get this thesis finished! Thank you to our wonderful, buzzing boys Rufus and Caspar who have had to put up with so many weekends of mummy ‘working again’. Let’s have some fun.

Chapter 1: Deintensification of radiotherapy for HPV positive Oropharyngeal Squamous Cell Carcinoma through biological response-based adaptation: Introduction

1.1 UK OPSCC epidemiology

There are approximately 12,200 new cases of head and neck cancer a year in the United Kingdom (UK); 3% of total new cancer cases. The highest incidence occurs in people aged 70 – 74 years. It is the 4th most common cancer in men, 14th most common in women, and accounted for 4,143 deaths in the UK between 2017 - 2019. Over the last 2 decades, head and neck cancer incidence has increased by a third; a greater increase has been seen in women (43%), than men (23%). Whilst the most common head and neck cancer originates in the larynx, the second most common head and neck cancer, and with the largest rise in incidence, is oropharyngeal squamous cell carcinoma (OPSCC)(1).

The incidence of OPSCC is rising in many countries worldwide. The UK incidence doubled between 1990 – 2006 and again in 2006 – 2010 (2). Historically a disease of traditional risk factors including smoking and alcohol excess, the current trend is primarily due to the increasing rates of infection with Human Papilloma Virus (HPV). HPV positive OPSCC is a separate disease entity to HPV negative OPSCC, with different epidemiology, disease biology and outcomes from treatment (3). HPV positive OPSCC tends to affect younger and fitter patients and has a superior prognosis compared to the HPV negative OPSCC (4).

Whilst a significant cause of OPSCC, HPV infection does not completely explain the current rise in the incidence of OPSCC. Schache et al (5) carried out a retrospective study to determine the proportion of HPV positive and negative OPSCC across the UK. They looked at archival blocks of over 1600 patients from 11 UK centres. The group found that 51.8% of cases were positive for HPV and this remained a constant throughout the decade 2002 – 2011. The OPSCC incidence, however, doubled in the same timeframe, suggesting a multifactorial aetiology. Other smoking related head and neck cancers did not exhibit the same rise and so it has been postulated that alcohol may well play a larger role in the development of OPSCC than previously thought.

1.2 HPV associated disease

HPV positive OPSCC is characterised by the presence of a high-risk HPV genomic DNA in the tumour. HPV is a small circular DNA virus with a genome of approximately 8 Kilobases. The viral genome is typically found either integrated as a single genome into cellular DNA, or as tandem repeats of the genome at a single genomic locus. In 95% of HPV positive OPSCC cases, the DNA is from the HPV-16 sub-type (6). There are over 100 subtypes of HPV including HPV18; infection with HPV-18 is also a risk factor for developing OPSCC.

HPV infection is an early event in the carcinogenesis process. The majority of the cancers arise from deep crypts in the lingual and palatine tonsillar region; primary cancers of the base of tongue and palatine tonsils are the predominant clinical presentation. Pathologically, the HPV infection typically gives rise to poorly differentiated basaloid squamous cell carcinoma histology (7).

In 2008 Gillison et al (8) described the predominant risk factors for HPV-16 positive OPSCC as sexual behaviour, HPV-16 exposure and HPV-16 oral infection. Incidence did not correlate with tobacco smoking, alcohol intake, reduced oral hygiene or a family history of head and neck cancer. HPV positive disease is genetically distinct from HPV negative with distinct patterns of loss of heterozygosity, chromosomal abnormalities and gene expression profiles. Like the common carcinogens' alcohol and tobacco, HPV inactivates the tumour suppressor genes p53 and pRb. It does this through the expression of oncoproteins E6 and E7. Stable integration of the viral genome into the host genome and subsequent action of E6 and E7 on the reduction of levels of p53 (Fig 1.1) and pRb leads to cellular transformation (9). Additional genetic changes are then required for full carcinogenesis, including the acquisition of invasive and metastatic phenotypes. Positive HPV-16 in situ hybridisation assays strongly correlate with the expression of E6 and E7 oncogenes, however 5 – 10% of HPV positive OPSCC are HPV-16 negative and associated with different HPV subtypes. To mitigate for this, the expression of P16 is now an established immunohistochemical biomarker for the function of E7 and a good

surrogate for all HPV subtypes (10). P16, also known as $P16^{INK4A}$ is a protein that highly correlates with HPV infection in OPSCC. It is encoded by the tumour suppressor gene, CDKN2A. In OPSCC and other HPV-driven cancers, P16 is overexpressed. This is due to the HPV oncoprotein E7 binding to and inactivating the tumour suppression gene Rb. Rb regulates P16 and the inactivation of Rb results in an overexpression of P16 in the tumour.

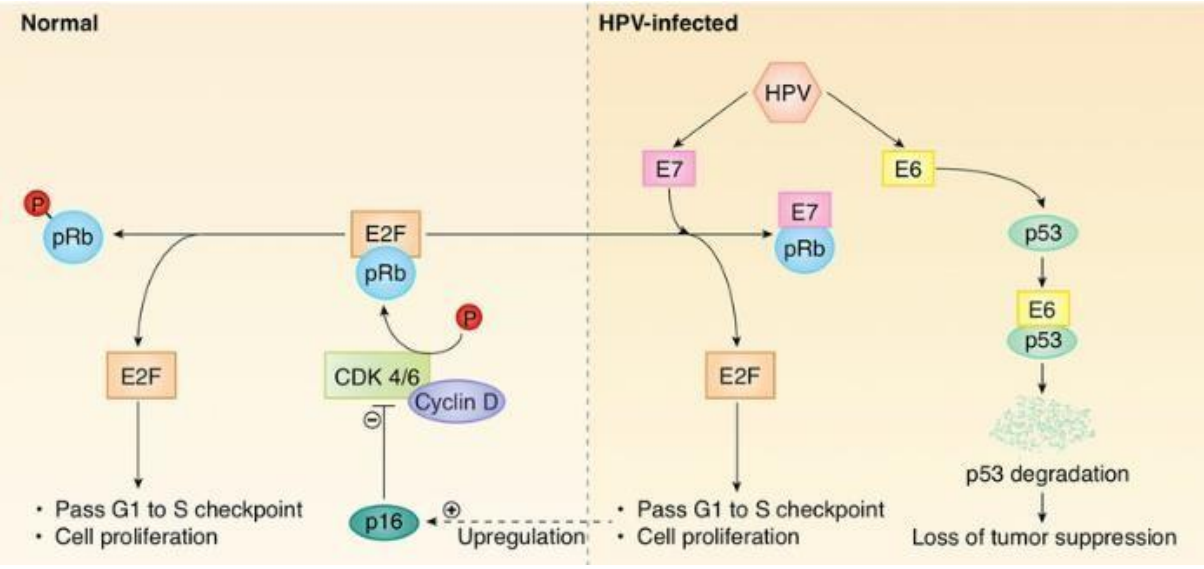

Figure 1.1 Molecular interactions of HPV oncoproteins E6 and E7 highlighting upregulation of p16 due to the inactivation of pRb by E7

Credit: Katherine Wai et al Molecular diagnostics in Human Papilloma Virus related Head and Neck Squamous Cell Carcinoma Cells 2020, 9, 500

In 2010, Ang et al (11) concluded HPV positivity to be a strong and independent prognostic factor for survival in OPSCC and endorsed clinical trials be specifically designed for HPV positive or negative patients – the diseases being separate entities with regards to prognosis.

The superior prognosis of HPV positive OPSCC versus HPV negative disease is multi factorial. Whilst an increased intrinsic sensitivity to radiation or improved radiosensitisation by cisplatin is reflected by longer periods of locoregional control, no specific molecular mechanism has

been found to account for the differences in rate of response to radiotherapy. HPV positive OPSCC also responds better to induction chemotherapy, although there is no difference in the impact of cisplatin on occult distant metastases (12). Although the rates of secondary malignancy are lower in HPV positive OPSCC patients compared to HPV negative OPSCC patients (mainly because the rate of smoking is much lower in patients with HPV positive OPSCC), the rates of death from a second malignancy are similar. This suggests the improved prognosis with HPV positive OPSCC is inherently due to the nature of the cancer, rather than patient specific biological factors namely genetic and physiological variables (13).

Whilst it is anticipated that the prophylactic HPV vaccination program, which covers both HPV 16 and 18 subtypes, will ultimately reduce the incidence of HPV positive OPSCC in the UK by a significant degree, there is likely to be a 30-year lag before we see cases fall in the clinic (14).

1.3. Oropharyngeal cancer staging and anatomy

1.3.1 Anatomy

The oropharynx involves the middle part of the pharynx (Fig 1.2). It extends vertically down from the soft palate to the superior aspect of the hyoid bone. It includes the posterior and lateral pharyngeal walls, the posterior third and base of tongue, the soft palate and the tonsils. Over 90% of oropharyngeal cancers are squamous cell carcinomas, arising from the squamous epithelium that lines the oropharynx (15).

The oropharynx is primarily responsible for swallowing and speech and is part of both the digestive and respiratory systems. The location of the oropharynx creates a challenge for the planning of surgical and non-surgical treatment. Many normal tissue structures – defined as Organs at Risk (OARs) - are in proximity including the spinal cord, brain stem, major salivary glands (parotid glands and submandibular glands) and structures involved in swallowing –

SWOARs – which include the superior, middle and inferior pharyngeal constrictor muscles, supraglottis, glottis and oesophagus. Damage to OARs can result in clinically apparent damage and detriment to their function in the early and late phases which can be severe.

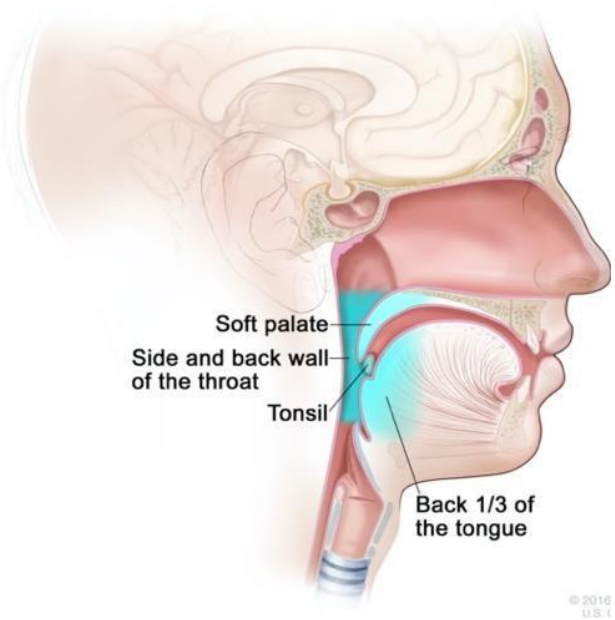

Figure 1.2 Anatomy of the oropharynx

Credit Terese Winslow LLC 2016 National Cancer Institute

Anterior border	Circumvallate papillae of the tongue and anterior tonsillar pillars
Posterior border	Soft palate cranially and pharyngeal constrictor muscles caudally
Inferior border	Epiglottis and glosso-epiglottic fold (larynx) and the pharyngoepiglottic fold (hypopharynx)

Table 1.1 Anatomical borders of the oropharynx

1.3.2 Staging

OPSCC is staged as per the American Joint Committee on Cancer TNM staging system. In response to the significant difference in prognosis, the latest edition of TNM staging (TNM 8) (16) distinguishes between HPV-positive and HPV-negative OPSCC (Table 2).

AJCC stage	Stage grouping	p16 (HPV)-positive oropharynx cancer stage description
I	T0, T1 or T2 N0 or N1 M0	The cancer is no larger than 4 cm (T0 to T2) AND any of the following: • It has not spread to nearby lymph nodes (N0) OR • It has spread to 1 or more lymph nodes on the same side as the primary cancer, and none are larger than 6 cm (N1). It has not spread to distant sites (M0).
II	T0, T1 or T2 N2	The cancer is no larger than 4 cm (T0 to T2) AND it has spread to 1 or more lymph nodes on the opposite side of the primary cancer or both sides of the neck, and none are larger than 6 cm (N2). It has not spread to distant sites (M0).
	M0	

	OR	
	T3 or T4 N0 or N1 M0	The cancer is larger than 4 cm (T3) OR is growing into the epiglottis (the base of the tongue) (T3) OR is growing into the larynx (voice box), the tongue muscle, or bones such as the medial pterygoid plate, the hard palate, or the jaw (T4) AND any of the following: • It has not spread to nearby lymph nodes (N0) OR • It has spread to 1 or more lymph nodes on the same side as the primary cancer, and none are larger than 6 cm (N1). It has not spread to distant sites (M0).
III	T3 or T4 N2 M0	The cancer is larger than 4 cm (T3) OR is growing into the epiglottis (the base of the tongue) (T3) OR is growing into the larynx (voice box), the tongue muscle, or bones such as the medial pterygoid plate, the hard palate, or the jaw (T4) AND it has spread to 1 or more lymph nodes on the opposite side of the primary cancer or both sides of the neck, and none are larger than 6 cm (N2). It has not spread to distant sites (M0).
IV	Any T Any N M1	The cancer is any size and may have grown into nearby structures (Any T) AND it might or might not have spread to nearby lymph nodes (Any N). It has spread to distant sites such as the lungs or bones (M1).

Table 1.2 Staging of HPV positive OPSCC (AJCC 8th edition)

1.3.3 Summary of changes between the American Joint Association of Cancer TNM 7th and TNM 8th editions of staging of HPV positive versus negative OPSCC

1. T Classification: Largely unchanged except carcinoma in situ (Tis). This reflects the nonaggressive pattern of invasion in P16 positive OPSCC and the absence of a distinct basement membrane in the Waldeyer's ring epithelium. T4b was removed as a result of the survival curves between T4a and T4b being indistinguishable.

2. N Classification: There is a newly defined difference between clinical and pathologic staging. Clinical staging is based on the laterality and size of nodes; the number of lymph nodes is no longer significant if radiotherapy is the primary mode of treatment, whereas contralateral nodes have an impact. Pathologic staging is based on the number of nodes and relevant for patients who have had surgery as their definitive form of treatment.

3. M Classification: Unchanged

4. Overall Stage: Stage IV reserved for M1 disease only

1.4 Management of HPV positive OPSCC

The currently recommended treatment for radically treatable OPSCC does not take into consideration HPV status. Outside of clinical trials, the recommended treatment of HPV positive and HPV negative OPSCC remains the same across consensus guidelines (17). As with most cancers, tumour stage and patient fitness play the most influential roles when selecting the most appropriate course of management.

1.4.1 Definitive treatment

For T1 – 2 OPSCC tumours with no nodal involvement, or a single node <3cm, single modality treatment with either surgery or radiotherapy is the recommended option. In retrospective analyses both have been shown to produce comparable survival outcomes (18). Patient choice is often a deciding factor when weighing up the practicalities involved for each modality as well as the risk of potential adverse effects each carries. Base of tongue tumours treated with surgery for example, leads to similar survival outcomes but poorer functional outcomes when compared to patients who received primary radiotherapy (19).

For locoregionally advanced tumours, the treatment is multimodality often involving surgery followed by post-operative (chemo)radiotherapy or definitive chemoradiotherapy with the option of salvage neck dissection or resection of the primary should an incomplete response be demonstrated. In definitive non-surgical management of locoregionally advanced OPSCC, a 5-year survival benefit of 6.5% was seen when concurrent cisplatin was given alongside radical radiotherapy (20), and this is the gold standard non-surgical treatment of locally advanced OPSCC in fit people under the age of 70 years. No survival advantage has been demonstrated with neoadjuvant chemotherapy despite a possible reduction in occurrence of distant metastases in patients with large primary tumours or multiple pathological nodes at presentation (21).

1.4.2 Post operative treatment

Standard post operative radiotherapy protocols are based upon results of studies including RTOG 73-03 (22) that demonstrated improved local control in locally advanced head and neck cancer following post-operative radiotherapy. A subsequent randomised study (23) explored the optimum dose for post-operative radiotherapy and recommended a minimum dose of

57.6Gy to the post operative tumour bed and involved lymph node areas, increasing the dose to 63Gy in 1.8Gy fractions to areas of higher risk including involved margins (<1mm) around the primary tumour and extra nodal extension of nodal disease in the neck. In the UK, most centres prescribe a dose of 60Gy in 30 fractions over 6 weeks to most patients who require post-operative radiotherapy (24), with the option of boosting high risk areas up to 66Gy. Historical studies on which these doses are based, are likely to contain only a small proportion of HPV positive patients.

Practices vary concerning the addition of chemotherapy to post-operative radiotherapy. Current practice is informed by two international studies; EORTC 22931 (25) and RTOG 9501 (26) which demonstrated an overall survival benefit when chemotherapy was added to postoperative radiotherapy in patients where there is evidence of involved margins or extranodal extension in the post-surgical specimen. It is unclear how relevant these results are to the HPV-positive OPSCC patient cohort. The question of whether doses of postoperative radiotherapy can be safely reduced, or chemotherapy omitted in HPV positive OPSCC is being addressed in current ongoing studies including PATHOS (27).

I will now outline the current standard of practice for definitive radiotherapy in OPSCC and its toxicity profile.

1.5 Radiotherapy: The therapeutic ratio and common toxicities in OPSCC

1.5.1 The therapeutic ratio

The objective of radiotherapy is to achieve tumour control whilst minimising damage to normal tissues manifesting as treatment-related toxicity.

The dose response curve (Fig 1.3) is based upon results of cellular level radiobiological studies (28). The curve predicts that the higher the dose of radiation, the higher the chance of destroying tumour cells and curing the patient. Unfortunately, increasing the delivered dose without changing radiotherapy techniques also leads to higher rates of side effects. The challenge is to deliver as high a dose as possible to the target volumes whilst minimising dose to the OARs.

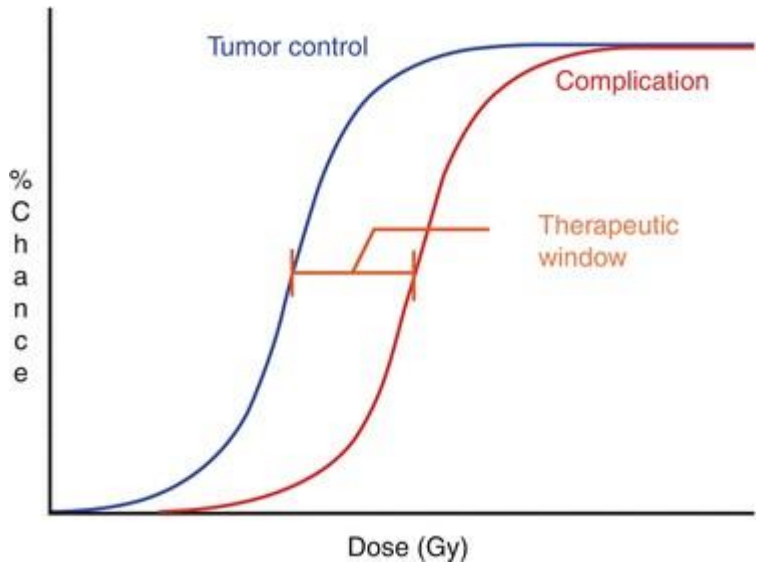

Figure 1.3 The therapeutic window Credit: Chang D,S et al Basic Radiotherapy Physics and Biology (Springer, Cham. 2021)

The therapeutic window is a description of the theoretical gap between the 2 sigmoidal curves representing the relationship between the dose required to cure or control a tumour (tumour control probability – TCP), and the likelihood of causing harm to the patient (normal tissue complication probability – NTCP). Above a threshold, the probability of tumour control and toxicity increases steeply with minimal increase in dose. The wider the separation between the 2 curves, the more the benefit/risk ratio tips towards benefit of treatment. The therapeutic ratio can be widened in several ways.

1. Concurrent radiosensitisers can move the TCP curve towards the left, with lower doses of radiation exerting the same impact as higher doses in the absence of radiosensitisers, assuming they don't increase the rate of dose-limiting side effects.
2. The fractionation of a course of radiotherapy can also impact upon the therapeutic ratio. By allowing a degree of normal tissue recovery from sublethal damage between fractions, the NTCP curve can be moved to the right.
3. Increased damage by radiotherapy to the tumour cells is also facilitated by fractionation by the reassortment of cells into more radiosensitive phases of the cell cycle (Fig 1.4c), and through reoxygenation. Both these processes move the TCP curve to the left.

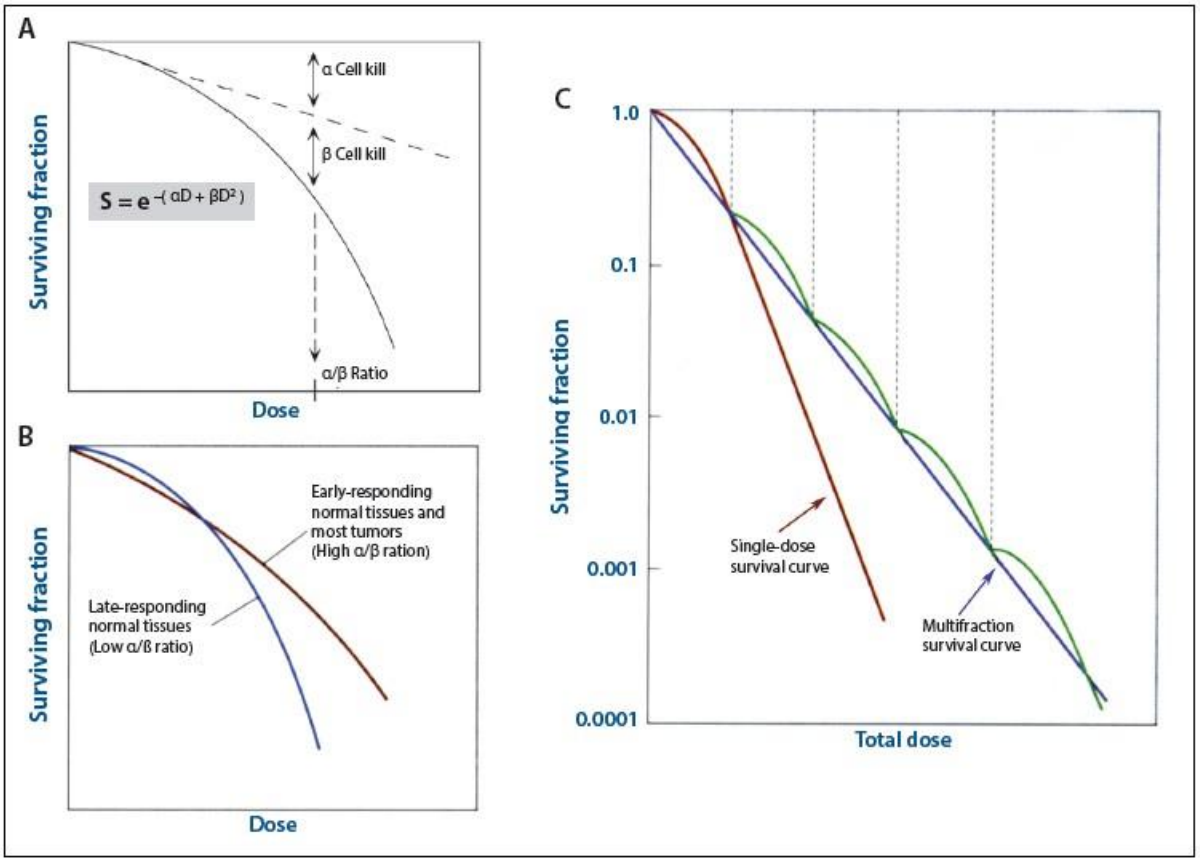

Figure 1.4 Biological rationale for the fractionation of radiotherapy Credit: Zeman E,M Biological basis of radiation oncology (Elsevier-Saunders 2012)

1.5.2 Dose Volume Histograms (DVHs)

Dose Volume Histograms (DVHs) are histograms that relate radiation dose to tissue volume in radiotherapy planning by summarising 3D dose distribution in a 2D graphical format (Fig 1.5). A DVH for clinical use will include all the target volumes and structures of interest in the radiotherapy plan, each plotted in a different colour.

DVHs can be used to compare outcomes of treated patients with or without critical late toxicities and form the derivatives of dose volume constraints. These constraints can then be used prospectively to reduce the incidence of toxicity for future patients by optimising radiotherapy plans and exploring new radiotherapy techniques by comparing different plans represented in a DVH format. Clinical studies have shown DVH metrics correlate with patient toxicity outcomes although a DVH cannot offer spatial information regarding whereabouts in a structure the dose is deposited. In addition, if there are changes to patient anatomy or the volume of the structures during a course of radiotherapy, the accuracy of the DVH reduces.

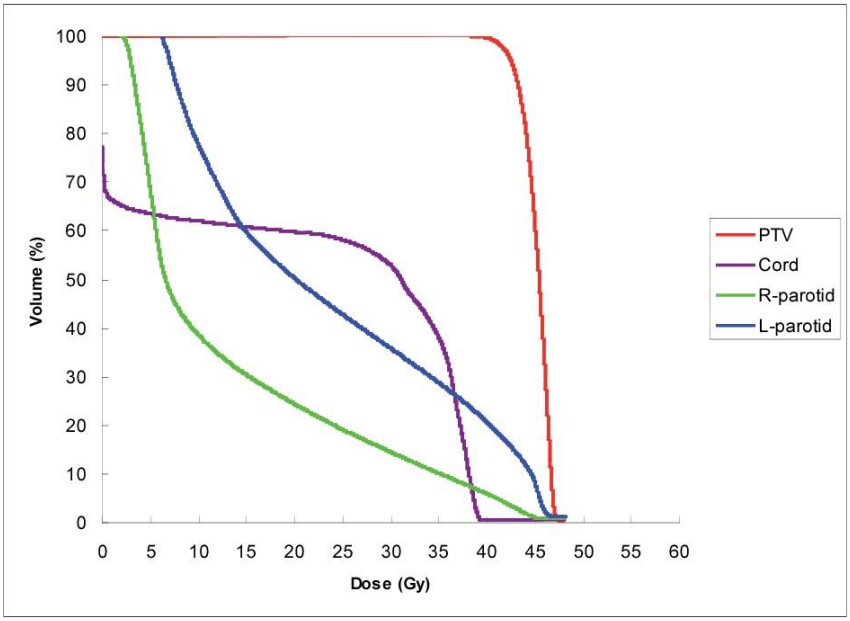

Figure 1.5 An example of a DVH

Credit: Teguh, D 2010 'Late morbidity in Head and Neck Cancer after radiotherapy using various treatment techniques.

An important concept to reduce dose received by normal tissues is to enable deposition of dose in a more accurate location. Intensity modulated radiotherapy (IMRT) including Volumetric Modulated Radiotherapy (VMAT) offers this opportunity.

1.5.3 Intensity modulated radiotherapy (IMRT)

Intensity modulated radiotherapy (IMRT) advances 3D conformal radiotherapy by delivering a more conformal dose distribution. By varying the intensity of multiple beams – classically 5 or 7 – and by shaping the beams with multi-leaf collimators, IMRT can mould the shape of the isodoses closely around the target volume, avoiding OARs more effectively and reducing dose received by them. IMRT can also deliver a simultaneous integrated boost so that different targets can be treated to different doses in the same number of fractions. The UK PARSPORT randomised controlled trial showed the advantages of IMRT in head and neck cancer treatment with reduced rates of xerostomia (dry mouth) following parotid sparing plans (30). Further improvement is required to tackle the other common head and neck radiotherapy related toxicities including dysphagia (swallowing dysfunction). The DARS study, reported in abstract form at the time of writing (40), investigated the impact of dysphagia optimised IMRT on swallowing outcomes. This is the first study to demonstrate that a reduction in dose to dysphagia related OARs improves swallowing outcomes.

1.5.4 Volumetric modulated arc therapy (VMAT)

Volumetric modulated arc therapy (VMAT) is a form of IMRT which delivers radiotherapy continuously as the treatment head rotates on the gantry around the patient. The beam shape, gantry speed and dose rate can all alter resulting in a more efficient delivery of radiotherapy. VMAT generally delivers the same dose in a shorter time, and with improved dose distribution, compared to standard IMRT.

1.5.5 Clinical dose constraints

The advent of IMRT and VMAT techniques has given rise to more conformal target coverage compared to 3D conformal radiotherapy, and the ability to limit the exposure of organs near high doses of radiation. Consequently, clinically apparent reductions in toxicity have been demonstrated, particularly a reduction in long term xerostomia (30).

To offer the optimal radiotherapy plan for patients, robust data is required regarding the relationship between dose received by an OAR, the volume of the OAR receiving it, and whether it makes any objective (clinician-graded) or subjective (patient-reported) impact on normal tissue complications and clinical outcomes.

An important point of reference for radiation dose-volume effects covering a large range of OARs is the Quantitative Analysis of Normal Tissue Effects in the Clinic (QUANTEC) initiative published in 2010 (32). It produced an update of the Emami paper (33) and suggested dosevolume parameters and their association with probability of normal tissue complications (Table 1.3).

OAR	Endpoint	Suggested dose-volume constraint	Expected complication rate if constraint met
Pharyngeal constrictors (superior pharyngeal constrictor muscle, middle pharyngeal constrictor muscle, inferior pharyngeal constrictor muscle)	Dysphagia	Mean dose <50Gy	<20%

Larynx	Aspiration Oedema	Mean dose <50Gy Mean dose <44Gy	<30% <20%
Parotid Glands	Xerostomia	Mean dose <25Gy for both glands Mean dose <20Gy for single gland	<20% <20%
Oesophagus	Acute Oesophagitis	V35 <50% V50 <40% V70 <20%	<30% <30% <30%

Table 1.3 QUANTEC recommended dose-volume parameters

SPCM = Superior Pharyngeal Constrictor Muscle, MPCM = Middle Pharyngeal Constrictor Muscle, IPCM = Inferior pharyngeal constrictor muscle

QUANTEC was largely based upon conformal 3D radiotherapy data and published over 10 years ago. IMRT has now become the established radiotherapy delivery method of choice in the UK for head and neck cancer (24). Various studies have been published since QUANTEC, attempting to clarify and identify important dose volume constraints which, if achieved, could significantly reduce toxicity experienced by patients. Brodin et al (34) reviewed the evidence published since QUANTEC and recommended additional dose volume constraints, highlighting additional key issues (Table 1.4).

Critical OARs	Toxicity/common definition or endpoint	Common validated measuring instruments	Important dosimetric thresholds	Important nondosimetric risk factors
Larynx Supraglottic larynx superior pharyngeal constrictor muscle/middle pharyngeal constrictor muscle	Dysphagia/aspiration	EORTC QLQ-H&N35 patient reported outcomes CTCAE MDADI	Larynx: V50 <27%, mean dose <40Gy Supraglottis: Mean dose <55Gy superior pharyngeal constrictor muscle/middle pharyngeal constrictor muscle: Mean dose <50 - 60Gy, V55 important*	Xerostomia Older age Concurrent chemotherapy Pretreatment dysphagia
Parotid gland (both) C/l parotid gland	Xerostomia/reduction in salivary function to <25%	Patient reported outcomes score after 6 months	Both parotid glands: Mean dose <26Gy V30 <50% contralateral Parotid Gland: Mean dose <20Gy	Pretreatment xerostomia Older age
Oral cavity	Oral mucositis Grade 2/3	CTCAE EORTC/RTOG scales	Mean dose ALARP V30 <73% D21cc <10.25Gy/wk	Concurrent chemotherapy Weight loss >5%
Oesophagus	Oesophagitis Grade 2/3	CTCAE EORTC/RTOG scales (Data often from lung patients)	V35 <20% V50 important*	Concurrent chemotherapy Female gender Tumour stage T3/T4

Thyroid gland	Hypothyroidism (Primary; NPC patients at risk of secondary due to dose to pituitary gland)	Elevated TSH/ Reduced free T4	V30 important* Mean dose 45Gy = 50% NTCP (lack of data)	Female gender Neck/thyroid surgery Caucasian Elective nodal irradiation
Mandible Maxilla	Osteoradionecrosis	Exposed bone failing to heal; variety of grading/timeframes No PROMs	V50 important V44 <42% V50 important	Smoking Alcohol Poor periodontal status

*Important dosimetric value; Lack of consensus among studies regarding percentage volume, but this dose volume is consistently shown to be a distinguishing factor of toxicity

Table 1.4 Summary of contemporary studies and recommendations Brodin et (34)

1.5.6 The relationship of toxicity to dose

The high dose of radiation required to radically treat OPSCC combined with the close proximity of many OARs in the head and neck results in the potential for high levels of treatment related toxicity, both reported by the patient and objectively measured in the clinic. Identifying the toxicities that have the greatest impact on the patient's symptoms or quality of life, relating them to specific OARs and the radiation dose the OARs receive, is a crucial step to innovating treatments which can reduce toxicity.

Radiotherapy-related toxicity is standardly referred to as either acute or late. Acute toxicity describes side effects experienced by the patient during a course of radiotherapy, or within 90 days following its completion. Common acute toxicities in radiotherapy treated head and neck cancer patients include oral mucositis and pain. Late toxicity describes side effects and detriment to function experienced after 90 days post-radiotherapy and can have a lasting impact on quality of life for the rest of a patient's life. Common late toxicities in radiotherapy

treated head and neck cancer patients include dysphagia, xerostomia and osteoradionecrosis (ORN).

Traditionally toxicity has been graded objectively by clinicians using scores including those developed by the World Health Organisation - CT/CAE - and EORTC/RTOG scores (Table 1.5). More interest and emphasis are now placed on Patient Reported Outcomes (PROs) including the EORTC QLQ H&N 35 score (35) and MDADI questionnaire (36). Patient Reported Outcomes are now frequently represented in clinical studies.

	Toxicity/ Grade	1	2	3	4	5
Acute	Mucositis	Asymptomatic or mild symptoms; intervention not indicated	Moderate pain; not interfering with oral intake; modified diet indicated	Severe pain; interfering with oral intake	Life threatening consequence; urgent intervention indicated	Death
	Skin reaction	Asymptomaticor mild symptoms, clinical observations only, intervention not indicated	Moderate; minimal, local or noninvasive intervention indicated; limiting age appropriate instrumental ADL	Severe or medically significant but not life threatening; hospitalisation or prolongation of existing hospitalisation indicated. Debilitating; limiting self care ADLs	Life threatening consequence; urgent intervention indicated	Death

Late	Dysphagia	Symptomatic, able to eat regular diet	Symptomatic and altered eating/drinking	Severely altered eating/swallowing; tube feeding or TPN or hospitalisation indicated	Life threatening consequence; urgent intervention indicated	Death
	Xerostomia	Symptomatic without significant dietary alteration. Unstimulated saliva flow >0.2ml/mi n	Moderate symptoms, oral intake alterations. Unstimulated saliva 0.1 – 0.2ml/min	Inability to adequately ailment orally. Tube feeding ot TPN indicated, unstimulated saliva 0.1ml/min	-	-

Table 1.5 CTCAE toxicity score version 5 for common toxicities of head and neck radiotherapy

1.5.7 Dysphagia

Swallowing is a complex process involving the pharyngeal constrictors, base of tongue, glottis, upper oesophageal sphincter and floor of mouth. Consistently the radiation dose to these structures increases the risk of dysphagia. Dysphagia is the late toxicity proven to have the greatest impact on quality of life (37). Dose to the pharyngeal constrictor muscles and the glottis is significantly correlated with functional outcomes (38). Dose received by the superior pharyngeal constrictor muscle, is the most significant risk factor overall for dysphagia (39). A mean dose of 56Gy gives a 25% aspiration risk and a mean dose of 63Gy gives a 50% aspiration risk. Multiple papers show that mean doses over 50 – 55Gy lead to a steep rise in aspiration risk, which can be used to derive NTCP curves. Amongst contemporary clinical studies, the commonly recommended mean dose to superior and middle pharyngeal constrictor muscle is <50Gy.

Dose received by the glottis also plays an important role in the development of dysphagia. A mean dose of 39Gy is associated with a 25% aspiration risk and a mean dose of 56Gy gives a 50% aspiration risk (39).

Recently, the DARS trial became the first to demonstrate reduced radiotherapy dose to dysphagia/aspiration related OARs improved swallowing (40). For its experimental arm, DARS set a mandatory dose constraint for the superior pharyngeal constrictor muscles lying outside of the high dose target volume to create a plan for dysphagia optimised IMRT (DO-IMRT). The median mean dose to the inferior pharyngeal constrictor muscle (28.4Gy versus 49.8Gy $p<0.0001$), and the superior/middle pharyngeal constrictor muscle (49.7Gy versus 57.2Gy $p<0.0001$), was significantly lower in patients randomised to DO-IMRT. Patient-reported swallowing function (MDADI score) at 12 months post-radiotherapy was significantly higher in patients randomised to the DO-IMRT arm compared to the standard arm (MDADI score 77.7 versus 70.3 ($p=0.016$).

Other factors that contribute to the risk of dysphagia include older age, the use of concurrent chemotherapy and the site of the primary tumour (41). On an individual patient level, it is the anatomical site of the primary tumour that influences which of the swallowing structures will receive the highest dose. Subsequently, minimising the dose to these structures is likely to have the largest impact on reducing toxicity. In OPSCC, the superior pharyngeal constrictor muscle is the most important, whereas in series of head and neck cancers including larynx cancer, dose to the inferior pharyngeal constrictor muscle is most significantly correlated with dysphagia (42) in keeping with where the highest dose is targeted anatomically.

1.5.8 Xerostomia

The most common definition of xerostomia has traditionally been a long-term reduction in salivary function to <25% of baseline (43). More recent years, however, have seen a shift to

the utilisation of patient reported outcomes to inform the assessment of the impact of treatment as experienced by the patient. As there is usually some degree of recovery over time following radiotherapy, xerostomia is often assessed and scored after 6, 12 and 24 months.

The risk of developing xerostomia is related to dose to the major salivary glands (parotid and submandibular glands), and minor salivary glands within the oral cavity. As a parallel organ, function of the parotid gland may depend upon a critical percentage receiving a low dose. Eisbruch found that a mean dose threshold of <24Gy preserved unstimulated saliva flow, and <26Gy preserved stimulated flow (38). As a result of this data, the commonly recommended mean dose to the contralateral parotid gland is <26Gy. The contralateral parotid gland is focused on for organ sparing as it is often assumed the ipsilateral parotid gland lies very close to, or is within, the primary and high dose nodal clinical target volumes (CTV) and so it's sparing is not possible without compromise to coverage of the planning target volumes (PTV). Quantitative analysis of normal tissue exposure found that with a mean dose to one parotid gland of <20Gy or to both of <25Gy, 40% of patients experienced significant xerostomia (44).

An important consideration for any fractionated course of radiotherapy attempting to calculate dose received by the parotid gland is that they tend to shrink and move medially with increasing radiation dose thus making the planned DVH less predictive of received dose than if the parotid gland did not change volume or position (45).

Whilst the mean dose to either the contralateral or combined parotid gland has been demonstrated to reliably estimate risk, contemporaneous data points to the compartments containing stem cells (stem cell rich regions) as being the most vital to function recovery. This suggests a heterogeneous radiosensitivity within the parotid gland and regional dose thresholds within the same OAR may be beneficial to preservation of organ function (46). This could be hard to demonstrate objectively, however. Steenbakker et al performed a recent study comparing salivary flow in patients randomised to stem cell rich region-sparing and standard radiotherapy plans (47). The group defined the stem cell rich regions using an in house METLAB algorithm and adapted it based upon the localisation of the main parotid gland

duct. Parotid gland salivary flow measurements were taken before and after the radiotherapy course up to 12 months. Whilst there was a trend to better flow, there was no statistical difference between the prevalence of a >75% reduction in salivary flow at 12 months and so the study was negative in terms of its primary end point.

Less is known about the dose response of the submandibular glands; Murdoch-Kinch showed that stimulated flow from the submandibular gland reduced exponentially by 1.2% per Gy as the mean dose increased up to 39Gy then plateaued near to zero at mean doses over 39Gy (48).

1.5.9 Oral mucositis

Oral mucositis is often the predominant severe acute symptom experienced by patients with OPSCC during radiotherapy. The pain of mucositis contributes to reduced nutritional intake, reduced engagement in swallowing exercises, and subsequent weight loss. Whilst considered a temporary side effect during treatment and after radiotherapy completion, it has a considerable impact on quality of life and can manifest as long-term taste disturbance (49).

1.5.10 Oesophagitis

The grade of oesophagitis in OPSCC patients can be severe and is worse when the target volumes are more central and caudal. Most data regarding dose volume constraints has been collected from lung cancer patients and so has to be interpreted with a degree of caution when applying them to head and neck cancer patients. Several dose-response models have been derived for acute oesophagitis incorporating mean dose (49) and also V50 (the percentage or absolute volume of an outlined structure that receives 50Gy), which maybe a better predictor of >grade 2 oesophagitis than V35 (50). Models including the surface mapping of the oesophageal wall dose have been trialled to see if they can improve predictions for >grade 2 oesophagitis over and above the conventional mean dose model but have not yet demonstrated an advantage (51).

1.5.11 Osteoradionecrosis (ORN)

Irradiated bone reduces its capacity for defence against trauma and avoidance of infection. Osteoradionecrosis (ORN) is a serious complication of radiotherapy in the head and neck when irradiated bone becomes necrotic and exposed and fails to heal over 3 – 6 months.

Whilst failure of exposed bone to heal is a common theme, the timeframes and severity scoring of osteoradionecrosis remains non-standardised with several different scales in popular use including the CTCAE and Notani systems (52). As grading of osteoradionecrosis as a toxicity varies widely between studies and clinicians, accurate NTCP models are difficult to produce and dose constraints hard to define. Consequently, QUANTEC did not release any data on dose constraints.

In general grade 1 osteoradionecrosis is minimal bone exposure, grade 2 requires minor surgical debridement, grade 3 has in the past been managed with hyperbaric oxygen, although this is no longer supported by the evidence, and grade 4 requires major surgical debridement. Mandibular osteoradionecrosis is more commonly reported than maxillary although there are some reports which include maxillary osteoradionecrosis (53).

Whilst there is evidence that poor periodontal care is a significant risk factor for osteoradionecrosis, the extraction of teeth prior to radiotherapy is still an area requiring further detail. Some studies have shown teeth extraction to be a risk factor rather than play a preventative role in osteoradionecrosis genesis (54). Whilst common clinical practice is to clear the mouth of teeth that are in poor condition prior to radiotherapy, the advantage of this may be more nuanced and dependent upon the extent of the clearance, the overall health of the oral mucosa, and patient behavioural factors including smoking and dental hygiene practices.

The change in the demographic of OPSCC may also influence the rate of osteoradionecrosis. Patients with HPV positive OPSCC is more likely to present with level 2 lymphadenopathy than their HPV negative counterparts (55), necessitating greater mandibular coverage. These patients also have more curable cancers and so may have many decades of risk for late sequelae, such as osteoradionecrosis, to develop.

1.5.12 Normal Tissue Complication Probability modelling in head and neck cancer

Dose/volume metrics described above can also help establish the parameters of NTCP models which can then be applied to individual plans for an estimation of toxicity risk. Comparing the differences between NTCP models for 2 or more different radiotherapy plans can also inform the clinician which plan has the lower risk of toxicity.

There are multiple types of NTCP models published in the literature with varying degrees of validation. Mavroidis et al (56) applied 4 different NTCP models to patient treatment plans from NCT01530997, an HPV positive OPSCC radiotherapy de-intensification study (57). Their aim was to determine the radiobiological parameters of these models. They aimed to describe the dose-response relationship of the pharyngeal constrictor muscles and major salivary glands, to the severity of dysphagia and xerostomia at 6 and 12 months post radiotherapy.

They defined clinically significant toxicity as an increase of at least 2 points in the CTCAE toxicity score.

The four models were generally equivalent with regards their 'goodness of fit' for xerostomia at 6 and 12 months. They found the best correlations of dose/volume metrics to toxicity were a combined volume of both the contralateral salivary glands with xerostomia at 6 and 12 months. The mean dose to combined salivary glands in those with/without toxicity was 33.8 +/- 7.7Gy and 21.5 +/- 9.0Gy, and 33.1Gy +/- 8.8Gy and 25.2 +/- 9.4Gy at 6 and 12 months post radiotherapy respectively.

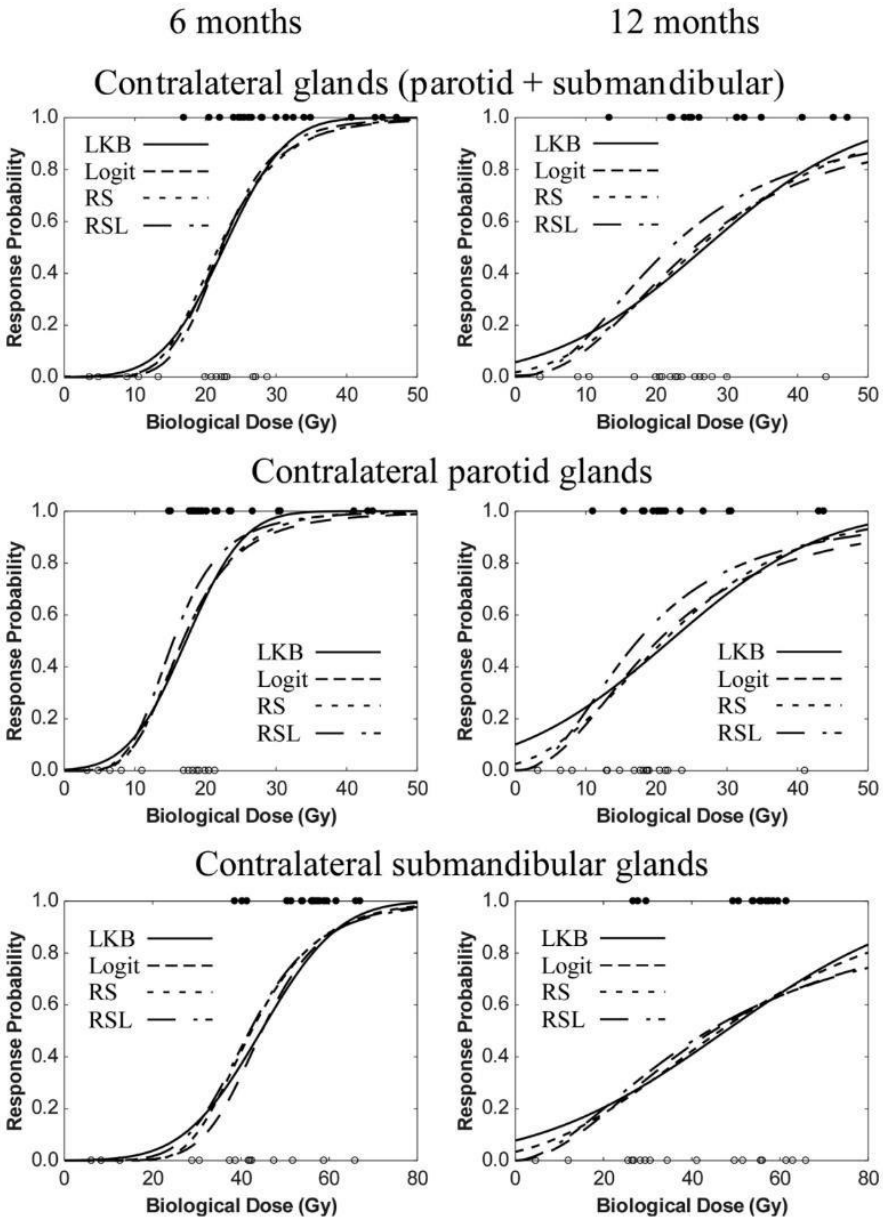

Figure 1.6 NTCP Curves for major salivary glands at 6 and 12 months Credit: Mavroidis et al (56)

The mean dose to both the combined pharyngeal constrictor muscles and superior pharyngeal constrictor muscle was reported. The superior pharyngeal constrictor muscle metrics were the better fit with an increase of at least 2 points on the dysphagia toxicity score at 6 months. The mean dose to superior pharyngeal constrictor muscle in those with/without toxicity was 60.1 +/- 3.9 and 56.6 +/- 3.4, and 59.1Gy +/- 2.8 and 56.3 +/- 3.4Gy at 6 and 12 months post radiotherapy respectively. This suggests that a reduction in mean dose of around 3Gy is theoretically enough to reduce the rate of clinically significant dysphagia in selected patients.

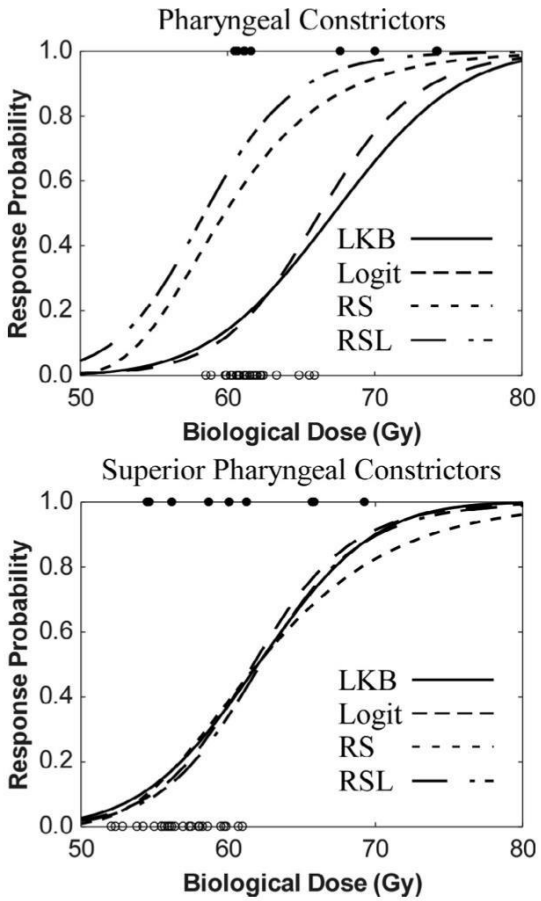

Figure 1.7 NTCP Curves for PCMs and superior pharyngeal constrictor muscle Credit: Mavroidis et al (56)

The dose response curve taken from the study, looking at all 4 NTCP models is shown in Figs 1.6 and 1.7 and illustrates the steep section of the curve where small changes in dose can result in larger changes in risk of toxicity. In addition to the dose/volume relationship for whole organ OARs, there is a growing interest in the heterogeneity of function within an OAR eg the parotid glands. Depending upon where in the OAR volume the dose is reduced, a modest reduction in dose may still have a clinically relevant impact on the dose response curves.

1.6 Standard Delineation in OPSCC

The definition of the target volume is the first step in determining how dose should be distributed within a plan.

1.6.1 Creation of the Clinical Target Volume (CTV)

In 2017 consensus guidelines were published for the delineation of the primary tumour clinical target volume (CTV) in head and neck squamous cell carcinomas including OPSCC (56). The CTV standardly includes macroscopic disease – the Gross Tumour Volume as defined by clinical and radiological examination, expanded to include a volume of surrounding tissue at risk of microscopic tumour infiltration. The consensus guidelines acknowledged several studies that looked at the pattern of microscopic tumour cell infiltration surrounding the GTV and, whilst they only included relatively small numbers of patients, they concurred that most of the microscopic tumour infiltration occurs within the first 10mm radiating from the GTV. The consensus group reviewed the Danish Head and Neck Cancer association (DAHANCA) geometric '5 + 5mm' expansion of the GTV and edited it to account for anatomy (57). The consensus recommends two CTVs for the primary tumour based upon geometric expansion of the primary GTV (GTV_P) (Fig 1.8): CTV1_P encompassing the area around the GTV at highest risk of harbouring microscopic disease – an expansion around the GTV of 5mm, and CTV2 encompassing a peripheral area at lower risk of microscopic disease – an expansion of 10mm from the GTV. CTV1 is prescribed a higher dose than CTV2. Whilst there is a risk that the 10mm CTV margin may not include the entirety of microscopic tumour extension in some cases, further enlargement of the CTV must be weighed against the potential increase in toxicity due to a higher dose of radiation received by surrounding normal tissue.

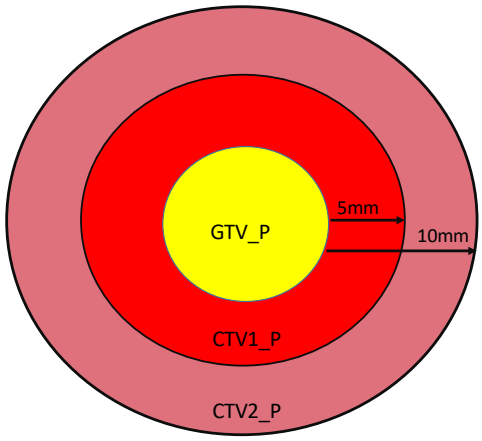

Figure 1.8 Standard expansion of Primary GTV (GTV_P) to Primary CTV1 and 2 (CTV1_P and CTV2_P)

The creation of the high dose nodal CTV (CTV_N) is based upon the pathologically and/or radiologically involved nodes (GTV_N) and follows the same 5+5mm expansion format (58). It has been demonstrated that the extent of extra nodal extension is <5mm in over 95% of pathological nodes with extra nodal extension examined in a pathological series, and always within 10mm. This creates nodal CTV1 and CTV2 (CTV1_N and CTV2_N).

In addition, there is a third nodal CTV, CTV3_N, which is a prophylactic anatomical CTV including the draining cervical nodal levels at risk of involvement (58). CTV3_N is prescribed a prophylactic dose intended to treat microscopic disease not yet manifesting as changes on imaging. The nodal levels to be included in the CTV3_N are determined by the site of the primary tumour, its proximity to the midline of the neck, and the site of any overtly involved nodes (Table 1.6).

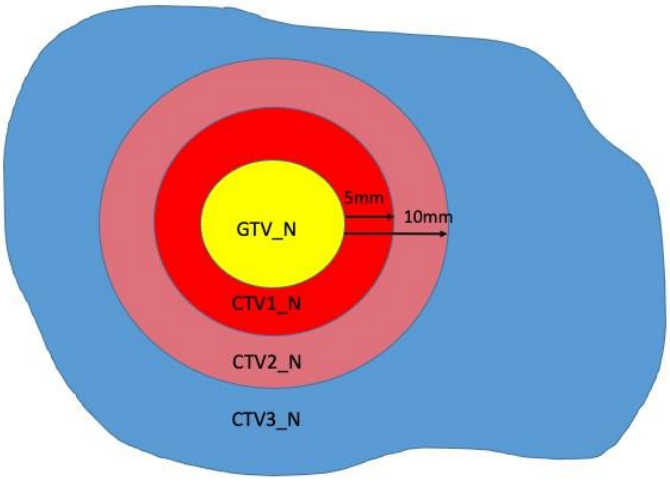

Figure 1.9 Standard geometric expansion of GTV_N to CTV1_N, CTV2_N, and anatomical expansion for CTV3_N

	Nodal status	CTV3_N
Lateralised tumour[1]	Node negative	Ipsilateral (1b)[2], II, III, IVa[3] + VIIa
	Node positive	Uninvolved ipsilateral 1b, II, III, IVa, Va+b Ipsilateral VIIa at the level of the oropharynx Ipsilateral VIIb (when II involved) Ipsilateral IVb+Vc (when Iva or V is involved)
Non-lateralised tumour[4]	Node negative	Ipsilateral II, III, Iva 1b[2] Contralateral II, III, Iva

	Node positive	Uninvolved ipsilateral Ib, II, III, IVa, Va+b Ipsilateral IIVa at the level of the oropharynx Ipsilateral VIIb (when II involved) Ipsilateral IVb +Vc (when IV or V is involved) Contralateral II, III, IVa Contralateral IIVa at the level of the oropharynx

1 Unilateral treatment is recommended for N0 – N1 tonsillar fossa tumour not infiltrating the soft palate nor the base of tongue.
2 Any tumour with extension to the oral cavity and/or the anterior pillar of tonsil and/or in the case of anterior involvement of level II.
3 Level IVb is included in case of involvement of level Iva
4 Non lateralised tumours refer to tumours involving the soft palate and posterior pharyngeal wall, or base of tongue tumours extending more than 1cm towards the midline.

Table 1.6 Recommended CTV3_N nodal levels according to clinical staging and laterality of the primary OPSCC tumour (58).

1.6.2 Creation of Planned Target Volume

The planned target volume (PTV) is based upon the CTVs shown in Fig. 1.7 and 1.8 with a margin of 3 - 5mm to account for machine inaccuracy and set up error. The PTV margin is defined in accordance with the set-up confidence of a specific treatment centre's equipment and verification procedures.

1.6.3 Dose Prescription

There is no difference in the management of OPSCC due to HPV status according to American (58) or European (59) guidelines.

Internationally the standard definitive radiotherapy dose of OPSCC is 70Gy in 35 fractions delivered over 7 weeks. In the UK many treating centres have adopted a mildly hypo fractionated equivalent regimen of 65-66Gy in 30 fractions over 6 weeks (24). In Velindre Cancer Centre we standardly prescribe 66Gy to PTV1, 60Gy to PTV2 and 54Gy to PTV3 in 30

fractions over 6 weeks. The gold standard treatment includes concurrent chemotherapy; 3 weekly cisplatin dosed at 100mg/m^2.

This section outlined the standard radiotherapy contouring method, the next section describes a range of alterations to this standard method that have been explored within the context of a clinical study with the aim of reducing toxicity.

1.7 Non-adaptive de-intensification of treatment in oropharyngeal squamous cell carcinoma

The greater radiosensitivity and improved prognosis of HPV positive locally advanced OPSCC has formed the basis for research into the de-escalation of treatment. Various strategies of de-escalation are being tested in clinical trials, with the aim of maintaining high cure rates whilst reducing treatment related toxicity. I have categorised them as adaptive and nonadaptive methods.

1.7.1 Reduction of total radiotherapy dose

In NRG HN-002 (60), a randomized phase II study, 295 patients with T1-2 N1 and T3 N0-N1 (stage I-II TNM8) HPV-positive OPSCC and a minimal (≤10 pack/year) smoking history were randomised to receive one of two de-intensified chemoradiotherapy treatment regimens, either reduced dose IMRT, 60Gy in 30 fractions over 6 weeks with concurrent weekly Cisplatin (40mg/m2) or moderately accelerated reduced dose IMRT alone, 60Gy in 30 fractions over 5 weeks. In order to establish acceptability as compared to the standard of care, at least one experimental arm had to achieve a 2-year progression free survival rate above the historical control rate in addition to a 1 year mean composite MDADI score of at least 60. The reduced dose IMRT with cisplatin arm demonstrated a 2-year progression free survival of 90.5% (expected 91%), however the IMRT alone arm did not achieve acceptable control rates. This

suggested that reduced dose radiotherapy of 60Gy in chemoradiotherapy regimens may be a safe option for these patients. This is currently being tested in larger studies.

In another prospective single-arm phase II study (61), 43 patients with stage I-II (TNM8) HPVpositive OPSCC and a minimal (≤10 pack/year) smoking history were treated with reduced dose IMRT (60Gy/30 fractions to the primary tumour and involved nodal PTVs and reduced dose (30mg/m^2) concomitant weekly cisplatin. The primary end point was pathological complete response based on the primary site biopsy and neck node dissection. Biopsies of the tumour sites following treatment demonstrated a complete pathological response rate of 98% at the primary site and 84% in the neck nodes. The one case of a positive primary site biopsy was resected, and no viable tumour was found. At a median of 36 months follow up for 42 patients, regional control was 100%, local control was 100% and overall survival was 95%. Whilst definitive comparisons require randomised controlled studies, treatment was associated with reduced toxicity rates when compared with contemporary studies (e.g., PARADIGM (62) where patients received 70Gy of radiation: 39% of patients (compared to 85%) required a feeding tube for a median of 15 weeks (range 5-22 weeks).

1.7.2 Induction chemotherapy-response based radiotherapy

Three studies show rates of loco-regional control after reduced total dose radiotherapy in patients following induction chemotherapy.

In one single arm phase II study (63), the 24 out of 44 patients with stage I-III (TNM8) HPV positive OPSCC who had a complete or partial response to two cycles of induction chemotherapy with carboplatin and paclitaxel, received 54Gy in 27 fractions of radiotherapy to the planning target volume encompassing the primary tumour and involved nodes, and 43Gy to the prophylactically treated uninvolved nodes, representing a ~20% reduction in total dose compared to standard doses of radiotherapy. Weekly paclitaxel chemotherapy was given alongside the radiotherapy. The trial demonstrated a 2-year progression free survival of 92%

(95% CI: 77-97%) and 2-year loco-regional control rate of 95% (95% CI: 80-99%), which compared favourably with historical studies, in addition to a reduced toxicity profile.

In another single arm phase II study of 80 patients with TNM8 Stage I (50 – 60%), Stage II (30 – 40%) and Stage III (10% T4 – no N3) HPV-positive OPSCC patients underwent 3 cycles of induction chemotherapy with docetaxel, cisplatin and 5-fluorouracil (64). The 70% of patients who had a complete clinical response went on to receive 54Gy in 27 fractions of radiotherapy to the primary tumour and involved nodes, and 51.3Gy to the uninvolved nodes, together with concurrent cetuximab. The trial demonstrated a 2-year progression free survival rate of 80% (95% CI: 65-89%) which was lower than expected. However, when they analysed the data, patients with T1-T3 N2 (stage I-II TNM8) disease who had a minimal (≤10 pack/year) smoking history did extremely well, with a 2-year progression free survival and 2-year overall survival rate of 96% (95% CI: 76-99%). It also demonstrated better swallowing and nutritional outcomes compared with contemporaneous controls.

In a third single arm phase II study, OPTIMA (65), 62 patients with HPV-positive OPSCC were staged according to the TNM 7th edition and stratified as having low risk disease (≤T3, ≤N2b, ≤10 pack year smoking history) or high-risk disease (T4, ≥N2c, >10 pack year smoking history). Patients received 3 cycles of induction chemotherapy with nab-paclitaxel; radiotherapy and concurrent carboplatin treatment was based upon response to induction chemotherapy. Low risk patients with more than 50% response to induction chemotherapy had 50Gy radiotherapy. Low risk patients with 30 – 50% response, or high-risk patients with >50% response received chemoradiotherapy with 45Gy. All other patients received standard chemoradiotherapy with 70Gy in 35 fractions. All patients who underwent de-escalated treatment had a biopsy of the primary and a neck dissection following treatment. The pathological complete response rate for 50Gy of radiotherapy and chemoradiotherapy with 45Gy was 94.7% and 89.3% respectively. After a mean follow up of 29 months, 2-year progression free survival and overall survival was 95% and 100% for the low-risk patients, and 94% and 97% for the high risk patients. Acute toxicity and long-term feeding tube use was significantly reduced compared to standard of care data.

These studies illustrate the importance of selecting the right risk group of patients for deintensification whilst appreciating that they are small single centre studies with a large potential for bias.

1.7.4 Reduced target volume expansion

An approach to reducing side effects is to reduce the volume receiving high dose radiotherapy therefore limiting the amount of irradiated normal tissue. The expansion of the GTV to high dose CTV is a significant contributor to the level of radiation received by normal tissues due to the impact on volume and surface area an increase in diameter has. In the context of the improved outcomes of HPV positive OPSCC, one group in Wisconsin, limited expansion of the GTV to a direct 3mm geometric growth to form the high dose PTV (66) without prior expansion to CTV. An intermediate CTV was created using a 10mm expansion from the GTV. They reported the outcomes in 134 cases treated with this reduced margin at a median follow up of 56 months. Local and regional control at 5 years remained high (91.5% and 90.8%) in line with expected rates. Of the 14 locoregional failures, 10 were in field. As this was a retrospective study the only objective toxicity data analysed was gastrostomy tube use at a year post-treatment (6%). This is in keeping with tube use rates seen in standard practice. These results supported the findings of other groups that 60 – 63Gy in the immediate periphery of the PTV (calculated from the expected dose fall-off that radially surrounds the PTV) is enough to sterilise the treatment volume of microscopic spread. The authors concluded that prospective evaluation was indicated to further explore this method of deintensification.

1.7.3 Positron Emission Tomography (PET) - based dose painting

Traditionally, the aim of radiotherapy is to deliver a homogenous radiation dose to a defined tumour volume. The response of tumour cells to treatment within the same tumour can be heterogenous, and a different approach, known as ‘dose-painting’, has been developed in

several settings in order to match up the magnitude of dose with the appropriate parts of the tumour.

A UK phase I study (FIGARO) (67) used pre-treatment PET scans to identify the PET-avid (biological) GTV left after 1 cycle of induction chemotherapy for a 10% dose escalation, in patients with poor prognosis (predominantly HPV-negative) OPSCC. Their results reported higher than expected late toxicity rates although comparative to other studies using standard dose radiotherapy. There was improved overall survival at 3 years compared to historical data on poor prognosis patients leading the authors to conclude further work was needed to explore the role of dose escalation in this patient cohort.

Another group performed a dose painting case matched control study (68). 72 patients who received boosts of up to 85Gy guided by FDG PET-CT scans were matched to controls. 5-year local control rates were higher in the dose escalation cohort (82.3% versus 73.6%) although this was non-significant ($p = 0.82$). Grade 3 dysphagia was seen in half the dose escalation patients with acute and late dysphagia being more common compared to controls ($p = 0.004$). The group concluded that having demonstrated the feasibility of increasing dose to tumour sub-volumes, tailoring of the volume and escalated dose was required to reduce the increased toxicity experienced by these patients.

Whilst these dose painting studies have investigated PET-based dose escalation in high risk or unselected risk patients, there are no published studies looking at PET-based deintensification of treatment specifically in better prognosis HPV positive OPSCC patients. As increased toxicity has been demonstrated with PET-based dose escalation, it is reasonable to anticipate a reduction in toxicity may be possible in patients where PET imaging informs a deintensification of treatment.

1.8 Adaptive PET-based de-intensification of treatment in OPSCC

Adaptive radiotherapy generally refers to making alterations to treatment volumes between fractions to account for inter-fractional organ motion caused by random or systemic changes in anatomy. It can also include alteration of the total treatment dose or time based on changes seen during treatment. When designing a novel adaptive radiotherapy protocol, it is paramount that safety is the first consideration, and that the adaptive strategy is carefully designed to fit the underlying clinical issues. Adaptive protocols can be used as a strategy to de-intensify treatment in responding patients, with the aim of improving long term functional and quality of life outcomes for patients without detrimental impact on tumour control.

1.8.1 Use of FDG PET-CT as basis for biological adaption

18F-fluorodeoxyglucose (FDG) PET is the most widely available method of functional imaging in the UK and the most used in head and neck cancer. FDG is a radio-labelled analogue of glucose which is preferentially taken up by cells with a high level of metabolic activity. FDG PET combined with CT can be helpful in the diagnosis of head and neck cancers; 90 - 100% of them can be detected using FDG-PET (69). There are alternative tracers that can be used e.g. 18F-fluoromisonidazole (FMISO), which is a hypoxia-associated tracer, and there is published work exploring the effect of chemoradiotherapy on FMISO PET scans, and the role of FMISO in identifying areas of the tumour that may respond to higher doses of radiation. Despite on going work in this field, results are mixed in terms of it's reproducability and correlation to long term head and neck cancer outcomes (152). There is also evidence that FDG-PET may be a valid surrogate for FMISO (153). In addition to the wider availability of FDG, most relapses after chemoradiotherapy occur in areas of tumour that were initially FDG-avid (70). In addition, FDG-PET avid volumes have been shown to represent tumours seen in histopathological samples following surgery more accurately than CT and/or MRI (71).

An ongoing European phase II study (ARTFORCE) (72) is recruiting patients diagnosed with lung or head and neck cancers. The head and neck project arm is a randomised phase II study

with a factorial design. It is comparing weekly concomitant cisplatin with weekly cetuximab, and conventional radiotherapy with a dose redistribution arm that redistributes dose based upon a pre-treatment PET CT with adaptive re-planning after 2 weeks using a repeat CT.

GTVs of head and neck tumours delineated based on PET scan images are significantly smaller than GTVs based upon CT and MRI (73). This is true for pre-treatment imaging and on imaging performed during radiotherapy. In one study of 8 patients, the average FDG PET defined GTV was shown to reduce during radiotherapy to approximately 70% of its original volume after 14Gy and to 55% of its original volume after 25Gy. The increase in volume between 14 and 25Gy may be attributable to radiotherapy-induced inflammation of the tumour (74). Reimaging with CT and MRI during treatment led to a less prominent reduction in GTV. Importantly, the FDG PET based GTV translated into subsequent reductions in both prophylactic and therapeutic CTVs and PTVs.

Residual FDG activity during chemoradiotherapy appears to be predictive for unfavourable local control and survival (75). FDG-PET CT scans therefore offer an imaging modality which could enable us to target the area in which most relapses will occur i.e., the volume that remains PET-avid after a proportion of radiotherapy treatment has been given. Re-planning based on changes in the disease seen on imaging during treatment offers the opportunity to dose-paint or re-distribute the dose to residual active (FDG avid) tumour, whilst reducing the dose to other areas of the initial tumour which have already responded to treatment.

One study looked at 18 patients with head and neck squamous cell cancer and repeated the FDG PET scan after a mean dose of 46Gy (76). They demonstrated that the irradiated volume defined by FDG PET was reduced by 15 – 40% when adaptive planning based on interim PET was used. It also demonstrated that by using FDG PET based adaptive radiotherapy, significant dose sparing to the ipsilateral parotid could be achieved (mean dose 38.6Gy vs 30.7Gy with a p value = 0.004). So adaptive radiotherapy based on interim PET-CT also has the potential to reduce dose to critical structures and lower toxicity.

1.8.2 Timing of prePET and iPET

In addition to potential prognostic information from baseline FDG-PET-CT, a small number of studies have investigated the role of FDG-PET-CT during radical radiotherapy for head and neck cancer in predicting response to treatment and prognosis. They have performed intra-treatment PET-CT scans at different time points and published some conflicting results. As described in a recent systematic review, various published reports demonstrate differing degrees of predictive and prognostic capabilities of FDG-PET-CT in the setting of head and neck cancer and it is yet to be determined at what time point(s), and with which parameters, PET scans during radiotherapy should be performed (77).

Castaldi et al (78), published their prospective study conducted on 26 head and neck cancer patients of varying subsites. Patients underwent a baseline FDG-PET-CT, another at 2 weeks into radiotherapy and finally one at 8 – 12 weeks post-completion of treatment. The post treatment FDG-PET-CT was predictive of clinical outcome, correlating with both relapse free survival and disease specific survival. The group was unable to confirm a role of the mid-treatment FDG-PET-CT as it did not have any features that significantly correlated with patient outcome and that further investigation of PET-CT after 2 weeks of radiotherapy is warranted.

In contrast to this study, in 2002 Brun et al (79) performed an FDG-PET-CT at baseline (PET1) and 5 – 10 days into radical head and neck cancer treatment (PET2) with radiotherapy (n=45) or chemotherapy (n=2) in a heterogenous head and neck cancer patient group. At a median follow up of 3.3 years, local control rate was 80%, 5-year overall survival 54%. Within this small population of patients, a low metabolic rate at PET2 in the primary tumour was strongly associated with complete remission, local control rate and survival. Survival was 72% and 35% in patients who had a low metabolic rate at PET2 vs a high one respectively. The hazard ratio for death was 4.5 vs 2.8.

These results were supported by more recent work performed by another group on a cohort of 37 patients with advanced head and neck cancer. Hentschel et al (80) found that the decrease in the maximum standard uptake value (SUVmax) from baseline FDG-PET-CT to the FDG-PET-CT performed after week 1 or 2 into radical radiotherapy, to be a potentially prognostic biomarker. 2-year overall survival and 2-year locoregional control were improved for patients who demonstrated a decrease in SUV max of the primary tumour of over 50% at the second FDG-PET-CT (88% vs 38% and 88% vs 40% respectively).

Despite the above findings Ceulemans et al (81) concluded that they could not replace the post-treatment FDG-PET-CT with an earlier, intra-treatment scan. When they compared FDG PET-CT conducted at the end of week 4 of radiotherapy (47Gy) to that of a scan at 4 months post- completion of treatment, the sensitivity, NPV and accuracy of detecting complete response was reduced (28.6% vs 42.5%, 31.0% vs 60.0% and 80.0% vs 88% respectively). Although the positive predictive value (PPV) and specificity was slightly higher in the week 4 scan (81.8% vs 75.0% and 80.0% vs 77%), this was not enough to warrant a change of imaging scheduling. One possible explanation of this difference in findings in the higher amount of radiation the Ceulemans patients were exposed to. It is now widely considered that after 2 – 3 weeks of radiotherapy, background radiation-induced inflammation can become an issue for the interpretation of FDG-based imaging.

1.8.3 Parameters of PET

Another important area of debate surrounds the choice of parameter to use when using interim FDG-PET-CT for predictive and prognostic means. Parameters most widely studied include the maximum SUV of the tumour (SUVmax), the Metabolic Tumour Volume (MTV) (the metabolically active volume of tumour segmented using FDG-PET-CT), and Total Lesion Glycolysis (TLG), which is the MTV multiplied by the mean SUV. Most work on this has been performed on the pre-treatment (pre_PET).

The primary tumour SUVmax on pre-PET has been demonstrated to be predictive of survival regardless of the size and stage of the tumour (80) although studies differ on their reported cut-off values, which range from SUVmax 4 – 10. The work by Hentschel et al used a relative reduction of 50% in SUVmax between pre_PET and iPET.

In some studies, the MTV has been shown to be more accurate in the prediction of outcome compared to SUVmax (69). One suggested explanation for this is that SUVmax may have less bearing on outcome because highly avid disease may be expected to have a better response to radiotherapy treatment. The MTV can be broadly determined in two ways. The first by a fixed background SUV cut off e.g MTV2.5, or 2 standard deviations of normal liver activity; or by using the SUVmax of individual tumour site regions up to a prefixed percentage of the SUVmax e.g., MTV40%. Dibble et al (84) showed the MTV (and TLG) on pre-PET to be significantly associated with survival and outcome. An MTV equal or greater than 7.7ml was predictive of overall survival. Kao et al (85) looked at the pre_PET of 64 patients with mixed pharyngeal tumours and found the MTV2.5 to be predictive of primary recurrence and DFS. Lim et al (86) looked at 176 patients with oropharyngeal cancer. They used an SUV42% to delineate MTV and compared SUVmax, MTV and TLG. They found the MTV and TLG to be strongly correlated with the development of distant metastases or death. An MTV of over 19.7cm^3 was strongly predictive of a high risk of death. Abgral et al (87) looked at 80 patients with mixed head and neck cancer and demonstrated a pre_PET MTV5.0 to be the best predictor of recurrence and death following treatment and an MTV5.0 of over 4.9ml to be predictive of poor event free survival and overall survival.

1.8.4 Definition of PET-avid disease on iPET

Key to the definition of residual PET-avid disease, is the use of a validated scoring system to define PET avidity in the context of background radiation-induced changes to the normal tissue.

A variety of groups have looked to validate a visual therapy response interpretation criterion, The Hopkins Criteria (82), for use on FDG-PET-CTs performed on head and neck patients during a course of radiotherapy. This objective and standardised visual grading system was intended to reduce inter-observer variability in assessing PET scans. Non-complete metabolic response on iPET is classed as avidity equal to or greater than the focal uptake of the liver and non-complete metabolic response on post-PET is classed as avidity equal to or greater than the mediastinum. Min et al (83) looked at 69 patients with head and neck cancer treated with radical radiotherapy. An FDG-PET-CT was performed at baseline, during week 3 of radiotherapy, and post-completion of treatment after a median interval of 13 weeks. They assessed the residual FDG uptake using the 5-point visual grading system and concluded that the Hopkins criteria was a useful predictor of response to treatment and patient outcome based both on the post-treatment FDG-PET-CT and the interim FDG-PET-CT. Whilst it did not demonstrate the same level of prognostic power as the post-treatment FDG-PET-CT, the interim PET had a very high negative predictive value. In the patients who had a complete metabolic response on the interim FDG-PET-CT, the Hopkins Criteria had an NPV of 91% for the primary site alone, and 100% if both primary and nodal disease demonstrated a complete metabolic response. The group postulated that it potentially offered a mechanism on which to base adaptive de-escalated radiotherapy. They also established optimal thresholds for the definition of the non-complete metabolic response group as focal grade 3 uptake more than, or equal to that of the liver. This is a higher threshold than that of the post-treatment FDGPET-CT to account for elements of increased FDG-uptake attributable to inflammation as a result of radiotherapy treatment.

1.8.5 Automated contouring with the Automatic Decision Tree-based Learning Algorithm (ATLAAS)

Being able to reliably identify and outline or segment the metabolically active tumour on a PET scan is of paramount importance. This can be done manually by a clinician, or it can be done automatically, using an automatic segmentation algorithm.

Manual outlining is prone to intra- and inter-observer variability but, despite its limitations, is still regarded as the 'gold standard' for clinical use.

A variety of PET automated segmentation methods have been proposed to overcome the limitations of manual outlining. However, one of their limitations is the large number of algorithms available and a lack of a standard protocol between centres. In addition to this, head and neck cancers are highly heterogenous and may not all be best segmented with the same PET algorithm.

ATLAAS (88) is a machine learning tool, designed and developed by our co-investigators in the department of engineering at Cardiff University using simulated and phantom based PET images; it can select the optimal PET automate segmentation method for use in each clinical setting as it contains nine algorithms that perform differently in differing conditions. ATLAAS estimates the tumour characteristics in the given PET images and uses a predictive model to select the most appropriate segmentation methodology for the given PET image. Initially developed and validated on oesophageal carcinomas, ATLAAS was applied to the PEARL pilot study head and neck cases and subsequently used on the PEARL study cases within a validation sub-study outlined in the PEARL protocol.

1.8.6 The PEARL Study

Most studies carried out to date evaluating the role of FDG-PET-CT as a basis for adaptive radiotherapy have included heterogenous patient groups, using a variety of PET assessment parameters. This may go some way to explain the disparate conclusions and cut offs that the research has produced.

The PEARL study, described in this thesis, was set up to build on the published data available and analyse the utility of an iPET for adaptive radiotherapy in a well-defined cohort of good prognosis patients with HPV-positive OPSCC.

As detailed in this chapter so far, the hypothetical advantage of reducing the high dose treatment volume based on FDG-based biological tumour response 2 weeks into a course of chemoradiotherapy is the consequential reduction of dose to OARS and toxicity experienced by the patient. Toxicity secondary to dose received by swallowing structures (dysphagia) and salivary glands (xerostomia) results in reduced quality of life for patients. The main OARs of interest in the PEARL study were therefore the major salivary glands and swallowing structures (SWOARs): the superior pharyngeal constrictor muscle (superior pharyngeal constrictor muscle), the middle pharyngeal constrictor muscle (middle pharyngeal constrictor muscle), and the glottis. Optimal dose constraints for these OARs were set based on published data and aligned as far as possible with other studies involving comparable patient cohorts.

The studies described in section 1.7.1 suggest that a reduction in prescribed dose to the primary PTV from an equivalent 2Gy per fraction dose (EQD2) of 70Gy, to an EQD2 of 60Gy appears safe, with no increased rates of treatment failure in phase II studies, although this awaits confirmation in randomised phase III trials. In PEARL, the total dose to the high dose PTV is maintained at EQD2 70Gy, although the volume receiving 70Gy is reduced in responders, based upon biological response on interim PET. Where some groups have used response to induction chemotherapy as a basis for treatment de-intensification, the strategy used in the PEARL study is using the PET-based response midway through chemoradiotherapy as a basis for adaptive radiotherapy. Patients in whom there is no response on iPET will not undergo adaptation. Re-planning based on changes in the disease seen on imaging during treatment offers the opportunity to dose-paint or re-distribute the dose to residual active tumour, whilst reducing the dose to other areas of the initial tumour which have already responded to treatment.

The PEARL study is also used to prospectively apply ATLAAS for the first time to PET-CT scans taken during treatment with chemoradiotherapy.

Due to the increased complexity of adaptive radiotherapy deigned for the PEARL study, and the pressures of the COVID-19 pandemic, we designed a method of automated planning to improve the turnaround of PEARL phase 2 plans.

1.9 Automated Planning

Automated planning of radiotherapy plans is a growing research field and automated planning is already being implemented within the clinical setting. The benefits of automated planning have been widely documented in the literature (89, 90).

The general concept of planning was described by Kevin Moore (91) as 'the process by which a radiotherapy device is programmed to deliver an amount of radiotherapy to a patient'. Over the past 2 decades, this process has transitioned from simply the length of time a beam is left on, to more complicated processes including conformal radiotherapy and VMAT whereby simulation of dose deposition into tissues is part of the planning method. For the purposes of planning, the patient is a set of digital medical images, and the delivery device is a computer algorithm. The quality of the modern planning process can be defined as the extent to which the simulated treatment maximizes the therapeutic ratio.

The planning process has commonly been classed as a manual task – machines have aided humans in achieving this task, but it has been generally steered by humans (Fig. 1.10). Manual planning places high demands on time and workforce. In busy healthcare settings, these can manifest as delays to patient treatment and potentially substandard treatment, as well as acting as hurdles to the research and implementation of adaptive radiotherapy.

A simplified model of the planning process can be described as Fig 1.9 below:

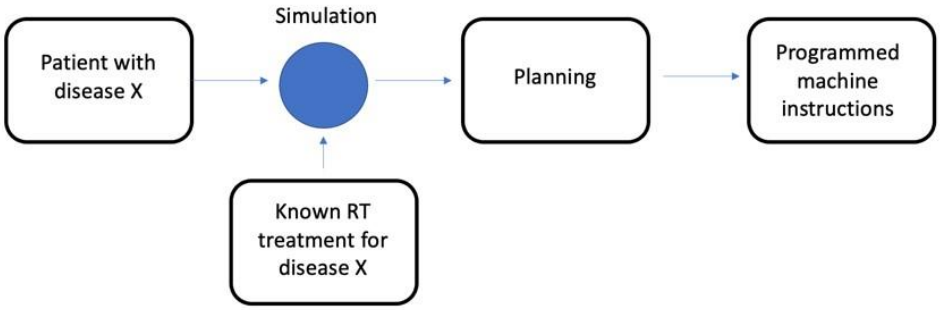

Figure 1.10 Simplified diagram of the radiotherapy planning process, adapted from Moore et al 2018 (91)

1.9.1 Automated Planning with EdgeVCC

EdgeVCC was developed at Velindre Cancer Centre (VCC) to address issues with the manual planning of radical radiotherapy treatments (92).

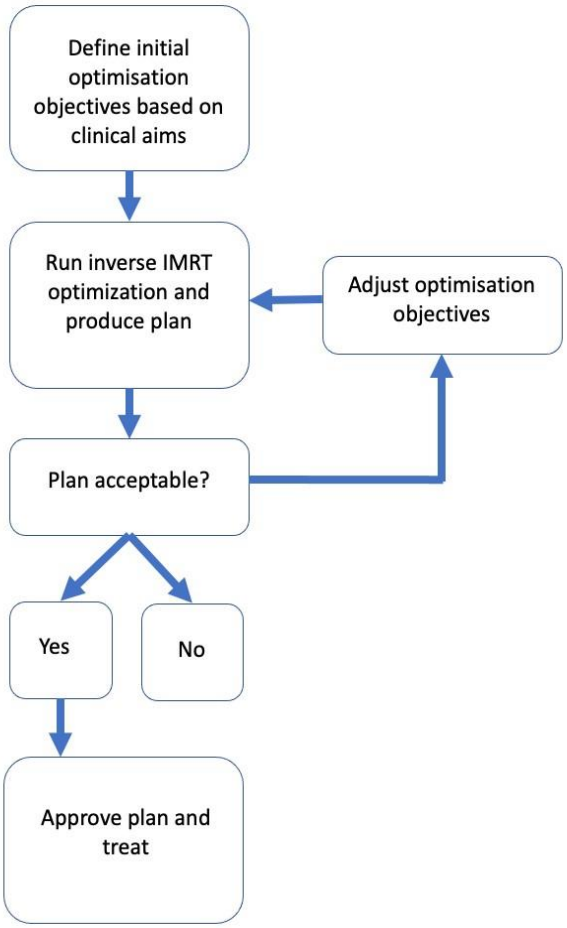

Figure 1.11 Simplified process of manual IMRT or VMAT planning, adapted from Moore et al 2018 (91)

To build the EdgeVCC automated planning protocol, the team initially used prostate VMAT cases. 10 prostate plans which had been previously clinically approved were acquired and used as 'calibration' patients. The plans were labelled VMATclin. The plan with the most representative anatomy of the 10 was chosen as a 'navigator' plan. The EdgeVCC protocol was developed on the navigator with clinical input, using 'trade offs' in the balance of dose between target volumes and OARs, to produce the most clinically acceptable plan. This

protocol was then applied to the rest of the calibration cases, using the exact same arc configurations as the VMATclin, to generate 10 VMATauto plans.

The VMATclin and VMATauto plans for each of the 10 cases were compared on local centre clinical goals and additional indices including D98%, D2% and a conformality index. In addition, clinicians performed a blindly qualitative study of the VMATclin and VMATauto plans for each patient, scoring them using a 5-point scale (1 – unacceptable, 2-poor, 3-satisfactory, 4-good, 5-excellent) and ranked them in order of preference. The overall results were favourable towards the VMATauto. The EdgeVCC team concluded that the automated protocol had incorporated the clinical decision-making on trade-off balancing successfully. I joined the EdgeVCC team to provide the clinic input whilst the process was repeated for head and neck patients. We demonstrated similarly favourable results towards VMATauto in this tumour site (unpublished data).

1.9.2 Role of automated planning in trial Quality Assurance (QA)

Most contemporary radiotherapy trials now include a mandatory radiotherapy quality assurance (RTQA) standard which must be passed by an investigator or treatment centre in order to treat patients within the trial. Whilst the passing of such a standard ensures an acceptable level of PTV coverage and OAR sparing, it does not guarantee a plan is at its optimum. In addition, a lack of conformality in plan quality across different planners and institutions is widely referenced in the literature. In large, randomised trials, this difference in quality, and sub optimal plans, is not considered in stratification. It could introduce bias, influence outcomes, and result in a need for higher sample sizes to demonstrate a difference between treatment arms.

The patient-specific nature of planning presents difficulties in quality assurance across different patient plans to assess plans as ‘good’ or ‘bad’. A good plan essentially requires the

planner to maximise the therapeutic ratio for that patient, similarly a bad plan does not meet the accepted clinical goals for that patient.

The RTQA process appraises patient specific and patient independent factors. Patient independent factors include simulation errors whereby patient, or radiation distribution is incorrectly represented, and treatment delivery errors concerning a mismatch between the treatment that is simulated, and that which is delivered to the patient. Errors of patient specific factors include the inaccurate contouring of the target or normal tissue structures, and problems with optimization where the planner fails to meet achievable plan quality for that patient. Patient specific factors are considerably more challenging to standardize and, consequently, apply RTQA to.

The most important patient specific factor determining plan quality is the anatomy of the patient. Human planners use a trial-and-error format to move the plan closer towards the limiting tradeoff between competing parameters e.g., target coverage and normal tissue sparing, or sometimes between 2 different OARs. Each patient has a different point at which the plan is at its most optimal but human planners do not know what this point is. A consequence of this is the challenge to objectively score individual patient plans. Features such as the distance to the 50% isodose line can be used but this is not sufficient. Whilst the DVH provides a way of representing dose distribution across targets and OARs, it can be misleading. 'Bad' DVHs can look good on a favourable patient plan, and vice versa.

Generally, once dose constraints are met, manual planning doesn't standardly push planning objectives further. This was illustrated in the QA for the RTOG 0126 study (93); the best plans were those which had been difficult to meet the criteria for and the planners had had to keep adding further iterations to bring the doses closer to the constraints. The worst plans were the cases which had easily met the constraints and so the planners had stopping pushing the planning objectives.

Automated planning removes the time spent on producing a manual plan. Instead of comparing a manual plan to a library or knowledge-based model, automated planning applies the patient specific model DVH to the initial plan optimization. Inverse optimization is DVH based. An estimated DVH from a modelled plan, based upon patient specific features in the database, can be entered into the optimization process. A single plan is then produced which has already been optimized to obtain the optimal dose distribution according to the DVH from the automated library or knowledge-based machine.

Examples of the assessment and validation of various automated planning methods are already in the literature. The complexity of head and neck planning makes it an ideal tumour site to explore the use of automated planning. Tol et al (94) performed a retrospective analysis of radiotherapy plans generated within the EORTC-1219-DAHANCA-29 Study. They used the Varian RapidPlan automated planning system which is based upon a library of 177 plans. By generating predicted DVHs for the actual plans used within the study, they found that they could reduce the mean dose to OARs including the parotid glands, submandibular gland and pharyngeal constrictor muscles by up to 9Gy.

1.10 Proton Beam Therapy

Proton beam therapy (proton beam therapy) as an alternative to photon beam radiotherapy is gaining in prominence and interest in head and neck cancer treatment. Whilst improvements to dosimetry have been by the introduction of IMRT and VMAT, there may be a ceiling to the conformality achieved by photons due to the limitations of their physical properties in addition to evidence that other toxicities including fatigue, hair loss and oral mucositis may be increased compared to 3D conformal radiotherapy due to IMRT/VMAT methods of delivery (30).

Protons have a physical profile distinct to photons and as a result, different radiobiological properties. The increased mass of protons offers a sharper lateral dose distribution compared to photons due to a sudden increase in dose deposition at the end of the particles range, giving rise to a feature known as the Bragg Peak (Fig.1.12 and 1.13). These steep dose gradients reduce the integral dose received by surrounding tissues and minimises to an insignificant amount the exit dose beyond the target volume.

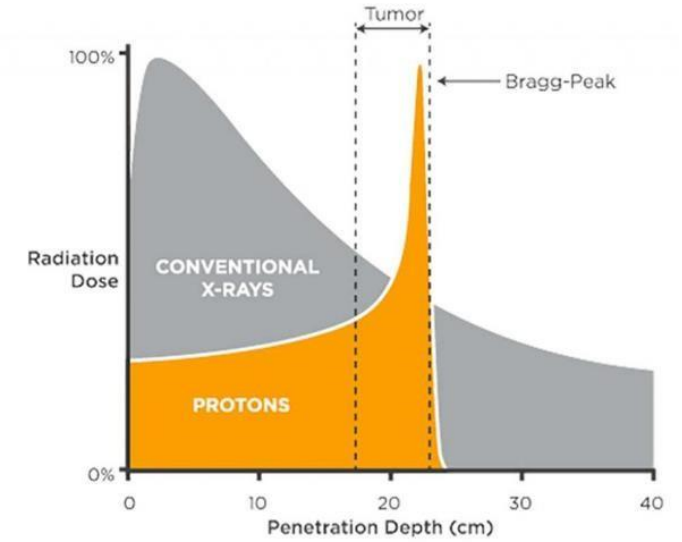

Figure 1.12 The Bragg Peak profile of a single proton beam compared to photon Credit: www.provisionhealthcare.com/about-proton-therapy

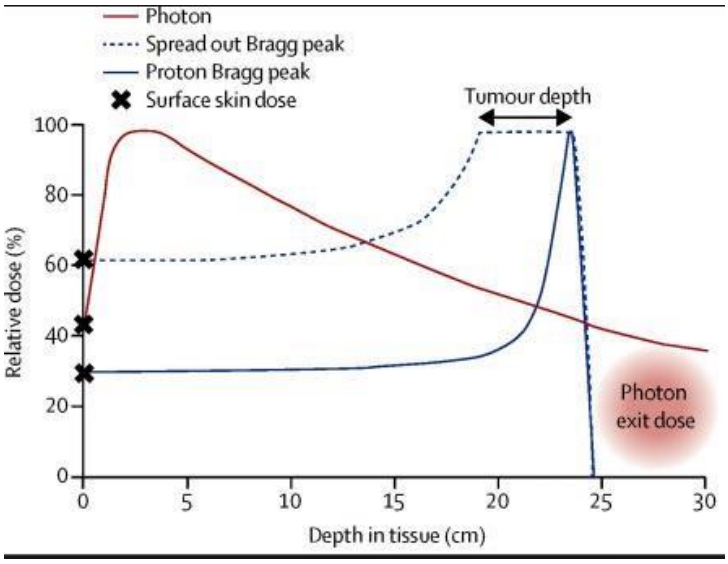

Figure 1.13 The beam profile of the Bragg Peak spread out to cover the tumour compared to single beam profiles of photons and protons Credit: Leeman, J et al The Lancet Oncology 2017

The delivery of proton beam therapy can be broadly divided into passive scanning and active scanning (pencil beam and intensity modulated proton therapy (IMPT)) techniques.

Passive Scanning	Active Scanning/IMPT
Less flexible than active scanning and requires patient specific devices Protons of different energies have different ranges. Scattering foil spreads out the beam, which results in the spreading out of the Bragg peak (SOBP) to ensure dose at depth and can lead to a higher entrance dose. Depth modulated by range compensators Beam conformed laterally by brass apertures which can be adjusted for range and set up uncertainty Creates secondary neutrons Reduced capacity or adaptive replanning	Most widely used method of proton beam therapy. Relies on magnetic properties of protons Different energies treat different depths within tumour A small beam creates a 'spot' the size of which impacts upon the penumbra therefore volume of peripheral tissue receiving a significant dose. More conformal than PS and more skin sparing Magnets deflect beam and conform it to the target volume

Table 1.7 Common methods of proton beam therapy delivery

Proton beam therapy is not without relative disadvantages. It is more sensitive to the physical and geometric uncertainties of a radiotherapy plan compared to IMRT and so this needs to be mitigated for both prior to, and during, treatment. The cost of proton beam therapy is also an important factor to consider. It generally costs 2-3 times as much as IMRT however in the right patients, this may be countered by an overall reduction in the cost of patient care on account of reduced toxicity (95).

Theoretical benefits of proton beam therapy must also be weighed up against the potential requirement for treatment volumes to be larger in order to offset lack of confidence in patient set up and proton range. With photon treatment, geometric uncertainties are dealt with by applying a margin to the CTV and creating a PTV. It does not account for anatomical changes during treatment and is known as a static dose cloud approximation. It is adequate for photons as it does not need to consider changes in tissue density, motion or variation of particle range. The magnitude of the CTV-PTV margin is in part dependent upon image guidance for treatment verification and with advances in imaging, it is likely these margins can continue to be reduced. In IMPT, uncertainties are mitigated for using robust optimization rather than the application of a PTV margin. 'Robustness' is how well the plan mitigates for uncertainties of set up, particle range and stopping power. Robust plan optimisation algorithms consider any range or set up variation that may occur during a course of treatment prior to treatment delivery. There are broadly two types of robustness; worst case scenario and stochastic/probabilistic programming which is based upon several different potential scenarios and how likely they are to occur.

IMPT optimisation can either be single field or multifield. Single field is when each field is optimised individually whereas in multifield, all fields are optimised simultaneously. Multifield is more conformal however incorporates a higher level of uncertainty and has more infield dose gradients. It can provide better organ sparing but is more vulnerable to changes in set up and anatomy. Inter- and intra-fractional motion can change the tissue density along the proton beam path and have significant ramifications for the position of the Bragg Peak and subsequent dose distribution.

1.10.1 Proton beam therapy toxicity and NTCP

The first published study in proton beam therapy to cancers involving the pharynx was Slater et al in 2005 (98). They used proton beam therapy to deliver a concomitant boost to a 3D conformal photon plan in 29 patients. At 5 years there was an acceptable locoregional control

rate of 88% and disease-free survival of 65%. Subsequent studies looking at clinical outcomes have been published including a case matched control study by Blanchard et al (99) which compared 50 IMPT plans with 1000 control IMRT plans. At 2 years overall survival was equivalent but G3 weight loss and PEG usage at 3 months and 1 year was significantly reduced in the IMPT group.

Whilst retrospective, there is accumulating evidence that IMPT reduces toxicity in a clinically meaningful way. Sio et al (100) collected and analysed patient reported outcomes of oropharyngeal cancer patients, 35 who were treated with IMPT and 46 treated with IMRT. Patient reported outcomes were assessed by the MD Anderson Symptom Inventory Head and Neck module (MDASI-HN). Changes in taste and appetite during the early and late phase favoured IMPT. The mean of the top 5 MDASI-HN scored symptoms (taste, xerostomia, swallowing/chewing, reduced appetite and fatigue) was reduced by 22% in the IMPT group.

One late toxicity where proton beam therapy may have a significant impact is in reducing the incidence of osteoradionecrosis which is notoriously challenging to treat. Known risk factors for the development of osteoradionecrosis include total radiation dose, dose per fraction and field size. It is often difficult to reduce radiation dose to the mandible in oropharyngeal cancer cases with photons due to the proximity of the primary or pathological nodes to the mandible.

The Introduction of 3D conformal radiotherapy, and then IMRT, has reduced the risk of osteoradionecrosis compared to parallel opposed photon fields, but the risk remains. A retrospective analysis by Zhang et al (101) looked at mandible dose and osteoradionecrosis rates in 534 patients with oropharyngeal cancer treated with IMRT and 50 with IMPT plans. IMPT reduced the minimal, mean and median dose to the mandible; the mean dose difference was 25.6Gy versus 41.2Gy. V5 – V70 were all reduced. They found the osteoradionecrosis events to be significantly associated with increasing mandible volumes V45 – V70. At a median follow up of 33.8 months, the clinical outcomes reflected the dosimetric data with 7% IMRT patients having G1 – G4 osteoradionecrosis and 2% IMPT patients having G1 only.

The results of 2 large prospective randomised controlled studies comparing IMRT with IMPT, TORPEDO (102) and NCT01893307 (103), will hopefully help to elucidate what benefits proton beam therapy may have and in patients with OPSCC.

Numerous acute and late adverse effects of radiotherapy have been shown to be dose and volume related. An increased dose to an increased volume escalates both the probability and severity of toxicity and organ dysfunction.

Considering the financial and practical implications of access to proton beam therapy, models have been developed with the purpose of predicting who is most likely to benefit from proton over photon-based radiotherapy. Normal Tissue Complication Probability (NTCP) scoring is a model-based approach designed to improve the cost effectiveness of proton beam therapy, which carries a considerably higher cost than IMRT (96). Patients are selected for proton beam therapy if the model calculates a reduction in NTCP of a certain amount or more e.g., a 10% reduction in grade 2 complications.

This system is limited as many models have been developed using cohorts of patients treated with an outdated method of photon-based radiotherapy and so may over-estimate the benefit of proton beam therapy. In addition, while contemporaneously, IMPT is the most widely used form of proton beam therapy, much of the head and neck proton beam therapy data published has been based upon passive scatter methodology.

Arts et al (97) looked at IMRT and IMPT plans generated for 78 patients with a range of margins and robust settings used respectively. When different levels of accuracy were applied to these plans, patient selection was affected, with differing patients reaching the threshold NTCP for proton beam therapy selection. The largest impact on the NTCP was from the degree of set up robustness. They concluded that treatment accuracy must be considered on a case-by-case basis when establishing which patients should be recommended for proton beam therapy.

They also acknowledged that it is not straightforward to compare margins to robustness settings for a fractionated course of radiotherapy of similar accuracy. Ultimately the plan is limited by what is clinically deliverable and the final decision must be taken with review of the plan once reconstructed by the treatment planning system.

In Chapter 6, the advantages of adaptive radiotherapy based on biological response seen on iPET are compared when planned with IMPT compared to VMAT, to examine whether additional organ sparing can be produced.

1.11 Treatment Verification

The improved conformality of radiotherapy methods such as IMRT, adaptive and proton beam therapy, requires optimal on-set verification to ensure the target volumes are covered appropriately by the 95% isodose, and irradiation of OARs are kept within mandatory dose constraints and as low as reasonably possible. Improved on set verification may also allow a smaller margin to be added to CTVs, reducing the volume receiving the prescribed dose and complementing the impact of adaptive radiotherapy.

Head and neck squamous cell carcinomas treated radically with radiotherapy are classed as category 1 tumours. There is evidence that prolonged treatment time leads to less favourable outcomes in this category. Re-planning midway through a course of radiotherapy treatment in a timely manner is very resource intensive and can take several days to turn around. Category 1 patients should not have unplanned breaks in their treatment course (103). Consequently, head and neck cancer patients who require replanning are treated on the original plan until the new one is ready, resulting in suboptimal radiotherapy accuracy during this time. Identification of features predictive for set up errors and the need for re-planning requirements could inform treatment pathways that then prospectively factor in a re-plan.

This would allow for a more streamlined and efficient process.

1.11.1 Treatment verification in head and neck radiotherapy

In-room imaging of the patient on the treatment couch is performed to verify patient position prior to treatment. Onboard imaging with either kilovoltage (kV) or megavoltage (MV) imaging modalities allows visualisation of the target volume, or a surrogate, in relation to OARs. 2D imaging with MV electronic portal imaging devices and KV planar imaging, or 3D imaging with linear accelerator-based kV cone beam CT (CBCT) or MV CBCT on tomotherapy units can be obtained. In Velindre Cancer Centre we use daily kV CBCT for verification of radical VMAT head and neck plans. KVCT imaging is generally viewed as having advantages over MVCT due to its higher resolution, reduced photon scatter and fewer artefacts. Despite these benefits, the supplementation of daily MVCBCT by a mid-course kVCT may not necessarily convey an advantage (105). MVCBCT can be optimized to allow for deformable image registration and delineation and recalculation of dose with up to 2 – 3% accuracy for clinically relevant parameters (106).

Treatment verification can be offline or online. Offline verification is performed to monitor systemic errors. The verification image is obtained prior to the radiotherapy treatment fraction and reviewed after the fraction has been delivered to assess set up error. Measurements and the correction of systemic errors regarding target positioning can then be performed by way of treatment couch shifts and applied to subsequent treatment sessions. Online verification, with adjustments performed whilst the patient is still on the treatment couch, and shortly before the treatment fraction delivery, allows for significantly more accurate correlation and can correct for both systemic and random errors.

1.11.2 PTV Margins

A major factor in the degree of toxicity experienced by patients undergoing head and neck radiotherapy is the size of the irradiated volume. Whilst the size of the tumour is not a variable

that can be changed, treatment margins added onto the GTV may well offer an opportunity for reducing the irradiated volume. As previously detailed in earlier chapters, the requirement for these margins is to account for invisible, microscopic tumour spread (GTV to CTV) and mitigate for uncertainty around set up and treatment delivery (CTV to PTV). On a practical basis, the CTV-PTV margin is employed to compensate for variability in treatment set up. It applies to specific delivery systems and verification protocols and is dependent upon the accuracy of radiotherapy delivery. The PTV margin can be adjusted according to the level of uncertainty and intensity of verification, and with the improvement of both these factors over recent years, it is a potential target for margin reduction.

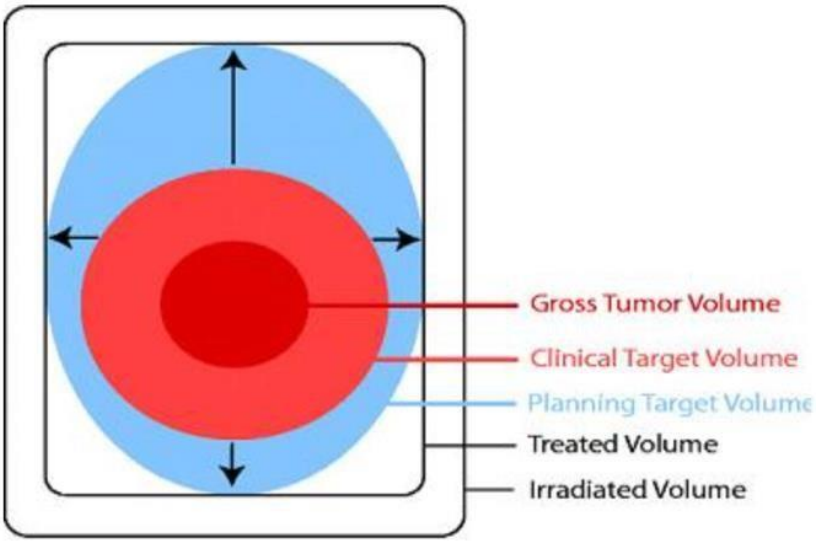

Figure 1.14 ICRU50 margins credit: Lena Sprecht

Reduction in the PTV margin has been demonstrated to have clinical benefits. Navran et al (107) compared 3mm to 5mm PTV margins in a retrospective study. In a cohort of over 400 Head and Neck cancer patients, the first half were treated with a PTV margin of 5mm, the latter half, 3mm. Daily online set up corrections were based on CBCT and any residual misalignment or anatomical change flagged up and evaluated by a radiation oncologist for consideration of adaptive planning. Locoregional control at 2 years for 5mm and 3mm was 79.9% and 79.2% respectively. The reduced margin was independently predictive for a reduction in any acute grade 3 toxicity, acute grade 3 mucositis and acute and late grade 3 dysphagia in a multivariate analysis. There was a significantly reduced mean dose to the parotid glands and pharyngeal constrictor muscles particularly in oropharyngeal primaries.

Mean dose was reduced by approximately 1Gy per 1mm reduction in margin. This study showed that reducing the PTV margin can produce clinically significant benefits to patients without jeopardizing disease control.

1.11.3 Common changes to anatomy during head and neck treatment and implications for target coverage and dose to OARs

1.11.3.1 Changes to coverage of the Target Volume

It is common for the primary GTV to be larger on the week 1 CBCTs than the planning CT due to tumour growth in the interval between the planning CT and starting treatment (108) – in practice an interval of up to 2 -3 weeks. In addition, weight loss/external contour change is often seen later in a course of radiotherapy in head and neck patients due to tumour response in the neck or reduced oral intake leading to weight loss. Weight loss is a significant predictor for a rise in cumulative D95 to the primary PTV (109).

1.11.3.2 Changes in delivered dose to OARs

In common practice, the ipsilateral parotid gland volume changes to a greater extent than the contralateral parotid gland due to the higher dose it receives as a result of its proximity to the primary tumour (110). Wu et al (111) demonstrated on modelled re-plans based on serial CBCTs, that the change in volume of parotid glands is more prominent than the CTV. In addition to gland shrinkage, parotid glands move position tending to drift medially, cranially and dorsally during a course of head and neck radiotherapy. Mean dose can increase by up to 10% if patients are not re-planned to mitigate for this change in size and location. Wu found the main benefit of re-planning was to preserve parotid sparing over target volume coverage and that by minimizing the CTV-PTV margin and re-planning when indicated, the mean dose to the parotids could be reduced by up to 30%. Whilst the percentage change can be large, it

is important to concede that the absolute change in mean dose received by the parotid glands may not be significant regarding correlation with the risk of xerostomia. Despite this, xerostomia is known to impact upon a head and neck patient's quality of life as mentioned earlier in this chapter, and any reduction in mean dose to parotid glands could contribute to reducing this impact.

1.11.4 Image guided radiotherapy (IGRT) and adaptive planning

Geographical target miss refers to when some–- or all–- of a tumour, or the intended margin around the tumour, is excluded from the delivered irradiated volume. Image Guided radiotherapy with onboard kilovoltage or megavoltage imaging facilities reduces the risk of geographical target miss and offers the potential to reduce the CTV to PTV margins by minimizing setup uncertainty.

Reactive re-planning can also be employed to reduce set up errors resulting from non-rigid anatomical deformations e.g weight loss and TV shrinkage by replanning radiotherapy on a new planning CT at a point during treatment.

Whereas conventional IGRT only corrects for set up errors, dose guided radiotherapy recalculates dose delivered per fraction and can identify patients who require adaption to mitigate for the underdosing of the target volume or overdosing of OARs.

A dose guided radiotherapy model was proposed by Von Kranen et al (112) who carried out a small retrospective study on 19 OPSCC patients. Delivered dose was modelled and evaluated using daily CBCT. Adaptive planning was employed if coverage of the target volume fell below a threshold. For each fraction, anatomy on CBCT was deformably registered with the planning CT and delivered dose calculated. This process was modelled with 3 different CTV-PTV margins (0mm, 3mm and 5mm). Candidates for adaption were identified if the accumulated dose to 99% of the volume (D99) to the CTV dropped by more than 2Gy. In nearly all the target

volumes identified, coverage was improved by more than 3Gy with a single adaptive intervention at fraction 10. Target volume coverage throughout the course of treatment was also more robust than predicted. The group hypothesized this may be due to multiple CTVs or concave TVs shifting into other PTVs as the deformations developed. Another reason is that the planned dose distribution doesn't perfectly conform with the PTV and consequently the treated volume (within the 95% isodose) is often larger than the PTV, allowing for an additional degree of set up error to be absorbed.

Close monitoring of the delivered dose and accurate prediction of the expected final dose to CTVs and OARS is required identify candidate patients for meaningful adaptive intervention.

To justify the increased resources required for verification and re-planning, there is a need for better clarification over what significant clinical benefit re-planning leads to. Noble et al (113) demonstrated that weight loss or shape change doesn't mandate radiotherapy replanning for spinal cord safety. This agreed with findings from Wu et al (111) who showed the dose to the spinal cord remained stable during treatment despite other anatomical changes occurring.

1.11.5 Features predictive for re-planning on treatment verification imaging

If radiological features early on in treatment were predictive of verification issues later, replanning and adaption could be factored into a course of radiotherapy up front. This could increase the efficiency of the treatment course, scheduling in the time for re-planning prospectively. Alternatively, PTV margins could be adapted on a patient-by-patient basis, accommodating for differences in set up tailored to the patient. In some patients this may reduce the irradiated volume and subsequent toxicity to normal tissues.

Hunter et al (114) looked at cumulative parotid dose throughout a course of treatment on daily online imaging. They demonstrated that the difference in parotid position between the planning CT and day 1 online imaging was highly correlated to the final discrepancy between

planned and delivered dose to the parotid glands. Van Kranen's (112) modelling study on 19 oropharyngeal cancer VMAT plans found where the CTV coverage was reduced by >2Gy due to reduced PTV margins, this could be corrected for by replanning based upon the average anatomy on the first 10 CBCTs.

Both Hunter and Van Kranen's work suggests that most re-planning is required due to systemic local misalignment e.g., neck flexion, rotational error, shoulder mal-position or physical tumour features, rather than progressive change (regression, weight loss,) as plans adapted early in the course of treatment were then accurate enough for the rest of the course.

Conversely, Van Beek et al (115) noted non-rigid anatomical changes including shape change, in addition to shifts in rigid internal structures e.g., thyroid cartilage or the hyoid bone, contributed to the need to re-plan. These types of anatomical changes cannot be corrected for by couch shifts and in most centers are observed and assessed daily by the treatment radiographers. Out of 416 consecutive head and neck patients, Van Beek's center replanned 9% due to anatomical changes either by recontouring on a new planning CT or adjusting existing TVs and OARs on the new planning CT. In the early weeks the most likely reason for replanning was an increase in TVs due to a reduction in external contour, or local shifting of target volumes.

In standard clinical practice, CBCT images are reviewed by the treatment radiographers and compared to the planning CT. A treatment couch correction can then be made to improve the correlation of bony anatomy demonstrated on the verification images with that seen on the planning CT. If couch correction does not improve the correlation of bony anatomy, or there is additional concern about coverage of the TV as a result of altered hyoid position or soft tissue anatomy changes, treatment radiographers refer the CBCT to the imaging team for further review. At this point clinicians alongside the imaging radiographers and physicists can assess the set-up error and decide if a repeat planning CT is required.

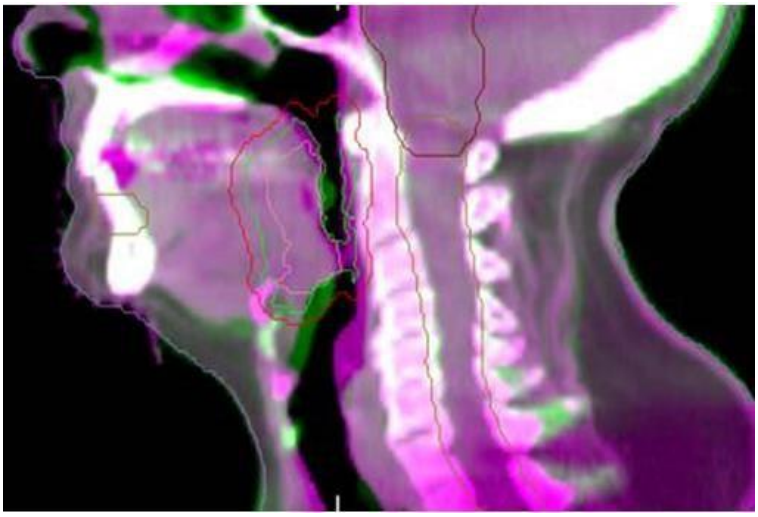

Figure 1.15 CBCT (green) at fraction 5 of a course of radical chemoradiotherapy demonstrating a hyoid drop from its position on the baseline scan (purple). In this example, the base of tongue also appears to have dropped.

1.11.7 Hyoid anatomy

The visualization of the hyoid bone on CBCT is an important frame of reference for treatment verification for radiographers on set.

The hyoid is unique in that it is the only bone in the body that does not directly articulate with another bone. It is a horseshoe structure in the anterior neck and at rest lies inferiorly to the skull, below the mandible at the level of the C3 vertebra (Fig. 1.16). The hyoid bone is suspended in the neck by the stylohyoid ligament which attaches the lesser horns to the styloid process, part of the temporal bone. It provides a surface for the attachment of ligaments and muscles. These, in turn stabilize and move the tongue and larynx (Fig. 1.17).

The hyoid is made up of the body, 2 greater horns–- or cornua–- and 2 lesser horns. The hyoid body is the central rectangular portion of bone with an anterior convex structure and posterior concave structure. A transverse ridge travels across the rough anterior body, dividing into a superior and inferior portion. This surface forms the base for multiple muscle attachments (table 8). The back of the body is smooth and is separated from the epiglottis by the hyothyroid membrane and loose areolar tissue.

The greater horns are the larger processes, extending laterally in the supra-posterior axis from either distal end of the hyoid body. The lesser horns are conical processes extending either side of the superior aspect of the hyoid body and are connected to the body by fibrous tissue in line with the transverse ridge. They point supra-posteriorly towards the styloid processes and are the attachments for the stylohyoid ligament.

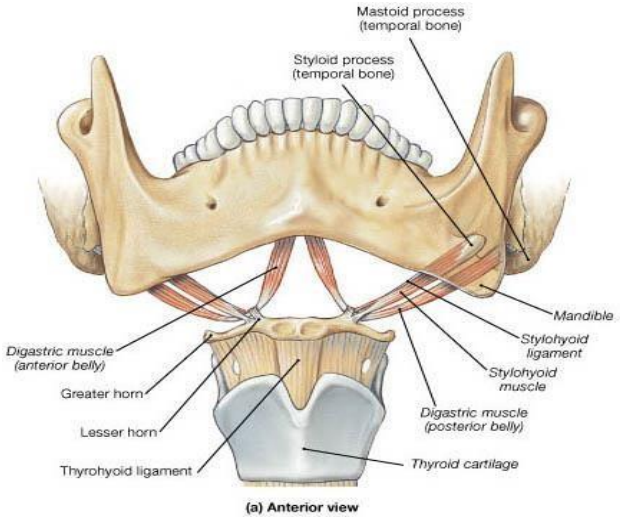

Figure 1.16 Anterior view of the hyoid bone and its relationship to surrounding structures.

Credit: www.anatomyinfo.com/hyoid-bone/

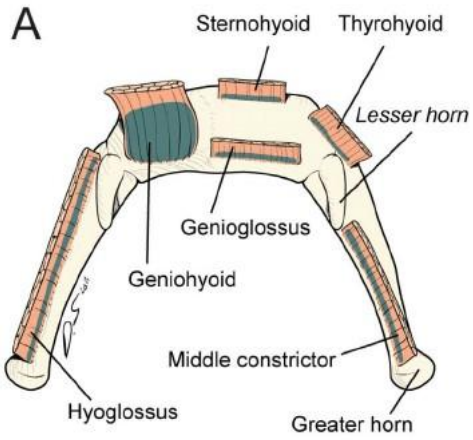

Figure 1.17 Superior view of the hyoid bone and the sites of muscle attachments.

Credit: Ha, J pLoS-ONE 2013

Muscle	Hyoid insertion	Attachment	Function
Suprahyoid			
Stylohyoid	Lesser horns Greater horns	Styloid process	Pushes tongue up against the palate in swallowing
Digastric	Greater horns	Digastric fossa of mandible/mastoid notch	Pushes tongue up against the palate in swallowing
Geniohyoid	Anterior surface of body	Interior mental spine of symphysis menti	Pulls hyoid up and forwards in swallowing
Mylohyoid	Anterior surface of body	Mylohyoid line of mandible	Elevates hyoid in swallowing
Oral Cavity/Pharynx			
middle pharyngeal constrictor muscle	Greater and lesser horns	Median pharyngeal raphe	
Hyoglossus	Anterior and posterior surface of body Greater horns	Lateral tongue	Depresses tongue during swallowing
Genioglossus	Posterior surface of body Tongue	Mandible	Tongue position
Infrahyoid			

Thyrohyoid	Greater horns Posterior surface of body	Superior thyroid cartilage	
Omohyoid	Anterior surface of body	Superior border of scapula	
Sternohyoid	Anterior surface of body	Posterior sternal manubrium	

Table 1.8 Anatomy and function of the dominant muscle attachments to the hyoid bone

1.11.8 Hyoid function

By providing anchorage for numerous muscles and ligaments of the larynx, pharynx, floor of mouth, and tongue, the hyoid bone plays a crucial role in many critical physiological functions including swallowing and phonation.

There is a paucity of published data on the movement of the hyoid throughout a course of OPSCC radiotherapy, and its relationship to the position of the primary GTV. Improved understanding of both these factors may allow for a more tailored approach to patient set up, better confidence in verification and potential reduction in the CTV-PTV margin.

1.12 Conclusion

Worldwide, efforts are ongoing to determine the optimal strategy to reduce late toxicity in patients with good prognosis HPV positive OPSCC who are undergoing definitive chemoradiotherapy. There is yet no consensus on the best way forward.

In my thesis, I explore three novel strategies that have the potential to reduce toxicity in these patients, namely FDG-PET-CT guided adaptive, proton beam therapy planning and predicting hyoid bone movement to improve treatment plan verification and reduce margins. The findings will contribute towards a better understanding of how toxicity can be reduced in this patient population, who want to survive their cancer whilst retaining their quality of life.

Hypotheses:

Hypothesis 1: Adaptive radiotherapy based on biological response to treatment seen on interim FDG-PET-CT scan during chemo-radiotherapy treatment can be used to reduce the dose received to the Swallowing Related Organs at Risk (SWOARs) and major salivary glands in patients with HPV positive OPSCC.

Adaptive radiotherapy using intra-treatment FDG-PET (iPET) creates an individualised, responsive treatment plan based on an individual patient's tumour biology and responsiveness to chemo-radiation. This adaptation has the potential to reduce the dose of radiotherapy received by SWOARS and major salivary glands thereby potentially reducing toxicity. As part of this MD, I will develop the protocol for PEARL: PET-based Adaptive Radiotherapy study, aiming to establish the feasibility of adapting radiotherapy plans based on PET-CT response after 2 weeks of chemoradiotherapy. Furthermore, I will perform dosimetric modelling studies on both pre-trial and on-trial plans to explore how a biologically adapted plans translate into reduced normal tissue irradiation.

Hypothesis 2: Adaptive radiotherapy based on biological response to treatment seen on interim FDG-PET-CT scan during chemo-radiotherapy treatment will be superior using proton beam therapy compared to VMAT in terms of sparing dose to organs at risk in patients with HPV positive OPSCC.

Proton beam therapy has physical characteristics that may improve dose conformality and normal tissue sparing compared to photon therapy. I will perform dosimetry modelling studies on pre-trial cases to determine whether proton beam therapy-based adaptive results in greater sparing of dose to OARs compared to photon-based adaptive.

Hypothesis 3: Hyoid bone movement can play a part in radiotherapy treatment verification, and better understanding hyoid movement during treatment may allow a reduction in CTV to PTV margins.

Reduction of intra- and inter-fraction movement offers the potential to reduce PTV margins and consequently the volume of tissue receiving high dose radiotherapy. I will explore how the hyoid bone may be used as a surrogate for the position of OPSCCs during radiotherapy and how a better understanding of how the hyoid bone moves during a course of treatment may allow optimal verification and the minimisation of set up uncertainty, which is essential with improved treatment conformality and adaptive radiotherapy.

CHAPTER 2: Development of a protocol for a novel PET-CT based Adaptive Radiotherapy Clinical Trial – The PEARL Study

2.1 The PEARL Study

As the PEARL Clinical Research Fellow, I developed a Clinical Trial Protocol and Radiotherapy Trials Quality Assurance (RTTQA) Program for PEARL, a Phase 2 PET-CT based adaptive radiotherapy clinical trial. In this chapter I will outline the following:

- Study Rationale
- Inclusion/Exclusion Criteria
- Primary and Secondary Objectives
- Planning PET-CT Protocol
- Benchmark Outlining and Planning Quality Assurance (QA)
- Development of PEARL Outlining Protocol
- Development of PEARL Planning Protocol
- Statistical Considerations
- Ethical Approval
- PEARL Sub-Studies

The full PEARL protocol and radiotherapy guidance document are in Appendices 1 and 2

2.2 PEARL Rationale

HPV-positive oropharyngeal squamous cell carcinoma (OPSCC) has a better response to chemoradiotherapy and has a younger average demographic compared to HPV-negative disease. Following radical treatment, good-risk HPV-positive OPSCC has a better prognosis; nearly double the survival of high-risk HPV negative OPSCC (4). The current standard of care for locally advanced OPSCC is 6–- 7 weeks of radical chemoradiotherapy. Chemoradiotherapy results in high cure rates, however many patients are left living with long term side effects that impact upon their quality of life (37). With high cure rates in radically treated HPVpositive OPSCC, survivorship issues become a focus for improvement.

The higher the dose of radiotherapy received by a volume of normal tissue, the greater the risk of significant toxicity. There is clear evidence for this dose volume effect, otherwise known as the therapeutic ratio. Radiobiological studies (38) of patients treated with the standard radiotherapy dose of 70Gy to a head and neck cancer demonstrate that when the composite volume of the pharyngeal constrictor muscles receiving 70Gy exceeds 30%, longer term feeding tube dependency increases with a higher number of patients requiring feeding tubes 1 – 2 years post-completion of radiotherapy. When the volume of pharyngeal constrictor muscle exceeds 50%, the risk of pharyngeal strictures increases. If >50% of the pharyngeal constrictor muscle volume receives 65Gy, aspiration increases. Finally, the probability of dysphagia increases with every 10Gy above 55Gy to the middle pharyngeal constrictor muscle and superior pharyngeal constrictor muscle. Minimizing this dose volume effect has recently been substantiated in a Phase 3 randomised controlled trial. The DARS study (NCT 25458988) demonstrated improved patient reported swallowing function in patients with head and neck cancer when dysphagia optimised IMRT (Do-IMRT) was used (40). This was the first randomised study to demonstrate improved functional outcomes from swallow sparing IMRT.

One strategy to improve the therapeutic ratio is to use adaptive radiotherapy. By adapting the treatment volume to imaging throughout a course of treatment, anatomical, metabolic, and morphological changes can be taken account of, and the resulting radiotherapy distribution become more conformal to the persistent tumour volume. Adaptive radiotherapy also offers the chance to escalate or de-escalate the prescribed treatment dose based upon individualized tumour response during treatment. There have been several dose escalation studies which demonstrate the challenges of dose escalation in head and neck cancer radiotherapy in delivering an acceptable therapeutic ratio. The Figaro study boosted the persistently PET-avid volume, following one cycle of induction chemotherapy, up to 77.9Gy EQD2. They have recently reported their late toxicity rates were higher than expected, although comparable to contemporary data for standard dose IMRT (76).

In contrast, dose de-intensification studies have demonstrated that reducing the treatment dose in good prognosis HPV-positive OPSCC patients can result in disease control rates equivalent to those seen with conventional dosing. As outlined in Chapter 1, there is emerging evidence that it could be safe to de-intensify treatment in these good-risk patients, however most are small phase 2 studies, many of which involve assessing response to induction chemotherapy which is not standardly used for treating OPSCC in the UK. In addition, the radiotherapy was not individually adapted based on response during treatment. Not all deintensification studies have been positive, however. The replacement of concurrent cisplatin with cetuximab in the De-Escalate HPV (118) and RTOG 1016 (117) studies showed inferior outcomes with concurrent cetuximab. It is therefore of paramount importance that any attempts to reduce toxicity with de-intensification of treatment are performed cautiously and not at the expense of reduced tumour control rates.

The increasing incidence of HPV-positive OPSCC, and the need to reduce the high toxicity rates in these patients, underpins the design of PEARL PET-based Adaptive Radiotherapy trial (NCT03935672). PEARL aims to maintain high cure rates in good prognosis HPV-positive OPSCC patients, whilst reducing dose to the normal tissue.

2.3 PEARL Design

Rather than reducing the prescription radiotherapy dose, or changing concurrent systemic therapy, PEARL offers personalised radiotherapy based upon the metabolic response of the primary tumour on an 18-F- Fluorodeoxyglucose (18-FDG) PET scan performed 2 weeks into a course of chemoradiotherapy. As discussed in Chapter 1, 18-FDG PET is the most common form of functional imagining routinely used for the assessment of response to treatment in head and neck cancer. The PET avid volume is the part of the primary tumour most likely to recur following treatment (70). When a primary tumour responds to treatment, the avid volume on 18-FDG PET reduces and offers the opportunity for adapting the high dose volume during a course of radiotherapy (74); ensuring the highest dose is delivered to the volume at greatest risk of recurrence.

In PEARL, a mid-treatment planning PET-CT (iPET) is performed after 2 weeks of chemoradiotherapy. A new plan is generated and implemented from the start of the fourth week of radiotherapy. This delivers the second phase (18 fractions) of the treatment course (Fig. 2.1). The central hypothesis of PEARL is that by reducing the primary tumour volume which receives the highest dose of radiation for the second phase of treatment, the total dose to the surrounding normal tissues, including the SWOARs and the major and minor salivary glands, will also be reduced, potentially lowering the rate of late toxicity for patients.

There are 2 main reasons why the nodal volumes will not be adapted based on response on PET in PEARL. The first is that most published data on head and neck cancer metabolic response to treatment on FDG PET has been on the primary tumour. The second reason is that cystic, necrotic nodes are common in HPV-positive OPSCC and may not have uniform 18FDG uptake consequently. This would make the interpretation of the activity of nodal disease challenging.

With the aim of reducing late toxicity rates, PEARL explores the feasibility of adapting an individual patient's radiotherapy plan based upon response of the tumour on interim PET scan (iPET_CT) after 2 weeks radical chemoradiotherapy. PEARL is the first study of its kind to redistribute radiotherapy in patients with HPV-positive OPSCC, based on FDG-PET-CT performed a third of the way through treatment.

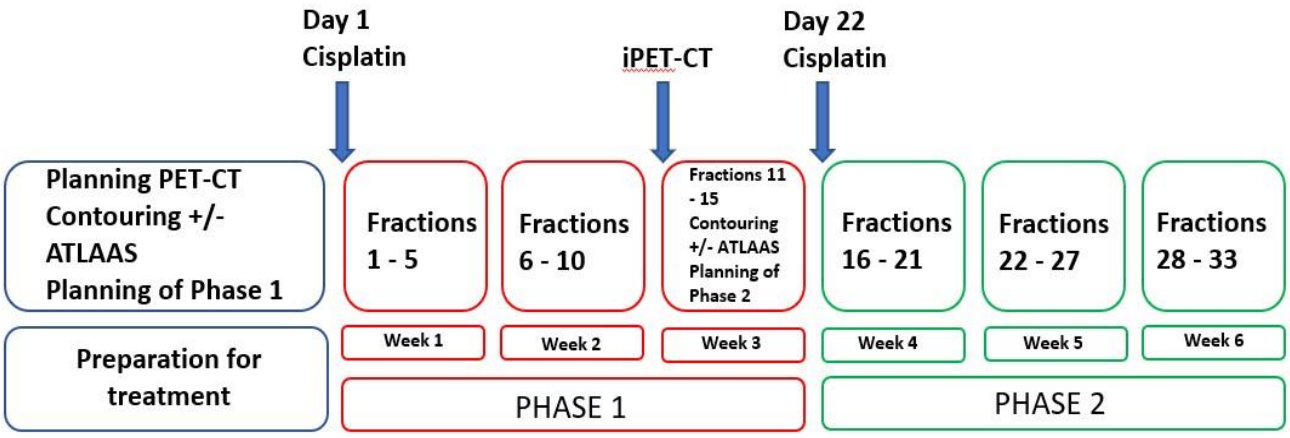

Fig. 2.1 Schema of radiotherapy treatment pathway in PEARL

The inclusion and exclusion criteria for PEARL reflects the good risk patient cohort most appropriate for de-intensification as per the survival-based risk stratification by Ang et al (4), as well as patient-specific appropriateness for radical treatment with chemoradiotherapy. Patients must have stage 1-2 disease as defined by TNM 8th edition.

2.3.1 Inclusion and exclusion criteria

Inclusion criteria

1. Histologically confirmed squamous cell carcinoma of the oropharynx
2. Positive p16 Immunohistochemistry on local testing
3. UICC TNM (8th edition) stage 1-2 (T1 – T3 N0 – N1-N2 M0)
4. Multidisciplinary team decision to treat with primary chemoradiotherapy
5. Patients considered fit for radical treatment with primary chemoradiotherapy (including sufficient renal function (GFR>50ml/min)
6. Aged 18 years or older
7. Not smoked in the last 2 years
8. Written informed consent provided
9. Patients with reproductive potential (male or female), who are sexually active during the duration of the trial consent to using a highly effective method of contraception for at least six months after the last dose of chemoradiotherapy.

Exclusion criteria

1. Known HPV negative squamous cell carcinoma of the head and neck
2. T1 – T3 tumours where primary treatment with chemoradiotherapy is not considered appropriate
3. T4 disease

4. Distant metastatic disease
5. Current smokers or smokers who have stopped within the past 2 years. Vaping is permitted and is considered as non-smoking status.
6. Any pre-existing medical condition likely to impair swallowing function and/ or a history of pre-existing swallowing dysfunction prior to index oropharyngeal cancer
7. Previous radiotherapy to the head and neck
8. History of malignancy in the last 5 years, except basal cell carcinoma of the skin, or carcinoma in situ of the cervix
9. Tumour non-avid on PET-CT or not visible on cross sectional imaging

2.4 PEARL study aims and objectives

Aim

To reduce doses to OARs implicated in late toxicity following chemoradiotherapy for HPV positive OPSCC by adapting radiotherapy treatment based on biological response seen on interim FDG-PET-CT scan carried out after 2 weeks of treatment.

Primary objective

To maintain a 2-year progression free survival rate of 90% (77 – 97% 95%CI) with biologically adapted radiotherapy in patients with good prognosis HPV positive OPSCC.

Secondary objectives:

- To demonstrate feasibility of recruitment
- To test if individualised, adaptive, biologically based radiotherapy planning is feasible and results in a significant change in the radiotherapy plan
- To maintain a complete response rate of over 88% 3 months after treatment
- To assess acute and late toxicity rates and in particular the effect of treatment on swallowing function using MD Anderson Dysphagia Inventory (MDADI) and CTCAE

toxicity scores at 1, 3-, 6-, 12- and 24-months post treatment, and feeding tube use at 1-, 3-, 6- and 12-months post treatment.

The PEARL study is designed to achieve the above aim through the re-contouring of the primary Gross Tumour Volume (GTV_P) after 2 weeks of chemoradiotherapy (Fig. 2.2), based on FDG-PET response. Re-planning with the new contours aims to reduce dose to the high dose primary PTV (PTV_P) and consequently the total dose received by significant OARs implicated in toxicity.

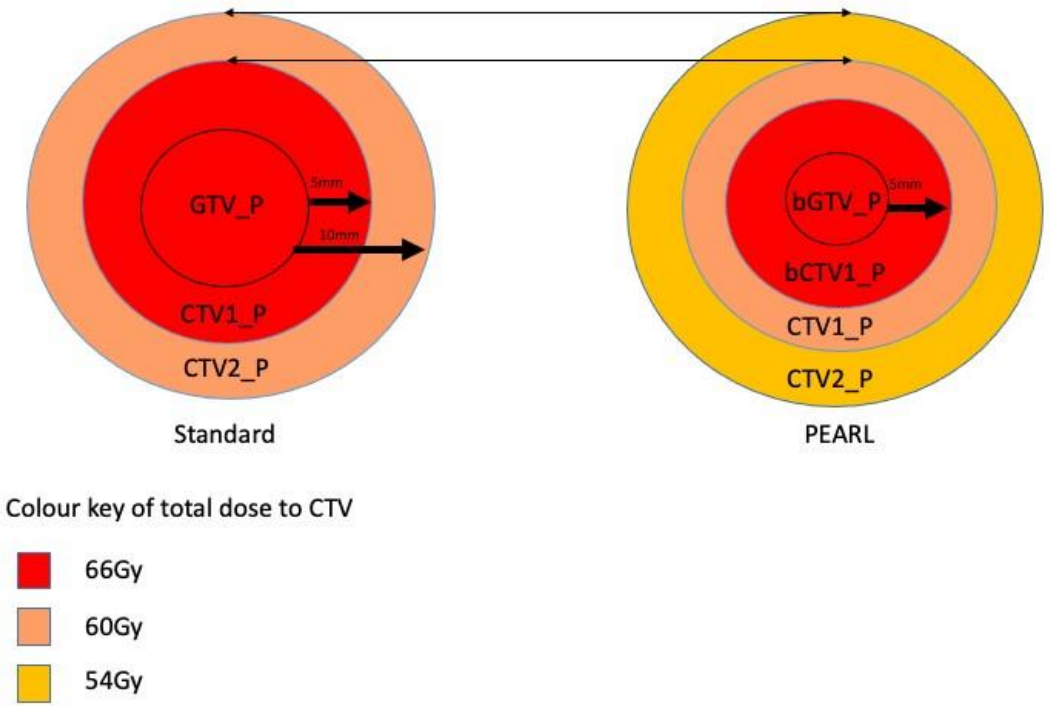

Fig. 2.2 Volume expansions based upon the Primary Gross Tumour Volume (GTV_P) in standard 5+5 expansion, and the Primary Biological Gross Tumour Volume (bGTV_P) in Phase 2 of PEARL. In the PEARL study, the total prescription dose remains the same (66Gy to the highest dose Primary Clinical Target Volume, (CTV) but the volume of tissue receiving 66Gy is reduced in Phase 2 if there is a biological response on PET-CT scan after 2 weeks of treatment. The original CTV1_P receives at least 60Gy (intermediate dose), the original CTV2_P receives at least 54Gy (prophylactic dose).

2.5 Statistical considerations

The statistical considerations for the PEARL Study are led by Dr Chris Hurt at the Centre for Trials Research at Cardiff University.

2.5.1 Sample size

To be certain that PEARL is not having a negative impact on progression free survival by adapting the radiotherapy plan, we must ensure that the progression free survival will be at least as high as expected after treatment with chemoradiotherapy in patients with similarly staged HPV-positive OPSCC. The E1308 trial (64) estimated the 2-year progression free survival to be between 95% (less than 10 pack year smoking history and lower stage than T4N2c) and 84% (non-T4a tumours) with 95% confidence in similar subgroups of patients who will be recruited to PEARL (T1 – T3, N1 (TNM8), low smoking history). If we assume that our point estimate may be as high as 90% then 44 patients would allow us to calculate confidence intervals that exclude 76% (77-97%). Comparable phase II studies have used similar assumptions. We have therefore decided to recruit 50 patients in order to allow for ~10% loss to follow up.

2.5.2 Main analysis

All patients who have an interim PET-CT (iPET_CT) are to be included in the main analysis.

2.5.2.1 Primary endpoint

Progression free survival will be calculated using Kaplan Meier estimation methods with 95% confidence intervals.

2.5.2.2 Secondary endpoints

1 To demonstrate feasibility of recruitment. Feasibility of recruitment will be demonstrated by rate of accrual, the percentage of patients screened who enter the trial, and achieving the recruitment of 50 patients within the 2-year time frame.

2 To test if individualized, adaptive, biologically based radiotherapy planning is feasible and results in a change in the radiotherapy plan. This will be demonstrated by the adaption of the radiotherapy plan based on the interim PET-CT resulting in a difference to the mean dose received by the organs at risk.

3 To maintain high complete response rates 4 months after treatment. The proportion of patients who have no residual tumour on PET-CT at 4 months as per the Hopkins response criteria will be presented.

4 To assess acute and late toxicity rates and the effect of treatment on swallowing function

Cumulative acute CTCAE toxicity score percentages during and up to 3 months after treatment will be presented. Toxicity scores will be presented at 6, 12, 18 and 24 months.
Water swallow test, MDADI and quality of life scores will be plotted over time (Fig. 2.3).

2.5.4 Trial schema

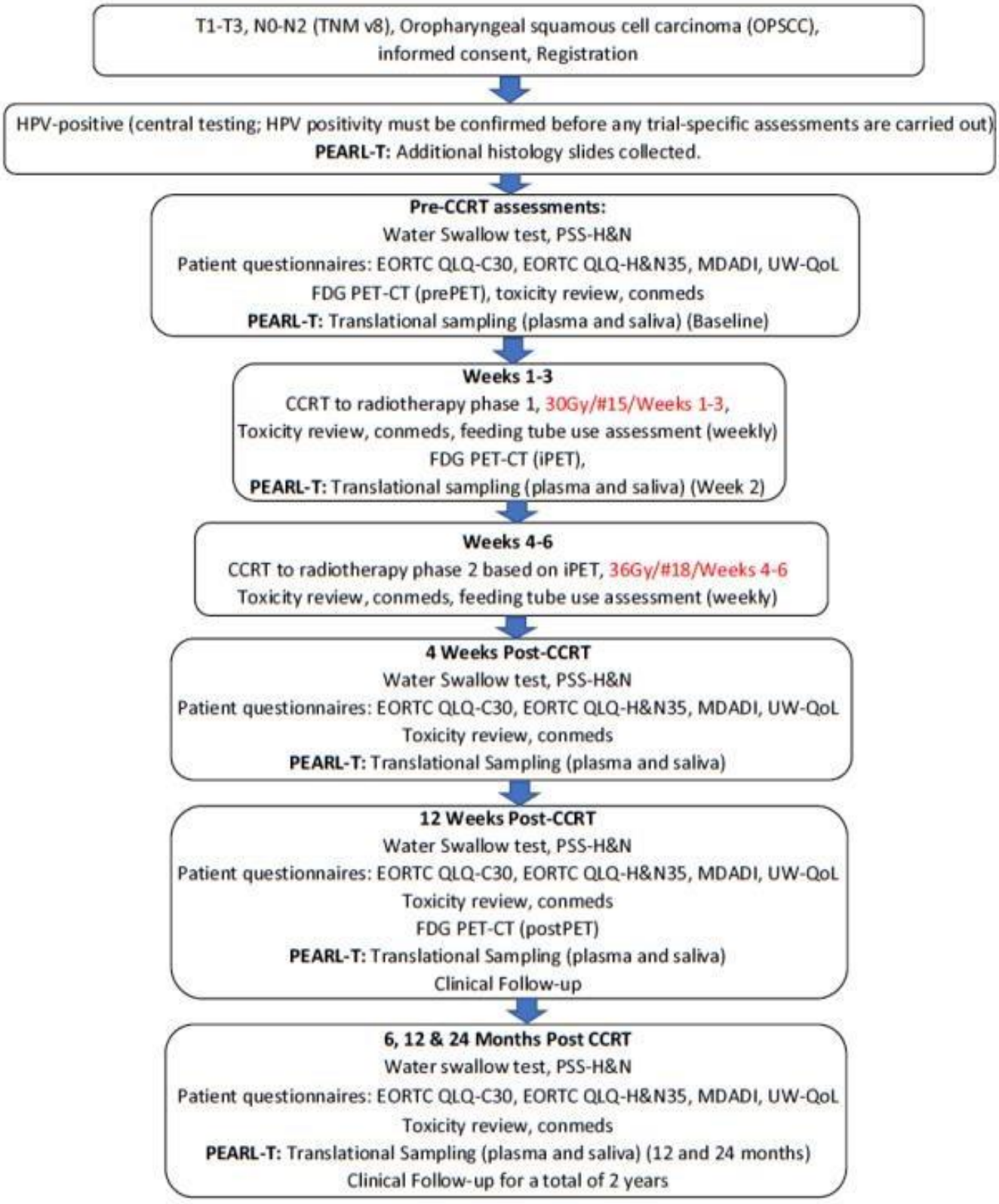

Fig. 2.3 Schema of trial including patient assessments and their time points

2.6 Trial Assessments

Whilst COVID-19 is a public health issue, the latest version of the COVID-19 PEARL recruitment policy should be followed as part of the screening and study procedures. This may include some trial visits or assessments being done remotely.

2.6.1 Baseline (pre-chemoradiotherapy) assessments

Patients should undergo the following assessments prior to chemoradiotherapy*:

1. PET-CT scan (prePET)
2. Toxicity assessment
3. Quality of life questionnaires - EORTC QLQ-C30 and EORTC QLQ-H&N35 (Appendix 4) and UW-QOL (Appendix 5)
4. A panel of swallowing assessments (Appendix 2)
5. MDADI score (MDADI questionnaire is in Appendix 3)
6. PSS-H&N
   100mL Water swallow test
7. Recording of feeding tube use
8. Clinical Review

*For centres where p16 and/or HPV testing is standard practice and the patient has been confirmed as HPV positive locally, trial specific assessments can be carried out prior to receiving confirmation of central HPV testing result.

Questionnaire-based assessments should be conducted prior to the water swallow test so that responses to questionnaires are not influenced by this procedure. The timing of assessments will be documented in the Case Report Form. All assessments can be carried out on the same day or staged, according to local resources. Speech and Language Therapists in individual centres may delegate functional assessments to appropriately trained research nurses or other members of the team. A member of the site Speech and Language Therapist team should oversee those performing study assessments to ensure temporal consistency in the results.

Baseline translational blood and saliva samples should be collected from participants who consented to take part in the PEARL-T sub study. Additional histology slides taken from the diagnostic biopsy should be sent to the All Wales Genetic Laboratory.

2.6.2 Assessments during treatment

The assessment schedule is outlined in Table 2.1. The worst grade toxicity as per CTCAE criteria v4.03 should be recorded weekly during chemoradiotherapy.

Toxicity should also be recorded 4 weeks (+/- 2 weeks), 6 months (+/- 4 weeks), 12 months (+/- 4 weeks) and 24 months (+/- 8 weeks) after the end of chemo-radiotherapy.

Recording of feeding tube to be performed weekly during chemoradiotherapy.

In addition, at two weeks into chemoradiotherapy, translational blood and saliva samples should be collected from participants who consented to take part in the PEARL-T sub-study.

PET-CT scan and disease assessment to be performed after 10 fractions of radiotherapy (at 2 two weeks into chemoradiotherapy) and the radiotherapy plan adapted based upon the remaining avid biological GTV (bGTV_iP) on the iPET.

2.6.3 Post-chemoradiotherapy assessments (4 weeks and 6, 12, and 24 months postradiotherapy)

All post-radiotherapy assessment time points should be timed from the end of chemoradiotherapy.

After 4 weeks post-treatment, visits can be conducted telephonically, and questionnaires emailed or posted where this remains in the best interest of the participant and the visit does not include statistically relevant assessments where hospital attendance is needed for them to be carried out.

4 weeks (+/- 2 weeks) post-chemoradiotherapy assessments:

As described above for pre-chemoradiotherapy assessments apart from the FDG-PET-CT scan. CTCAE toxicity should be recorded. Translational blood and saliva samples should be collected from participants who consented to take part in the PEARL-T sub-study.

12 weeks (+/- 2 weeks) post chemoradiotherapy assessments:

As described above for pre-chemoradiotherapy assessments including the post treatment PET-CT scan (postPET). The PostPET can be completed within 10 and 16 weeks. Disease assessment should also be performed. Translational blood and saliva samples should be collected from participants who consented to take part in the PEARL-T sub-study.

6 months (+/- 4 weeks) post-chemoradiotherapy assessments:

As described above for pre-chemoradiotherapy assessments apart from the FDG-PET-CT scan. CTCAE toxicity should be recorded.

12 months (+/- 4 weeks) post-chemoradiotherapy assessments:

As described above for pre-chemoradiotherapy assessments apart from the FDG-PET-CT scan. CTCAE toxicity should be recorded. Clinical review and Swallowing support summary is also required. Translational blood and saliva samples should be collected from participants who consented to take part in the PEARL-T sub-study.

24 months (+/- 8 weeks) post-chemoradiotherapy assessments:

As described above for pre-chemoradiotherapy assessments apart from the FDG-PET-CT scan. CTCAE toxicity should be recorded. Clinical review is also required. Translational blood and saliva samples should be collected from participants who consented to take part in the PEARLT sub-study.

As before, questionnaire-based assessments should be conducted prior to water swallowing testing so that responses to questionnaires are not influenced by these investigations.

Procedures	Screening	During CCRT			Post CCRT				
		Baseline	Weekly	Fraction 10	4 Weeks	12 weeks	6 months	12 months	24 months
Informed consent	x								
Demographics	x								
Medical History	x								
Eligibility Assessment	x								
Pregnancy test*	x								
Central HPV testing		x							
FDG PET-CT		x		x		X***			
MDADI Score		x			x	x	X	x	x
PSS- H&N		x			x	x	X	x	x

Procedures	Screening	During CCRT			Post CCRT				
		Baseline	Weekly	Fraction 10	4 Weeks	12 weeks	6 months	12 months	24 months
Water Swallow test		x			x	x	X	x	x
Feeding tube use		x	x		x	x	X	x	x
Swallowing support summary								x	
QoL (EORTC QLQ-C30, EORTC H&N35 and UW-QOL)		x			x	x	X	x	x
CTCAE Toxicity (v 4.03)		x	x		x	x	X	x	x
Clinical review		x	x		x	x	X	x	x
Disease assessment	x			x		x			

Procedures	Screening	During CCRT			Post CCRT				
		Baseline	Weekly	Fraction 10	4 Weeks	12 weeks	6 months	12 months	24 months
Translational Blood Sampling		x		x	x	x		x	x
Translational Saliva sampling		x		x	x	x		x	x
Histology slides from the diagnostic biopsy		X**							

Table 2.1 PEARL schedule of assessments

*As applicable

** Histology slides should be cut for PEARL-T at the same time as cutting the slides for the HPV centralised test provided the participant has consented to tissue collection.

***PostPET scan can be completed within 10 to 16 weeks post treatment.

2.7 Chemotherapy

All patients must have sufficient renal function (GFR>50ml/min) to receive concurrent chemotherapy with the radiotherapy. If Cisplatin is not appropriate, carboplatin may be substituted.

Chemotherapy will be administered according to local practice in each centre. Precise scheduling and dose reductions are at the discretion of the treating oncologist.

Whilst COVID-19 is a public health issue, the latest version of the COVID-19 PEARL recruitment policy should be followed as part of the screening and study procedures.

2.7.1 Scheduling

Cisplatin is delivered as per local practice in each centre, according to the following recommended schedule: Cisplatin 100 mg/m^2 administered intravenously on day 1 for 2 cycles, that is day 1 (day 1 of cycle 1) and day 22 (day 1 of cycle 2) of the radiotherapy schedule (Fig. 2.1). Cisplatin given within 24hrs of the required day for cycle 1 and within 48hrs for cycle 2 is acceptable.

On the day of chemotherapy, Cisplatin should, whenever possible, be administered prior to radiotherapy.

In the event of Cisplatin substitution by Carboplatin, Carboplatin is delivered as per local practice in each centre, using AUC5 to calculate dose.

2.8 Safety reporting

The Principal Investigator is responsible for ensuring that all site staff involved in this trial are familiar with the content of this section.

All SAEs must be reported immediately (and within 24 hours of knowledge of the event) by the PI at the participating site to the CTR PV and safety specialist or Trial team unless the SAE is specified as not requiring immediate reporting.

The Principal Investigator (or another delegated medically qualified doctor from the trial team) will assess each SAE to determine the causal relationship and the Chief Investigator (or another appropriately qualified member of the Trial Management Group) can also provide this assessment where necessary

The Chief Investigator (or another delegated appropriately qualified individual) will assess each SAE to perform the assessment of expectedness.

2.8.1 Termination of the trial

To alleviate concern that we are having a detrimental impact on treatment efficacy, we will have an early stopping rule based on complete response at the primary site at 4 months following treatment (defined as having no disease at the 4-month PET and no disease on any subsequent biopsy). A recent study (63) found that 43/44 (98%, 95% CIs: 88%-100%) of patients had complete response. This correlated with excellent outcomes at 2 years with local control, regional control, cancer specific survival, distant metastasis free survival and overall survival rates at 100%, 100%, 100%, 100% and 95% respectively. Any accumulated data will be reviewed regularly at Interim Data Monitoring Committee meetings. When presenting data to the Interim Data Monitoring Committee we will generate 95% confidence intervals around our estimate of 4-month complete response rate and ensure that they include 88%.
We will conduct an interim analysis after 15 patients complete 3 months of follow-up and are assessed for complete response and the IDMC will have the mandate to stop the trial for harm if we see less than 10 complete responders.

2.9 Follow-up

Clinical follow up after treatment (for disease recurrence/death) should be carried out as per routine practice for at least 5 years in accordance with National guidelines (NICE IOG guidance 2004). Specifically, patients should undergo regular full examination of the head and neck

according to the following schedule: year 1 – every 4 – 6 weeks; year 2 – every 8 – 10 weeks; year 3 – every 3 - 5 months; years 4 and 5 – approximately every 6 months. The patient will be followed up by the trial team for the first 2 years after treatment. Patient status will be collected at the end of the trial in order to obtain up to date progression free survival data. Translational blood and saliva samples should be collected from participants who consented to take part in the PEARL-T sub-study as per Section 14.5 Trial assessment table.

2.10 Ethical approval

Ethical approval was sought from the Wales Research Ethics Committee (REC) in November 2018 and PEARL was assigned a REC registration reference: 18/WA/0391.

2.11 Informed consent

The participant's written informed consent must be obtained using the PEARL trial Consent Form, which follows the Participant Information Sheet. The participant should be given at least 24 hours after the initial invitation to participate before being asked to sign the Consent Form. Informed consent must be obtained prior to the participant undergoing procedures that are specifically for the purposes of the trial.

2.12 The PEARL radiotherapy guidance

The development of the radiotherapy protocol for PEARL considered international consensus guidelines on the contouring of the primary and nodal clinical target volumes (CTVs) in OPSCC and trial protocols including the PATHOS swallowing atlas previously developed by the team at Velindre University NHS Trust (Appendix 3). The radiotherapy guidance was designed to be applicable to multiple cancer centres outside of Velindre, including centres in London, Bristol and Glasgow. The full version is in Appendix 2.

I led on specific pieces of work performed to inform the development of the radiotherapy guidance. These included an RTTQA workshop and the pilot study for PEARL. The pilot study is described in Chapter 3.

2.12.1 Planning PET-CT scan protocol for PEARL

Patients have baseline and interim planning PET-CT scans performed in a head and neck immobilisation shell and treatment position. Patients are immobilised in a thermoplastic shell with their neck in a neutral position. No mouth bite is used. The planning PET-CT scans are performed in the shell and reconstructed at appropriate thickness (2 to 3 mm). Use of intravenous contrast is recommended in order to facilitate accurate delineation. The PET-CT scan includes both shoulders and extends from vertex to liver as a minimum. Follow up PETCT scan (postPET) is carried out as per standard protocol.

2.12.2 CT Quality Assurance (QA)

A quality assurance program is in place to assess the quality of the CT data (including geometry, image quality and electron density). The CT component of the PET-CT scanner is subject to the same rigorous testing as a conventional radiotherapy-dedicated CT simulation machine. The daily QC is performed weekly (on account of reduced throughput of patients) but must be carried out on the day of scanning a patient in the radiotherapy treatment position.

2.12.3 Planning PET-CT process QA

The input of all patient data and scanning parameters is the responsibility of the PET-CT staff. On a quarterly basis a quality assurance check is commissioned by a member of medical physics from the treating centre, and it is the responsibility of medical physics at the treating centre to liaise with the PET-CT centre to ensure suitable access to the scanner.

2.12.4 Determining the optimal timing of the interim PET (iPET)

It is crucial for accurate adaptive radiotherapy planning that interim imaging is performed at the optimal time. The timing of the iPET scan is based both on the predictive nature of the scan at this time point, and to minimise the impact of radiation-induced inflammation on PET image interpretation.

As covered in detail in Chapter 1, a variety of different research groups have found background inflammation to be significant only after three weeks of radiotherapy and others have found the 2-week time point a favourable time to re-contour the GTV due to low levels of radiation-induced inflammation at that point (77). Based on this data, 2 weeks was selected as the optimal time point for the iPET in the PEARL protocol, after the high dose primary CTV has received 18Gy. This allows a week within which to turn around the phase 2 plan, before starting phase 2 treatment in week 4.

2.12.5 Planning PET-CT data acquisition and transfer to Velindre for contouring

For patients recruited at Velindre Cancer Centre the planning PET-CT scans are performed at The Positron Emission Tomography Imaging Centre (PETIC) at Cardiff University. The patients are set-up in the radiotherapy treatment position on a flat top couch with full immobilisation for both PET and CT scans. To get the most accurate alignment between PET and CT data, the planning CT scan is acquired directly after the PET scan using an integrated PET-CT scanner.

Once the PET-CT data is acquired it is transferred to the Prosoma Treatment Planning System at Velindre by a direct DICOM link. This is then transferred to Velocity by a direct DICOM link and the biological primary GTV (bGTV_P) delineated on the PET scan. The dataset is then transferred back to Prosoma by direct DICOM link for completion of contouring (Fig 4).

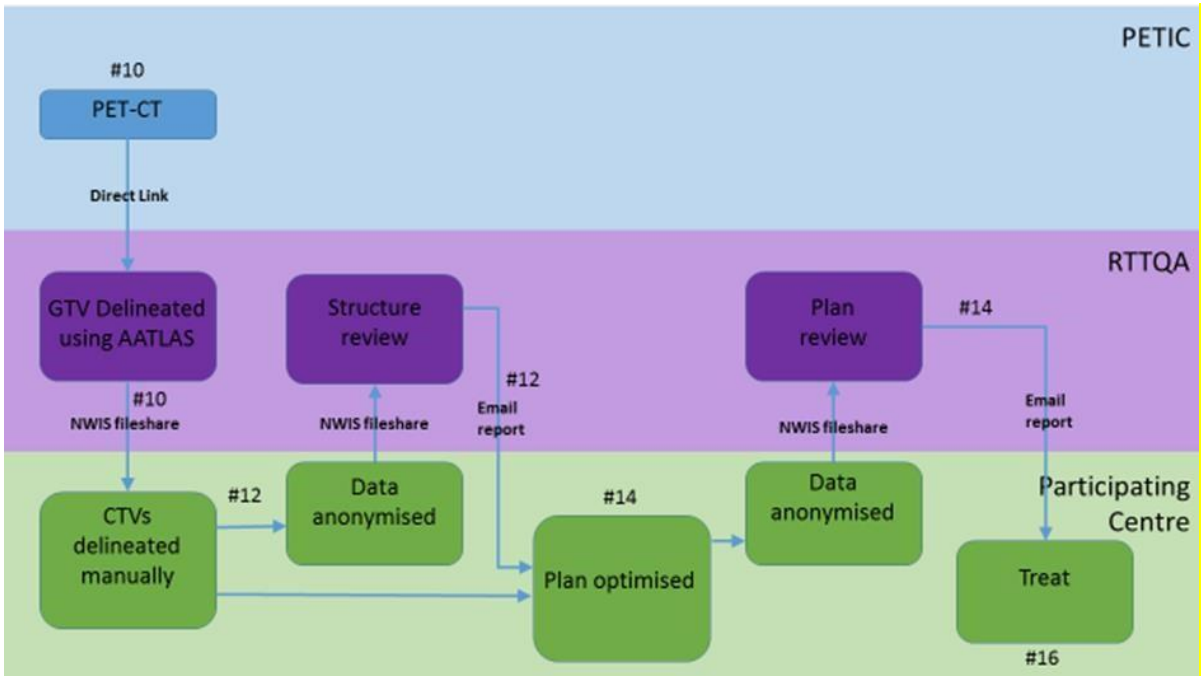

Fig 2.4 Pathway of datasets of a patient in the PEARL Study at Velindre Cancer Centre

2.12.6 Primary Tumour Categorisation

Prior to target volume delineation, the primary tumour is categorised as lateralised or nonlateralised, based on the site of primary and the extent of involvement of midline structures. The recommendation is that this categorization be based on clinical examination findings including flexible nasendoscopy and pandendoscopy under anaesthetic, and imaging including CT and MRI. For ease of comparison with outcomes from suitable studies, the definitions are in line with those of other appropriate head and neck studies including PATHOS (NCT02215265), NIMRAD (NCT01950689), and CompARE (NCT04116047).

Definition of a lateralised tumour

Tumour confined to the tonsillar fossa/lateral pharyngeal wall extending onto or into the adjacent base of tongue and/or soft palate by <1 cm and with >1cm clearance from midline

Definition of a non-lateralised tumour

Tonsillar/lateral pharyngeal wall tumour that involves the adjacent base of tongue and/or soft palate by ≥1 cm or with ≤1cm clearance from midline

OR

A tumour that arises from a midline structure (base of tongue, soft palate or posterior pharyngeal wall primary tumour)

2.12.7 Treatment of the neck

All patients with lateralised tumours receive unilateral neck radiotherapy, regardless of the nodal stage of the ipsilateral neck, and all patients with non-lateralised tumours undergo bilateral neck radiotherapy.

2.12.8 Definition of Treatment Volumes

To maintain the highest clinical standards, outlining of the target volumes is carried out using a geometric approach as per the current international consensus guidelines. Diagnostic imaging, clinical findings including pan-endoscopy reports, and pathology information are to be used to delineate target volumes. To maximise accuracy, the diagnostic CT and MRI scans can be co-registered with the planning PET-CT scan (prePET).

So that adaption of the primary GTV can be based upon response to treatment on iPET, radiotherapy is prescribed in 2 phases.

Phase 1 includes #1 – 15 (week 1 to 3 of treatment) and is prescribed prior to the start of treatment. Phase 2 includes #16 – 33 and is prescribed after the radiotherapy plan has been adapted based on the iPET.

The nodal volume is not adapted based on biological tumour activity seen on iPET. However, the nodal volumes can be transferred across from prePET to iPET and edited, when required, for anatomical change, or re-outlined de novo on the CT component of iPET without reference to avidity.

2.13 Guidelines for target volume and organ at risk delineation

2.13.1 Nomenclature and definition of targets and avoidance structures

Standardization of the nomenclature for target volumes, and organs at risk ensures accurate dose reporting and structure definition between treatment centres, and practitioners within the same centre. It also allows for clear bilateral communication within the RTTQA review process.

bGTV_preP	Clinician defined biological primary GTV in Phase 1
GTV_P	Gross Primary Tumour Volume
CTV1_P	GTV_P + 5mm
CTV2_P	GTV_P + 10mm
bGTV_iP	Biological primary GTV in Phase 2
bCTV1_P	bGTV_iP + 5mm
GTV_N	Gross Nodal Tumour Volume

CTV1_N	GTV_N + 5mm
CTV2_N	GTV_N + 10mm
CTV3_N	Prophylactic Nodal Volume
SpinalCord	Spinal Cord
BrainStem	Brainstem
Parotid_IL	Ipsilateral Parotid Gland
Parotid_CL	Contralateral Parotid Gland
submandibular gland_CL	Contralateral Submandibular Gland
PCM_Superior	Superior Pharyngeal Constrictor Muscle
PCM_Middle	Middle Pharyngeal Constrictor Muscle
PCM_Inferior	Inferior Pharyngeal Constrictor Muscle
Cricopharynx	Cricopharyngeus Muscle
Oeso_Inlet	Oesophageal Inlet
Cervical_Oeso	Cervical Oesophagus
Larynx_SG	Supraglottic Larynx

Larynx_G	Glottic Larynx
Oral_Cavity	Oral Cavity

Table 2.2 Nomenclature of target volumes and organs at risks for the PEARL clinical trial

2.13.2 Primary target volume delineation

2.13.2.1 First Phase

Primary biological Gross Tumour Volume (bGTV_preP) (Orange)

It is the FDG uptake on the PET component of the prePET-CT that directs the drawing of the bGTV_preP, rather than any abnormality seen on the CT component. The definition of the avid volume is performed by a nuclear medicine consultant in collaboration with the clinical oncologist. The nuclear medicine consultants contributing to PEARL have been accredited by the RTTQA(UK) PET QA group based at Guys and St Thomas's Hospital NHS Foundation Trust to ensure standardised definition of the avid volumes.

The bGTV_preP does not include areas of soft tissue/tumour on CT that have low grade FDG uptake or areas not FDG avid. The bGTV_preP may include areas which do not contain tumour e.g., the airway, because of scatter. This is adjusted by the clinical oncologist or nuclear medicine consultant in the radiotherapy treatment planning system and the volume edited out of bone (unless involved) and/or air (Fig. 2.5).

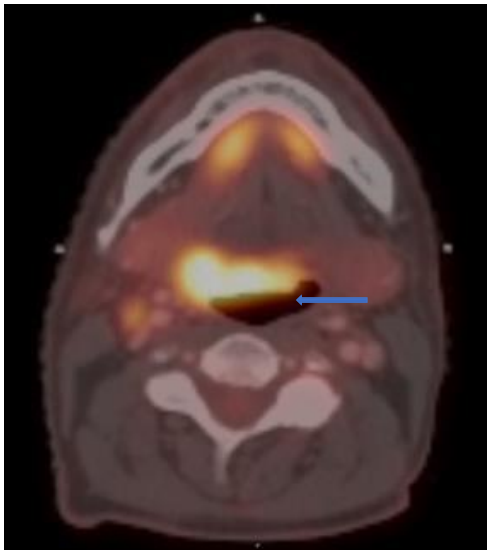

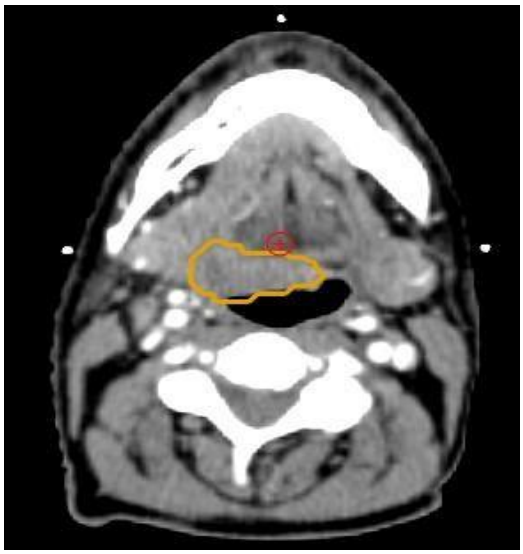

2.5a 2.5b

Fig. 2.5a and 2.5b Cross sectional imaging of the phase 1 planning PET-CT. Avid area contoured as bGTV_preP is marked by the blue arrow in Fig. 5a. bGTV_preP is seen in orange in Fig. 5b

Primary Gross Tumour Volume (GTV_P) (Red)

This volume includes the primary tumour. It is delineated taking into consideration all the information available from the diagnostic CT (and MRI if available) as well as the bGTV_preP generated from the prePET scan, and findings from clinical examination including the panendoscopy report (Fig. 2.6).

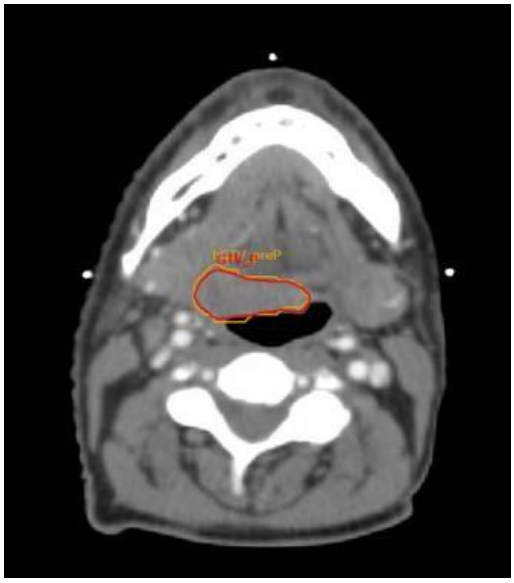

Fig. 2.6 Cross sectional imaging of the phase 1 planning CT. bGTV_preP contoured in orange, final GTV_P in red

Primary Clinical Target Volume 1 (CTV1_P) (Green)

This volume includes the primary tumour (GTV_P) with an isotropic margin of 5mm, edited for anatomical barriers e.g. air, fascia and bone. The editing for platysma is permissible. The CTV margin allows for potential microscopic spread around the primary tumour (Fig.2.7).

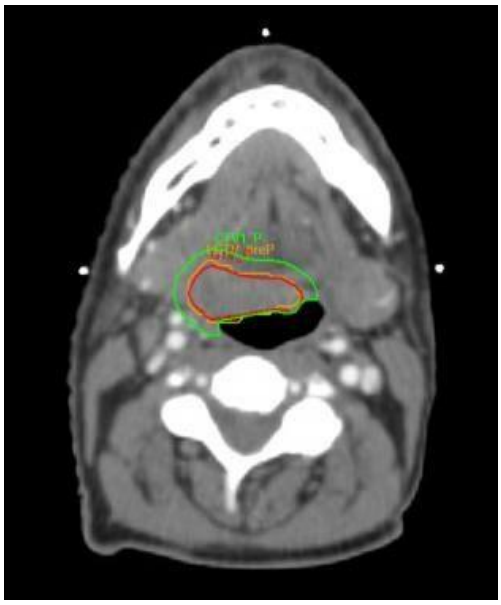

Fig. 2.7 Cross sectional imaging of the phase 1 planning CT. bGTV_preP contoured in orange, final GTV_P in red and CTV1_P in green.

Primary Clinical Target Volume 2 (CTV2_P) (Pink)

This volume includes the primary tumour (GTV_P) with an isotropic margin of 1cm, edited as above (Fig. 2.8).

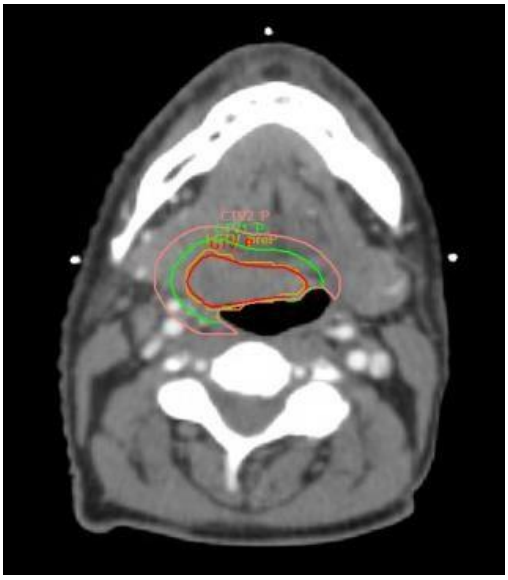

Fig. 2.8 Cross sectional imaging of the phase 1 planning CT. bGTV_preP contoured in orange, final GTV_P in red, CTV1_P in green, and CTV2_P in pink

2.13.2.2 Second Phase

Phase 2 is to be commenced at fraction 16 but is outlined & planned on an interim planning PET-CT scan which is carried out after fraction 10 of radiotherapy. Phase 1 treatment continues during fractions 11-15 as the phase 2 is outlined and planned.

Primary biological Gross Tumour Volume (bGTV_iP) (Blue)

Defining the bGTV_iP: The region of the GTV_P that remains avid on PET-CT after fraction 10 of radiotherapy (Fig. 2.9a and 2.9b). If there is a complete metabolic response at this time point, no bGTV_iP is created. If there is clinical concern about any residual avidity, the decision to include a bGTV_iP defined by the nuclear medicine consultant and the clinical oncologist is made at the treating clinician's discretion.

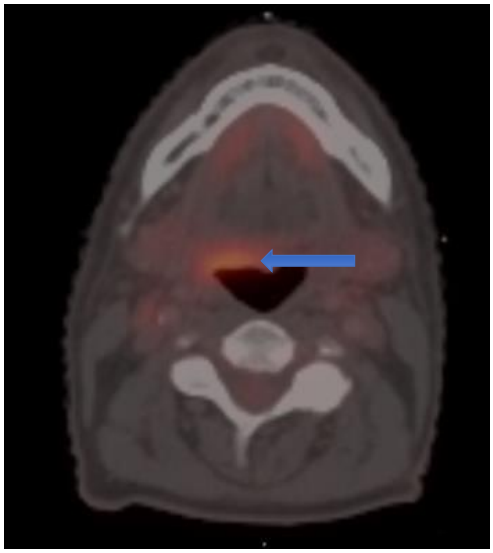

2.9a

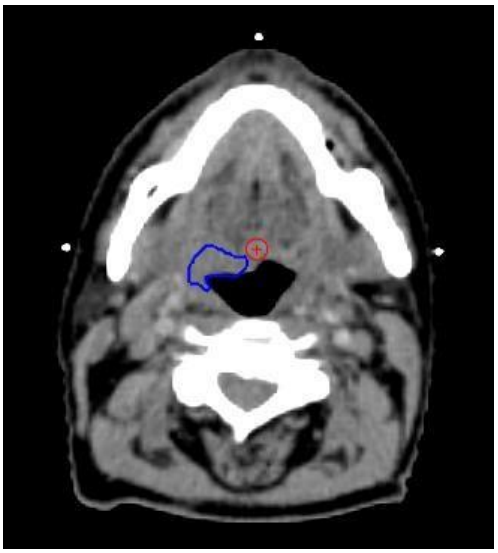

2.9b

Fig. 2.9a and 2.9b Cross sectional imaging of the phase 2 planning PET-CT. Remaining avid area contoured as bGTV_iP marked by the blue arrow on the PET component and contoured in blue on the CT component.

Primary biological Clinical Target Volume (bCTV1_P) (Green)

This volume includes the bGTV_iP with an isotropic margin of 5mm edited for anatomical barriers (Fig. 2.10).

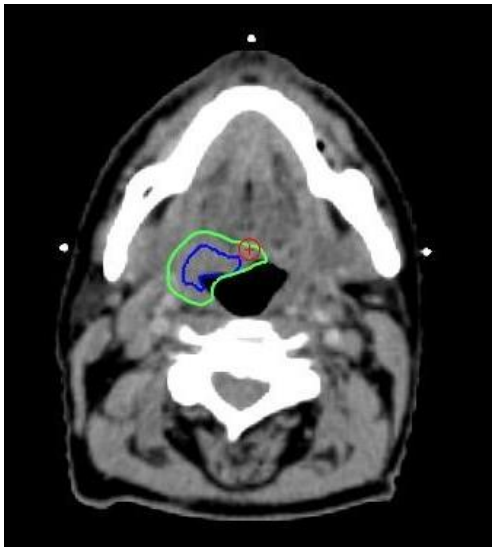

Fig. 2.10 Cross sectional imaging of the phase 2 planning CT. bGTV_iP contoured in blue, bCTV1_P in green

Primary Clinical Target Volume 1 (CTV1_P) (pink) and Primary Clinical Target Volume 2 (CTV2_P) (light blue)

Volumes are defined as per phase one. To mitigate for the mismatch of CTV_P volumes between the prePET and iPET, the phase one GTV_P can be rigidly registered with the iPET. The geometric expansion by 5mm and 10mm in all directions to form CTV1_P and CTV2_P respectively can then be performed again. CTV1_P and CTV2_P can then be edited for anatomical barriers as previously described (Fig. 2.11).

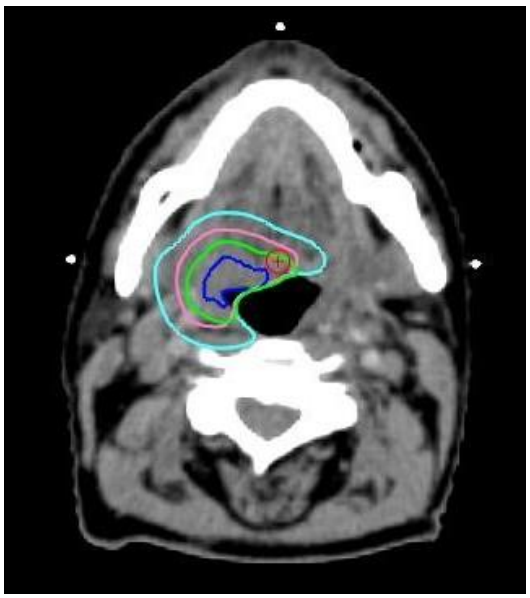

Fig. 2.11 Cross sectional imaging of the phase 2 planning CT. bGTV_iP contoured in blue, bCTV1_P in green, CTV1_P in pink and CTV2_P in light blue

2.13.3 Nodal target volume delineation

The nodal volumes are either transferred from the Phase 1 scan (prePET_CT) to the Phase 2 scan (iPET_CT) and edited, or they are re-contoured on the CT component of the iPET_CT for anatomical volume changes. They are not adapted based upon any biological response seen on the iPET_CT. The definitions and nomenclature of all the nodal target volumes remain the same.

Nodal Gross Tumour Volume (GTV_N) (red)

This volume includes the pathologically involved nodes. It is delineated taking into consideration all the information available from the diagnostic CT (and MRI if available), USS and FNA/core biopsy, as well as the prePET_CT scan and findings from clinical examination (Fig. 2.12).

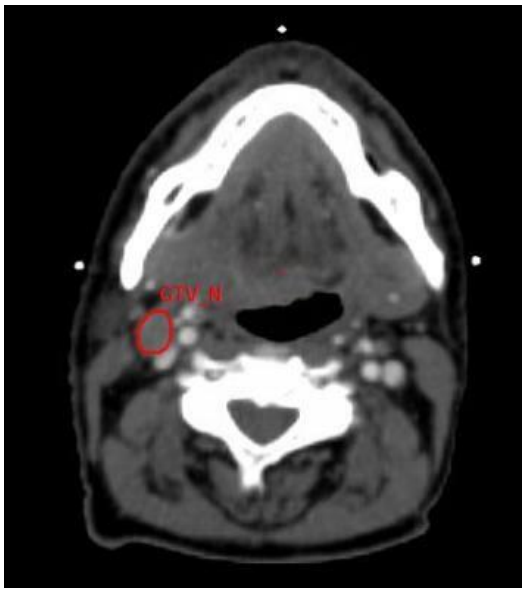

Fig. 2.12 Cross sectional imaging of the phase 1 planning CT. GTV_N contoured in red

Nodal Clinical Target Volume (CTV1_N) (green)

This volume includes the GTV_N with a 5mm margin in all directions edited for anatomical barriers as detailed above. The CTV margin allows for potential microscopic spread around the involved nodes (Fig. 2.13).

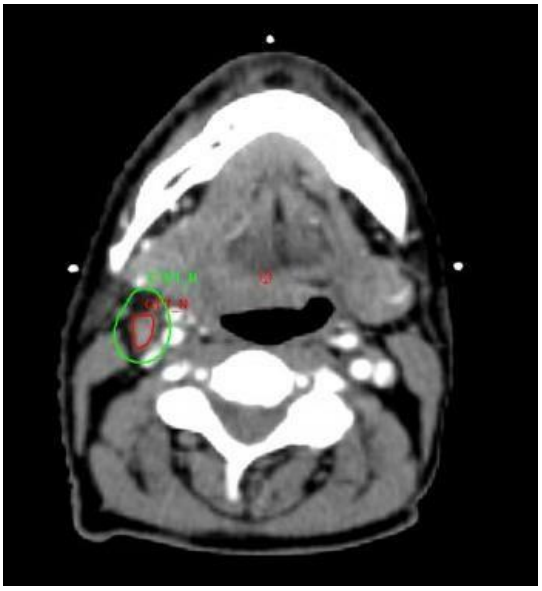

Fig. 2.13 Cross sectional imaging of the phase 1 planning CT. GTV_N contoured in red, CTV1_N in green

Nodal Clinical Target Volume (CTV2_N)

This volume includes the GTV_N with a 10mm margin in all directions edited for anatomical barriers (Fig. 2.14).

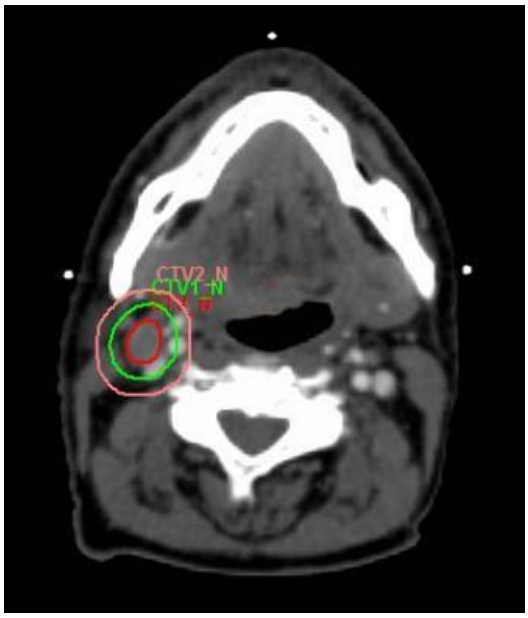

Fig. 12.4 Cross sectional imaging of the phase 1 planning CT. GTV_N contoured in red, CTV1_N in green, CTV2_N in pink

Prophylactic Nodal Clinical Target Volume (CTV3_N) (light blue)

This volume includes the rest of the involved nodal level(s) and all at risk non-pathological nodal levels appropriate for prophylactic irradiation as defined by the updated consensus guidelines and atlas (Table 4). The contours for CTV3_N include the entire level regardless of any overlap with CTV1_N or CTV2_N (Fig. 2.15).

	Nodal status	CTV3_N
Lateralised tumour	Node negative	Ipsilateral (1b)[2], II, III, IVa[3] + VIIa*
	Node positive	Uninvolved ipsilateral 1b, II, III, IVa, Va+b Ipsilateral VIIa at the level of the oropharynx Ipsilateral VIIb (when II involved) Ipsilateral IVb+Vc (when IVa or V is involved)
Non-lateralised tumour	Node negative	Ipsilateral II, III, IVa, IIVa 1b[2] Contralateral II, III, IVa, VIIa
	Node positive	Uninvolved ipsilateral Ib, II, III, IVa, Va+b Ipsilateral IIVa at the level of the oropharynx Ipsilateral VIIb (when II involved) Ipsilateral IVb +Vc (when IV or V is involved) Contralateral II, III, IVa Contralateral VIIa at the level of the oropharynx

Table 2.3 Levels for prophylactic nodal irradiation according to lateralisation of tumour, and pathological nodal involvement

*In PEARL, the recommendation is that the cranial border of the retropharyngeal nodal level (level VIIa) be defined as the upper edge of the body of C1 or the upper extent of the hard palate, whichever was more cranial. This is in line with other UK contemporaneous head and neck clinical trials including the PATHOS and NIMRAD studies.

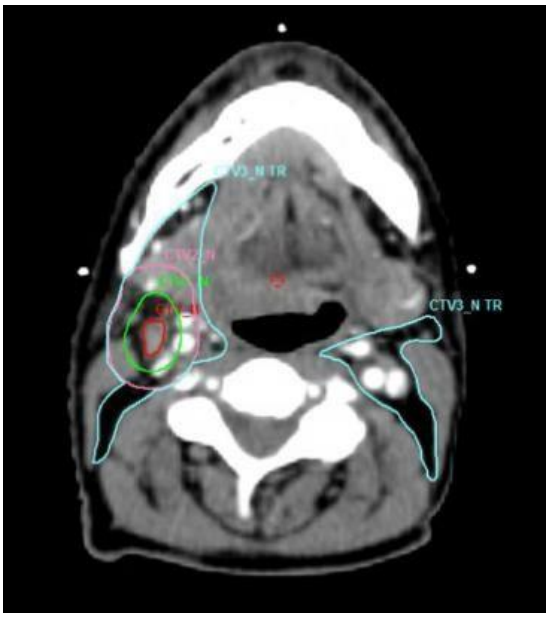

Fig. 2.15 Cross sectional imaging of the phase 1 planning CT. GTV_N contoured in red, CTV1_N in green, CTV2_N in pink, and bilateral CTV3_N in light blue

2.13.4 Contouring of OARs and SWOARs

OARs are outlined on prePET_CT and can be transferred by deformable fusion methods onto iPET_CT for Phase 2 planning. They can then be modified on iPET_CT by the consultant clinical oncologist as appropriate. Alternatively, the OARS for phase 2 can be outlined de novo on the iPET_CT if this is felt to be a more accurate method of maintaining consistency between the 2 phases.

The following normal tissue structures should be delineated as per Table 2.4.

Spinal Cord

The spinal cord (not the spinal canal) from the lower border of foramen magnum to 2.5 cm inferior to PTV is included. Isotropic expansion of 3-5mm (depending on local practice and immobilisation) to create the PRV. Please contact the RTTQA team if your centre wishes to create a PRV volume outside of 3-5mm.
Brainstem
The entire brainstem up to the lower border of foramen magnum is included. Isotropic expansion of 35mm (depending on local practice and immobilisation) to create the PRV. Please contact RTTQA team if your centre wishes to create a PRV volume outside of 3-5mm.
Parotid Glands (ipsilateral and contralateral)
Both superficial and deep lobes should be included. When blood vessels (external carotid artery and retromandibular vein) are encased by the gland, these should be included. If there is an accessory lobe to the parotid, this should be included in the volume. Outline the visible parotid glands with reference to the diagnostic MRI if available.
Submandibular Glands (ipsilateral and contralateral)
The submandibular glands should be included bilaterally with reference to the diagnostic MRI if available.
Swallowing-related Structures
The swallowing-related structures (SWOARS) are outlined for every patient according to published guidelines and the PATHOS atlas for contouring swallowing related structures. These structures include the pharyngeal constrictor muscles (superior PCM, middle PCM and inferior PCM), supraglottic/glottic larynx, cricopharyngeus, oesophageal inlet, cervical oesophagus and oral cavity. The superior and middle pharyngeal constrictor muscles will often be in the treated volume but the other SWOARs can all be used for treatment plan optimisation.

Table 2.4 Normal Tissue Structures for delineation in PEARL

Comprehensive guidelines for outlining the swallowing-related structures in PEARL are included in Appendix 3.

The dose constraints for OARs and their planning OAR volume (PRV) are given in Table 2.5. No constraint is given for the ipsilateral parotid gland as it often overlaps or abuts the PTV; this should be kept as low as possible but not at the expense of PTV coverage.

All doses to critical OARs must be within tolerance for both phases, as though each phase is being planned for the entire 33 fractions.

Structure	**Volume Constraint**	**Optimal Dose Constraint**
Spinal cord	Max	<48Gy*
	$1cm^3$	<46Gy*
Spinal cord PRV	$1cm^3$	<48Gy*
Brain stem	Max	<55Gy*
	$1cm^3$	<54Gy*
Brain stem PRV	$1cm^3$	<55Gy*
Contralateral Parotid (Lateralised Tumour)	Mean	<14Gy
Contralateral Parotid (Non-lateralised Tumour)	Mean	<24Gy
Ipsilateral Parotid	Mean	ALARP

Contralateral Submandibular Gland	Mean	<35Gy
Supraglottic Larynx	Mean	<55Gy
Glottic Larynx	Mean	<45Gy
Superior Pharyngeal Constrictor Muscles	Mean	<50Gy
Middle Pharyngeal Constrictor Muscles	Mean	<50Gy
Inferior Pharyngeal Constrictor Muscles	Mean	<20Gy
Cricopharyngeus/oesophageal inlet	Mean	<20Gy
Cervical oesophagus	Mean	<20Gy
Oral Cavity (low priority for optimisation)	Mean	<30Gy

*Mandatory dose constraint

Table 2.5 Dose constraints for OARs and PRVs

2.14 RTTQA workshop

To mitigate for variables other than the study intervention, and to ensure compliance with the PEARL Radiotherapy Trials Quality Assurance (RTTQA) process, I designed and led a multicentre RTTQA workshop. All clinical and planning staff involved in the set-up of PEARL at their centre were invited. The aim of this workshop was to familiarise participating clinicians and planners with the PEARL contouring and planning methods, to review submitted

benchmark cases, and discuss feedback and points of contention in order to reach a consensus.

It is widely accepted that radiotherapy protocol compliance plays a crucial role in the outcome of clinical studies. Studies, including head and neck trials, have demonstrated that noncompliance to trial protocols can lead to a significant reduction in tumour control and survival (118). Consensus building for contouring is a critical step in assuring the highest possible trial RTTQA, safeguarding the subsequent relevance and objectivity of trial results.

Prior to opening PEARL at a participating centre, a programme of pre-trial quality assurance must be completed, and centres must achieve VMAT credentialing from the PEARL RTTQA group in order to enter patients into the PEARL trial. Attendance at the RTTQA workshop was accepted as adequate pre-trial QA for clinical attendees.

Attending clinical oncologists, planners, and physicists were sent the draft PEARL radiotherapy guidance document. This was used to contour and plan the benchmark cases I provided. All attendees were encouraged to submit the benchmark cases prior to the workshop. The final contours and plans were reviewed anonymously at the workshop collaboratively by all the attendees. The outcomes of subsequent discussions assisted in honing the contouring and planning guidance to ensure it was robust, clear to follow, and reflected a consensus of the multiple practices of the attendees.

2.15 Pre-Accrual Target Delineation Benchmark Case

The local Principal Investigator (PI) at participating centres is required to complete the target delineation benchmark case and to be involved in completion of all on-trial cases by any noncredentialed clinicians at their centres.

The aim of outlining the benchmark cases is to ensure consistency of outlining across study centres.

Primary and nodal GTVs are contoured by the PEARL RTTQA team based on pre_PET-CT and iPET-CT from the PEARL pilot study cases and sent to the Principal Investigator (PI) being accredited.

As the benchmark cases were chosen from prePET_CT and iPET_CT data sets transferred from another treatment centre, and the GTVs predefined, only basic clinical and radiological information was provided alongside them.

2.15.1 Analysis of the submitted contours

All structures delineated and submitted were transferred onto the same scan so conformality and comparison between different practitioners could be assessed (Fig. 2.16). Though anonymised, each practitioner was informed of the colour of their contours so they could see how they related to others. The datasets were scrolled through in the axial, sagittal and coronal plains so that the extent of each volume could be assessed, comparisons made, and deviations discussed. Whilst the volumes were scrolled through, analysis of the contours took the form of a verbal discussion regarding any deviations. For all submitted CTVs, there was clinical consensus that they were passable with only minor deviations from the RTTQA team contours.

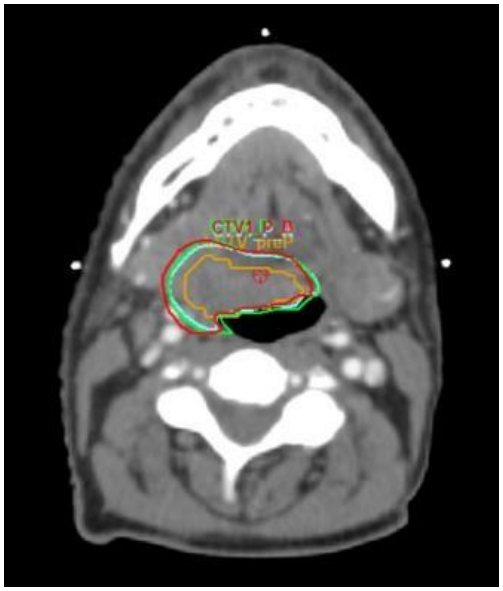

Fig. 2.16 Example of submitted CTV1_P contours from 2 PI's using the RTTQA group defined GTV_P. Red contour = RTTQA team, green and blue contours = PIs.

Issues discussed and alterations made to the radiotherapy guidance document as a result of the RTTQA day:

Contouring issues
- Clarification of CTV3_N structure: Where the same nodal level has sections in CTV1_N and CTV2_N; CTV3_N will be one structure, encompassing the entire nodal level rather than divided up into sections abutting parts of the level already included in higher dose CTVs. - Trimming of the platysma is permissible - Nodes can be re-outlined on iPET-CT de novo for phase 2, if the transfer of phase 1 structures onto the iPET-CT does not result in acceptable contours.
RTTQA issues
- Confirmation that PEARL QA will require submission of the phase 1 and phase 2 outlines for the first patient per clinician for real time RTTQA - Confirmation that GTV_N will be provided for future benchmark cases

Radiotherapy guidance content issues
- Addition of screenshots displaying the nodal contouring process - Improve phrasing so it is clear the nodal GTVs are not to be adapted based upon biological response on iPET.

Table 2.6 Consensus alterations to radiotherapy guidance as a result of RTTQA workshop discussions

2.16 Development of the PEARL planning protocol

During the set-up of the PEARL study and recruiting the initial patients during the COVID pandemic, the PEARL planning protocol evolved to make it easier for physics departments across different sites to implement. The initial adaptive radiotherapy method, 'ADAPTIVE', is described in this chapter. This was used for the PEARL pilot study and for planning the first 6 patients recruited to PEARL. In later chapters this initial planning solution developed for the Pilot Study and used for the first 6 patients recruited to PEARL, will be referred to as 'ADAPTIVE_A' for comparison to the subsequently implemented 'ADAPTIVE _B' protocol which will be described in Chapter 5.

The PEARL planning protocol was developed alongside physics and planning colleagues using Prosoma and RayStation in a pilot study of 4 pre-trial cases. The pilot study was based upon cases from Leeds and is explained in more detail in Chapter 3.

2.16.1 Adaptive radiotherapy in the PEARL study: The 'ADAPTIVE' planning method

ADAPTIVE uses 5 dose/fraction levels in phase 2 to reduce the total dose to PTV1_P and PTV2_P (Fig. 2.17).

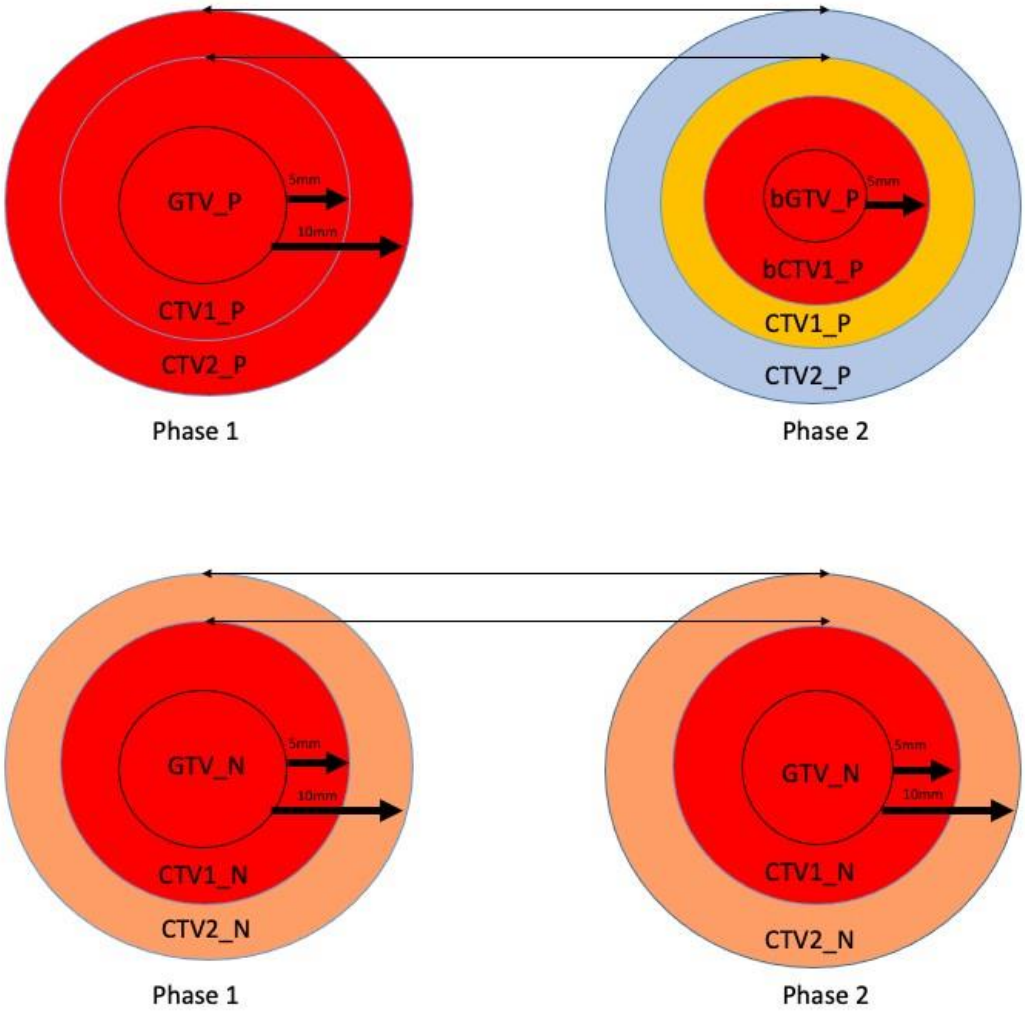

The dose/fraction to the prophylactic nodal level is not altered between Ph1 and Ph2 and is treated at 1.63Gy per fraction across both phases

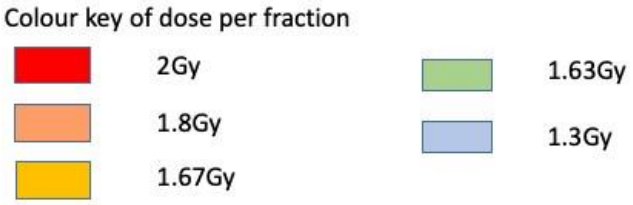

Fig. 2.17 Schematic diagram representing the different dose per fraction levels for phase 1 and phase 2 for the primary and nodal CTVs in ADAPTIVE. Note there is no adaption of the nodal volumes between phases.

Phase 1				Phase 2			Total	
		Dose/Fraction	BED 2Gy		Dose/Fraction	BED 2Gy	Dose/Fraction	BED 2Gy
bPTV1_P	N/A	N/A	N/A	36Gy/18F	2	43	66Gy/33F	79
PTV1_P	30Gy/15F	2	36	30Gy/18F	1.67	35	60Gy/33F	
PTV2_P	30Gy/15F	2	36	24Gy/18F	1.3	27	54Gy/33F	

Table 2.7 Total dose and dose/fraction to primary PTVs for Phase 1 and Phase 2 using the ADAPTIVE planning method

2.16.1.1 ADAPTIVE Phase 1

Planning phase 1 for ADAPTIVE broadly follows standard practice. Target coverage and OAR doses are initially planned for the full treatment course to ensure adequate coverage and overall plan safety.

2.16.1.2 ADAPTIVE Phase 2

This phase is more complex due to introduction of new dose levels. There is a total of 5 dose levels for phase 2 (Fig. 2.17). The dose per fraction to some areas within Phase 1 volumes is reduced as a result of the high dose volume being adapted (Table 2.7). As for Phase 1, it is planned as if to be used for the full 33 fractions.

2.16.2 Pre-Accrual Planning Benchmark Case

Participating centres are required to submit two planning benchmark cases – one for each phase of treatment (Fig. 2.18). The plan is optimised on a pre-outlined case (targets and OARs) provided by the RTTQA group. Cases are imported and optimised by the physics and planning

team as described in the PEARL trial Radiotherapy Guidance document (Appendix 2). Centres grow the PTVs and PRVs using their own margins as determined by their local immobilisation and set up techniques. On completion, the Plan Assessment Form is completed, and approval sought for submission from the local PI. This is returned to the RTTQA group to assess adherence to protocol, suitability of the planning technique and quality, in addition to agreement of dose/volume recording between participating centre and RTTQA group.

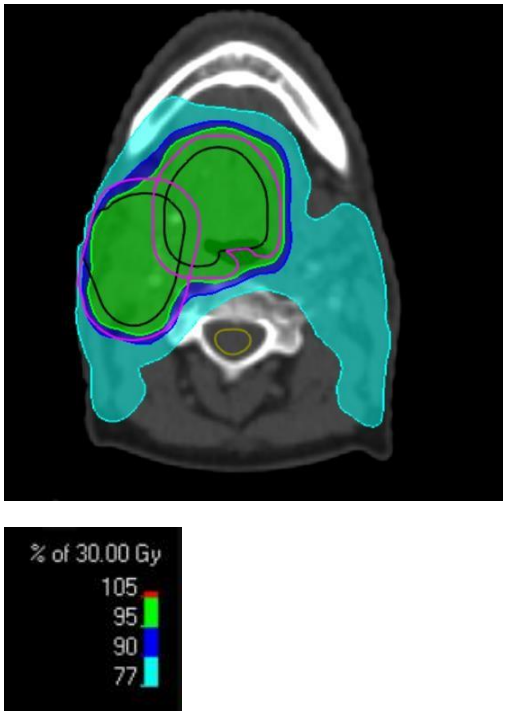

Fig. 2.18a

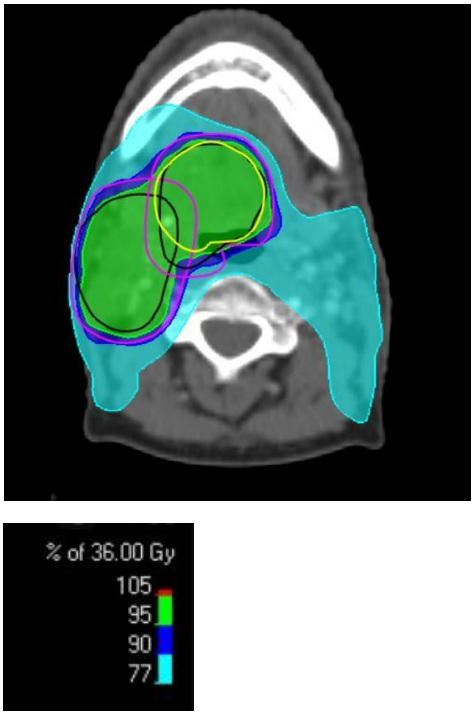

Fig. 2.18b

Fig 2.18a and 2.18b Axial CT slices of Phase 1 and Phase 2 plans for the PEARL planning benchmarking case and their respective isodose keys. For simplicity, only the bPTV_1 (yellow), PTV_1 (black) and PTV_2 (cerise) are shown.

2.16.3 Verification of Electronic Transfer of Data

During the typical patient pathway, data is transferred both anonymised and nonanonymised. As such, transfer between participating centres and the RTTQA group is undertaken via the NHS Wales Informatics Service (NWIS) Fileshare Service.

The intended transfer method between RTTQA and participating centre is followed using the benchmark case in the trial setup stage to ensure this transfer is successfully achieved and to identify any issues that require resolution prior to commencing on-trial cases.

2.17 Radiotherapy Treatment Quality Assurance

2.17.1 Dosimetry Audit

Audits are carried out either by the RTTQA group in person (with participating centre support) or via a postal audit using RTTQA equipment and performed by the participating centre. Centres can start entering and treating patients into the trial prior to the dosimetry site visit. However, the dosimetry audit should be completed as soon as possible following general pretrial QA approval.

2.17.2 Streamlining of Outlining, Planning and Audit process

There is no streamlining of target delineation or planning from having completed credentialing for other head and neck radiotherapy trial(s). Phase 1 and Phase 2 delineation must be completed and submitted for structure baseline case. As Phase 2 is the more complex, centres are only required to submit a baseline planning case for Phase 2, and standardly, only the first Phase 2 cases undergo real-time target delineation and planning quality assurance.

A dosimetry audit is required per technique, not per trial. As such, completion of a dosimetry audit for the purposes of a previous trial within an appropriate timescale is suffice for credentialing subsequent trials. This is checked by the RTTQA centre.

2.17.3 On-Trial Prospective Case Review

All trial cases undergo a real-time QA of target delineation prior to plan optimisation. Independent review is conducted by any available Trial Management Group Clinical Oncologist. To allow for this, the delineation and submission must be completed in a timely manner, especially in the case of the more tightly time-bound phase 2 turnaround, and sufficient clinical history had been submitted to include as a minimum:

- Site of primary disease
- Categorisation of primary tumour
- Involved nodal levels on pathology
- TNM stage
- Treatment start date

Review is organised by the RTTQA centre to ensure that timescales and communication methods are agreed in advance of submission to allow for maintenance of required trial planning timescales.

Following successful completing of target delineation QA, real-time plan QA is completed through submission of the optimised plan and completed plan assessment form and review by RTTQA. This must be successfully completed prior to patient commencing radiotherapy.

A map of the real-time review process for phase II is shown below in Fig. 2.19.

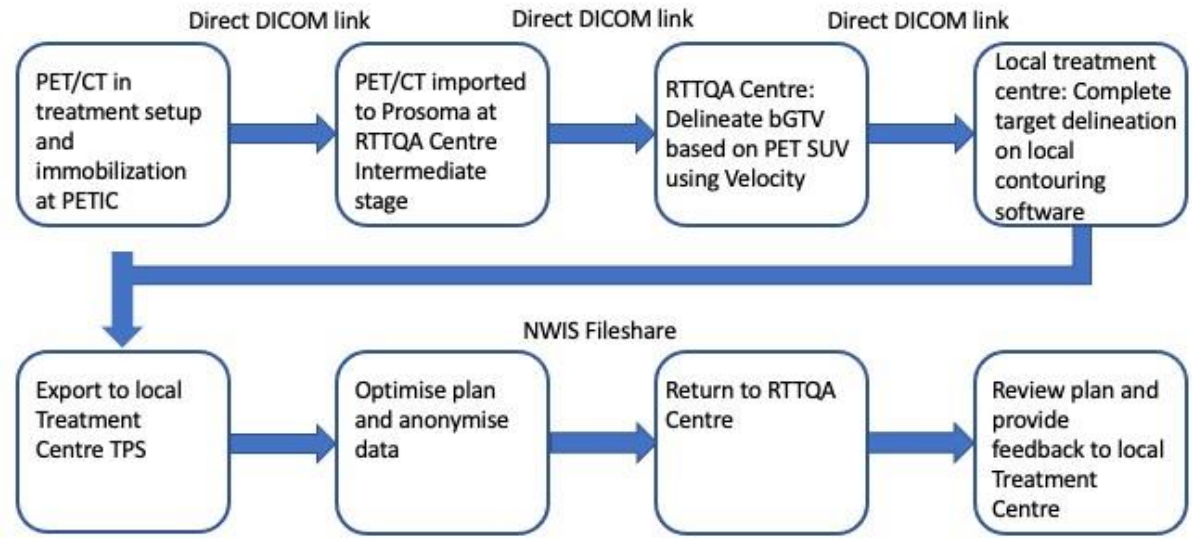

Fig. 2.19 Map of the real time RTTQA review process

2.18 PEARL ATLAAS Sub-Study

As detailed in chapter 1, the PEARL study offers an opportunity to validate the machine learning tool ATLAAS by comparing it's automatically generated bGTV_P with those manually defined by the nuclear medical and clinical oncology consultants (Fig. 2.20). Practically, the ATLAAS segmentation is not performed in real time in the PEARL Study due to time pressure of adaptive radiotherapy and the limited availability of the ATLAAS software across the local treatment centres.

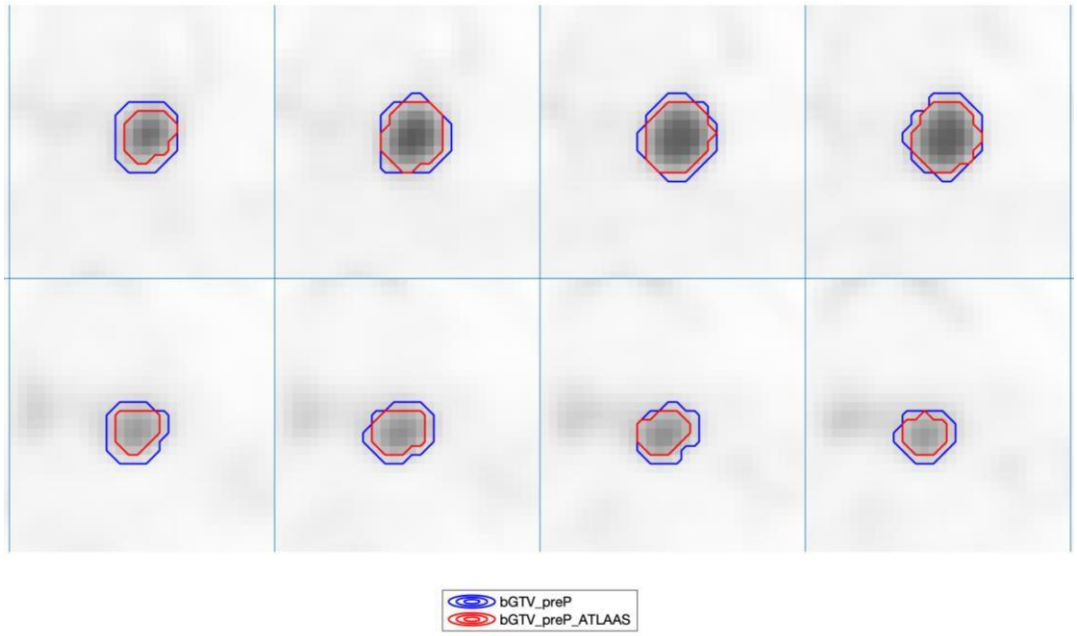

Fig. 2.20 Example of ATLAAS segmentation of the four pilot study cases. Top row images are taken from the prePET and bottom row from the iPET. Contours of the PET avid primary tumours (red) are compared to clinician defined contouring (blue).

The results of the ATLAAS sub-study are not within the scope of my MD and will be presented by the ATLAAS group separately.

2.18.1 Process for bGTV_P segmentation by ATLAAS

The region of the primary that is avid on prePET-CT and iPET-CT is defined by ATLAAS to create bGTV_preP_ATLAAS and bGTV_iPET_ATLAAS respectively. The PET and CT scans are reviewed with all relevant clinical information to inform the subsequent review of the segmented volumes. This distinguishes tumour uptake from physiological uptake or causes for increased FDG uptake such as any infective/inflammatory causes. If there is a complete metabolic response at this time point, ATLAAS will not generate a bGTV_iP.

Further technical detail concerning the ATLAAS sub-study can be found in the PEARL Study Protocol in Appendix 1.

2.19 Conclusion

I have presented the protocol for a novel adaptive radiotherapy study, PEARL. Following the presentation of the PEARL Study to the Regional Ethics Committee, the team was praised for a clear protocol to deliver research that explores an important research question. Subsequent feedback from the Trial Steering Committee includes the comment that PEARL is a very well-designed study.

I have outlined the rationale for PEARL; a novel method of de-intensifying the radical treatment of good prognosis, HPV associated OPSCC, through adaptation of the primary target volume based on biological response. For the novel ADAPTIVE plan to be deliverable within multiple cancer centres, clear radiotherapy guidance was developed to ensure the standardisation of processes regarding patient set up, image acquisition, target volume and OAR contouring, and radiotherapy planning.

During the development of the PEARL Radiotherapy Guidance, a pilot study was required to test the guidance for clarity, robustness and reproducibility. Given the complexity of the trial set up, the pilot study was run contemporaneously with the trial set up process. This allowed dynamic development of the trial protocol and helped ensure that PEARL could be open to patient recruitment soon after any issues raised by the pilot study were addressed. My next chapter will present the design, set up and results of the PEARL pilot study. This was a modelling planning study based on PET datasets of patients previously treated at an external site but imaged with PET-CT at 2 weeks into chemoradiotherapy for an unrelated research project.

Chapter 3: A pilot planning study to test the feasibility of PEARL, investigate tumour response, and analyse the dosimetric impact of the PEARL protocol

3.1 Introduction

The concept of de-escalating therapy in patients with good prognosis head and neck cancer having radical chemo-radiotherapy is attractive as toxicity rates of treatment are high. Our concept of individualising de-escalation based on each patient's response to the initial phase of treatment is highly novel.

In this chapter I define an optimised treatment planning protocol that considers dose to swallowing OARs (SWOARs) for use as a non-adaptive comparison to the ADAPTIVE plans produced as per the PEARL protocol.

I investigate the degree of clinical benefit that may be seen by adaptation with a modelling study comparing non-adaptive to adaptive plans. To do this, I compare mean doses received to OARs in modelled adaptive plans to mean doses received in modelled non-adaptive plans.

In addition, I look at the impact of radiotherapy on the volume of salivary glands. The dose received by the salivary glands during a course of radiotherapy may be greater than originally planned due to the change in position of the glands as they shrink in response to irradiation. Performing an iPET-CT after two weeks of chemoradiotherapy offers the opportunity to measure the volume of salivary glands during treatment, record their degree of shrinkage, and look at any movement in their position that occurs consequently on the CT component of the iPET-CT.

As I did not have any appropriate local datasets, I conducted my pilot planning study using FDG-PET-CT datasets from an external collaborating centre.

3.1.1 Objectives

The main objectives of the modelling pilot study:

1. Define a non-adapted radiotherapy plan that is optimized to reduce dose to Swallowing Organs At Risk (SWOARs) and salivary glands
2. Demonstrate an objective response to treatment can be seen on an iPET-CT scan carried out 2 weeks into the course of chemoradiation
3. Show it is feasible to adapt radiotherapy based on primary tumour (GTV_P) response to chemoradiation seen on iPET-CT
4. Demonstrate objective dosimetric advantage to i) Optimizing standard radiotherapy plans to reduce dose to the SWOARS and ii) Adaptive Radiotherapy in which the high dose CTV is adapted after 2 weeks of radiotherapy to a shrinking biological tumour volume (bGTV) seen on iPET-CT as per the PEARL study protocol.
5. Compare volumes of the parotid and submandibular glands on planning CT to their volumes on iPET_CT

3.2 Methods

3.2.1 Identifying datasets for the modelling planning study

I performed a literature search for studies that included an iPET-CT scan at 2 weeks of chemoradiation. I identified a study that presented data on changes in the primary GTV volume comparing pre-treatment PET-CT with a PET-CT performed after 2 weeks of chemoradiotherapy, the same timeline as we had designed for PEARL. It had also been conducted in the UK and so any data transfer was likely to be more straightforward. I approached the authors, a research group in Leeds led by Dr Robin Prestwich. They had published a study that included PET-CT scans performed at similar times during radiotherapy to those stipulated in the PEARL protocol (74). The Leeds study was an observational study

evaluating the changes in the size of the GTV_P between baseline and interim PET-CTs performed after fraction 11 and fraction 21 of chemoradiation. Unlike PEARL, the group did not adapt the patient's treatment based upon an interim response and so the Leeds patients had standard non-adapted treatment. I led a modelling planning study to look at the theoretical changes to target volumes and to the doses received by the OARs if plans had been adapted based upon the fraction 11 iPET-CTs in these patients, as per the PEARL protocol.

As a result of the agreed collaboration, 8 diagnostic imaging datasets of patients previously treated in Leeds were anonymised and sent by the Leeds team in DICOM format over the NHS Wales Informatics Service (NWIS) file share system. These were then downloaded and imported into RayStation at Velindre Cancer Centre. In addition to the DICOM files, we received an MS excel spreadsheet containing anonymised scan reports and clinical summaries for each case. The imaging datasets included a prePET-CT and iPET-CT for each patient. The prePET-CT was a standard hemibody and contrast enhanced diagnostic CT with PET acquisition of the head and neck region in a beam-directing shell. The iPET-CT was a contrast enhanced CT and head and neck region PET, also performed in the shell. Out of the 8 patient cases sent, 4 were selected for our pilot study based on anatomical site of primary being in the oropharynx, and completeness of the data sets on electronic transfer. Clinical and radiological information of the selected 4 cases is outlined in Table 3.3.

I used the Leeds prePET-CT and iPET-CT scans to contour the target volumes and OARs for each of the 4 patient cases as per the PEARL protocol described in Chapter 2, in order to perform the modelling planning study. The GTVs, CTVs, PTVs and OARs were all contoured by me then manually planned by Dr Owain Woodley, a Velindre radiotherapy planner with clinical guidance from myself and Dr Thomas Rackley, Consultant Clinical Oncologist and Co-Chief Investigator for PEARL.

3.2.2 Defining the standard non-adaptive planning technique

In order to accurately establish the impact PEARL adaptive has on dosimetry, it was paramount that the non-adapted plan, which served as the standard, was optimised to reduce the dose to normal tissue as much as possible. This served to mitigate for potentially incorrectly attributing dose reduction in the PEARL adaptive plan to the adaptation.

In standard practice, Velindre Cancer Centre's routine head and neck planning protocol considered dose to the contralateral submandibular gland and parotid glands with optimal mean dose constraints of <35Gy to the contralateral submandibular gland, and <14Gy (lateralised tumour) and <24Gy (non-lateralised tumour) to the contralateral parotid gland. Dose constraints to swallowing OARs (SWOARs) however, were not part of our centre's head and neck class solution. Even if delineated by the clinician, they were not added as an objective to the optimisation and therefore dose to the SWOARs was not specifically minimised. We produced a standard plan for each of the Leeds cases, using our standard class solution. In order to establish the impact of optimising to the SWOARS, we also produced a plan which included optimal dose constraints for the SWOARs as per Table 3.2. Finally, we produced a third plan which optimised to the SWOARS and included adaptive radiotherapy.

In summary, the following plans were produced for each of the 4 pilot study cases:

1. Non-optimised for SWOARS, 'NON-OPTIMISED'

Standard treatment plan i.e. For the primary and nodal targets, 66Gy prescribed to PTV1 (GTV+5mm=CTV1), 60Gy to PTV2 (GTV + 10mm = CTV2), 54Gy to PTV3 (prophylactic nodal volume). The CTV to PTV margin is 4mm.

2. Optimised for SWOARS, 'OPTIMISED'

As per NON-OPTIMISED but considering dose to SWOARs in the optimisation process as per Table 3.2.

3. Adaptive radiotherapy as per the PEARL protocol, 'ADAPTIVE'

A 2-phase adaptive radiotherapy plan based upon the PEARL protocol described in Chapter 2. Optimisation for SWOARs as per Table 3.2. For the primary target, 66Gy was prescribed to bPTV1, 60Gy to PTV1 and 54Gy to PTV2.

	Primary CTV definition	Number of fractions	Dose/fraction to high dose PTVs (Gy)	Total dose to high dose PTVs (Gy)
NON-OPTIMISED	GTV+5mm GTV+10mm	33 33	2 1.82	66 60
OPTIMISED	GTV+5mm GTV+10mm	33 33	2 1.82	66 60
ADAPTIVE Phase 1 Phase 2	 GTV+10mm bGTV+5mm GTV+10mm	 15 18 18	 2 2 1.67	 30 36 30

Table 3.1 Summary of primary CTV margins and dose/fractionation for the 3 different plans: NON-OPTIMISED, OPTIMISED, AND ADAPTIVE. CTV to PTV margin is 4mm.

3.2.3 Quantification of biological primary GTV (bGTV_P) response to radiotherapy using the SUVmax

The SUV is a simple image-based measure widely used in clinical practice to represent metabolic activity of biological tissue. It is a semi-quantitative measurement of uptake of a radioactive isotope in tissue and can be significantly influenced by the accuracy of dose calibration, time between injection and imaging as well as the weight of the patient, motion artefacts and blood glucose levels. I concluded that the SUVmax as defined by the Leeds nuclear medical consultant analysing the scans in real time, would be the most accurate

compared to retrospectively reviewing the scan datasets we had been sent. The reasons for this include:

- The Leeds reporting nuclear radiologist would have had access to all the information needed to report the SUVmax on their reporting software.
- The SUVmax is the most widely reported SUV-related variable in the analysis of malignancy on PET-CT and refers to the highest SUV signal in a particular volume of interest. It therefore makes my results more comparable to published literature.
- The SUVmax has very high inter-observer reproducibility, providing a useful parameter for PET comparison studies.

SUVmax is calculated as the maximum ratio of tissue radioactivity concentration (in kBq/ml) at a given time, divided by the administered dose at the time of injection (MBq) divided by the body weight (Kg). I use the change in SUVmax of the bGTV_P on the prePET and iPET as a surrogate for biological tumour response, in addition to the change in the PET-avid volume.

3.2.4 Defining the biological GTV (bGTV)

The bGTV is defined as the region of primary tumour avid on PET-CT and consists of the high FDG uptake volume based upon suitable windowing levels.

All PET images are displayed in the SUV scale on the Velocity platform. The standardised display settings for the PET are:

a. Zoom: 150-200%

The zoom tool is used to better define the bGTV but it is with awareness that increasing the zoom too much meant that larger volumes were likely to be outlined, which may overestimate the metabolic volume.

b. SUV scaling: 0 - 10

c. Colour scale: Inverse Linear

In preparation for defining the biological GTV (bGTV), the PET-CT is reviewed by myself in collaboration with Dr Nicholas Morley, Consultant in nuclear medicine. PET and CT components of the scans are reviewed with any relevant clinical information to inform review of the bGTV e.g., to distinguish tumour uptake from physiological uptake or causes for increased FDG uptake such as any infective/inflammatory causes. In addition, a volume produced by automated contouring with the ATLAAS software (bGTV_ATLAAS) as per the PEARL Sub Study, is used to inform the final manually contoured bGTV (described below).

3.2.4.1 Use of ATLAAS to define bGTV_ATLAAS

The ATLAAS contouring uses CERR software and is transferred to Velocity. The FDG uptake on the PET directs the drawing of the bGTV_ATLAAS, rather than the CT abnormality. If there is a discrepancy (i.e., the tumour is not well visualised on the CT scan) the volume defined as the bGTV_ATLAAS remained the metabolically active volume. The bGTV_ATLAAS sometimes includes areas which did not contain tumour e.g., the airway because of scatter.

3.2.5 Measurement of dosimetric impact on SWOARs and major salivary glands for OPTIMISED and ADAPTIVE plans

To demonstrate the dosimetric impact of different planning methods, I focus on the mean dose of radiotherapy (Gy) received by the SWOARs, contralateral parotid and contralateral submandibular glands over the course of treatment. The mean dose is the most widely published dosimetric parameter of head and neck SWOARs and salivary glands in the literature, and is the parameter derived from normal tissue complication probability (NTCP) models most used in clinical practice to define the optimal dose constraints for these head

and neck OARs. By looking at the differences in mean doses due to a change in optimization or adapted radiotherapy, I can look at whether optimal dose constraints are met as a result of the ADAPTIVE plans.

Optimal dose constraints for SWOARS and contralateral parotid and submandibular glands used for OPTIMISED and ADAPTIVE plans are shown in Table 3.2. It is important to note that the optimal dose constraint to the contralateral parotid gland is already included in the NONOPTIMISED plan.

Structure	Volume constraint	Optimal dose constraint
Contralateral Parotid Gland (lateralised primary)	Mean	<14Gy
Contralateral Parotid Gland (non-lateralised primary)	Mean	<24Gy
Contralateral Submandibular Gland (lateralised and non-lateralised primaries)	Mean	<35Gy
Supraglottic Larynx	Mean	<55Gy
Glottic Larynx	Mean	<45Gy
Superior Pharyngeal Constrictor Muscle	Mean	<50Gy

Middle Pharyngeal Constrictor Muscle	Mean	<50Gy
Inferior Pharyngeal Constrictor Muscle	Mean	<20Gy
Oral cavity	Mean	<30Gy

Table 3.2 Optimal dose constraints for contralateral major salivary glands and SWOARs for OPTIMISED and ADAPTIVE plans.

The mean dose is also the simplest way to sum the dose received to OARs across 2 phases delivered on 2 different planning scans in the ADAPTIVE plans.

To calculate mean dose to OAR in the ADAPTIVE plans:

$$\frac{Mean\ dose\ to\ OAR\ in\ phase\ 1}{33} \times 15 + \frac{Mean\ dose\ to\ OAR\ in\ phase\ 2}{33} \times 18 = Total\ mean\ dose\ for\ ADAPTIVE\ plan$$

3.2.6 Measurement of parotid and submandibular gland volumes

I contoured the parotid and submandibular glands on Raystation for Phase 1 and 2 of the ADAPTIVE plans and used the volumes generated in cm^3 to compare the phases.

3.3 Results

3.3.1 Comparison of OPTIMISED and NON-OPTIMISED plans for pilot study cases

The OPTIMISED plans reduced the mean dose to the majority of OARs in all 4 cases when compared to the NON-OPTIMISED plans (Fig. 3.1). The magnitude of reduction was between 0.13 - 2.87Gy with the greatest reduction was seen in the oral cavity in Case 1 (2.87Gy). The optimal dose constraint was met because of this reduction. No additional optimal dose constraints were met for OPTIMISED versus NON-OPTIMISED plans. The mean dose to glottis was reduced by 1.22 – 2.48Gy in all four cases but the optimal dose constraint had already been met in the NON-OPTIMISED plan. The oral cavity and inferior pharyngeal constrictor muscle also had reduced mean doses in all 4 cases. Smaller changes were seen in the major salivary glands and no dose reduction seen in the ipsilateral parotid gland in any of the cases.

Case	Clinical information	Radiological information	prePET-CT	iPET-CT (after 11 fractions)
1 T4N1M0 Squamous cell carcinoma base of tongue/vallecula	Nasendoscopy – Bulky base of tongue/vallecular tumour	MRI – Base of tongue tumour 3.5cm diameter extending into the vallecular and supraglottis.	Large primary tumour within base of tongue arising on the left but extending across midline measuring 4.8 x 4.3cm. SUVmax 21.9.	Significant reduction in size of primary tumour. Primary tumour 2.5 x 2.9cm and SUVmax 3.3.
2 T2N2bM0 Squamous cell carcinoma right base of tongue	Clinical exam – Subtle mass felt in the right posterior tongue.	CT – Soft tissue mass in the right tongue base measuring 3.8cm in maximal dimension. Extends inferiorly into the right side of the vallecula, crosses the midline in the region of the lingual tonsils which are involved. Involves the palatine tonsil superiorly and right oropharyngeal wall.	Right sided base of tongue mass extending across midline and into right vallecula. 4.1cm in longest dimension with an SUVmax 11.9.	Primary tumour measures 2.9cm in longest axis and has an SUVmax of 9.1.
3 T2N2bM0 Squamous cell carcinoma right base of tongue	Nasendoscopy – Nothing abnormal to see on clinical examination. Full tongue movements. EUA – Subtle abnormality of right tongue base.	MRI – Multiple enlarged cystic level II/III lymph nodes. Irregularity of the mucosa region of the right lingual tonsil and vallecula which shows asymmetric increased enhancement. Slight asymmetry of the soft tissues in the right lateral oropharynx.	Right base of tongue tumour 2.6cm in longest axis and SUVmax 14.8. No invasion into surrounding structures.	Primary tumour has not significantly changed in size – 2.6cm - but SUVmax has reduced to 10.9.
4 T1N2bM0 Squamous cell carcinoma left base of tongue	Not available	MRI – 18mm enhancing mass arising in the left tongue base and bulging into the left vallecula. Numerous necrotic left sided lymph nodes	Left base of tongue primary tumour 2.5cm in longest axis. SUVmax 13.3.	Primary has not significantly changed in size – 2.5cm – but there is an interval reduction SUVmax to 4.1.

Table 3.3 Clinical and radiological characteristics of the 4 Pilot Study cases

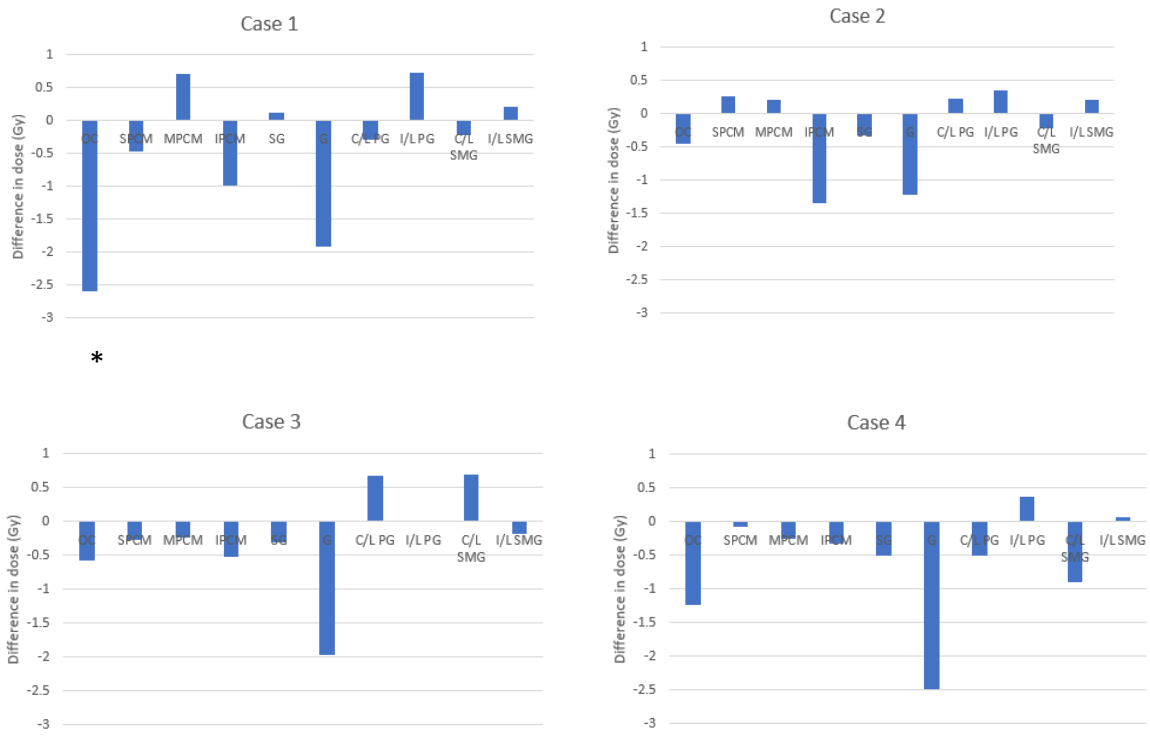

Fig 3.1 Waterfall plots demonstrating the difference in mean dose received by OARs in non-adapted pilot study plans as a result of implementing a planning class solution optimized to reduce dose to SWOARs (OPTIMISED plans) compared to a planning class solution not optimized for the SWOARs (NON-OPTIMISED plans). * Optimal dose constraint met as a result of optimisation

Key: OC = Oral Cavity, SPCM = Superior pharyngeal constrictor muscle, MPCM = Middle pharyngeal constrictor muscle, IPCM = Inferior pharyngeal constrictor muscle, SG = Supraglottis, G = Glottis, C/L PG = Contralateral parotid gland, I/L PG = Ipsilateral parotid gland, C/L SMG = Contralateral submandibular gland, I/L SMG = Ipsilateral submandibular gland

3.3.2 Quantifying tumour responses using SUVmax on interim iPET-CT scans after 2 weeks of chemoradiation in pilot study patients.

An SUV max of 2.5 or higher is generally considered indicative of malignancy although a range of values are reported. It is also widely recognised that non-malignant tissue can have SUV max of over 2.5, in addition to malignant tumours having values below 2.5. In all 4 cases, the

primary demonstrated an SUVmax value on prePET consistent with malignancy (123). In all 4 pilot study cases, the SUVmax of the primary tumour was reduced after 2 weeks of chemoradiotherapy (range of SUVmax 23.5 – 84%; mean 50.7%) (Fig. 3.2).

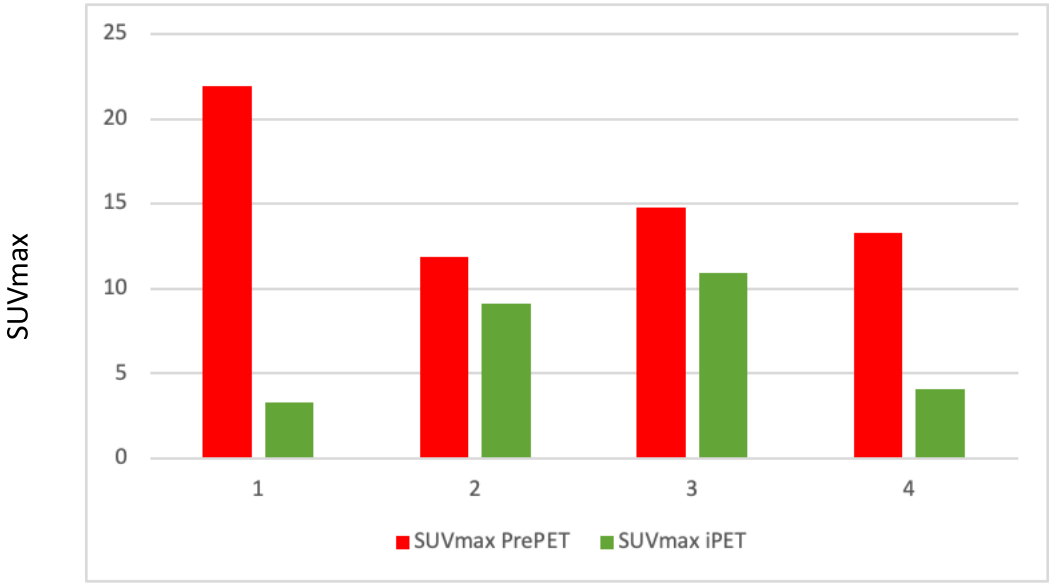

Fig 3.2 SUVmax of primary tumours on prePET and iPET for the 4 pilot study cases

3.3.3 Changes in PET-avid primary tumour volumes on interim iPET-CT scans after 2 weeks of chemoradiation in pilot study patients.

The PET-avid GTV reduced in volume in Cases 1 and 2 by 66.12 and 33.98%. For cases 3 and 4, which had much smaller bGTV_preP volumes, the volume increased by 2.64 – 4.44% (Fig. 3.3). The reduction in size for cases 1 and 2 is demonstrated on the axial and sagittal CT components of the prePET-CT and iPET-CT (Fig. 3.4 and 3.5) and reflected in the PTV, which is created by GTV expansion (Fig. 3.6, 3.7, 3.8).

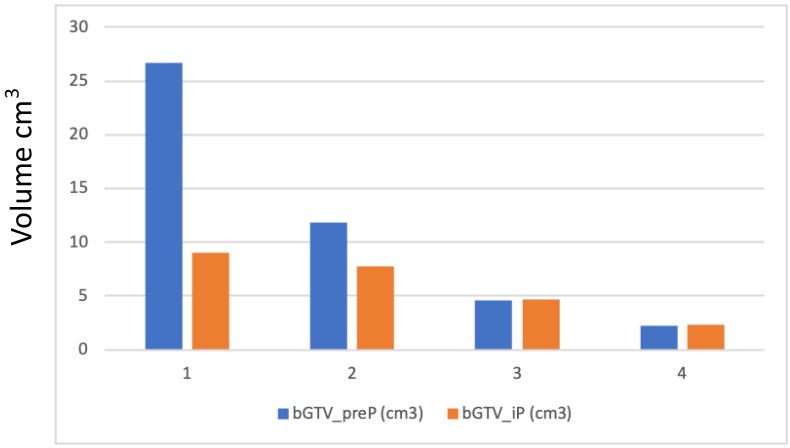

Fig. 3.3 Graphical representation of the change in bGTV after 10 fractions of chemoradiation for the 4 pilot study cases. bGTV_P on prePET (blue) and iPET (orange).

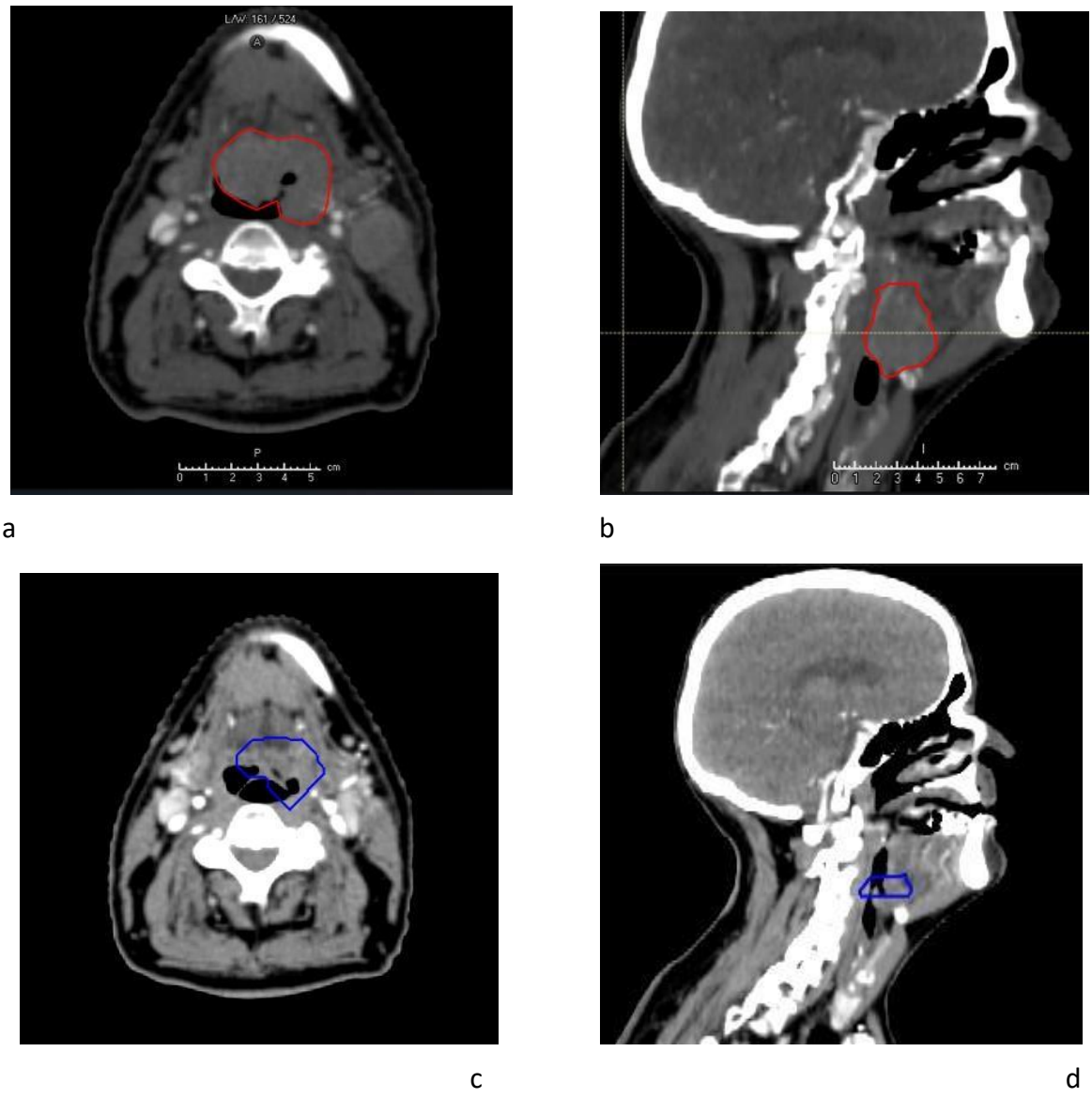

a b

c d

Fig 3.4 Transverse and sagittal slices of prePET (a+b) and iPET (c+d) CT components for case 1. GTV_P outlined in red, bGTV_iP outlined in blue.

Case 2

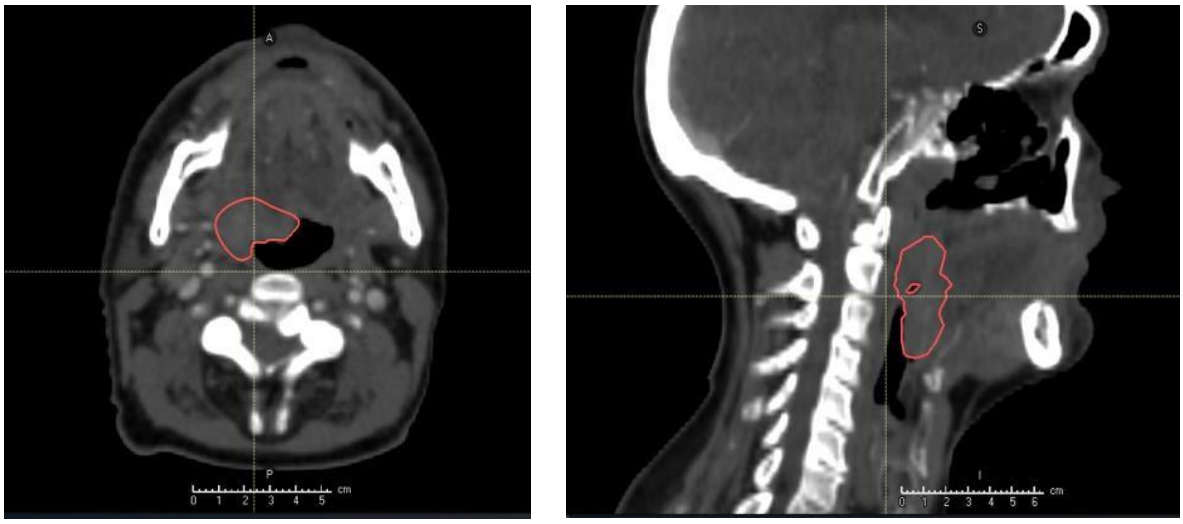

a b

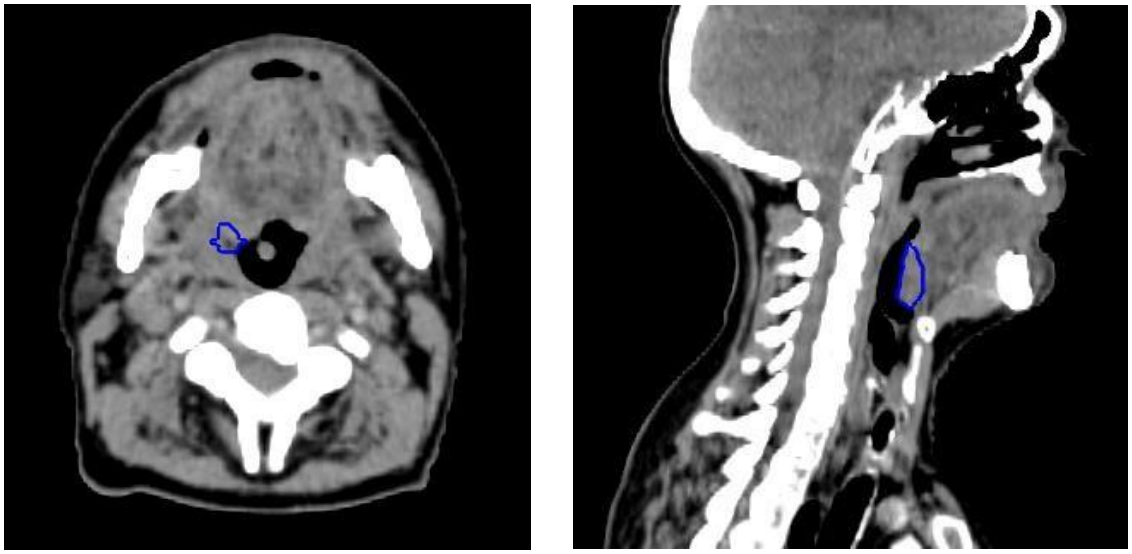

C d

Fig 3.5 a – d Transverse and sagittal slices of prePET-CT (Fig. 3.5 a+b) and iPET-CT (Fig. 3.5 c+d) CT components for case 2. High dose GTV_P outlined in red, bGTV_iP in blue

3.3.4 Changes in high dose primary PTVs in Pilot Study cases 1 - 4

The volume of the high dose PTV_P is reduced in Phase 2 across all 4 cases with a mean of 33.97% (range 9.5 – 56.74%). The largest percentage reductions are seen in case 1 and 2, which also had the largest PTV_P volumes prior to starting radiotherapy. It is feasible to adapt

radiotherapy based on tumour (GTV_P) response to head and neck radiotherapy seen on iPETCT.

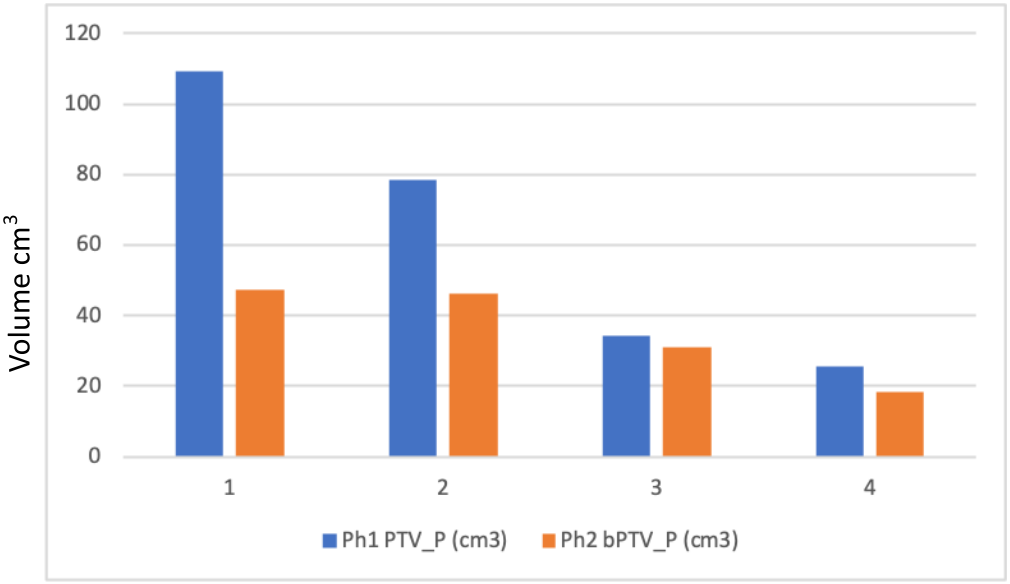

Fig 3.6 Graphical representation of the change in high dose PTV_P after 10 fractions of chemoradiation for the 4 cases from Leeds. Volume of high dose PTV_P on prePET-CT (blue) and iPET-CT (orange).

Case 1

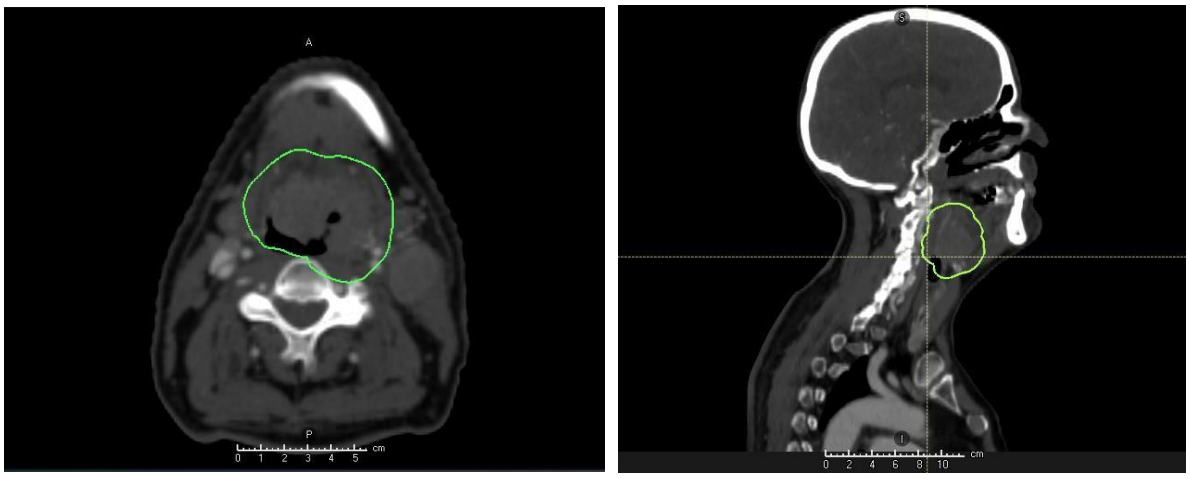

a b

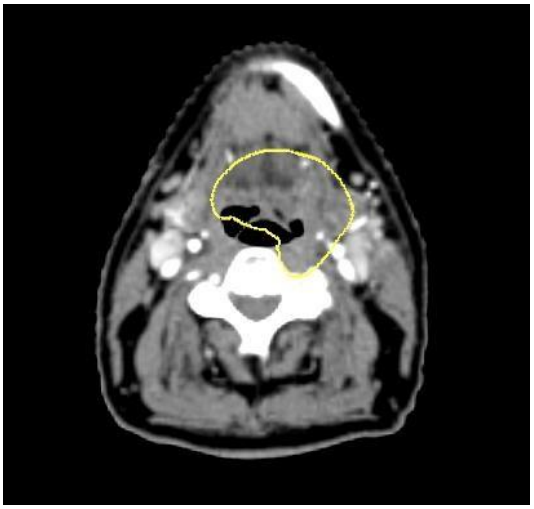

c d

Fig. 3.7 a – d Transverse and sagittal slices of prePET-CT (Fig. 3.7 a+b) and iPET-CT (Fig. 3.7 c+d) CT components for case 1. PTV1_P outlined in green, bPTV_P in yellow

Case 2

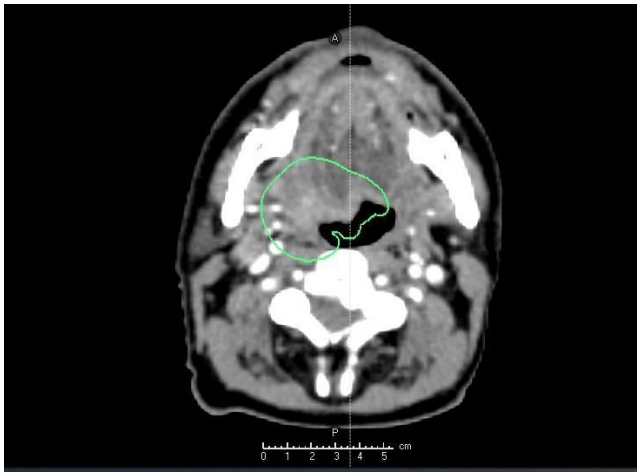

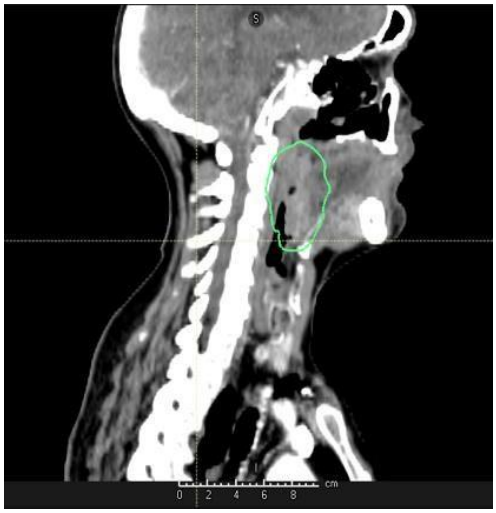

a b

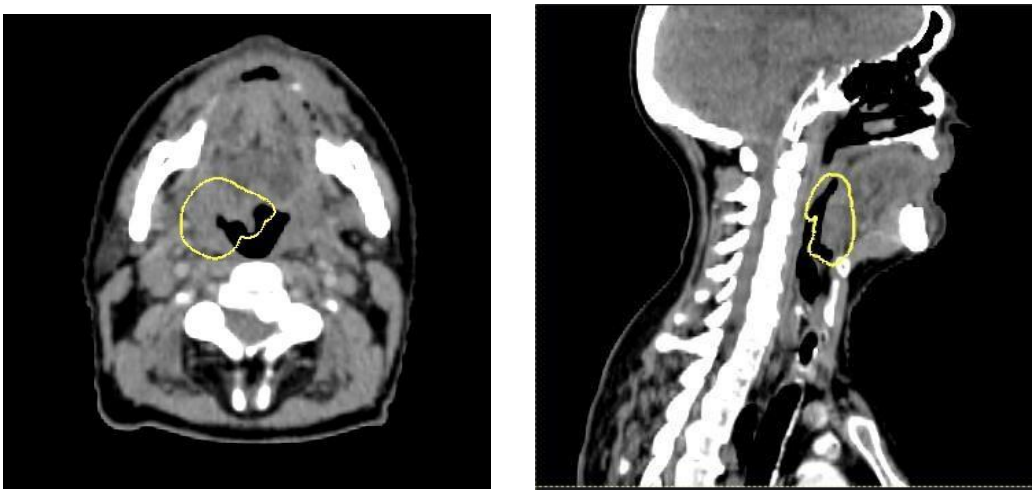

c d

Fig 3.8 a-d Transverse and sagittal slices of prePET-CT (Fig. 3.8 a+b) and iPET-CT (Fig 3.8 c+d) CT components for case 2. PTV1_P outlined in green, bPTV1_P in yellow.

3.3.5 Modelled dosimetric changes resulting from PEARL adaptive in pilot study cases

Fig. 3.9 c and d is an example of changes in dose distribution following re-planning to the new primary target volumes after 2 weeks of chemoradiation. The 95% (orange) isodose lines demarcate a smaller area around the primary site in phase 2. There is a shrinkage of the isodoses particularly around the medial and anterior aspect of the high dose PTV in Fig. 3.9 c and d corresponding to the tumour response and reduction in the GTV_P demonstrated in Fig. 3.9 and b.

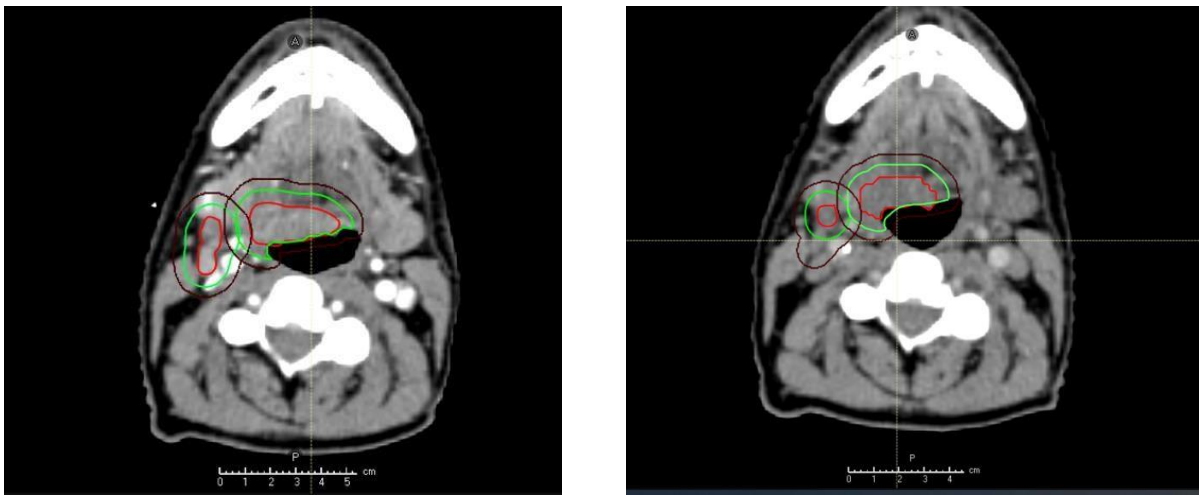

9a 9b

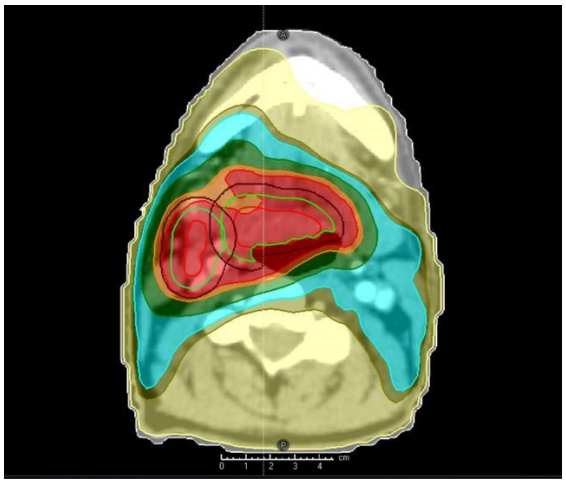

9c

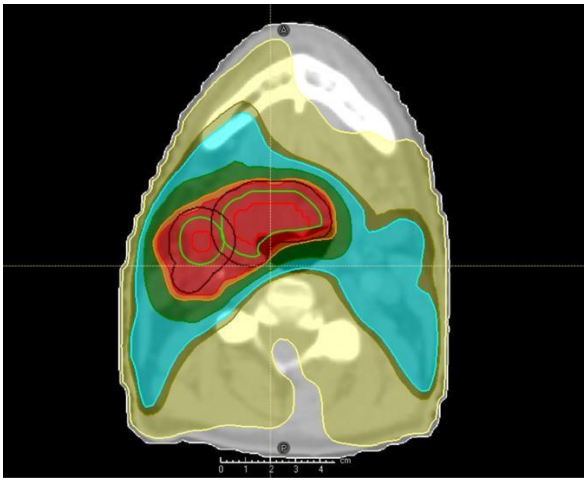

9d

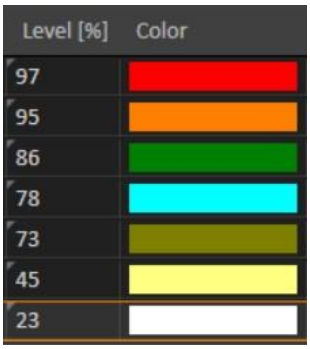

10e

Fig 3.9 a – d Axial CT slices showing primary and nodal CTVs for Phase 1 (Fig. 3.9a) and Phase 2 (Fig. 3.9b) of ADAPTIVE and the corresponding plans (Fig. 3.9c and Fig. 3.9d) for Case 2. Isodose level key demonstrated in fig. 3.9e for percentage of prescribed dose.

3.3.6 Comparison of the OPTIMISED and ADAPTIVE plan for pilot study cases

The ADAPTIVE plan reduced the mean dose to SWOARS consistently across all 4 pilot study cases by a mean of 3.1Gy per SWOAR (range 0.6 – 7.47 Gy) (Table 3.4 and Fig. 3.10). The greatest reductions were seen in the glottis and supraglottis. In Case 3, the optimal dose constraint to the supraglottis was met as a result of ADAPTIVE planning (mean dose 54.63Gy). The optimal dose constraint for the glottis had already been met by OPTIMISED planning for all cases but was further reduced by ADAPTIVE. There were reductions in mean dose to the pharyngeal constrictor muscles (SPCM range 0.6 – 3.42Gy, MPCM range 1.63 – 2.61Gy, IPCM range 1.92 – 4.61Gy) but no additional dose constraints were met as a result.

The impact on the major salivary glands was more variable and of generally smaller magnitude (range 0.15 – 2.89Gy). In Case 1, the optimal dose constraint to the contralateral parotid gland was met due to the ADAPTIVE planning (mean dose 23.48Gy). The contralateral submandibular gland had the most consistent benefit from ADAPTIVE with the mean dose reduced in 3 out of the 4 cases (range 0.56 – 2.64Gy).

Case	Oral Cavity			SPCM			MPCM			IPCM			Supraglottis			Glottis		
	OP	AD	AD-OP	OP	AD	AD-OP	OP	AD	AD-OP	OP	AD	AD-OP	OP	AD	AD-OP	OP	AD	AD-OP
1	28.99	30.22	1.23	57.27	54.77	-2.5	61.83	59.57	-2.26	42.33	38.70	-3.63	62.91	56.62	-6.29	39.83	35.09	-4.74
2	36.96	34.22	-2.74	60.65	57.23	-3.42	57.08	55.18	-1.9	43.02	40.63	-2.39	51.58	46.16	-5.42	42.75	40.69	-2.06
3	32.74	30.23	-2.51	48.54	46.84	-1.7	58.34	56.71	-1.63	44.56	42.64	-1.92	57.03	54.63	-2.4	35.11	33.66	-1.55
4	26.55	27.49	0.94	43.52	42.92	-0.6	60.45	57.84	-2.61	43.53	38.92	-4.61	60.07	57.99	-2.08	38.87	31.4	-7.47

Case	C/L parotid			I/L parotid			C/L SMG			I/L SMG		
	OP	AD	AD-OP	OP	AD	AD-OP	OP	AD	AD-OP	OP	AD	AD-OP
1	26.37	23.48	-2.89	37.98	41.26	3.38	61.14	58.5	-2.64	62.95	63.92	0.97
2	28.31	29.6	1.29	35.24	35.95	0.71	53.17	53.73	0.56	65.28	64.35	-0.93
3	29.91	28.88	-1.03	50.6	50.89	0.29	52.26	51.33	-0.93	64.6	65.39	0.79
4	25.85	24.62	-1.23	45.41	46.31	0.9	50.4	49.18	-1.22	65.19	65.04	-0.15

Table 3.4 Absolute values and change in mean dose (Gy) to SWOARS and major salivary glands for ADAPTIVE (AD) compared to OPTIMISED (OP) for the pilot study cases. Blue shading demonstrates a reduction in mean dose to OAR with ADAPTIVE.

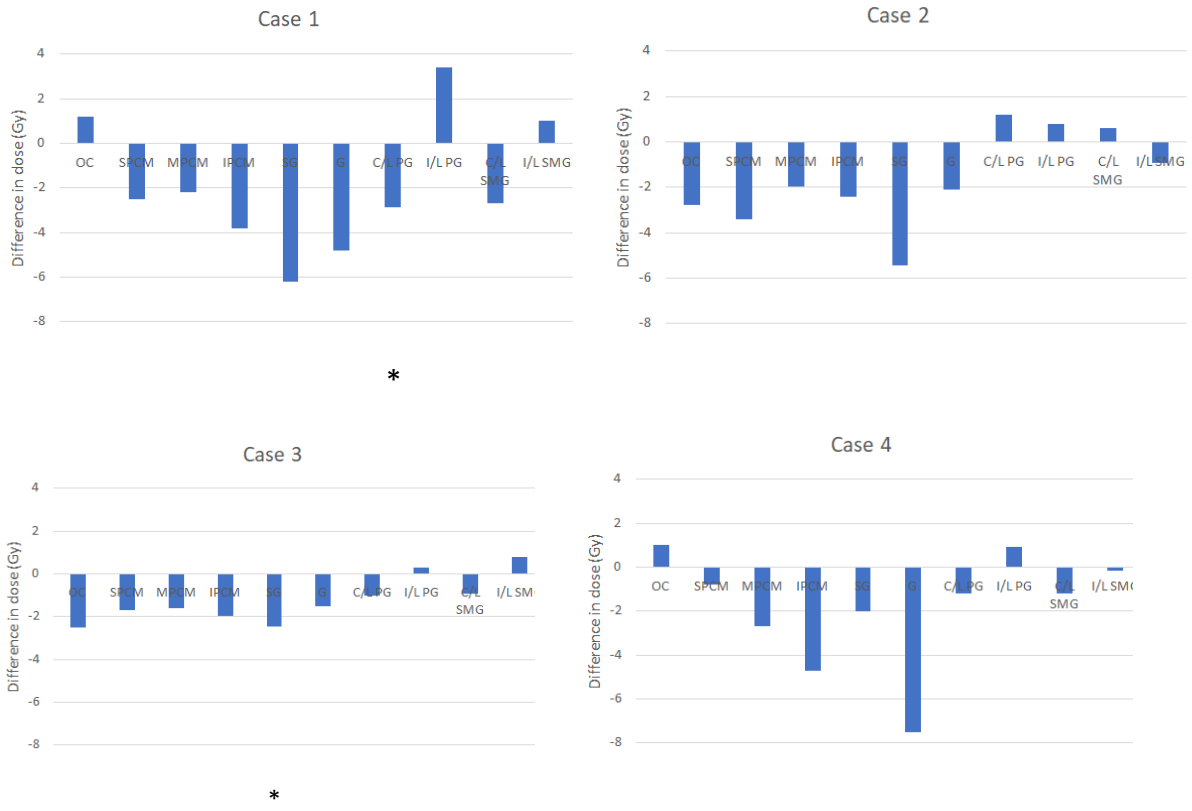

Fig 3.10 Waterfall plot demonstrating change in mean dose received by OARs in pilot study plans as a result of ADAPTIVE compared to OPTIMISED.

* Optimal dose constraint met as a result of ADAPTIVE planning.

Key: OC = Oral Cavity, SPCM = Superior pharyngeal constrictor muscle, MPCM = Middle pharyngeal constrictor muscle, IPCM = Inferior pharyngeal constrictor muscle, SG = Supraglottis, G = Glottis, C/L PG = Contralateral parotid gland, I/L PG = Ipsilateral parotid gland, C/L SMG = Contralateral submandibular gland, I/L SMG = Ipsilateral submandibular gland

3.3.7 Changes in salivary gland volumes on interim PET-CT (iPET-CT) compared to pre-treatment PET-CT

In general, there is shrinkage in the volume of all major salivary glands across all 4 cases. The exceptions are case 3 where all the glands increased in volume, and the contralateral parotid gland which increased in volume in all cases apart from case 1.

CASE	contralateral parotid gland	ipsilateral parotid gland	contralateral submandibular gland	ipsilateral submandibular gland
1	-12.67	-1.2	-9.27	-20.53
2	12.03	-1.09	-5.92	-12.23
3	2.28	4.9	16.92	29.3
4	2.9	-6.05	-12.51	-10.4

Table 3.5 Modelled Percentage change in volume of contralateral and ipsilateral parotid and submandibular glands using anatomical information from CT component of iPET-CT compared to CT component of pretreatment PET-CT

3.4 Discussion

To inform the PEARL clinical trial development and set up, I conducted an exploratory modelling planning study using PET-CT datasets from an external centre to model theoretical dose distribution to target volumes and OARS as a result of ADAPTIVE planning.

I defined the standard radiotherapy planning method as OPTIMISED planning, which considers dose to SWOARS, for comparison to ADAPTIVE.

The pilot study demonstrated that an iPET-CT performed after 2 weeks of chemoradiotherapy can demonstrate a biological response to treatment through reduction in SUVmax, and volume of the FDG-avid primary tumour in the two largest tumours. The study also showed the feasibility of adapting radiotherapy based on this response, and that there are dosimetric advantages in doing so, to the OARs implicated in dysphagia (superior/middle/inferior pharyngeal constrictor muscles, supraglottis, glottis, and oral cavity) and xerostomia (parotid and submandibular glands).

3.4.1 Impact of considering dose constraints to SWOARS in modelled planning process: OPTIMISED versus NON-OPTIMISED

As mentioned in Chapter 1, in 2020 the DARS study (NCT 25458988) was the first randomised study to demonstrate improved functional outcomes from dysphagia-optimised IMRT which included a mandatory dose constraint to the pharyngeal constrictor muscles (DO-IMRT) (40). There are important differences between the contouring the pharyngeal constrictor muscles in DARS and in PEARL.

1. PEARL requires the superior, middle and inferior pharyngeal constrictor muscles to be contoured as separate OAR volumes. Optimal dose constraints to the superior and middle pharyngeal constrictor muscles in PEARL are identical; a mean dose < 50Gy. For the inferior pharyngeal constrictor muscle, the optimal dose constraint is a mean dose of < 20Gy.
2. Optimal, and not mandatory dose constraints are set to all SWOARs in PEARL, and only oropharyngeal primaries are included.
3. DARS reports dose to the OAR volume that remains once the primary PTV is subtracted from the pharyngeal constrictor. PEARL reports mean dose to the entire constrictor including regions within the primary PTV.
4. DARS includes both oropharyngeal and hypopharyngeal primaries and specified how the constrictor muscle OARs were contoured according to the site of the primary. For OPSCC, the superior and middle pharyngeal constrictor muscles were delineated as one OAR volume with a mandatory dose constraint to the region of OAR outside of the primary PTV. For hypopharyngeal primaries, DARS delineated the inferior pharyngeal constrictor muscle as the OAR with a mandatory dose constraint.

To assess the impact of ADAPTIVE planning as per the PEARL protocol compared to nonadaptive radiotherapy, I had to first define a standard radiotherapy method so that any advantage seen with the ADAPTIVE plan could be ascribed to the adaptive element of PEARL alone. In my pilot study, I compare the dosimetry between a non-SWOARs optimised method

(NON-OPTIMISED), and a SWOARs optimised method as per the PEARL protocol dose constraints (OPTIMISED) to assess what, if any dosimetric advantage optimising for SWOARs conveyed.

Overall, the general trend was a reduction in mean dose to SWOARs and the major salivary glands across all 4 cases with OPTIMISED planning. Dose to the glottis demonstrated the largest and most consistent reduction with OPTIMISED overall (Fig. 3.1) with a mean reduction in the mean dose of 1.9Gy (range 1.22 – 2.48Gy). The optimal dose constraint for the glottis had already been met by the NON-OPTIMISED plans in all cases.

Mean dose to the oral cavity was also reduced by a mean of 1.28Gy (range 0.45 – 2.87Gy) and in Case 1, the optimal dose constraint was met in the OPTIMISED plan. There was a smaller change to the mean dose to the superior and middle pharyngeal constrictor muscles in all cases. For Cases 3 and 4, the mean dose was already less than the optimal dose constraint using NON-OPTIMISED but for cases 1 and 2, OPTIMISED did not bring the superior pharyngeal constrictor muscle mean dose below the <50Gy objective. None of the cases achieved the dose constraint for middle pharyngeal constrictor muscle with either NON-OPTIMISED or NON-OPTIMISED due largely in part to the position of the high dose primary PTV which overlapped with the middle pharyngeal constrictor muscle volumes.

The optimal dose constraint placed on the contralateral parotid gland (mean dose <24Gy) was not met in Cases 1- 4 with either NON-OPTIMISED or OPTIMISED. In general, there was not much improvement in dose to the contralateral parotid in any of the cases by applying OPTIMISED (Fig 3.1). This is to be expected given that the NON-OPTIMISED method already includes the contralateral parotid gland in its optimization priorities. What is reassuring is that in all cases apart from Case 3, there was not an increase in mean dose to the contralateral parotid gland as a result of optimising dose to the SWOARs.

As a result of the improved dosimetry for the glottis and oral cavity, without any sizeable increase in mean dose to other OARS, we selected OPTIMISED as our standard non-adaptive radiotherapy plan to use for comparison to ADAPTIVE. OPTIMISED will be referred to as the 'NON-ADAPTIVE' plan for the remainder of the thesis.

3.4.2 SUVmax response of primary tumour

All four pilot study cases demonstrated varying degrees of SUVmax reduction in the primary tumour on iPET compared to the prePET in keeping with a metabolic response to treatment. The largest response in the primary disease was seen in case 1 with a relative reduction in SUVmax of 84% (Table 3.2). Case 1 also started with the highest prePET primary SUVmax (21.9), and the largest volume of disease (4.8cm) (Fig. 3.3). These results should be interpreted with a degree of caution as the number of cases is so small, and other factors can influence the SUVmax. The volume of a tumour can have an impact upon the SUVmax due to the Partial Volume Effect. Soret et al (119) explains that two components of the Partial Volume Effect can influence the SUV and alter its value. The first component is the 3D image blurring. This is a consequence of the detector design and reconstruction process which limits the spatial resolution capabilities of the imaging system. 3D image blurring can distort the 3D shape of the structure in question and result in smaller volumes appearing larger and with a lower SUVmax than they really have. The second component is image sampling. This relates to the discordance between the sampled radiotracer on a voxel grid and the actual contours of the area the tracer involves. This is compounded by most voxels containing different types of tissue. `Spilling out' and 'spilling in' of the tracer throughout voxels peripheral to the target can lead to active parts of a tumour appearing less aggressive and necrotic areas looking more active. The overall Partial Volume Effect can be challenging to predict as the spilling out is rarely balanced by the spilling in. A certain amount of mitigation against Partial Volume Effect can be performed by ensuring a large enough volume is drawn around the tumour as Partial Volume Effect doesn't affect the total activity of the tumour.

In addition to SUV signal, the Partial Volume Effect can also have an impact upon the apparent size of the tumour. The actual tumour volume may well be larger than the metabolically active part due to the limits of spatial resolution of fused PET-CT. Likewise, the CT aspect doesn't always include the entire metabolically active part of the tumour as it is restricted to demonstrating the attenuating properties of the tumour only.

Whilst Partial Volume Effect can impact upon the tumour's perceived size, the size of the tumour can conversely impact upon the influence of Partial Volume Effect. Smaller tumours can produce underestimations of the uptake value and so different sized tumours with the same uptake value may produce images with different degrees of brightness, leading to changes in the apparent uptake. Several studies have shown a non-linear correlation between SUV and tumour size; small tumour appearing less aggressive than they are. This is important to bear in mind when interpreting tumour response on PET. If the size of the tumour shrinks, it could give the impression that the SUV has reduced more than it has.

3.4.3 Volumetric response of primary tumour

In all four cases, the bGTV_P reduced in volume on iPET compared to prePET. The largest baseline GTV_P, in case 1, had the largest absolute and relative reduction in volume (71.99%) whereas Cases 3 and 4 had much more subtle reduction of 7.54% and 9.27% respectively. The largest GTV_P volume response correlated with the largest SUV response in the example of Case 1 but the other cases did not demonstrate this relationship. There remain many questions around why some tumours respond better, or faster than others during radiotherapy. Many published studies report differential responses on mid treatment PET-CT.

Not only was there variation in the magnitude of volumetric response, but there were also differences in how the GTV_P reduced in terms of its gross morphology. Case 1, a T4a base of tongue/vallecula tumour reduced in size predominantly in the craniocaudal dimension. Case

2, a smaller T2 base of tongue tumour shrunk more significantly in the transverse dimension. In theory both directions of shrinkage could result in a lower dose to the OARs and subsequent reduction in toxicity. A craniocaudal reduction will reduce the length of pharynx receiving a higher dose of radiation and a transverse reduction could reduce dose to parotid glands and, depending on the degree of shrinkage, spare normal tissue on the contralateral side.

There is a paucity of published data concerning the change in shape of a tumour as it responds to radiotherapy. It is of interest because changes in tumour volume, in addition to other anatomical changes such a weight loss, will impact upon the dosimetry to the surrounding tissues. Random motion during a course of radiotherapy can cause a blurring of dose distribution but systemic changes can lead to a shift of dose. This can lead to under treatment of the target or overdosing to critical structures. The anatomical changes due to tumour response are not only longitudinal but are progressive and may well impact more upon dosimetry than random or systematic changes.

Most publications concern computerised modelling using CT scans and look at ways to predict shape change, rather than comment on the actual way the tumour changes shape. One study (120) that gave information on changes of the actual tumour dimensions during radiotherapy looked at the primary or nodal disease of 14 head and neck cancer patients with GTVs over 4cm. They performed 3 CT scans a week during treatment and determined the volume and positional changes relative to a central bony reference point. Overall, the centre of mass of the shrinking tumours changed position with time suggesting the GTV reduction was asymmetrical. At completion of treatment, the median centre of mass displacement was 3.3mm (0 – 17.3mm) and the GTV volume reduced by 1.8% a day (0.2 – 3.1%). Contrary to this, Takao et al (121) studied pathological lymph nodes in 6 patients using surface geometry mapping. During treatment with 66 – 70Gy in 2Gy/F, they concluded that the tumours reduced uniformly. Yock et al (122) looked at whether the morphological pattern of tumour response could be predicted. A total of 35 tumour volumes were studied, 17 primary and 18 nodal. Morphologies were mapped using landmarks at the surface. 3 computer models were used to forecast the changes in morphology during 70Gy of radiotherapy and concurrent

chemotherapy. The models were able to anticipate longitudinal changes and to some extent characterise the patient specific response. A greater understanding of how tumours reduce in size and volume and whether there is any correlation with stage or site of primary could help improve treatment verification in future and refine PTV margins.

Interestingly, in addition to size and SUV uptake, the Partial Volume Effect also depends upon the shape of the volume. A compact shape has a lower surface area: volume ratio and forms a shape closer to a sphere. The less compact a shape is, the more susceptible it is to being affected by the Partial Volume Effect as a larger part of the volume is close to the edge of the tumour and so more prone to the spilling in/out phenomenon.

3.4.4 Dosimetric impact of ADAPTIVE plans on Organs At Risk

Apart from the contralateral parotid in Case 2, the mean dose to the superior and middle pharyngeal constrictor muscles, the supraglottis, glottis and contralateral parotid gland was reduced by adaptive planning using the PEARL protocol. Case 1 contralateral parotid gland achieved the optimal dose constraint (mean dose < 24Gy) by adaption, with a reduction in mean dose of 2.89Gy, from 26.37Gy to 23.48Gy. This was an unexpected benefit of adaptation, as the contralateral parotid gland was already considered in the optimisation of the NON-ADAPTIVE plan.

Case 2 was a T2N2b right base of tongue tumour that crossed the midline and involved the nodes on the ipsilateral side. The dose to the contralateral parotid increased in this case despite a reduction of the primary tumour volume in the transverse dimension (Fig. 3.5). One possible factor is that the re-contoured volume of the contralateral parotid increased by 12.03% (Table 3.4), which increased its proximity to the high dose volume.

Case 1 T4aN1 Base of tongue/vallecula SqCC	All mean doses across the OARs were reduced in case 1 apart from the oral cavity. Apart from the contralateral parotid gland, no other OARs were brought into tolerance by the ADAPTIVE plan, although all the SWOARs had a reduction in dose. This may reflect the magnitude of response seen on iPET; Case 1 had the largest absolute and percentage change in PTV_P volume on iPET (61.94cm^3, 56.74%) as well as reduction in SUVmax (from 21.9 to 3.3, an 84% reduction).
Case 2 T2N2b Right base of tongue SqCC	ADAPTIVE reduced the mean dose in all OARs apart from the contralateral parotid gland, as previously mentioned. The largest impact seen on the superior pharyngeal constrictor muscle (3.42Gy). The superior pharyngeal constrictor muscle remained over the optimal dose constraint. Case 2 had the second largest reduction in PTV_P volume on iPET (32.52cm^3, 41.35%) and a modest SUVmax reduction of 2.8 (11.9 to 9.1).
Case 3 T2N2b Right base of tongue SqCC	ADAPTIVE reduced the mean dose in all SWOARs, despite the modest reduction in the PTV_P volume on iPET (3.25cm^3). The mean superior pharyngeal constrictor muscle dose was already in tolerance from the OPTIMISED plan and was reduced from 48.54Gy to 46.84Gy. All other SWOARs mean doses remained over the optimal dose constraint.
Case 4 T1N2b Left base of tongue SqCC	ADAPTIVE reduced the mean dose in all SWOARs. The most marked reduction was seen in the glottis. This may be due in part to the reduction in the cranio-caudal dimensions of the PTV_P. Case 4 had the third largest reduction in PTV_P volume (7.21cm^3, 28.3%).

Table 3.6 Summary of impact of ADAPTIVE on dose to OARs

One limitation to my analysis of the impact of ADAPTIVE planning is that I compare it to NON-ADAPTIVE plans which are single phase treatments based on the pre-treatment PET-CT (preCT-PET). The NON-ADAPTIVE plans do not account for changes in anatomy during treatment and may well generate more favourable dosimetry to OARs across the 6 weeks of chemoradiotherapy than is the case. A greater magnitude of impact by ADAPTIVE may be seen by comparing the phase 2 of ADAPTIVE treatment, to NON-ADAPTIVE plans transferred onto iPET-CT. At the time of my data gathering, this was not a feasible option as resource constraints meant that experienced planners were not available to collaborate on this work with me. Whilst I have trained in head and neck VMAT planning, I am unlikely to produce plans of the standard of experienced planners. This would have created bias in my results. It is important to note however, that in everyday clinical practice, we make decisions to accept plans based on dosimetry calculated on the pre-treatment planning scan alone in many cases. Since my initial work on the pilot study for PEARL, physics colleagues Dr Philip Wheeler and Dr Salvatore have presented modelled data using the phase 2 comparisons I have outlined above. I will summarise their work in Chapter 8.

3.4.5 Salivary gland volume changes

Several studies have tracked the size and position of the parotid glands during radiotherapy treatment. The general expectation is for parotid glands to shrink and move medially as the radiation dose received builds up. This has implications for parotid sparing in head and neck cancer radiotherapy as the glands tend to move closer to the high dose volume. Barker et al (124) demonstrated parotid gland volume reduced on average by 0.19cm^3/day (0.04 – 0.84cm^3) and shifts medially by 3.1mm over the course of treatment. This correlated with patient weight loss. Similar findings were published by Castelli et al (125). Brouwer et al (126) who performed a systematic review of publications reporting anatomical changes of OARs in head and neck cancer radiotherapy treatment. Again, the most common anatomical change was a reduction in parotid gland volume and a medial shift of the whole parotid gland. Ricchetti et al (127) performed weekly kV CT on 26 patients and by week 7 the average absolute change in parotid volume was 10ml, the largest relative change was 30%. Some

studies found there was also carinal and dorsal shift. Unfortunately, there was little reference to whether the glands studied were ipsilateral/contralateral to the primary tumour being treated, and whether the treatment involved high dose radiotherapy to both sides of the neck or just unilaterally. Sanguineti et al (128) found that parotid gland shrinkage was not linearly distributed throughout radiotherapy, and that most of the volume change occurred during the first half of the treatment course. The average dose increased to the parotid glands because of these anatomical changes, across all 24 papers reviewed, was 2.2Gy +/- 2.6Gy. Depending on what the intended dose was, an increase of 2.2Gy to the parotid could be significant and move a mean dose into a higher risk bracket for xerostomia. No clear relationship was found between weight loss, parotid volume loss and parotid gland dose; but volume loss and an increased parotid dose had the strongest association.

There is far less information available on radiation induced submandibular gland changes. Brouwer's review concluded submandibular gland lose an average of 22% of their volume by the end of a radical course of head and neck radiotherapy. Wang et al (129) demonstrated significant correlation between planned submandibular gland dose and volume reduction and concluded irradiated submandibular glands tended to move superiorly as well as medially which may result in them having a closer proximity to the high dose region.

The change in volume of the salivary glands is hard to appreciate on cross-sectional imaging. The absolute differences in volume (V) are small; if we assume the glands are spherical-like in shape, the calculation of a sphere is $V=4/3\pi r^3$, the r (radius) is an even smaller component.

In the 4 pilot study cases, there was no unifying pattern of volumetric change for the parotid or submandibular glands. Generally, most glands showed a degree of shrinkage on the CT component of the iPET-CT; the submandibular glands had a greater percentage reduction in volume than the parotids. The exception to this was case 3 which demonstrated enlargement of all 4 major salivary glands. This could be indicative of early radiation induced inflammation. One limitation of our pilot study, however, was that the majority of the OAR delineations were transferred across from the baseline planning PET-CT scan and adjusted on the iPET-CT, rather

than being re-contoured. It may be there is an element of inaccurate delineation or poor volume reconstruction. Based on this, we stipulated in the PEARL trial protocol that all OARS should be reviewed and re-contoured for phase 2 if the conformation is poor on transfer of the OAR volumes from phase 1 to phase 2.

There are 2 possible reasons for the higher degree of submandibular gland volume reduction versus the parotid. The first is that the Leeds planning system may have been optimized to prioritise a reduced dose to the contralateral parotid gland and so it may be that more dose was deposited by the clinical plans more inferiorly at the level of the submandibular glands. Alternatively, because the primary and nodal disease are commonly in closer proximity to the submandibular glands than the contralateral parotid gland, they are exposed to higher doses due to their position. I do not have the delivered dosimetric data for these cases so was unable to correlate volume change to the actual dose the salivary glands received.

In all cases apart from Case 1, the contralateral parotid gland increased in volume with treatment. The increase in size of the contralateral parotid gland may be due to inflammatory effects as it has occurred at an early timepoint to be explained by compensatory mechanisms. One explanation for the shrinkage of the contralateral parotid in case 1 may be the higher dose it received. Case 1 has the largest high dose PTV which crosses the midline, so the contralateral parotid is likely to have been exposed to a high dose.

3.5 Conclusion

I have demonstrated that optimising radiotherapy plans to consider dose to SWOARs, and adapting radiotherapy plans as per the PEARL protocol, have dosimetric advantages. As a result, both methods were taken forward as the standard comparator and the intervention.

Adapting the radiotherapy plan based upon the primary GTV response on iPET reduced most of the dose parameters to the SWOARs in all 4 pilot cases. Crucially, the mean dose was consistently reduced, with a very few exceptions. In some cases, optimal constraints were met when the ADAPTIVE planning was applied. The greatest impact of adaptation was seen in case 1, which demonstrated the largest volumetric, and SUVmax reduction of the bGTV_P. For the other cases there were other aspects to consider, such as the position and size of the primary tumour, as well as its pattern of volume reduction.

Whilst I have demonstrated a broad benefit of adaptation as per the PEARL Study, further cases and more data is required to make more specific conclusions and recommendations for future treatment. My next chapter applies ADAPTIVE planning to the first 4 patients prospectively recruited to the PEARL study, to determine whether there is a continued dosimetric benefit to adaptive radiotherapy within the context of real-world patients recruited to a clinical trial.

Chapter 4: Evaluating tumour response and the dosimetric impact of the PEARL protocol in the first four patients recruited to the PEARL clinical trial.

4.1 Introduction

By modelling plans for the Leeds datasets, the PEARL pilot study outlined in Chapter 3 demonstrated the feasibility of adapting the high dose primary GTV to the FDG avid volume remaining after 2 weeks of chemoradiotherapy. This pilot study also produced objective evidence that adapting radiotherapy as per the PEARL Study protocol, reduced mean dose to OARs associated with toxicity detrimental to quality of life including the superior and middle pharyngeal constrictor muscles, the supraglottis, glottis and contralateral parotid gland. In addition, the optimal dose constraint was reached as a result of adaptation for a proportion of OARs across the pilot study cases.

The PEARL study opened at its first centre, Velindre University NHS Trust, in January 2020. 4 patients were recruited within the first 3 months. Recruitment was subsequently suspended for over 4 months in response to the re-prioritisation of resources within the NHS during the COVID pandemic. In this chapter I present the dosimetric data from these first 4 patients treated on ADAPTIVE plans and compare it to modelled NON-ADAPTIVE plans.

Once PEARL recruitment was open again, the pace of accrual was limited by constraints on numbers of patients that could be accommodated by the radiotherapy department due to the ongoing effects of the pandemic on the department. Other sites due to open PEARL were delayed due to research resources prioritising COVID-related studies.

Subsequent workforce restrictions at Velindre University NHS Trust, in addition to my secondment back to clinical work during the pandemic, impacted on my ability to deliver the original research plan for my MD work. Consequently, I adapted my research plan to accommodate these changes and developed new research questions. One alteration involved the replacement of manual planning with automated planning to produce modelled NONADAPTIVE plans using a novel in-house automated planning system, EdgeVCC. These NONADAPTIVE plans were compared to the manually planned ADAPTIVE plans PEARL patients were treated on. Because of this alteration, in

this chapter I include an assessment of whether automated planning results in dosimetric differences compared to manual planning.

4.1.1 Objectives

1. To apply the novel PEARL adaptive radiotherapy protocol to treatment planning in an NHS clinical setting and deliver ADAPTIVE plans to patients prospectively recruited to the PEARL study.
2. Quantify tumour response seen on iPET-CT after 2 weeks of chemoradiotherapy within the PEARL Study with regards to the size of the primary FDG-avid tumour volume, and its intensity of FDG uptake.
3. Model the potential impact of using a novel in house automated planning technique (EdgeVCC) compared to manual planning in PEARL study patients.
4. Investigate the dosimetric impact of ADAPTIVE plans by reviewing the mean dose received by OARs associated with xerostomia, dysphagia and comparing to NONADAPTIVE plans.
5. Quantify impact of 2 weeks of chemoradiotherapy on the volume of major salivary glands.

4.2 Methods

4.2.1 Prospective recruitment of the first patients to the PEARL Study

The PEARL Study opened to recruitment in January 2000 at the Velindre University NHS Trust. Patients presented at the Southeast Regional Head and Neck Multidisciplinary Meeting are screened for eligibility. The first 4 patients eligible for recruitment accepted the study and have their planning PET-CT scan (pre_PET-CT) performed at The PETIC Centre at Cardiff University.

The PEARL study radiotherapy protocol is subsequently applied, and the patients are treated with ADAPTIVE plans as set out in the PEARL study protocol (Chapter 2). Manual planning was used to generate the ADAPTIVE plans these patients were treated on.

4.2.2 Assessment of tumour metabolic response and the impact on the volume of primary tumour targets after 2 weeks of chemoradiotherapy

4.2.2.1 Defining the biological GTV (bGTV)

The biological GTV (bGTV) is defined as the region of primary tumour avid on PET-CT and consists of the high FDG uptake volume based upon suitable windowing levels.

In preparation for defining the biological Gross Tumour Volume (bGTV), the PET-CT is reviewed by myself in collaboration with Dr Nicholas Morley, Consultant in nuclear medicine. PET and CT components of the scans are reviewed with any relevant clinical information to inform review of the bGTV e.g., to distinguish tumour uptake from physiological uptake or causes for increased FDG uptake such as any infective/inflammatory causes. In addition, a volume produced by automated contouring with the ATLAAS software (bGTV_ATLAAS) is used to inform the final manually contoured bGTV (described fully in Chapter 2).

4.2.2.2 Tumour response according to biological GTV (bGTV) volume

The volume of the primary tumour bGTV on the baseline PET-CT (bGTV_preP) is compared to the volume of the primary tumour bGTV on the PET-CT performed after 2 weeks of chemoradiotherapy (bGTV_iP). Volume measurements calculated by RayStation are recorded.

4.2.2.3 Tumour response according to SUVmax

I use the change in SUVmax of the bGTV_P on the prePET and iPET as a surrogate for tumour response, in addition to the change in the PET-avid volume. For each case, metabolic tumour response is calculated by comparing the SUVmax for the primary tumour reported by Dr Nicholas Morley, nuclear medicine expert, on the PET component of the pre-PET-CT and iPETCT. The PET-avid primary target volume for each case is defined following the PEARL protocol were calculated within Raystation for the biological GTV on the pre-treatment planning PETCT (bGTV_preP) and biological GTV on the interim PET-CT scan performed after 2 weeks of chemoradiotherapy (bGTV_iP).

4.2.3 Contouring of target volumes and organs at risk

The target volumes and OARs for each of the 4 patient cases are contoured as per the PEARL protocol described in Chapter 2. The primary and nodal GTV, clinical target volumes (CTV), planning target volumes (PTV) and organs at risk (OARs) are contoured by me and Dr Thomas Rackley, Consultant Clinical Oncologist and Co-Chief Investigator for PEARL, then manually planned by Dr Owain Woodley, a Velindre radiotherapy planner with clinical guidance from myself and Dr Thomas Rackley.

The schematic previously presented in Chapter 2 is shown again below in Fig. 4.1, demonstrating the expansion of the primary and nodal GTVs for the ADAPTIVE plans as per the PEARL protocol. ADAPTIVE uses 5 dose/fraction levels in phase 2 to reduce the total dose to PTV1_P and PTV2_P. The dose levels for ADAPTIVE and NON-ADAPTIVE plans are outlined in Table 4.1.

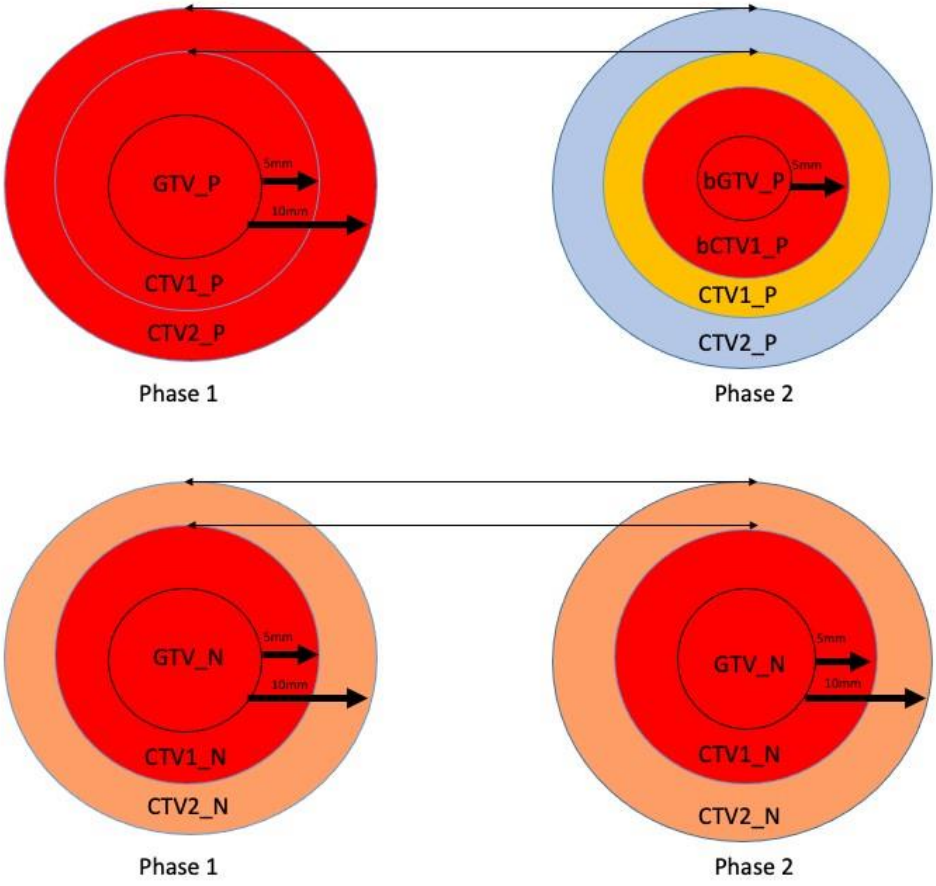

The dose/fraction to the prophylactic nodal level is not altered between Phase 1 and Phase 2 and is treated at 1.63Gy per fraction across both phases

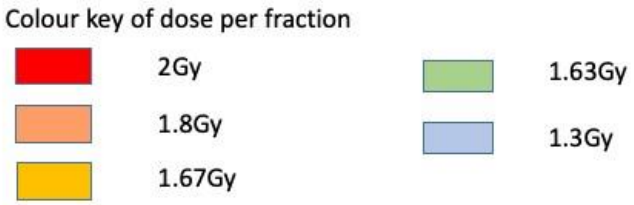

Fig. 4.1 Schematic diagram representing the different dose per fraction levels for phase 1 and phase 2 for the primary and nodal CTVs in ADAPTIVE. Note there is no adaption of the nodal volumes between phases.

	Primary CTV definition	Number of fractions	Dose/fraction to high dose PTVs (Gy)	Total dose to PTVs (Gy)
NON-ADAPTIVE	GTV+5mm GTV+10mm	33 33	2 1.82	66 60
ADAPTIVE Phase 1 Phase 2	 GTV+10mm bGTV+5mm GTV+5mm GTV+10mm	 15 18 18 18	 2 2 1.67 1.3	 30 36 30 54

Table 4.1 Dose levels for the primary CTVs for ADAPTIVE and NON-ADAPTIVE radiotherapy plans

4.2.4 ADAPTIVE plan generation

ADAPTIVE plan generation including the planning prioritisation of non-critical OARs and definition of mandatory dose constraints followed the PEARL Study protocol developed in chapter 2. Dose levels to target volumes are summarised in Fig. 4.1.

4.2.5 Dosimetric impact of adaptive radiotherapy on mean dose to OARs: ADAPTIVE plans compared to NON-ADAPTIVE plans

To demonstrate the dosimetric impact of different planning methods, I focus on the mean dose of radiotherapy (Gy) received by the SWOARs, contralateral parotid and contralateral submandibular glands over the course of treatment. I also look at whether optimal dose constraints are met as a result of the adaptation compared to non-adaptive plans

Identical optimal dose constraints for SWOARS and contralateral parotid and submandibular glands are used for NON-ADAPTIVE and ADAPTIVE plans and are previously described in Chapter 3, Table 3.2.

In order to evaluate the dosimetric impact of ADAPTIVE plans in the first 4 patients treated within the PEARL study, we generated modelled NON-ADAPTIVE plans for comparison. Manually generating NON-ADAPTIVE plans for comparison with ADAPTIVE plans were not feasible at the time due to COVID workforce constraints within the physics department. Instead, an automated planning solution developed in-house at Velindre, EdgeVCC (described in Chapter 1) alongside the physics team led by Dr Philip Wheeler, was used to produce modelled NON-ADAPTIVE plans for each PEARL patient. These are referred to in this chapter as 'NON-ADAPTIVE_AUTO' plans, to distinguish them from manually planned equivalents.

I had been involved in developing the automated solution for head and neck planning (EdgeVCC, described in Chapter 1), alongside the physics team led by Dr Philip Wheeler at Velindre University NHS Trust, to produce modelled non-adaptive plans for each PEARL patient (NON-ADAPTIVE_AUTO).

I was the clinical reviewer in the EdgeVCC team in the development of the automated planning protocol for head and neck NON-ADAPTIVE_AUTO plans. We used the Leeds datasets from the PEARL pilot study to develop the head and neck automated planning protocol and used it to generate automated plans for the first 4 patients recruited to PEARL
(Fig. 4.3).

I looked at the average mean dose to each OAR across the four patients for NONADAPTIVE_AUTO and ADAPTIVE_AUTO.In addition, I looked at whether any optimal dose constraints were met as a result of the adaptation of the plans.

4.2.6 The impact of automated planning on mean dose to organs at risk: Automated ADAPTIVE_AUTO compared to manual ADAPTIVE

Comparing manual ADAPTIVE plans to automated NON-ADAPTIVE plans may introduce confounding factors due to the two different planning methods. To avoid the potential for automated planning to affect the dosimetric impact of adaptation, we also produced automated adaptive plans for each patient which were used for the planning study but not for treatment, referred to in this chapter as 'ADAPTIVE_AUTO' plans. By comparing ADAPTIVE_AUTO plans to ADAPTIVE plans I was able to examine the impact of automated planning on mean dose to OARs.

I used EdgeVCC to generate adapted model plans (ADAPTIVE_AUTO) to compare to modelled NON-ADAPTIVE_AUTO plans, eliminating the potential bias of comparing different planning techniques. This allowed me to ascribe any differences between the two, to the impact of PEARL adaptation alone.

To investigate the impact of using automated and manual planning, I compared the manually planned ADAPTIVE plans used for treatment, to modelled automatedly planned ADAPTIVE_AUTO plans.

I looked at the mean dose to each OAR across the four patients for ADAPTIVE_AUTO and ADAPTIVE. In addition, I looked at whether any optimal dose constraints were met as a result of the automated planning of the plans.

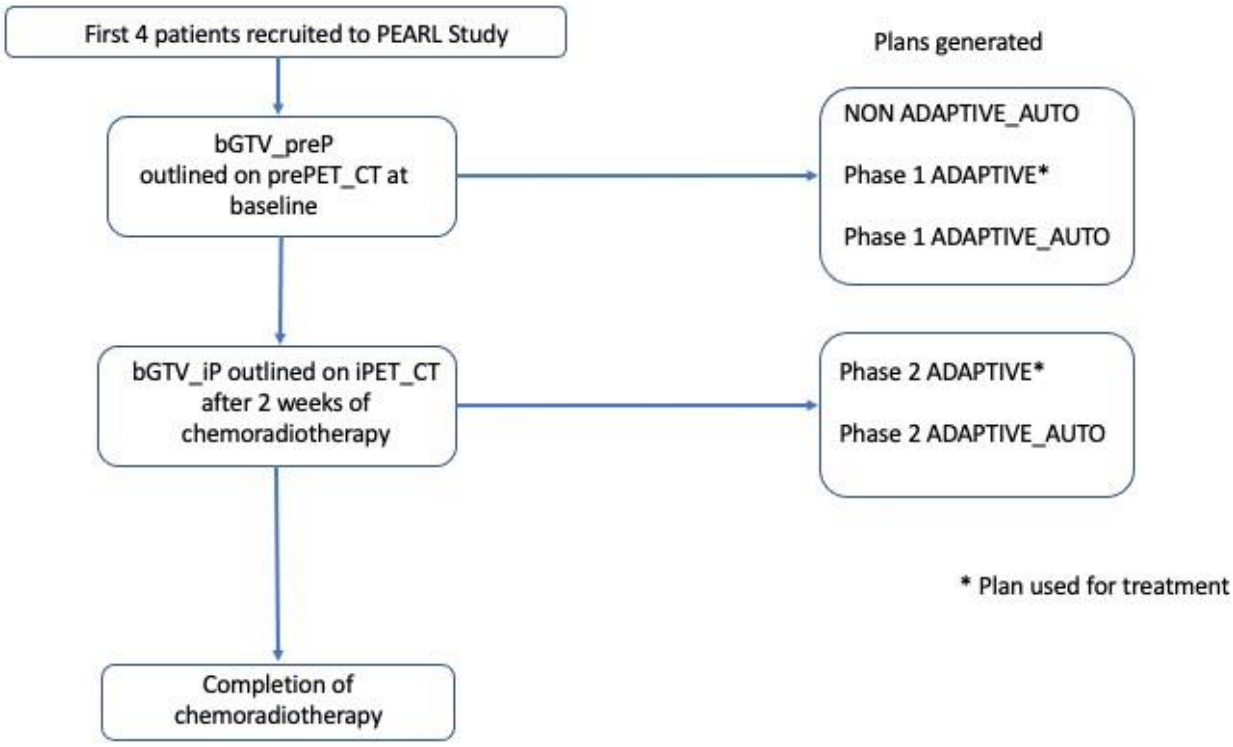

Fig. 4.2 Outline of different plans generated for the first 4 patients recruited to assess impact of adaptive planning and automated planning

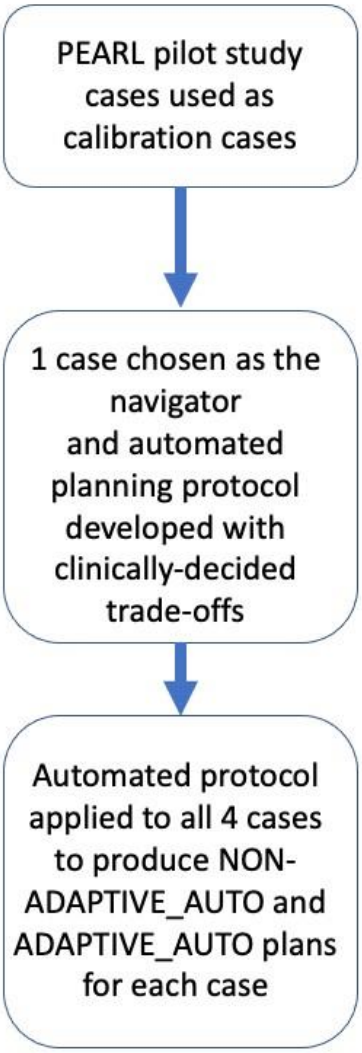

Fig. 4.3 Simplified process of developing the EdgeVCC automated protocol for Head and Neck VMAT planning

4.2.7 Impact of automated planning on PEARL planning workflow compared to manual planning

The planners and physicists working on the PEARL Study were consulted on what differences, if any, the introduction of automated planning had on the turnaround of the Phase 2 plans for PEARL.

4.2.8 Impact of 2 weeks of chemoradiotherapy on major salivary gland volumes

The change in parotid and submandibular gland volumes were calculated from Raystation's measurements of the gland volumes on the CT component of baseline pre-PET_CT and interim iPET_CT.

4.3 Results

4.3.1 Recruitment to the PEARL clinical study and application of the PEARL protocol to patients within a real-world NHS setting

Clinical and radiological details of the first 4 patients recruited to PEARL are described below in Table 4.2. Patients were recruited between January and March 2020, before the PEARL Study had to halt recruitment due to the COVID-19 pandemic. The acceptability rate of the first 4 patients was 100%. Whilst the patient pathway was more complex than a standard treatment pathway, the incorporation of the interim PET-CT after 2 weeks of treatment did not result in any delays to treatment or any missed scanning appointments.

Case	Radiological information	Clinical Information
1 T3N1M0 L tonsil	Well defined tumour left tonsillar fossa. Additional portion fills the vallecula. 5cm long, fixed to pharyngeal wall. Multiple partially necrotic ipsilateral lymph nodes	Large left tonsillar mass fixed to lateral pharyngeal wall and involving glossotonsillar sulcus. Extends to soft palate and anterior tonsillar pillar

2 T2N1M0 R tonsil	Asymmetric right tonsil, 4.1cm. Contacts right inferior soft palate. Abuts glossotonsillar fossa and posterior pharyngeal wall. 2 ipsilateral level 2 lymph nodes up to 1.9cm.	Large right tonsil tumour into soft palate fixed to posterior pharyngeal wall.
3 T2N1M0 L tonsil	Large left tonsil mass involving ipsilateral glossotonsillar fossa, posterior pharyngeal wall and soft palate. Large nodal mass involving level 2 and 1b in addition to nodes in levels 3 and 4.	Enlarged and firm left tonsil
4 T2N1M0 R tonsil	Large well defined right tonsil mass extending from the soft palate to just above the epiglottis. Fills the glossotonsillar fossa and involves posterior pharyngeal wall. Multiple ipsilateral lymph nodes including retropharyngeal and levels 1b, 2 – 4.	4cm firm irregular right tonsil mass. Invades lateral soft palate but not base of tongue.

Table 4.2 Clinical details of first 4 patients recruited to the PEARL study using UICC TNM 8th edition staging

4.3.2 Quantifying tumour response based on SUVmax of the primary seen on iPET-CT scans after 2 weeks of chemoradiation in PEARL patients

In all 4 cases, the primary demonstrated an SUVmax value on prePET consistent with malignancy. In Cases 2 - 4, the SUVmax of the primary tumour was reduced by approximately

50% after 2 weeks of chemoradiotherapy whereas the avidity of the primary tumour in Case 1 increased by 28.5% (Fig. 4.4).

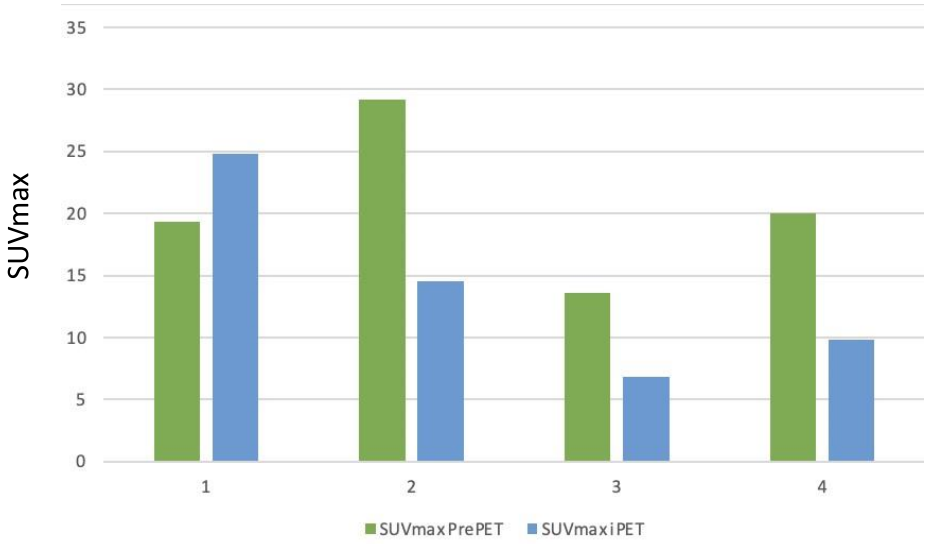

Fig. 4.4 PEARL Patients 1 – 4 comparing SUVmax of biological GTV on pre_PET and iPET

4.3.2 Quantifying tumour response based on the change in volume of the biological GTV on the interim PET-CT scans after 2 weeks of chemoradiation in PEARL patients

In all four patients, the PET-avid volume of the primary tumour on the iPET was reduced compared to the prePET volume, with patients 2 – 4 demonstrating the largest reductions, over 73% reduction in each case (Fig. 4.5). The Phase 2 high dose PTV was consequently reduced for all patients (range 32.43 – 69.38%) (Fig. 4.6).

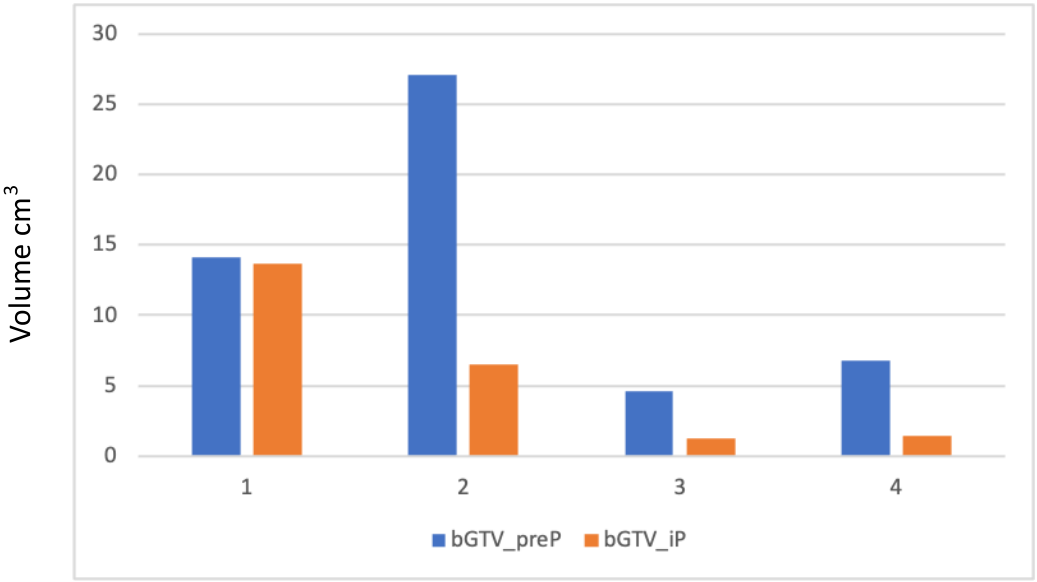

Fig 4.5 Volume of bGTV_prePET and bGTV_iPET for PEARL patients 1 - 4

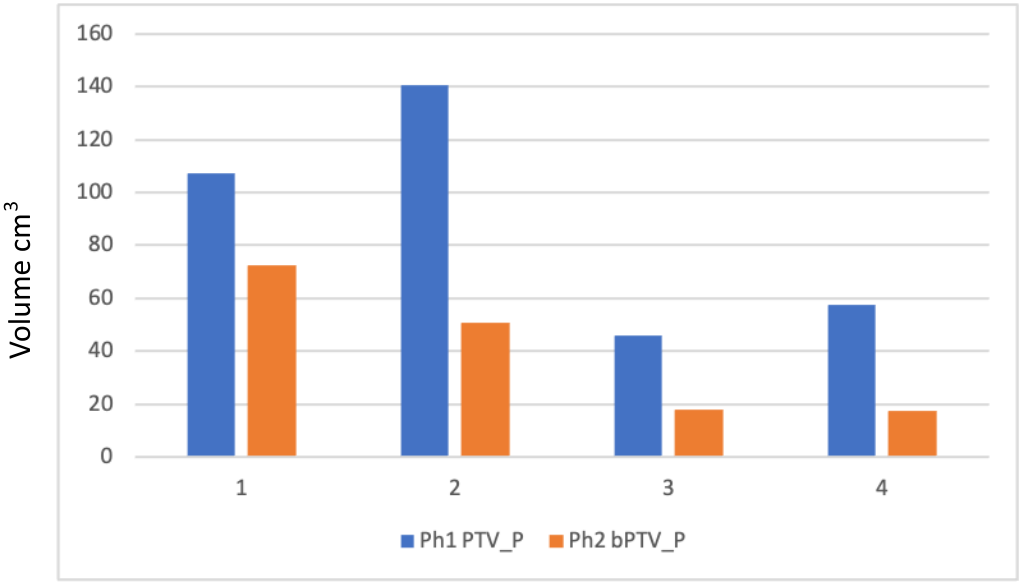

Fig 4.6 Volume of high dose primary PTVs for phase 1 and 2 for PEARL patients 1 - 4

All 4 patients demonstrated a reduction of the FDG avid volume in both the radial and craniocaudal direction after 2 weeks of chemoradiation (Fig. 4.7 – 4.10).

Patient 1

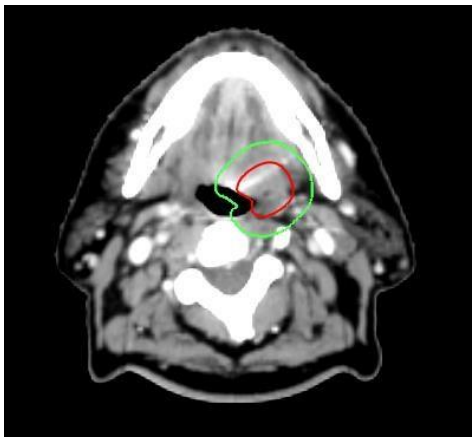

4.7a

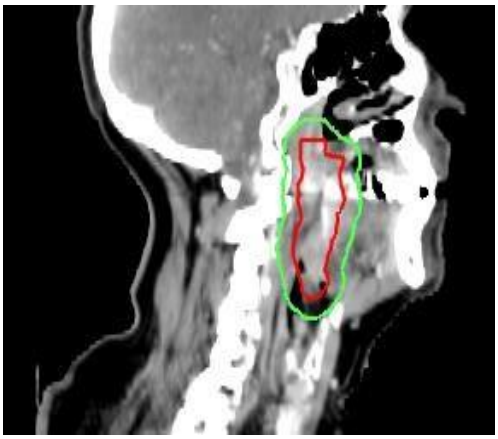

4.7b

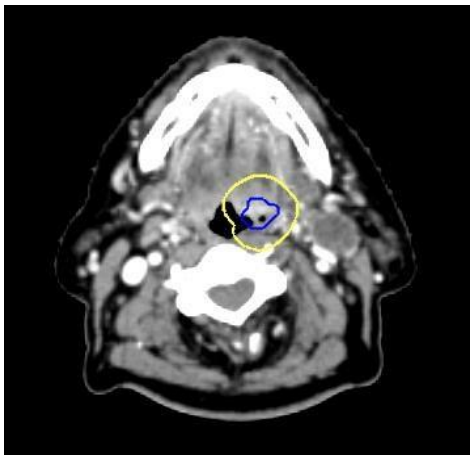

4.7c

4.7d

Fig. 4.7 a – d Transverse and sagittal slices of the CT components of prePET (Fig. 4 a+b) and iPET (Fig. 4 c+d) for Patient 1. GTV_P outlined in red, PTV1_P in green, bGTP_iP in blue, bPTV1_P in yellow.

Patient 2

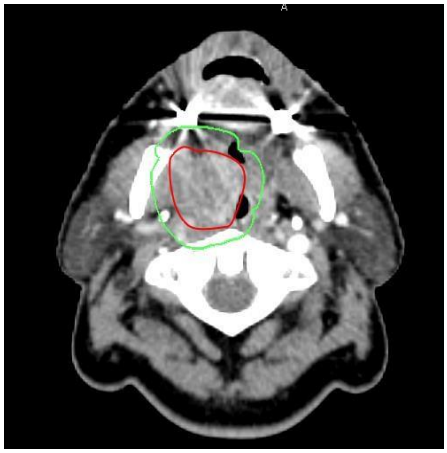

4.8a

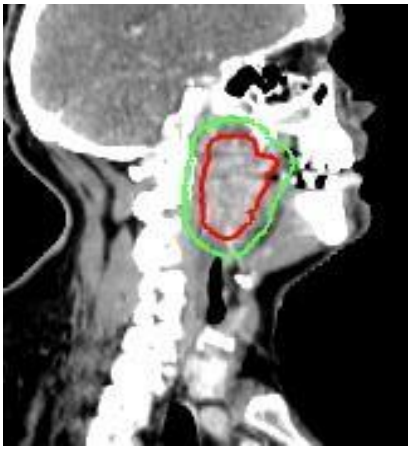

4.8b

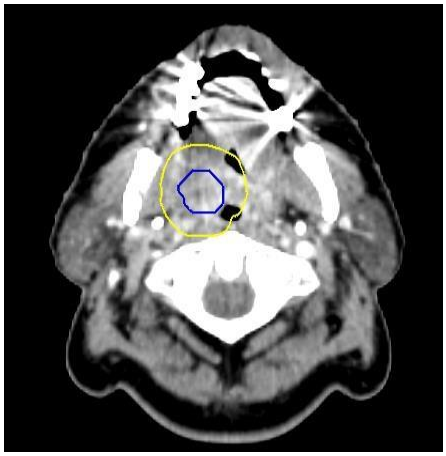

4.8c

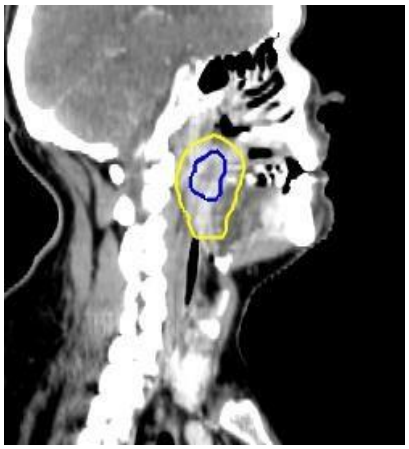

4.8d

Fig 4.8 a- d Transverse and sagittal slices of the CT components of prePET (Fig. 4.8 a+b) and iPET (Fig. 4.8 c+d) for Patient 2. High dose GTV_P outlined in red, PTV1_P in green, bGTV_iP in blue, bPTV1_P in yellow.

Patient 3

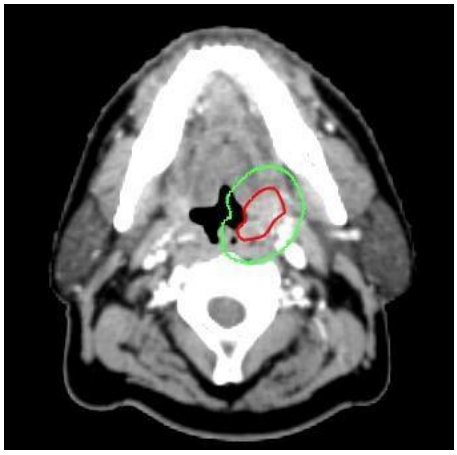

4.9a

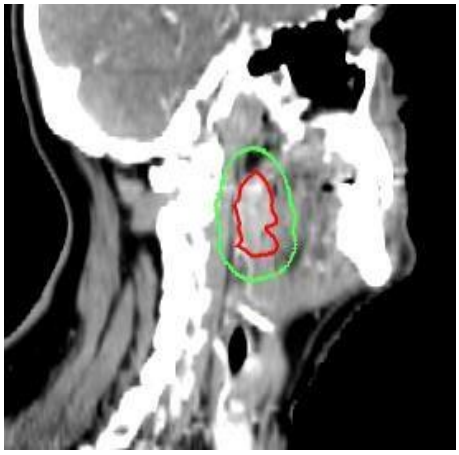

4.9b

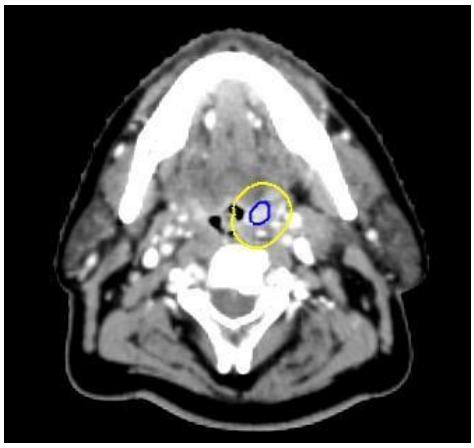

4.9c

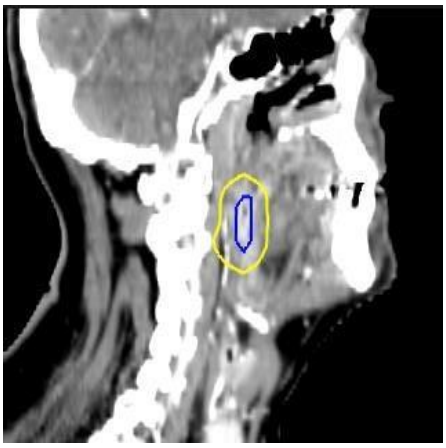

4.9d

Fig. 4.9 a - d Transverse and sagittal slices of the CT components of prePET (Fig. 4.9 a+b) and iPET (Fig. 4.9 c+d) for Patient 3. GTV_P outlined in red, PTV1_P in green, bGTV_iP in blue, bPTV1_P in yellow.

Patient 4

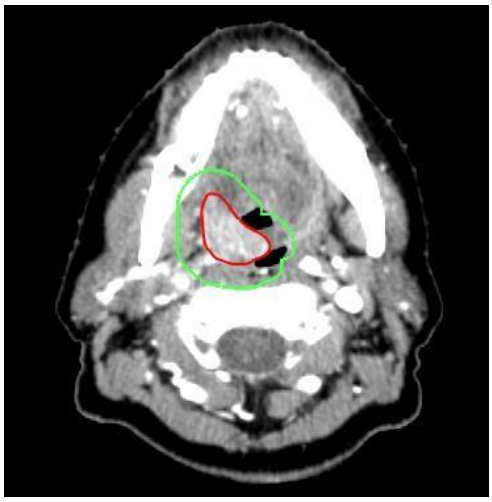

4.10a

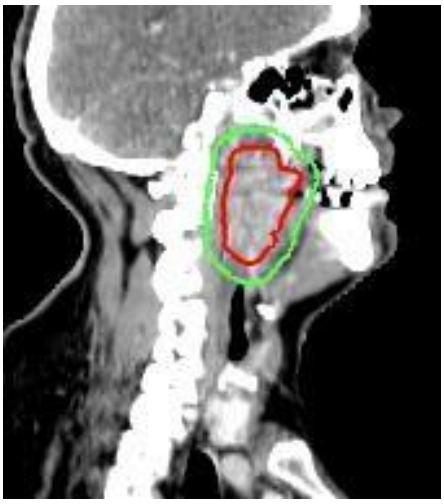

4.10b

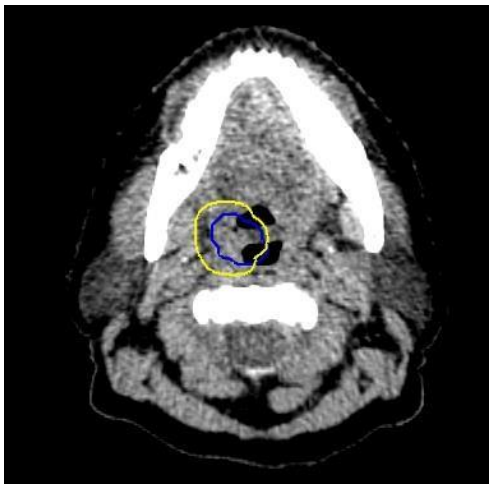

4.10c

4.10d

Fig. 4.10 a – d Transverse and sagittal slices of the CT components of prePET (Fig. 4.10 a+b) and iPET (Fig. 4.10 c+d) for Patient 4. GTV_P outlined in red, PTV1_P in green, bGTV_iP in blue, bPTV1_P in yellow.

4.3.3 Modelled dosimetric changes resulting from ADAPTIVE plans in PEARL Patients 1-4: ADAPTIVE_AUTO compared to NON-ADAPTIVE_AUTO

Fig. 4.11 demonstrates differences in dose distribution following modelled adaptation as per the PEARL protocol using automated planning in Patient 3. Fig. 4.11 a and c show the

NONADAPTIVE plan (synonymous with Phase 1 of the ADAPTIVE_AUTO plans). Fig. 4.11 b+d show Phase 2 of the ADAPTIVE_AUTO plan. In both axial and coronal planes, the 95% isodose (green) is reduced in the Phase 2 ADAPTIVE_AUTO plan based the biological GTV shrinking after 2 weeks of chemoradiotherapy.

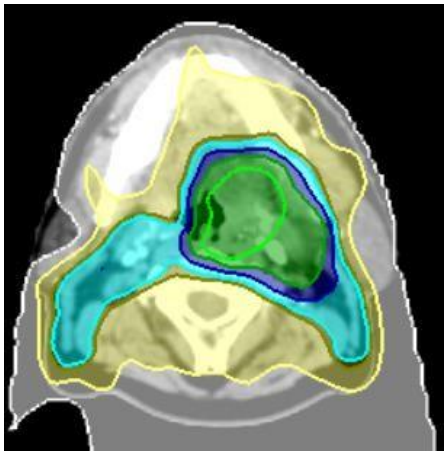

4.11a Patient 3 NON-ADAPTIVE_AUTO

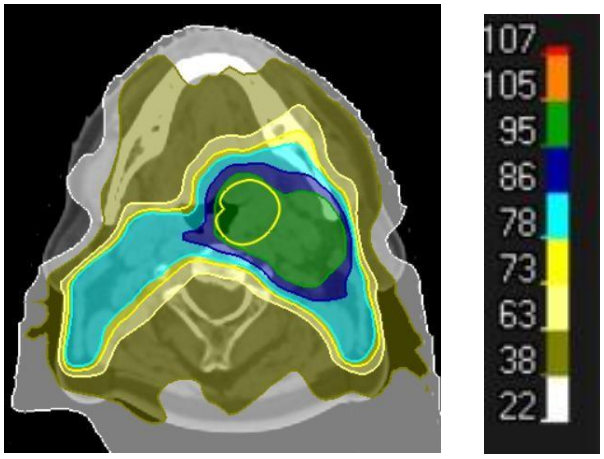

4.11b Patient 3 Phase 2 ADAPTIVE_AUTO

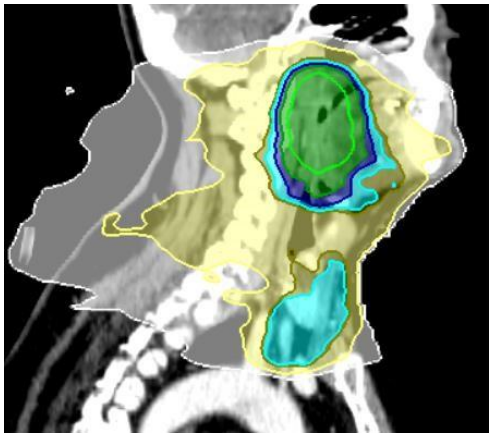

4.11c Patient 3 NON-ADAPTIVE_AUTO

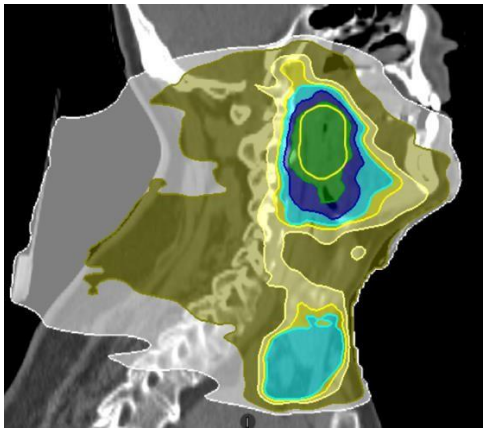

4.11d Patient 3 Phase 2 ADAPTIVE_AUTO

Fig. 4.11 a – d Example slices of plans for Patient 3 demonstrating differences in the dose distribution of NONADAPTIVE_AUTO and Phase 2 ADAPTIVE_AUTO in both the axial and coronal plans. Colour key demonstrates percentage of prescribed dose.

4.3.4 Modelled impact of adaptation on mean dose to organs at risk: ADAPTIVE_AUTO compared to NON-ADAPTIVE_AUTO

The average mean dose to each OAR across all 4 patients for adapted plans was compared to non-adapted plans.

Automated planned adaptive plans resulted in an average mean dose reduction to SWOARs of -0.02Gy per SWOAR (range +3.81Gy - -3.37Gy) when compared to automated planned non-adaptive plans.

A large proportion of SWOARs received a higher mean dose due to adaptation. The superior pharyngeal constrictor muscle was the only SWOAR to have a reduced mean dose in all 4 patients (-0.27 - -2.08Gy), conversely the mean dose to the inferior pharyngeal constrictor muscle was consistently increased by adaptation (0.21 – 3.77Gy).

The greatest reduction in mean dose due to adaptation was seen in the oral cavity and the superior pharyngeal constrictor muscle in Patient 4 (-3.37Gy and -2.08Gy respectively), and the supraglottis in Patient 1 (-3.5Gy). Whilst the supraglottis and glottis had already met optimal dose constraints in all patients with NON-ADAPTIVE_AUTO plans, Patient 4's oral cavity was the only SWOAR to achieve its dose constraint as a result of ADAPTIVE_AUTO (Fig. 4.12 d).

Patient 1 appeared to benefit most consistently from ADAPTIVE_AUTO in terms of reduction in mean dose to SWOARS. Patient 1 also had the highest reduction in any mean dose, 3.5Gy reduction to the supraglottis.

The contralateral parotid gland had already met optimal dose constraints with the NONADAPTIVE_AUTO plans, the ADAPTIVE_AUTO plans generally had a negligible impact on

the glands mean dose. An exception was Patient 3 where the dose was reduced by 2.66Gy. The contralateral submandibular gland was reduced in all 4 patients (range -0.43 - -1.56Gy) but no optimal dose constraint was met.

The ipsilateral parotid gland and submandibular glands displayed a general rise in mean dose in all the cases, up to 3.9Gy increase to the ipsilateral parotid gland in Patient 4 and a 6.73Gy increase to the ipsilateral submandibular gland in Patient 1.

No patient had a consistent reduction in mean dose across all the major salivary glands with adaptive planning.

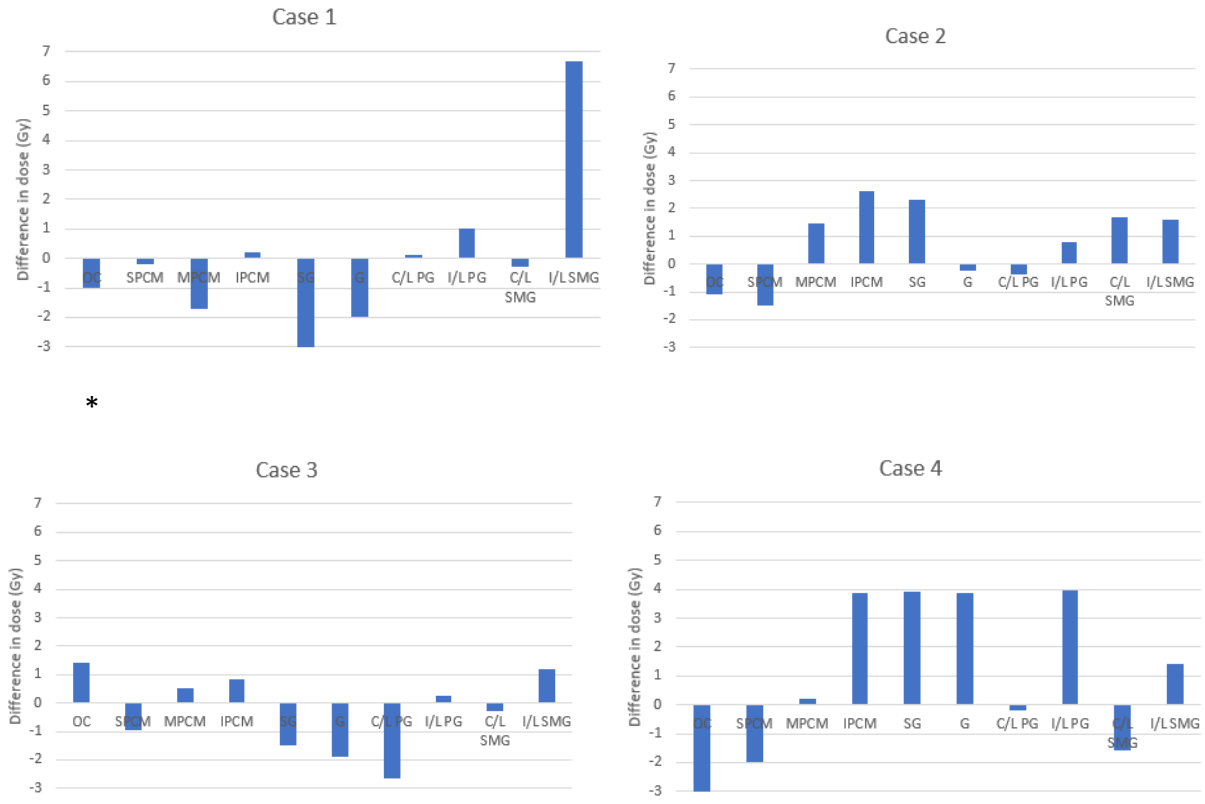

*

Fig. 4.12 a – d Waterfall plots demonstrating change in mean dose received by OARs in PEARL Patients 1 – 4 as a result of ADAPTIVE_AUTO compared to NON-ADAPTIVE_AUTO

* Optimal dose constraint met as a result of adaptation

Key: OC = Oral Cavity, SPCM = Superior pharyngeal constrictor muscle, MPCM = Middle pharyngeal constrictor muscle, IPCM = Inferior pharyngeal constrictor muscle, SG = Supraglottis, G = Glottis, C/L PG = Contralateral parotid gland, I/L PG = Ipsilateral parotid gland, C/L SMG = Contralateral submandibular gland, I/L SMG = Ipsilateral submandibular gland

	Difference in mean dose for OARs (ADAPTIVE_AUTO – NON-ADAPTIVE_AUTO)									
Patient	Superior pharyngeal constrictor muscle	Middle pharyngeal constrictor muscle	Inferior pharyngeal constrictor muscle	Supraglottis	Glottis	C/L Parotid gland	I/L Parotid gland	C/L SMG	I/L SMG	Oral Cavity
1	0.27	1.5	-0.21	3.5	1.83	-0.1	-0.97	0.43	-6.73	1.07
2	1.52	-1.43	-2.64	-2.32	0.23	0.3	-0.79	1.7	-1.63	1.07
3	0.94	-0.51	-0.82	1.98	1.86	2.66	-0.27	-0.2	1.2	-1.33
4	2.08	-0.27	-3.77	-3.81	-3.77	0.28	-3.91	1.56	1.2	3.37

Table 4.3 Average mean dose to OARs for the first 4 patients recruited to PEARL with modelled adaptive and non-adaptive automated plans C/L = Contralateral I/L = Ipsilateral SMG = Submandibular gland

4.3.5 Modelled impact of automated planning on mean dose to organs at risk: Manual ADAPTIVE compared to automated ADAPTIVE_AUTO plans

The average mean dose to each OAR across all 4 patients for manually planned adapted plans was compared to automated planned adapted plans(Table 4.4).

There was a trend of reduction in the mean dose to most SWOARs across all 4 patients with automated planning when compared to manual, with a mean reduction of 2.9Gy per SWOAR (range +5.03Gy - -17.42Gy). Patient 2 was the only patient not to have a reduced mean dose due to automated planning across all SWOARs.

The greatest absolute benefit of automated over manual planning was seen in the more caudal structures; inferior pharyngeal constrictor muscle, supraglottis and the glottis, which saw a reduction in mean dose across all four patients. The glottis was the OAR to benefit the most from automated planning and had dose reductions up to 17.42Gy (range -13.36 – -17.42Gy) compared to manual planning.

Smaller differences between manually and automated planning methods were seen in the superior pharyngeal constrictor muscle and middle pharyngeal constrictor muscle. For patient 2, automated planning conferred a higher mean dose compared to manual.

The only optimal dose constraint met as a result of automated planning was the oral cavity in Patient 4. The supraglottic and glottic mean doses were already within optimal constraints with manual ADAPTIVE plans.

Automated planning produced a lower mean dose to the major salivary glands compared to the manually planned. The contralateral submandibular gland in Patient 4 had the greatest

absolute reduction in mean dose (-9.33Gy) with automated planning and in the same patient, the contralateral parotid gland mean dose was reduced by 7.38Gy, meeting the optimal dose constraint as a consequence. The contralateral parotid mean dose was consistently lower with automated planning compared to manual across all 4 patients with a range of -1.19 - 7.38Gy.

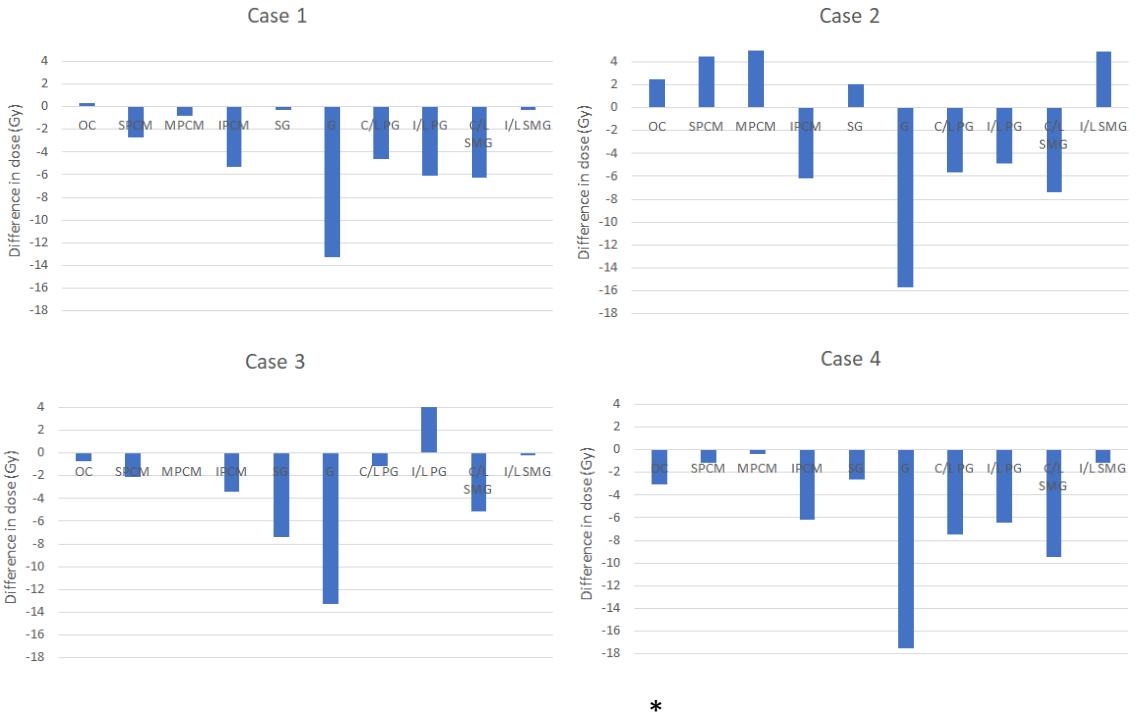

*

Fig 4.13 Waterfall plots demonstrating change in mean dose received by OARs in PEARL Patients 1 – 4 as a result of ADAPTIVE_AUTO compared to manually planned ADAPTIVE plans.

* Optimal dose constraint met as a result of automated planning

Key: OC = Oral Cavity, SPCM = Superior pharyngeal constrictor muscle, MPCM = Middle pharyngeal constrictor muscle, IPCM = Inferior pharyngeal constrictor muscle, SG = Supraglottis, G = Glottis, C/L PG = Contralateral parotid gland, I/L PG = Ipsilateral parotid gland, C/L SMG = Contralateral submandibular gland, I/L SMG = Ipsilateral submandibular gland

	Difference in mean dose for OARs (ADAPTIVE – ADAPTIVE_AUTO)									
Patient	Superior pharyngeal constrictor muscle	Middle pharyngeal constrictor muscle	Inferior pharyngeal constrictor muscle	Supraglottis	Glottis	C/L Parotid gland	I/L Parotid gland	C/L SMG	I/L SMG	Oral Cavity
1	-2.64	-0.71	-5.18	-0.33	-13.36	-4.59	-6.21	-6.48	-0.3	0.39
2	4.42	5.03	-6.16	1.86	-15.33	-5.61	-4.58	-7.09	4.84	2.7
3	-2.17	0.08	-3.27	-7.3	-13.31	-1.19	4.0	-5.2	-0.1	-0.61
4	-1.15	-0.5	-6.31	-2.55	-17.42	-7.38	-6.43	-9.33	-1.1	-3.08

Table 4.4 Average mean dose to OARs for the first 4 patients recruited to PEARL with manual adaptive and modelled automated adapted plans

C/L = Contralateral I/L = Ipsilateral SMG = Submandibular gland

4.3.6 Impact of automated planning on PEARL planning workflow compared to manual planning

Time to plan an automated plan was reduced compared to manual planning by up to 360 minutes. In addition, 3 members of the physics team were able to independently produce automated plans following the PEARL protocol, whereas only one member of staff was independent at manual planning.

4.3.7 Changes in salivary gland volumes as a result of 2 weeks of chemoradiation

There was an inter- and intra-individual variety of different responses seen in regard to volume of the major salivary glands at 2 weeks of chemoradiation across the 4 cases. The contralateral parotid gland volume reduced in two cases by 6.11% and 39.1% and increased in the remaining two by 0.6% and 45.34%. In two cases, the contralateral submandibular glands shrunk by 4.82% and 21.95% and increased by 0.57% and 14.76% in the other two. The ipsilateral parotid glands reduced in size (range 9.23 – 40.53%) after 2 weeks of chemoradiation in 3 of the 4 cases, and the ipsilateral submandibular glands reduced in all 4 cases by 4.43 – 62.19%. The ipsilateral submandibular glands were the only major salivary glands to shrink in all 4 cases. Case 3 demonstrated the largest percentage reductions and was the only case to show a reduced volume of all 4 major salivary glands after 2 weeks of treatment.

Patient	Contralateral Parotid Gland	Ipsilateral Parotid Gland	Contralateral Submandibular gland	Ipsilateral Submandibular gland
1	0.6	-1.35	-4.82	-12.68
2	-6.11	-9.23	0.57	-4.43
3	-39.10	-40.53	-21.95	-62.19
4	45.34	28.65	14.76	-19.02

Table 4.5 Percentage change in volume of parotid (parotid gland) and submandibular glands (submandibular gland) on iPET-CT.

4.4 Discussion

In this chapter I have presented work that meets the objectives set out in Section 4.1. The PEARL study opened to recruitment, and I was involved in the successful recruitment of the first four patients. Currently the PEARL trial is still open and recruiting new patients in 4 sites across the UK. An additional site is about to open. Across the UK recruitment is below target, partly due to covid-19, although recruitment within Velindre has been excellent with 100% percent of eligible patients approached to enter the trial accepting enrolment.

Challenges to recruitment include resource constraints on clinical trial units resulting in trials sitting in set up pipelines for prolonged amounts of time. Other difficulties arise from variations in treatment paradigms between cancer centres e.g., whole tonsillectomies in place of targeted tonsillar biopsies. The removal of the primary tumour makes the patient ineligible for PEARL as there would be no avid primary on the baseline PET-CT.

I have demonstrated the feasibility of applying the novel PEARL adaptive radiotherapy protocol to patients in a real time NHS setting, and the treating of them with manually planned adaptive radiotherapy.

I have quantified the response of the tumour after 2 weeks of chemoradiation both in terms of avid tumour volume, and the intensity of the FDG uptake by this volume. I have presented data on changes to dosimetry as a result of adaptive manual planning. I have also assessed the impact of automated planning by producing automated adaptive plans to compare with manual adaptive plans.

4.4.1 Treatment response in the primary tumour

The baseline biological primary GTV in all 4 PEARL cases had a SUVmax of 13.6 – 29.2 on the baseline planning scan, consistent with a diagnosis of primary OPSCC and in line with the SUVmax seen on the prePET-CT of the pilot study case studies presented in Chapter 3 (11.9 – 21.9).

Patients 2 – 4 all demonstrated a similar percentage reduction in the SUVmax on the iPET-CT after 2 weeks of chemoradiation (-49.0 - -50%) which was less varied than the percentage reduction seen in the pilot study (-23.4 - -84%). Patient 1 was an outlier and demonstrated an increase in SUVmax on the iPET-CT.

As previously discussed in Chapter 2, the optimal timing of the iPET-CT was defined after reviewing the literature. The consensus is that performing the iPET-CT after 10 – 14 days of chemoradiotherapy, or up to approximately 20Gy of radiotherapy is the optimal time, balancing the opportunity for impact of radiotherapy on the tumour with the potential for radiotherapy-induced inflammation causing a temporary rise in SUVmax. It is likely that the increase in avidity for case 1 was caused by radiotherapy-induced inflammation. For the purposes of the PEARL study however, the impact of PEARL adaptive radiotherapy relies more on the volumetric change in the avid tumour rather than the change in avidity. Patient 1 did demonstrate a reduction in the avid volume (bGTV_P) on iPET-CT, even though it had the smallest percentage change (-4.9%) of all the cases. The percentage change of the bGTV_P volume for Cases 2 – 4 was very similar (83.1 - 86.9%).

It is probably more relevant to PEARL adaptive, and potential to organ spare, to look at the absolute changes in volumes of the bGTV between the prePET-CT and iPET-CT as this will result in the change in volume of the high dose primary PTV which receives the full treatment dose. This varied more widely amongst the cases, from 6.1 – 40.27cm^3 with Case 2 having the largest

absolute reduction in volume and translating in the largest reduction of the high dose primary PTV (140cm^3 to 47cm^3).

The morphological changes in the avid volumes between the prePET-CT and iPET-CT included shrinkage in both the craniocaudal and radial directions with a larger reduction generally seen in the caudal and lateral extensions of the avid tumour. This offers the potential for both sparing of the pharyngeal lumen in addition to the more lateral structures including the parotid glands.

4.4.2 Impact of adaptation on modelled mean dose to OARs: ADAPTIVE_AUTO versus NON-ADAPTIVE_AUTO

The impact of adaptive planning compared to non-adaptive planning on the mean dose to SWOARs and xerostomia-associated OARs using automated planning was not as I had expected from the results of the PEARL Pilot Study presented in Chapter 3. No patient benefitted from automated adaptive planning to the same extent in terms of absolute reduction in mean doses to SWOARs compared to the pilot cases which had all been manually planned.

The greatest differences in the mean dose to OARs between the automated adaptive and automated non-adaptive plans was seen in the more caudal swallowing structures; inferior pharyngeal constrictor muscle, supraglottis and glottis. The impact was mixed however, with some patients having a mean dose reduction and others an increase. This could be the result of a combination of different tumour locations and the way the different planning methods drive down dose to OARs to achieve optimal dose constraints.

The two cases with the largest absolute reduction in high dose PTV volume (Patient 2 and 4), also showed the greatest reduction in mean dose to superior pharyngeal constrictor muscle as a result of adaptive radiotherapy but this came at the expense of an increase in mean dose

for the other SWOARs. There are a few possible reasons for this. The first is that the superior pharyngeal constrictor muscle is often in very close proximity to the primary oropharyngeal tumour. Consequently, adapting the radiotherapy plan for any reduction in the volume of the primary is likely to reduce the dose away from the midline in a similar axial plane to the superior pharyngeal constrictor muscle resulting in its exposure to a lower dose. Another explanation is that because the superior pharyngeal constrictor muscle is often so close to the oropharyngeal primary, the optimal superior pharyngeal constrictor muscle dose constraints are rarely met, and so the optimisation algorithm works harder to bring the mean dose to the superior pharyngeal constrictor muscle down at the expense of other OARs where the dose constraint is already met, or at a lower priority.

The superior pharyngeal constrictor muscle was the only OAR which benefited from automated adaptive planning, compared to automated non-adaptive planning, across all cases (mean dose reduced by 0.27 – 2.08Gy) although no optimal dose constraint was met as a result.

3 of the 4 patients had a reduction in mean dose to the contralateral salivary glands with the automated adaptive plan compared with the automated non adaptive plan. The mean dose to the ipsilateral salivary glands increased, possibly because of the prioritisation of the contralateral glands and the primary tumour regressing away from the pharyngeal lumen and contralateral OARs, but not moving position in relation to the ipsilateral parotid gland and submandibular gland due to constraints by the anatomy.

After review of these initial results, the case for continuing recruitment into the PEARL study was carefully considered. Manual adaptive planning did not demonstrate the benefit compared to automated non-adaptive planning that was expected based on the results of the PEARL Pilot Study presented in Chapter 3. I concluded that it was likely that the impact of adaption as per the PEARL protocol, is confounded by the difference in planning technique, with automated planning *per se* resulting in reductions in mean doses to OARs that were greater than those seen with adaption. I therefore collaborated with the EdgeVCC team to

produce automated adaptive plans to compare with manual adaptive plans to investigate the extent to which mean OAR dose is altered by the different planning techniques.

Considering the observed limited impact of ADAPTIVE compared to NON-ADAPTIVE_AUTO, and on the advice of the PEARL Trial Steering Committee, the PEARL RTTQA team are currently in the process of looking at the dosimetry of Phase 2 for the first 20 patients recruited to PEARL to assess the impact of adaption in a prospective cohort of patients where automated adapted and non-adapted plans were generated. The results of the first 10 patients demonstrate that adaptation significantly reduced dose to the superior and middle pharyngeal constrictor muscles, and the supraglottic larynx, with no increased dose to other OARs. Whilst the mean dose metrics were reduced by <1.2Gy, the reduction in the high (prescription) dose was reduced by up to 12%. This provided objective data that PEARL was producing a dosimetric benefit and reassurance that the PEARL study should remain open to recruitment.

4.4.3 Impact of automated planning on mean dose to OARs

The trend in lower mean dose to OARs with automated adaptive plans compared to manual adaptive plans suggests that automated planning improves organ sparing compared to manual planning in keeping with published literature appraised in Section 1.9. This may explain why a smaller benefit to adaptation is seen when automated non adaptive plans are compared to automated adaptive plans. To assess the impact of adaptation without the influence of automation, manually - planned non-adapted plans are required, as presented in the results of the PEARL Pilot study in Chapter 3. As a clinician trained in planning but with limited planning experience, I was unable to produce these plans myself with sufficient expertise to avoid introduction of bias. The standard of plan I can produce would not be as high as plans produced by the experience planner who produced the manual adaptive plans for PEARL. The unavailability of these manual nonadaptive plans, alongside the small number of patient cases, is an important limitation to this chapter. I discuss on going work by a collaborating physics team responding to this limitation in Chapter 8.

4.4.4 Changes in volume of major salivary glands

As demonstrated in the pilot study, there was no uniform pattern of volume change in the parotid and submandibular glands (submandibular glands) in Cases 1 – 4 of the PEARL study. It is common for salivary glands exposed to radiation to shrink and move medially. submandibular glands can also move superiorly. In the context of primary oropharyngeal cancers, this change in size and position often brings the glands closer to the primary and therefore areas of high dose. This change may well offset any advantage of a smaller high dose volume. The other issue is that when using the metric of mean dose, the reduction in glandular volume will influence the mean dose value if a greater percentage of the glands are in the high dose region.

The ipsilateral submandibular gland consistently shrank to a greater extent than the contralateral (-4.43 – 62.19% versus 14.76 - - 21.95%). This is logical as it would be expected for the ipsilateral submandibular gland to be closer to the primary and so receive a greater dose of radiotherapy than the contralateral submandibular gland. Brower et al (143) showed that the submandibular glands lose an average of 22% of their volume by the end of a course of radiotherapy in line with my findings.

The parotid glands were more variable, and in some cases, increased in volume between the prePET-CT and iPET-CT. This may be as a result of radiotherapy-induced inflammation and/or due to technical artefacts including poor reconstruction of the OARs onto the iPET-CT. Sanguineti (145) showed that due to their change in position and morphology during a course of radiotherapy, parotid glands could receive an additional 2.2Gy on average. I have shown in my dosimetry results that re-planning after a proportion of radiotherapy has been received, can reduce the mean dose received by the contralateral parotid glands. This may be in part due to the adaption of the parotid gland contours to their new size and positions.

4.4.5 Impact of automated planning on PEARL planning workflow compared to manual planning

In addition to dosimetric advantages, automated planning reduces the preparation time for patient radiotherapy treatment. Based on the Velindre Cancer Centre's experience to date, the average automated planning time for a typical head and neck VMAT plan is 60 – 80 mins, approximately a third of the time spent manually planning the same case. This has obvious benefits for a radiotherapy department in terms of human resources in addition to improved availability of hardware and treatment planning system software licences. The NHS radiotherapy department I was based in at the time was already over-stretched regarding number of treatment planners trained to manually plan head and neck VMAT plans. The impact of the COVID pandemic compounded this pressure. The option of a planning method that was quicker and required less human input was an important mitigating factor for this. Working with Phillip Wheeler and the automated planning development team allowed me to use the automated planning technique to plan NON-ADAPTIVE_AUTO and ADAPTIVE_AUTO plans for use in my research whilst simultaneously assisting their work towards gaining approval for the clinical implementation of EdgeVCC into the clinical workstream.

Automated planning looks very promising in regard to its role in RTTQA for studies and in the potential benefits to patients if the OAR sparing converts into clinically significant reductions in toxicity. However, it is also likely that the use of automated planning may also reduce the impact of adaptive planning as demonstrated by my results so far. As far as I am aware, there is no published data comparing the impact of adaptive versus automated planning to a manual non adapted plan.

4.4.6 Unexpected findings on interim PET-CT (iPET-CT) and subsequent changes in patient management

The performing of an interim PET-CT after 2 weeks of chemoradiotherapy offered a unique opportunity to assess the tumour's response to treatment. In some cases, it also added additional information that changed the patient's treatment in a variety of ways.

4.4.6.1 Radiological diagnosis of COVID-19

In one case, the iPET-CT scan demonstrated new bilateral lung changes consistent with pneumonitis. The patient was asymptomatic at the time, but a radiological diagnosis of COVID-19 was made. Subsequent testing by polymerase chain reaction confirmed the diagnosis of COVID-19. Consequently, the patient was advised to self-isolate as per the national guidance and take the precautions mandated at the time. In addition, their treatment slots in the radiotherapy and chemotherapy departments were moved to the final slot of each day to allow for deep cleaning after each session to reduce the risk of infecting staff and other patients.

4.4.6.2 New contralateral avidity on iPET

In another case, the iPET-CT demonstrated avidity in the contralateral neck which had not been seen on the pre-PET-CT. The imaging was reviewed by both a nuclear medical expert, and head and neck radiologist. The consensus was that this was likely to represent a pathological lymph node. Because of the change in staging, the high dose nodal CTVs were changed to include the contralateral avid lymph node and additional contralateral nodal levels included in the prophylactic nodal volume.

Had the patient been diagnosed with contralateral disease at the time of staging, they would not have been eligible for the PEARL study as the exclusion criteria for nodal staging at the time was N2 or N3 disease. However, the PEARL study was planned for an intention to treat analysis and so, after discussion with the PEARL statistical team, the patient has been included in the study for follow up of results.

4.4.7 Limitations

My work has several important limitations to consider when interpreting the results.

1. Small patient numbers: This means I can only perform limited analyses on my data, and report trends rather than statistical significance. To partly mitigate for this, I have presented data on 3 different plans for each patient, assessing both the impact of adaptation and automated planning on mean dose to OARs.

2. Mean Dose metric: It is possible that by using the mean dose metric, there are dosimetric advantages of adaptive radiotherapy that are hidden from my analysis. As explained in Chapter 2, mean dose is the most uniformly used metric when defining optimal dose constraints for SWOARs and major salivary glands. This is based on the NTCP modelling work referenced to earlier in my thesis. Mean dose, however, does not allow for analysis of the impact of a heterogenous dose within an OAR. As I have mentioned in Section 4.4.4, work performed by the PEARL RTTQA team which looked further into other dose/volume metrics may revealed additional dosimetric advantages of PEARL adaptive radiotherapy. I outline on-going research addressing this in Chapter 8.

3. Lack of manually planned non-adapted plans: I have demonstrated that the method of planning – manual versus automated - can impact on the mean dose to OARs to a similar or greater extent as the PEARL adaptation process and must be factored into future analyses looking at the dosimetric impact of adaptive radiotherapy.

4.5 Conclusion

The PEARL Study opened and recruited the first 4 patients eligible to enter.

The clinical implementation of the PEARL Study protocol was successful in delivering biological response-adapted radiotherapy to the first 4 patients recruited. The impact of the COVID pandemic resulted in the need to re-think my research plan and working with the automated planning development group at Velindre, I was able to develop model nonadapted VMAT plans for comparison. The impact of PEARL adaptation seen in the pilot study was not reflected in the findings of this comparative study, consequently, I altered my research question to include a closer look at the potential confounding impact of using automated planning instead of manual planning.

The potential benefit of automated planning is clear, from a practical perspective, and a dosimetric advantage. Practically, automated planning reduces the time of planning by up to 3 – 4 hours compared to manual VMAT planning. It is also easier to train additional planners to plan automatedly compared to manually. Considering these advantages, patients subsequently recruited to PEARL from Velindre Cancer Centre, were planned with an automated technique. Automated planning also has an important role to play in the standardisation of patient plans for trial QA and presents an efficient alternative to manual planning which many pressured healthcare systems could benefit from. Its superior dosimetry – particularly in head and neck planning - has been described in the literature and this is reflected in my work to date. This dosimetric advantage may well translate into clinical benefit to the patient.

In this chapter, I have demonstrated that automated non-adaptive plans often produce similar, if not greater, reductions in mean dose to OARs compared to manually planned adaptive and so may negate the advantage of PEARL adaptive radiotherapy to some extent.

It will be of utmost importance that the results of the PEARL study, with the benefit of greater patient numbers, are analysed with this as a consideration before final conclusions about the impact of PEARL adaptation are drawn.

Chapter 5: Development of an alternative planning protocol for The PEARL Study

5.1 Introduction

After the first 4 PEARL Study patients were recruited and completed their treatment, the PEARL Trial Management Group reviewed the protocol. There were 2 main concerns highlighted:

1. The length of time the manual planning of Phase 1 and Phase 2 was taking the planners to complete. As presented in Chapter 4, the manually planned adaptive VMAT radiotherapy plans (ADAPTIVE) took approximately 360 minutes of planner time to fully plan. Moreover, due to the complexity of Phase 2 of the PEARL planning protocol, there was only one planner who was fully skilled to independently plan for PEARL in Velindre at the time PEARL was opened. There was also a reduced number of general head and neck planners in the department which resulted in pressure on the time spent planning head and neck plans. When the COVID pandemic started, this pressure increased, and the process of planning became more complicated, due to constraints on the number of planners able to work in the department at any one time. In addition, the need to open PEARL in multiple centres across the UK meant that simplicity and ease of adoption of the protocol was of upmost importance.

2. The second concern was that the dose per fraction to PTV2_P in Phase 2 of ADAPTIVE receives 1.3Gy (Table 7, Chapter 2, p53). Some members of the TMG felt this was potentially suboptimal for effecting a microscopic tumoricidal impact.

The TMG wanted to simplify the PEARL planning process whilst increasing the minimal dose/fraction. Throughout discussions regarding alterations to the PEARL planning protocol, consideration was given to the potential impact on radiation dose received by OARs due to a new planning protocol, and whether any planning protocol change could be a confounding factor in the interpretation of the results of PEARL and their attribution to adaptive radiotherapy.

5.1.1 Objectives

1. To simplify the PEARL planning process by adjusting the prescription doses per fraction for Phase 1 and 2, with the intention of reducing time required for planning PEARL patients, and simultaneously increasing the prescription to all PTVs above 1.3Gy/fraction throughout treatment.
2. To assess the impact of the new PEARL planning protocol by comparing mean dose received by OARs with original PEARL protocol.

5.2 Methods

I formed a working group including the PEARL chief investigators, physics leads, and radiotherapy planners, in addition to head and neck clinical oncologists at Velindre Cancer Centre, to discuss ways to simplify the PEARL planning process. I chaired a meeting to discuss the impact of PEARL planning on resources, and the low dose per fraction to PTV2_P in Phase 2. Potential solutions were presented and debated.

The PEARL planning method (ADAPTIVE) was studied. A smaller number of dose/fraction levels in Phase 2 ADAPTIVE was identified as the adjustment most likely to reduce the time taken to plan and simplify the training of other head and neck planners for PEARL both within Velindre and in additional sites across the UK.

5.2.1 Simplification of the PEARL planning process

The initial PEARL planning protocol (from now on referred to as 'ADAPTIVE_A') included the prescription of a total of 3 different dose per fraction levels in Phases 1, and 5 dose levels for Phase 2 (Fig. 5.1). This enabled a reduction in dose to the areas of the primary CTV that could

be safely de-intensified due to biological response on the PET component of the iPET_CT in Phase 2.

Following consensus from the working group, a new planning protocol 'ADAPTIVE_B' was developed with only 3 dose levels for Phase 1 and 2. This is achieved by keeping the dose to PTV1_P and PTV2_P consistent between Phase 1 and Phase 2 and using a simultaneous integrated boost to increase dose to the bPTV1_P and PTV1_N in Phase 2. Primary and nodal dose levels are aligned and are all prescribed to a minimum of 1.63Gy/F (Fig. 5.2). The total dose delivered to each PTV at the end of both phases remained the same in ADAPTIVE_B as it was in ADAPTIVE_A (Table 5.1).

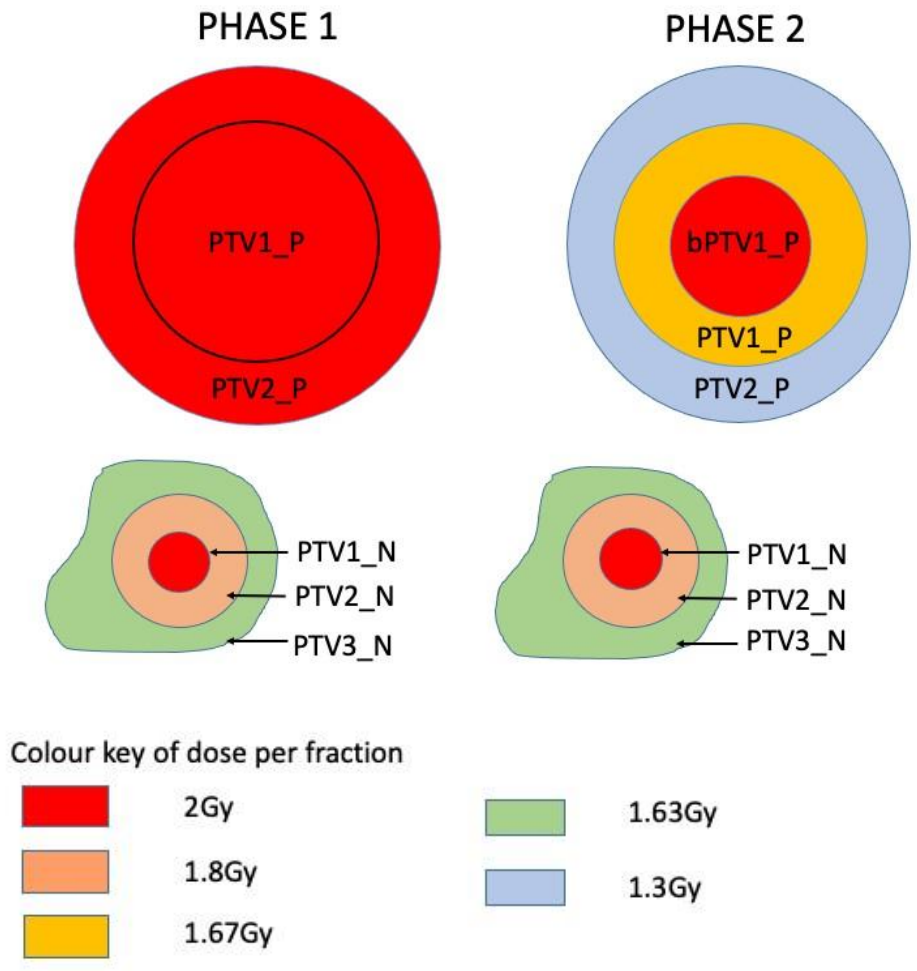

Fig 5.1 Schematic diagram representing the 5 different dose per fraction levels for primary (_P) and nodal (_N) PTVs in Phase 1 and Phase 2 of planning method ADAPTIVE _A

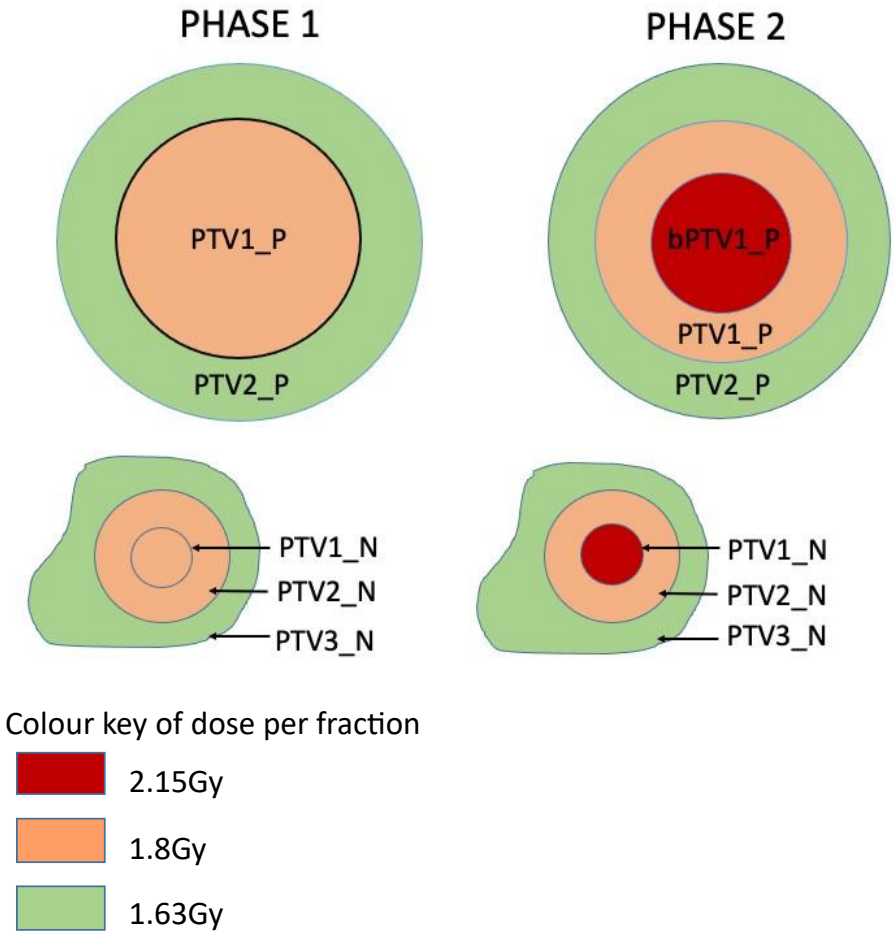

Fig 5.2 Schematic diagram representing the 3 different dose per fraction levels for primary (_P) and nodal (_N) PTVs in Phase 1 and Phase 2 of planning method ADAPTIVE_B

PTV	ADAPTIVE_A				ADAPTIVE_B			
	Total dose Ph 1	Total dose Ph 2	Total dose Ph 1+2	BED	Total dose Ph 1	Total dose Ph 2	Total dose Ph 1+2	BED
bPTV1_P	(30Gy/15F)*	36Gy/18F	66Gy/33F	79.20	(27.3Gy/15F)*	38.7Gy/18F	66Gy/33F	79.25
PTV1_P	30Gy/15F	30Gy/18F	60Gy/33F	71.01	27.3Gy/15F	32.7Gy/18F	60Gy/33F	70.90
PTV2_P	30Gy/15F	24Gy/18Gy	54Gy/33F	63.12	24.5Gy/15F	29.5Gy/18F	54Gy/33F	62.80
PTV1_N	30Gy/15F	36Gy/18F	66Gy/33F	79.20	27.3Gy/15F	38.7Gy/18F	66Gy/33F	79.25
PTV2_N	27Gy/15F	30Gy/18F	60Gy/30F	66.87	27.3Gy/15F	32.7Gy/18F	60Gy/33F	70.90
PTV3_N	24.5Gy/15F	29.5Gy/18F	54Gy/30F	61.87	24.5Gy/15F	29.5Gy/18F	54Gy/33F	62.80

Table 5.1 Total dose and the Biological Equivalent Dose (BED) to the primary and nodal PTVs for Phase 1 and Phase 2 using ADAPTIVE_A and ADAPTIVE_B

*Included within PTV1_P

5.2.2 Ensuring coverage of target volumes by ADAPTIVE_B and comparison of mean dose to OARs with ADAPTIVE_A and ADAPTIVE_B planning protocols

In order to ensure that the new planning protocol resulted in clinically acceptable plans, manual ADAPTIVE_B plans were planned for the 4 pilot study cases previously planned with ADAPTIVE_A in Chapter 3. The coverage of the PTVs by ADAPTIVE_B was checked, and the mean doses received by OARs with ADAPTIVE_B were compared to those from the original ADAPTIVE_A, to look for differences between the two different planning protocols.

5.3 Results

5.3.1 Comparison of mandatory PTV coverage with PEARL A and PEARL B planning protocols

The mandatory goals for primary and nodal PTV coverage (D99 >90% and D95 >95%) were met by ADAPTIVE_B for all the PTVs across all 4 patients (data not shown). The primary PTVs and PTV1_N received a lower total dose in phase 1 and a higher total dose in phase 2 with ADAPTIVE_B compared to ADAPTIVE_A due to the different division of dose between the 2 phases for each.

5.3.2 Comparison of mean dose to OARs with ADAPTIVE_A and ADAPTIVE_B planning protocols

The average mean dose for each OAR was compared between ADAPTIVE_A and ADAPTIVE_B techniques for each case. Fig. 5.3 a – d show the individual mean doses to OARs for each case. Most dots representing ADAPTIVE_A and ADAPTIVE_B are close or overlap. The range of difference is -1.44 – 2.61Gy. The largest difference is seen in Case 3 middle pharyngeal constrictor.

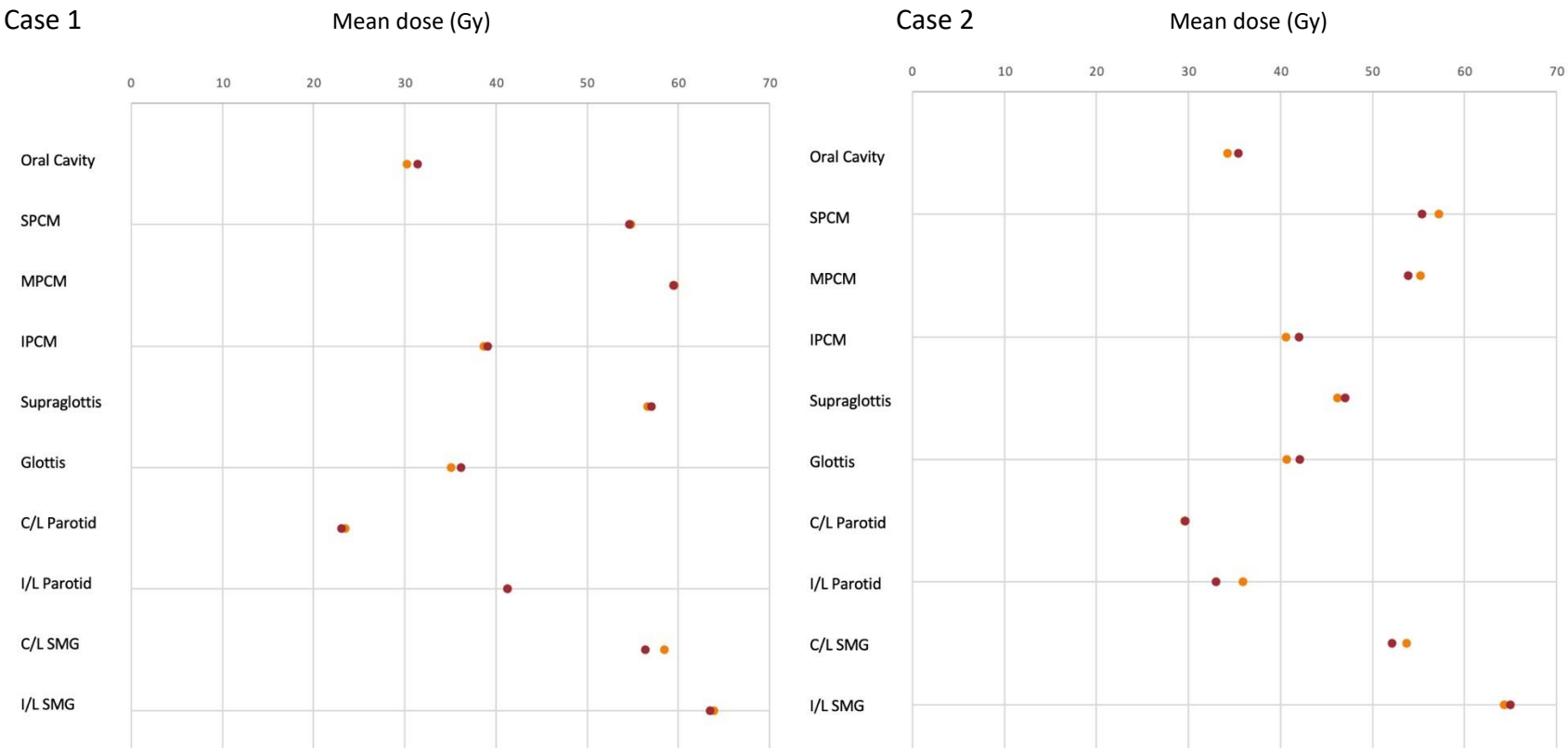

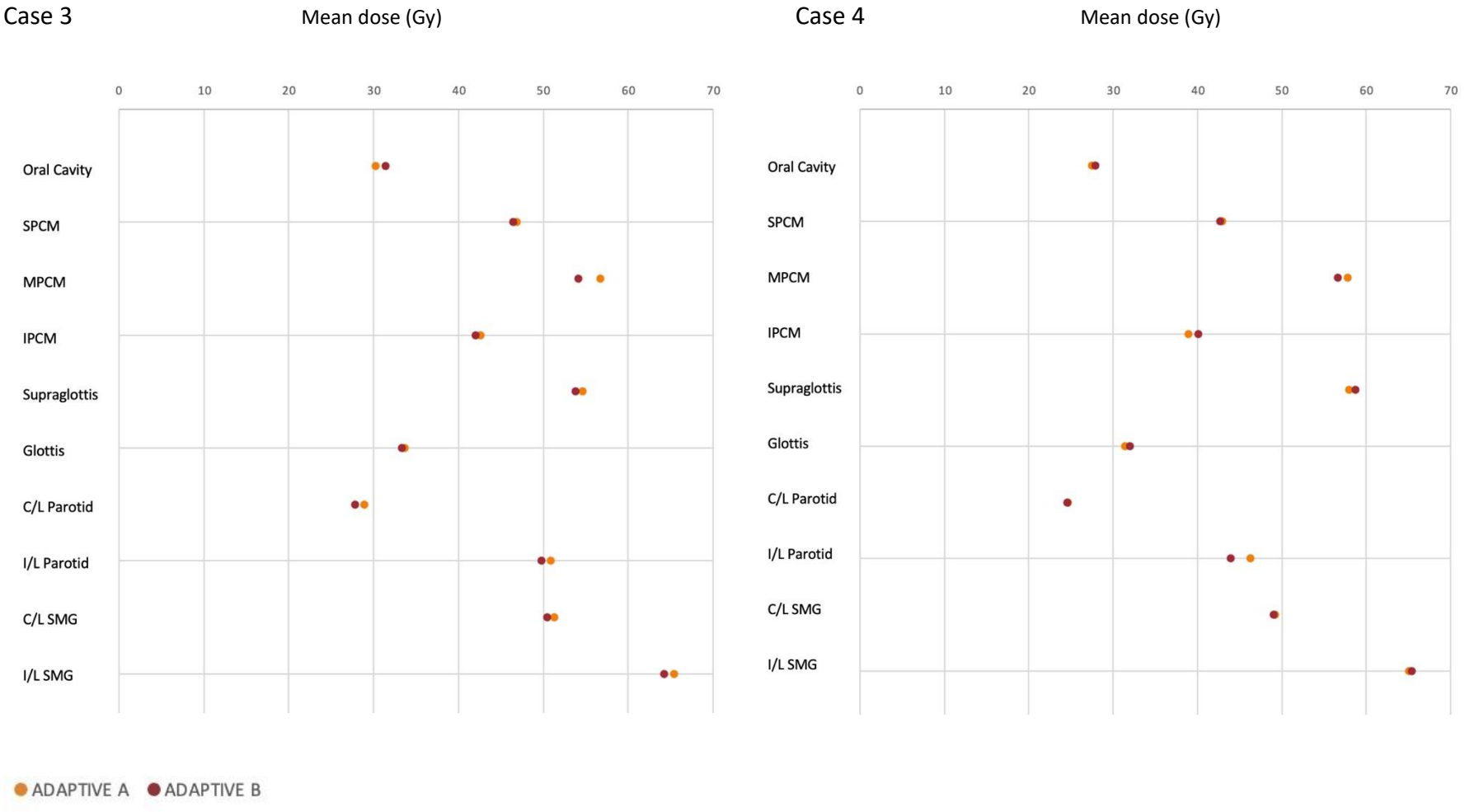

Fig. 5.3 a – d Scatter plots for Pilot Study Cases 1 – 4 showing mean dose to OARs for ADAPTIVE_A (yellow) and ADAPTIVE_B planning methods

	Superior pharyngeal constrictor muscle	Middle pharyngeal constrictor muscle	Inferior pharyngeal constrictor muscle	Supraglottis	Glottis	C/L parotid gland	I/L parotid gland	C/L SMG	I/L SMG	OC
ADAPTIVE_A	58.84	54.23	35.64	39.76	20.98	17.5	32.2	39.33	60.33	32.03
ADAPTIVE_B	57.55	53.17	35.31	38.86	20.7	17.4	32.14	39.05	60.77	30.96

Table 5.2 Average mean doses (Gy) across the four PEARL patients: Mean doses received to OARs in modelled adapted plans: ADAPTIVE_A and ADAPTIVE_B

5.4 Discussion

Time and human resource pressures, and a concern over a low dose per fraction (1.3Gy) delivered to the PTV2 in phase 2, drove the development of an alternative planning protocol, ADAPTIVE_B. Here I have presented the rationale for altering the protocol and the dosimetric effects of implementing the ADAPTIVE_B method. I achieved the objectives set out at the start of this chapter. ADAPTIVE_B is a simplified planning method which also increases the minimum dose/fraction to 1.63Gy. In addition, I have demonstrated that any difference between ADAPTIVE_A and ADAPTIVE_B in PTV coverage, and difference in dose to SWOARs and major salivary glands, is unlikely to result in clinically relevant differences in toxicity.

5.4.1 Simplification of the PEARL planning protocol

To reduce the time burden on an overstretched planning department, and allow for planners to be trained on the PEARL protocol in a shorter amount of time, I led the development of a new planning protocol, ADAPTIVE_B. The previous 5 dose levels in ADAPTIVE_A were reduced to 3 for ADAPTIVE_B which was based upon a more traditional design with a sequential boost to the high dose PTV in Phase 2. ADAPTIVE_B uses the same volumes and expansions as ADAPTIVE_A and has the same total dose delivered to the low, intermediate and high dose PTVs across both phases.

Whilst not formally timed, when compared to planning the ADAPTIVE_A method, planners felt that time taken to plan Phase 2 for ADAPTIVE_B was reduced by up to 10-15%. An additional unexpected benefit was clinical review of Phase 2 plans was more straightforward for the clinicians due to the reduced dose levels that required coverage checking. This was also not formally timed but was an observation commented on.

5.4.2 Increase of the dose/fraction delivered to prophylactic nodal volume

As well as simplifying the planning technique and reducing the time taken to plan, ADAPTIVE_B also eliminated the 1.3Gy/F dose level to the prophylactic nodal volume in Phase 2 of ADAPTIVE_A, which had been highlighted as a concern by the Trial Management Group in their review because of the risk of undertreatment.

Other than total dose, the size of the fraction is the most important influence on risk of late tissue effects, the larger the fraction size, the greater the risk of late toxicity. Too small a dose per fraction could theoretically fail to cause lethal damage to tumours, encouraging the emergence of radioresistant clones to dominate.

Whilst there is some evidence (130) that a fraction size of 1.4Gy may be effective enough for eliminating microscopic disease in prophylactic levels, there is no phase 3 data demonstrating this. The consensus of the Trial Management Group was that a smaller fraction size of 1.3Gy may undertreat microscopic disease despite it being delivered within the same overall treatment time as common UK practice. It was of paramount importance that every effort taken to ensure trial participants are not put at risk of under treatment. In accordance with this, the increased minimum dose/fraction size in ADAPTIVE_B of 1.63Gy provided additional reassurance.

5.4.3 Comparison of ADAPTIVE_A and ADAPTIVE_B on PTV coverage

PTV coverage for ADAPTIVE_A and ADAPTIVE_B was adequate and in line with ICRU regulations. The decrease in dose to PTV1_P and bPTV1_P in phase 2 of ADAPTIVE_B reflects the difference in dose per fraction between the 2 planning methods (data not shown). Whereas ADAPTIVE_A starts with a higher dose per fraction to the PTV1_P and PTV2_P, then reduces it in phase 2 to the non-avid volume, ADAPTIVE_B starts with a lower dose per fraction in phase 1 then increased, or ‘boosted’ the area defined by the residual avidity. The dose and dose per fraction to PTV2_N and PTV3_N are unchanged.

5.4.4 Comparison of PEARL A and PEARL B on mean dose to OARs

Theoretically, the combination of a change in dose per fraction to the dose levels across 2 phases, and simultaneous change in volume and position of OARs between Phase 1 and 2, could impact upon a difference in mean dose received by the OARs comparing ADAPTIVE_A and ADAPTIVE_B. For example, in ADAPTIVE_A Phase 1, 2Gy per fraction is delivered to the primary PTV2. In ADAPTIVE_B Phase 1, primary PTV2 is treated at 1.63Gy per fraction. OARs close to the primary PTV2 will receive a higher dose in ADAPTIVE_A compared to ADAPTIVE_B during Phase 1. Whilst total dose to PTV2 across Phase 1 and 2 remains the same, the higher dose per fraction in Phase 1 may exert a greater impact for OARs that change volume and position with radiotherapy e.g., the ipsilateral parotid gland. To ensure that the change in the planning protocol did not introduce bias into the PEARL results, I assessed the mean doses to OARs for the ADAPTIVE_A and ADAPTIVE_B in the 4 cases used in the pilot study.

5.5 Conclusion

The alteration in the PEARL planning protocol allowed for a more efficient and more straightforward turnaround of PEARL plans. This was especially important for the PEARL Phase 2 plans that need to be completed within 3 – 4 days. The benefits of a shorter planning process, and approval of plans, to an overstretched and pressured department are clear. Any differences between ADAPTIVE_A and ADAPTIVE_B are unlikely to have any noticeable impact on the patient or the results of PEARL. In addition, the new minimal dose per fraction level was increased to 1.63Gy which was felt by the Trial Management Group to be a more acceptable dose to treat potential microscopic disease.

The ADAPTIVE_B method was subsequently taken through as the new planning method for subsequent patients recruited to the PEARL Study and ratified by a minor amendment to the protocol.

Chapter 6: Modelling the dosimetric impact of the PEARL protocol using Intensity Modulated Proton Beam Therapy (IMPT) planning

6.1 Introduction

6.1.1 Proton Beam Therapy

With the wider availability of proton beam therapy in the form of Intensity Modulated Proton Therapy (IMPT) as a potential option for radiotherapy in the management of OPSCC, in addition to substantial cost implications, improving methods to determine the patients who will benefit most from proton beam therapy is required. The organ sparing benefits of proton beam therapy are well documented and summarised in Section 1.10. In this chapter I investigate if these benefits of proton therapy can be improved by applying biological response-based adaptation as per the PEARL Study planning method.

6.1.2 Normal tissue complication probability (NTCP) modelling in proton beam therapy

The development of radiotherapy toxicity is multi-factorial and not purely dictated by dosimetry i.e., toxicity experienced by two patients may vary even when the dosimetry is identical. For these reasons, not all patients will derive the same level of benefit from proton beam therapy compared to IMRT/VMAT. The comparison of Dose Volume Histograms (DVHs) alone to assess differences between plans is limited as a result of OAR contouring discrepancies between clinicians, differences between various Treatment Planning Systems software, and corrupt dosimetry information. Normal Tissue Complication Probability (NTCP) models aim to determine which patients are at low or high risk of developing toxicity in a more sophisticated way than simple DVH comparison. NTCP modelling can consider patient specific factors and tumour characteristics to estimate an individualised risk for the development of toxicities and assist the clinician in selecting the optimal radiotherapy plan for their patient. Various NTCP models have been validated and are already in use to select the patients with the most to gain from IMPT.

Whilst the foundation of an NCTP model is the DVH for a specific OAR, clinical factors including the smoking status, age/sex of the patients, as well as whether concurrent chemotherapy will be

given, may affect the risk of toxicity development and can be included in NTCP models too. For these reasons, differences between NTCPs (ΔNTCP) are expected to better represent actual clinical outcomes compared to DVH comparisons alone.

The widely published theoretical benefits of proton beam therapy in some head and neck cancer patients has been supported by, and driven the development of, a range of different NTCP models for head and neck cancer radiotherapy plans. In most cases, these models have been internally validated in single centre studies.

6.1.2.1 Impact of proton beam therapy on risk of dysphagia and xerostomia

A recent systematic review (131) reported 48 studies and 8 validation studies of NTCP modelling to predict late effects of proton beam therapy in head and neck cancer patients. Most studies (25) focus on xerostomia, 7 on dysphagia and the remainder on other toxicities including taste change and hearing loss. There were no studies published at that time on osteoradionecrosis. In line with my thesis, the most used dose parameter for the parotid glands, submandibular glands and pharyngeal constrictor muscles, is the mean dose. Some of the models incorporate additional information including baseline xerostomia, weight loss and the use of chemotherapy. Over half the studies (58%) used patient cohorts of over 100 patients but the majority lacked any degree of internal or external validation. 5 models across 4 studies included patients treated with proton beam therapy, the remaining were based upon patients who had been treated with IMRT/VMAT.

One modelling study by Rwigema et al (132) aims to develop an NTCP model to predict any acute toxicity benefit with proton beam therapy. They calculated the NTCP based upon 175 IMRT and 30 proton beam therapy OPSCC patients and validated it on a comparison of the 30 proton beam therapy plans and modelled equivalent IMRT plans. The NTCP model predicted differences in the mean NTCP values for each endpoint at 6 months, the most significant differences corresponding to grade 2 or above dysphagia and xerostomia at 6 months post-radiotherapy. When compared to actual clinical data, the model over predicted the rate of xerostomia. The group concluded larger clinical cohorts were required to validate their model.

The Netherlands have been at the forefront of proton beam therapy in head and neck cancer, and in the development of NTCP models to inform which patients will benefit the most from proton beam therapy over IMRT/VMAT. Approximately 2000 head and neck cancer patients a year have radiotherapy treatment in the Netherlands of which 30 – 40% are deemed eligible for proton beam therapy funding. The National Protocol for proton beam therapy for head and neck cancer Patients – 'NIPP-head and neck cancer' - was developed by Langendijk et al and published in 2021 (96). The protocol compares estimated NTCP profiles of optimal photon and proton beam therapy plans for xerostomia, dysphagia and feeding tube dependency based upon dose distribution parameters in OARs, and other clinical/treatment factors including the use of any chemotherapy and changes in weight. Prioritisation of OAR sparing is both parotid glands, superior pharyngeal constrictor muscle/inferior pharyngeal constrictor muscle/cricopharyngeus, and the oral cavity. The expected clinical benefit from the ΔNTCP profile between the IMRT/VMAT and proton beam therapy plans is calculated for each patient.

The NTCP models used in the NIPP-head and neck cancer are selected on the basis that they had been externally validated on large numbers within similar patient cohorts, receiving similar treatment techniques. They use the mean dose for the contralateral parotid glands, and the superior pharyngeal constrictor muscle and supraglottis, as a predictor for xerostomia and dysphagia respectively. The thresholds of the ΔNTCP are based upon CTCAE toxicity scores Grade 1 - 4. Minimal thresholds arbitrarily chosen and approved by the NIPP-head and neck cancer working group are set at ≥10% G2, ≥5% G3 or ≥2% G4 for xerostomia and dysphagia, in recognition of the increasing impact upon activities of daily living with grade severity. The patients who reach any of these thresholds are eligible for reimbursement of the cost of proton beam therapy (Fig 6.1).

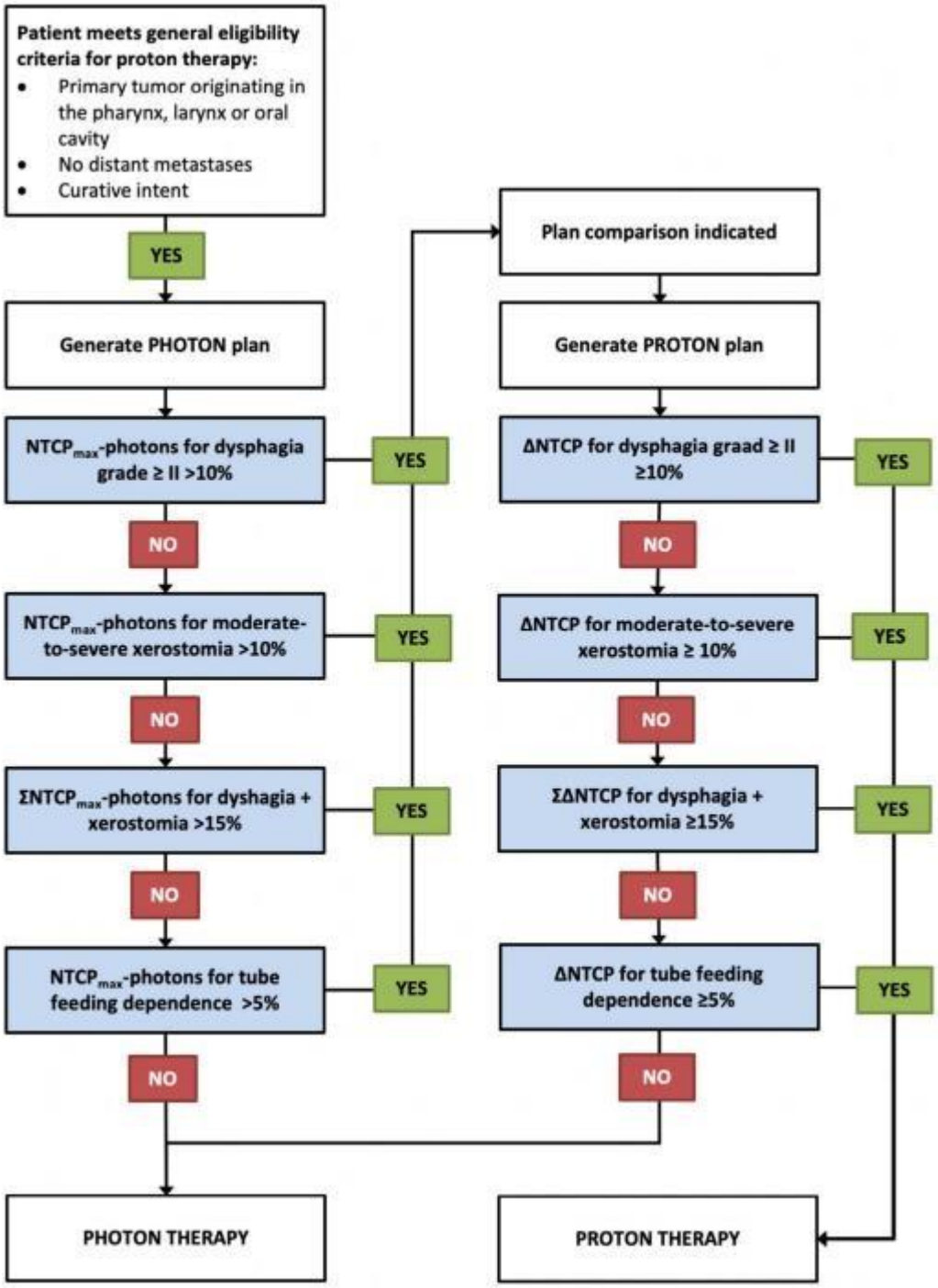

Fig. 6.1 NIPP-head and neck cancer pathway Courtesy of Langendjik et al (96)

Flowchart for selecting patients for a plan comparison and proton beam therapy as per The Netherlands national system. For each toxicity endpoint, the maximum ΔNTCP (ΔNTCPmax) between VMAT and proton beam therapy techniques must be calculated.

Clinical details of patients assessed by the NIPP-head and neck cancer from January 2018 to September 2019 (133) demonstrate those who qualify for proton beam therapy are more likely to have more locally advanced disease, pharyngeal tumours, receive concurrent chemotherapy, and have a higher degree of PTV overlap with the parotid gland, superior pharyngeal constrictor muscle, oral cavity and ipsilateral submandibular gland on their radiotherapy plans. The mean dose to these OARs is also higher for the IMRT/VMAT plans in those who qualified for proton beam therapy compared to those who did not (Fig. 6.2). The most common NTCP criteria for proton beam therapy was the reduction in the risk of dysphagia or the summed risk of ≥grade 2 toxicity.

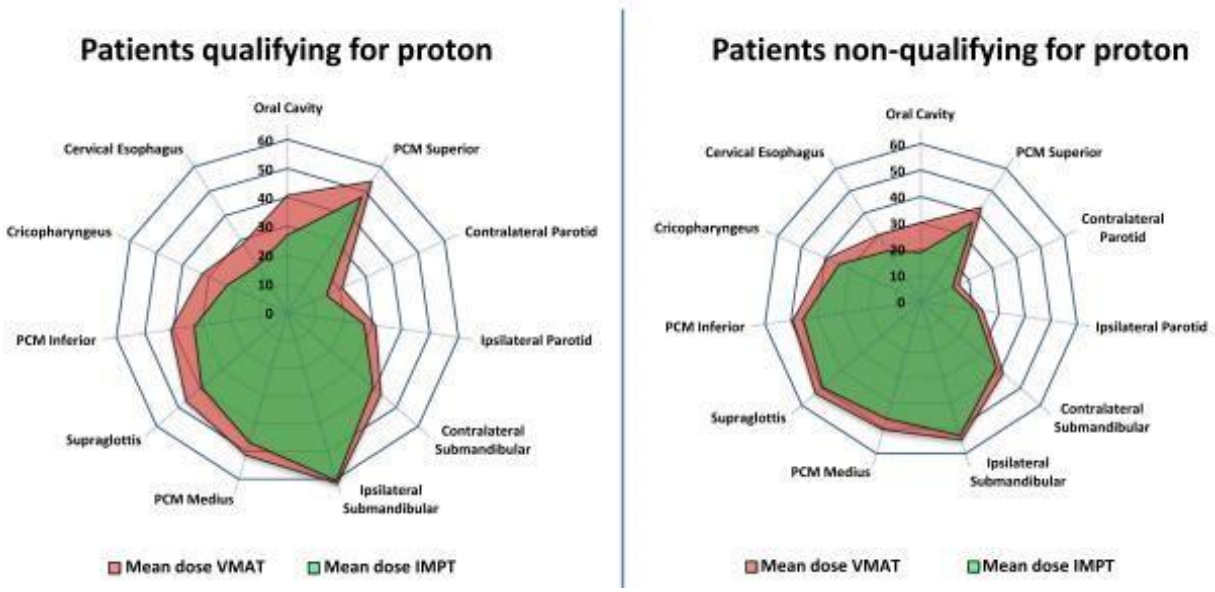

Fig 6.2 Radar diagrams demonstrating the average mean doses of OARs as a result of VMAT and IMPT Courtesy of Tambas et al (133)

Radar diagrams demonstrating the average mean doses of OARs as a result of VMAT and IMPT planning in the population of patients between January 2018 to September 2019 qualifying for proton beam therapy in the Netherlands, and the population of patients who did not.

6.1.2.2 Impact of proton beam therapy on risk of osteoradionecrosis

The reduced distal beam path dose of a proton beam therapy beam supports the theory that the risk of osteoradionecrosis could be significantly reduced by proton beam therapy. NTCP prediction could play a role in the tailoring of follow up schedules specifically to patients identified at increased risk with the incorporation of radiological and clinical review. This may facilitate the early detection of disease recurrence and optimise the number of options available for intervention including salvage surgery. Various dosimetric parameters have been suggested as optimal constraints for the mandible in efforts to lower the risk of osteoradionecrosis. A particular issue is the lack of consensus of osteoradionecrosis definition and grading.

The mean dose, V50 and V60 have all been proposed from osteoradionecrosis rates in large retrospective studies (134, 135). Despite this, there was no published NTCP model for the risk of osteoradionecrosis until Van Dijk et al in 2021 (136). To develop an NTCP model for osteoradionecrosis, they reviewed 1259 head and neck cancer patients treated with IMRT radiotherapy at the MD Anderson Cancer Centre between 2005 – 2015. To mitigate for the complexity of defining osteoradionecrosis, the endpoint was defined as osteoradionecrosis of any grade developed at any time point after radiotherapy. Variables including age, sex, subsite and smoking were also included.

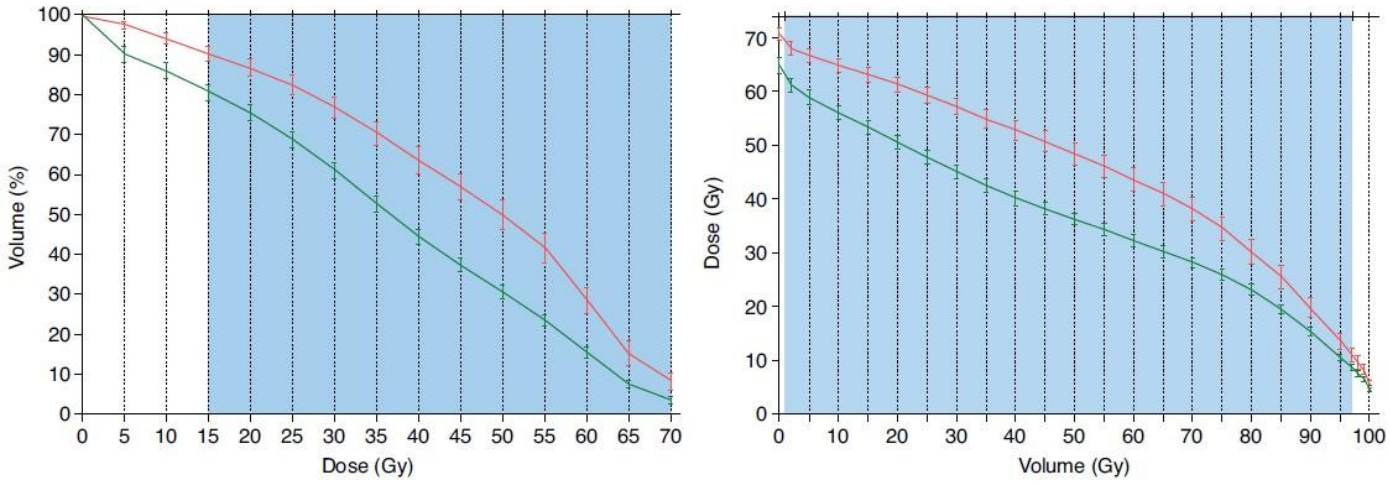

Fig. 6.3 Courtesy of Van Djik et al 2021 (136)

Average DVH for patients who develop osteoradionecrosis, n = 173, (red) versus those who do not, n = 1086, (green) for volume and dose parameters to the mandible. Blue shading indicates univariate significance of parameters. D2% - D98% and V15Gy – V70Gy were significant with a P<0.0001.

Patients who didn't get osteoradionecrosis (n = 1086) had an average D30 of 46Gy +/- 16Gy, those who did get osteoradionecrosis (n = 173) had an average D30 of 57Gy +/- 9Gy (Fig. 6.3). As a result of their finding, the final NTCP model was based around 2 parameters; tooth extraction prior to radiotherapy and the D30%. The group suggested that to reduce the risk of any grade osteoradionecrosis to ≤5%, the D30% should be kept below 42Gy if no tooth extractions were performed prior to radiotherapy, and below 35Gy if they were.

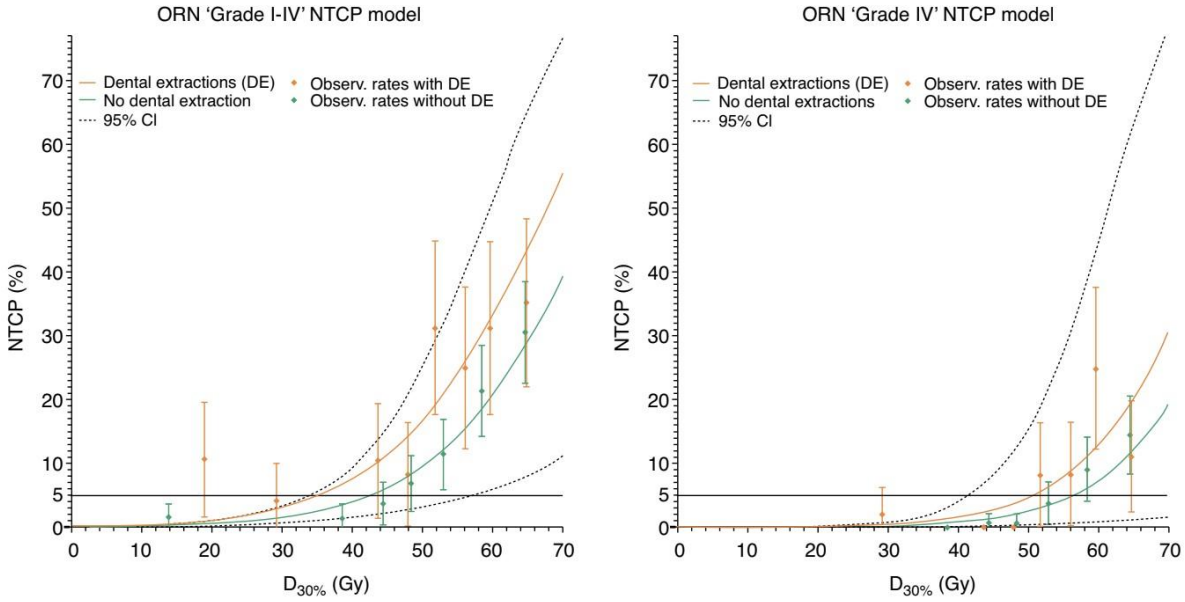

Fig. 6.4 osteoradionecrosis NTCP models courtesy of Van Dijk (136). NTCP curves plotted against D30% split into patients with pre-treatment dental extractions (orange lines) and those without (green lines) for NTCP models for osteoradionecrosis of any grade (left) and Grade 4 (right). The dotted line indicates the most outer 95% confidence interval (CI) limits of the NTCP curves.

Compared to the Mavroidis (56), NTCP curves included in Chapter 1 (Fig. 1.6 and 1.7), the Van Dijk osteoradionecrosis NTCP curves in Fig. 6.4 are shallower, reflecting the lower rates of incidence of osteoradionecrosis compared to xerostomia and dysphagia in OPSCC patients following chemoradiotherapy.

Small differences in mean dose to mandible have also been demonstrated to impact upon whether a patient develops osteoradionecrosis. A retrospective study (137) compared 534 IMRT patients to 50 IMPT patients. Mean dose received to mandible in the IMRT group was 41.2Gy, compared to 25.6Gy in the IMPT group. Those without osteoradionecrosis received a mean dose of 39.3Gy compared to 46.8Gy in those who developed it, a difference of 7.1Gy.

6.1.2.3 Role of NTCP modelling in the clinic

Ultimately the NTCP model only considers a proportion of factors that inform treatment decision making and provides only an estimation of risk. NTCP values must be used only as an adjunct to, rather than a replacement for, the clinician's clinical assessment.

6.1.3 Adaptive techniques in proton beam therapy

The physical and radiobiological features of proton beam therapy give it an inherent susceptibility to uncertainties regarding dose deposition (as discussed in Section 1.10). Anatomical changes in patients during a course of proton beam therapy leads to up to 40% of head and neck cancer patients requiring plan adaption (138).

6.1.3.1 Adaption for anatomical changes

The most widely published studies in adaptive radiotherapy for proton beam therapy look at reactive replanning of proton beam plans in response to anatomical changes e.g. weight loss rather than tumour response to treatment.

The optimal frequency of replanning for anatomical changes throughout a course of proton beam therapy has not yet been defined. Bobic et al (139) compared daily to weekly online adaptation

by retrospectively evaluating the daily CBCTs of 10 patients. They tracked the doses to CTVs and OARs with no adaption and compared with a theoretical adaption on a daily, and weekly basis. They concluded that whilst daily re-planning reduced random delivery errors, weekly replanning was equivalent in terms of clinical goals. Both daily and weekly replanning improved the CTV coverage and OAR sparing to the same extent compared to no adaption. They concluded that weekly replanning was sufficient for these patients.

6.1.3.2 Response based adaption in proton beam therapy

The improved conformality conveyed by IMPT may synergise with response-based adaption and result in a greater degree of dosimetric improvement. Conversely, the improved dosimetry by IMPT at baseline, may mean that the impact of adaption is reduced, as seen with automated planning in Chapter 4.

There is a paucity of published studies looking at response-based adaption of the high dose CTV during proton beam therapy treatment. There are no published studies looking at the dosimetric impact of PET-based response adaption in head and neck cancer proton beam therapy. In this chapter I demonstrate the organ sparing benefits of IMPT by comparing non-adaptive manual VMAT to IMPT plans for my pilot study cohort cases. I then model the dosimetric impact of biological response-based adaptive planning following the PEARL protocol, on IMPT plans and compare to non-adaptive IMPT plans. Finally, I compare dosimetric differences between non adapted and adaptive IMPT to published data, and address whether biological response-based adaption in IMPT is likely to confer additional benefit regarding the probability of toxicity.

6.1.4 Objectives

1. Investigate the dosimetric impact of IMPT by comparing mean dose received by OARs between non-adaptive VMAT and non-adapted IMPT plans
2. Investigate the dosimetric impact of adaptation by comparing dose received by OARs between non-adaptive IMPT and adapted IMPT plans
3. Investigate the relative dosimetric impact of adaptation by comparing dose received by OARs between adaptive VMAT and IMPT plans
4. Identify whether adaptation as per the PEARL Study protocol would influence the ΔNTCP threshold for proton beam therapy funding in The Netherlands

My hypothesis is that non-adapted IMPT will show dosimetric advantages in terms of OAR avoidance compared to VMAT for non-adapted planning, and that adapted IMPT will be superior to both non-adaptive IMPT and adaptive VMAT planning.

6.2 Methods

I performed a dose modelling study using IMPT to investigate the impact of IMPT and adaptation, on dose received to OARs including OARs associated with dysphagia, xerostomia and osteoradionecrosis. I specifically look at the mean doses to dysphagia and xerostomia-associated OARS, and D30 to the mandible, to align my data to published literature on proton beam therapy.

This modelling study was performed in collaboration with Jamil Lambert, Principal Physicist at The Rutherford Cancer Centre in Newport, Wales. The Rutherford Cancer Centre is a private healthcare provider with IMPT planning and delivery capability.

6.2.1 Identifying datasets for the IMPT modelling planning study

To allow accurate comparison of VMAT and IMPT techniques, the anonymized patient datasets used in the pilot study to model VMAT plans were used for the IMPT modelling study. Datasets included the planning PET-CT images, target volumes and OAR structures for each patient.

6.2.2 The standard and PEARL adaptive planning techniques

The ADAPTIVE_B planning method was used for work presented in this chapter.

The following plans were generated based upon the PEARL Pilot Study cases:

1. 'NON-ADAPTIVE': Manually planned non-adapted VMAT – Previously planned at Velindre Cancer Centre using RayStation VMAT planning protocol for the PEARL pilot study detailed in Chapter 5.
2. 'ADAPTIVE': Manually planned adapted VMAT – Previously planned at Velindre Cancer Centre using RayStation VMAT planning protocol for the PEARL pilot study detailed in Chapter 5.
3. 'NON-ADAPTIVE_PROTON': Manually planned non-adapted IMPT – Specifically planned at The Rutherford Cancer Centre for this project using RayStation proton beam therapy planning protocol.
4. 'ADAPTIVE_PROTON': Manually planned adapted IMPT – Specifically planned at The Rutherford Cancer Centre for this project using RayStation proton beam therapy planning protocol.

The target volumes and organ at risk structures defined for the VMAT pilot study in Chapter 3 were used for the IMPT modelling study.

	High dose CTV definition	CTV to PTV margin	Robustness parameters	Number of fractions	Dose/fraction to high dose CTV (CGE*)	Total dose to high dose CTV (CGE*)
Nonadaptive VMAT	GTV+5mm	10mm	N/A	33	2	66
Adaptive VMAT	GTV+10mm bGTV+5mm	10mm	N/A	15 18	1.8 2.15	27 38.7
Nonadaptive IMPT	GTV+5mm	N/A	3mm positional uncertainty 3.5% range uncertainty	33	2	66
Adaptive IMPT	GTV+10mm bGTV+5mm	N/A	3mm positional uncertainty 3.5% range uncertainty	15 18	1.8 2.15	27 38.7

Table 6.1 Comparison of adapted and non-adapted VMAT and IMPT plans' high dose CTV and dose/fractionation *Cobalt Gray Equivalent N/A = Not applicable

6.2.3 Transfer of pilot study datasets and structures to RCC

The planning and interim PET_CT datasets and structures were exported from Raystation at Velindre Cancer Centre as DICOM files and sent to RCC via the NWIS Fileshare system. The DICOM files were then imported into The Rutherford Cancer Centre's Raystation system.

6.2.4 IMPT plan generation (in collaboration with Jamil Lambert, Principal Physicist at Rutherford Cancer Centre, Newport)

Multifield optimisation on RayStation version 9A was used to generate the IMPT plans. We modelled the delivery of IMPT with pencil beam scanning using the IBA ProteusONE cyclotron.

The IMPT plans were robustly optimised such that doses received by target volumes and OARs were recalculated based upon multiple scenarios to take into consideration set up error (3-5mm) and range uncertainty, which functions as the equivalent of adding a PTV margin in photon planning. This leads to multiple CTV and OAR doses from each plan as discussed below.

For my study, the combined primary and nodal target volume was split into an inferior section extending to 2cm inferior to the chin, and a superior section from above the shoulders. The inferior section was treated with a single anterior beam and the superior section with either two posterior oblique beams to spare the parotids, or two posterior oblique beams and an anterior oblique beam on the side of the primary. Specific beam angles were selected during manual planning based upon several factors due to the specific physical and radiobiological nature of proton beams. These factors vary between individual patients and include regions of tissue density heterogeneity, termination of multiple beams at the same point in critical structures and the presence of non-biological implants e.g., dental amalgam.

The anterior beam was positioned to avoid travelling through the chin or teeth and the posterior oblique beams positioned to avoid the shoulders, due to the day-to-day variability in the positioning of the body. The posterior oblique beams only treated the nodes on the same side, e.g., the right posterior oblique beam did not treat the left nodal volume. The section in the neck where both the anterior and posterior oblique beams covered the target had a gradient dose junction to minimise the risk of over- or under treatment.

The plan was created by robustly optimising the dose to the CTV volume with a 3mm positional uncertainty and a 3.5% range uncertainty. The RayStation planning system had the option to shift the beams independently from each other as part of the robust optimisation process, which was used in the superior-inferior direction only, to create the gradient dose junction.

For the adaptive IMPT plans, the two phases were planned independently. The planning priority order for the optimisation of non-critical OARs, and the mandatory dose constraints, were as per the PEARL protocol used for the VMAT pilot study. The mandatory dose constraints were applied to the worst-case scenario generated during the robust IMPT planning rather than the planning organ at risk volume (PRV) used in VMAT planning.

The total dose for each IMPT plan was calculated as:

Phase 1 dose on baseline planning PET- CT x 15F/33F

+

Phase 2 dose on interim planning PET-CT x 18F/33F

The phase 2 dose was optimised based on the sum of the phase 1 plan and the phase 2 plan on the interim planning scan as was the standard process for planning phase 2 IMPT plans at The Rutherford.

6.2.5 Target volume coverage and OAR dose constraints

As per the PEARL protocol and previously detailed in Tables 2.5 and 5.1.

6.2.6 Transfer of IMPT plans from RCC to VCC for analysis

The IMPT plans generated on Raystation at RCC were sent back to Velindre Cancer Centre by email as DICOM files. The DICOM files were then imported into the Velindre Cancer Centre Raystation planning system for review and analysis.

6.2.7 Assessment of dose to OARs

Mean dose to OARs are reported for NON-ADAPTIVE_PROTON and ADAPTIVE_PROTON plans. There were compared to ADAPTIVE and NON-ADAPTIVE VMAT plans presented in Chapter 3. Optimal dose constraints to OARS achieved using IMPT or adaptive planning were recorded.

6.2.8 NTCP calculations for dysphagia risk in non-adapted and adapted VMAT plans for comparison with non-adapted IMPT plans

NTCP calculations for dysphagia risk we performed using the validated dysphagia model described by Christianen et al (140). Individual calculations were performed on each case comparing adapted and non-adapted VMAT plans to non-adapted IMPT plans to explore whether they reached the threshold for proton beam treatment funding as per The Netherlands scheme. Mean dose to the superior pharyngeal constrictor muscle and the supraglottis is entered into the following calculation:

$$\text{NTCP} = \frac{1}{(1+e)^{-s}}$$

where s = -6.09 + (mean dose to the superior pharyngeal constrictor muscle x 0.057) + (mean dose to the supraglottis x 0.037)

6.3 Results

6.3.1 Comparison of non-adapted VMAT and non-adapted IMPT plans

6.3.1.1 Impact on OARs by IMPT planning

All the mean doses to all studied OARs in the 4 pilot study cases were markedly lower with the non-adaptive IMPT plans compared to the equivalent VMAT plans (Fig 6.5a-d) and (Table 6.2).

The most marked difference was seen in the more caudal structures (inferior pharyngeal constrictor muscle and glottis) and the oral cavity. The mean dose to the glottis was markedly reduced by 17.99 – 24.73 Gy across the 4 cases.

In the pharyngeal constrictor muscles the largest degree of sparing by IMPT was seen in the superior pharyngeal constrictor muscle with reductions in mean dose between 10.07 – 19.31Gy. The oral cavity was spared by IMPT up to 25.16Gy in every case (range -9.59Gy - -25.16Gy).

Multiple optimal dose constraints were met across the different cases and SWOARs as a result of non-adaptive IMPT planning. The inferior pharyngeal constrictor muscle dose constraint was met in all 4 cases. 3 out of 4 cases met constraints to the middle pharyngeal constrictor muscle and supraglottis. Constraints to the superior pharyngeal constrictor and oral cavity were met in 2 cases.

The contralateral submandibular gland (9.67 – 18.46Gy) and ipsilateral parotid gland (11.76 - 21.21Gy) had the greatest reductions in mean dose with IMPT planning. One case achieved the optimal dose constraint to the contralateral submandibular gland with IMPT planning. The mean dose to the contralateral parotid gland was reduced by 1.99 – 9.24Gy and the optimal dose constraint was met for all 4 cases as a result. The smallest difference between non adapted VMAT and IMPT plans was seen in the ipsilateral submandibular gland (0.8 – 2.71Gy).

IMPT reduced the mean dose to the mandible across all 4 cases compared to VMAT with a reduction of 9.57 – 21.28Gy (Table 6.7). The D30 was >42Gy for all cases planned with nonadapted VMAT plans and was improved by non-adaptive IMPT planning; Cases 1 and 2 met the dose constraint of D30 <42Gy, cases 3 and 4 had D30 <35Gy.

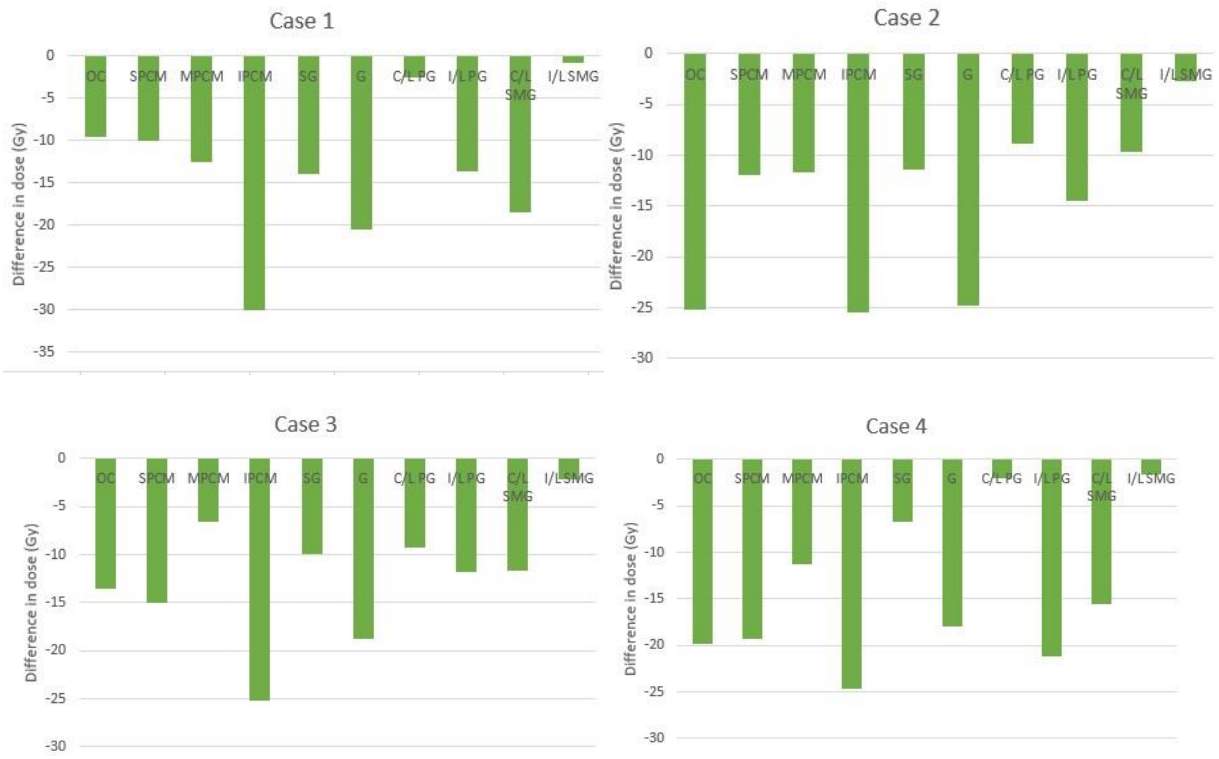

Fig. 6.5 Waterfall charts demonstrating change in mean dose received by OARs for Pilot Study cases 1 – 4 as a result of IMPT non adaptive planning compared to VMAT non-adaptive planning

Key: OC = Oral Cavity, SPCM = Superior pharyngeal constrictor muscle, MPCM = Middle pharyngeal constrictor muscle, IPCM = Inferior pharyngeal constrictor muscle, SG = Supraglottis, G = Glottis, C/L PG = Contralateral parotid gland, I/L PG = Ipsilateral parotid gland, C/L SMG = Contralateral submandibular gland, I/L SMG = Ipsilateral submandibular gland

	Difference in mean dose for OARs (NON-ADAPTED IMPT – NON-ADAPTED VMAT)									
Patient	Superior pharyngeal constrictor muscle	Middle pharyngeal constrictor muscle	Inferior pharyngeal constrictor muscle	Supraglottis	Glottis	C/L Parotid gland	I/L Parotid gland	C/L SMG	I/L SMG	Oral Cavity
1	-10.07	-12.48	-30.09	-13.97	-20.46	-2.57	-13.69	-18.46	-0.8	-9.59
2	-11.99	-11.68	-25.44	-11.36	-24.73	-8.81	-14.54	-9.67	-2.71	-25.16
3	-15.04	-6.59	-25.21	-9.98	-18.83	-9.24	-11.76	-11.63	-2.19	-13.56
4	-19.31	-11.3	-24.63	-6.73	-17.95	-1.99	-21.21	-15.52	-1.61	-19.84

Table 6.2 Average mean doses to OARs across all 4 Pilot Study cases comparing non-adaptive VMAT plans to non-adaptive IMPT plans.

	Mandible							
	Case 1		Case 2		Case 3		Case 4	
	Mean	D30	Mean	D30	Mean	D30	Mean	D30
NON-ADAPTIVE	39.81	46.67	38.82	44.25	38.17	42.79	35.98	42.64
NON-ADAPTIVE_PROTON	22.71	36.33	21.95	37.97	28.6	16.14	14.16	31.55
NON-ADAPTIVE_PROTON – NON-ADAPTIVE	-17.1	-10.34	-16.87	-6.28	-9.57	-26.65	-21.82	-11.09

Table 6.3 Mean dose and D30 to mandible for NON-ADAPTIVE(Gy), NON-ADAPTIVE_PROTON (Gy/RBE) and the difference between the two techniques (Gy).

6.3.2 Comparison of non-adapted IMPT and adapted IMPT planning

6.3.2.1 OARs

In most OARs across all 4 cases, the dose with IMPT was reduced further with adaptive IMPT planning compared to non-adaptive IMPT planning (Table 6.4). Overall difference in doses was smaller than the difference seen between the non-adaptive VMAT and non-adaptive IMPT plans. Across the 4 cases adaptation also increased the dose to 14 OARs. This was <1Gy in 9 OARs and most pronounced in the ipsilateral parotid gland, ipsilateral submandibular gland for cases 2 – 4, and the oral cavity in case 2.

Mean dose to the middle pharyngeal constrictor muscle was consistently reduced by adaptive IMPT planning (1.53 – 8.62Gy) as was dose to the supraglottis (0.12 – 19.42Gy) and glottis (0.28 – 5.29Gy) although there was wide inter-individual variation. The effect on the mean dose to the superior pharyngeal constrictor muscle was inconsistent, reducing dose in cases 1

and 4 by up to 1.72Gy and increasing the dose in Cases 2 and 3 by less than 0.5Gy. In addition to most optimal dose constraints being met by non-adaptive IMPT planning, adaptation did attain an extra dose constraint for the middle pharyngeal constrictor muscle in Case 3 by reducing the mean dose from 51.75Gy to 43.13Gy.

Mean dose to the contralateral parotid was reduced in Cases 1 and 4, and to the contralateral submandibular gland in Cases 2 and 3 with small increases in mean dose in the other cases. The ipsilateral parotid was spared 3.04Gy in mean dose by adaptation in case 1 but received a greater mean dose in the other cases (0.43 – 5.29Gy).

Adaptive IMPT planning had a mixed impact on the mandible mean dose, from a reduction by 10.45Gy in Case 3, to an increase of 1.98Gy for case 4 (Table 6.5). D30 was reduced for 2 cases to under 35Gy and was increased for Case 3 although the absolute value was low (22.15Gy), and Case 4 was only minimally changed, remaining under 35Gy.

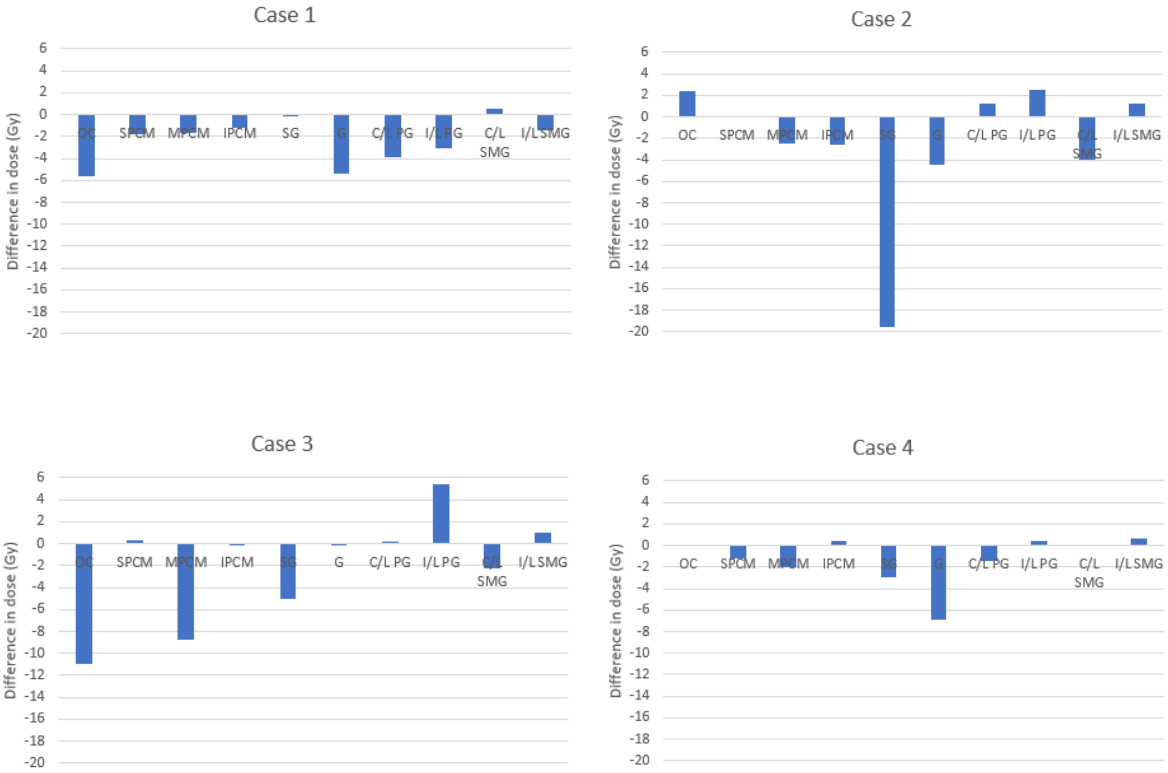

Fig. 6.6 Waterfall charts demonstrating change in mean dose received by OARs for Pilot Study cases 1 – 4 as a result of IMPT adaptive planning compared to IMPT non-adaptive planning

Key: OC = Oral Cavity, SPCM = Superior pharyngeal constrictor muscle, MPCM = Middle pharyngeal constrictor muscle, IPCM = Inferior pharyngeal constrictor muscle, SG = Supraglottis, G = Glottis, C/L PG = Contralateral parotid gland, I/L PG = Ipsilateral parotid gland, C/L SMG = Contralateral submandibular gland, I/L SMG = Ipsilateral submandibular gland

	Difference in mean dose for OARs (ADAPTED IMPT – NON-ADAPTED IMPT)									
Patient	Superior pharyngeal constrictor muscle	Middle pharyngeal constrictor muscle	Inferior pharyngeal constrictor muscle	Supraglottis	Glottis	C/L Parotid gland	I/L Parotid gland	C/L SMG	I/L SMG	Oral Cavity
1	-1.72	-1.53	-1.19	-0.12	-5.29	-3.78	-3.04	0.52	-1.37	-5.49
2	0.36	-1.96	-2.81	-19.42	-4.35	1.33	2.33	-3.46	1.08	2.3
3	0.44	-8.62	-0.15	-4.87	-0.28	0.32	5.29	-2.45	1.02	-10.98
4	-2.0	-2	0.42	-2.99	-6.86	-1.42	0.43	0.08	0.60	0.11

Table 6.4 Average mean doses to OARs across all 4 Pilot Study cases comparing adaptive IMPT plans to non-adaptive IMPT plans.

Dose (Gy/RBE)	Mandible							
	Case 1		Case 2		Case 3		Case 4	
	Mean	D30	Mean	D30	Mean	D30	Mean	D30
NON-ADAPTIVE_PROTON	22.71	36.33	21.95	37.97	28.6	16.14	14.16	31.55
ADAPTIVE_PROTON	22.14	34.74	22.23	24.82	18.15	22.15	16.14	31.86
ADAPTIVE_PROTON – NON-ADAPTIVE_PROTON	-0.57	-1.59	0.28	-13.15	-10.45	6.01	1.98	0.31

Table 6.5 Mean dose to mandible for NON-ADAPTIVE_PROTON (Gy/RBE), ADAPTIVE_PROTON (Gy/RBE), and the difference between the two techniques (Gy/RBE).

6.3.3 Comparison of adaptive VMAT and adaptive IMPT planning

6.3.3.1 OARs

Adaptive IMPT planning resulted in lower mean doses to all the studied OARs across all 4 cases compared to adaptive VMAT planning. The largest differences were seen in the oral cavity (mean difference 19.78Gy), glottis (20.63Gy) and inferior pharyngeal constrictor muscle (23.89Gy).

Adaptive IMPT planning resulted in lower mean dose to the mandible compared to adaptive VMAT planning across all the cases. The D30 was also lower with ADAPTIVE_PROTON compared to ADAPTIVE. None of the ADAPTIVE cases had a D30 <35Gy but cases 3 and 4 had D30 less than 42Gy. All the ADAPTIVE_PROTON cases had a D30 of <35Gy.

	Difference in mean dose for OARs (ADAPTED – ADAPTED IMPT)									
Patient	Superior pharyngeal constrictor muscle	Middle pharyngeal constrictor muscle	Inferior pharyngeal constrictor muscle	Supraglottis	Glottis	C/L Parotid gland	I/L Parotid gland	C/L SMG	I/L SMG	Oral Cavity
1	-9.29	-11.79	-26.67	-7.8	-21.01	-3.46	-20.01	-15.3	-3.14	-16.31
2	-8.21	-11.74	-25.86	-25.36	-27.02	-8.77	-12.92	-13.69	-0.7	-20.12
3	-12.9	-13.58	-23.44	-12.45	-17.11	-7.89	-6.76	-13.15	-1.96	-22.03
4	-19.83	-10.69	-19.6	-7.64	-17.38	-2.18	-22.00	-14.22	-0.86	-20.67

Table 6.6 Average mean doses to OARs across all 4 Pilot Study cases comparing adaptive IMPT plans to adaptive VMAT plans.

Mean dose (Gy/RBE and Gy)	Mandible							
	Case 1		Case 2		Case 3		Case 4	
	Mean	D30	Mean	D30	Mean	D30	Mean	D30
ADAPTIVE	38.03	44.6	39.82	45.3	36.51	41.1	34.52	39.54
ADAPTIVE_PROTON	22.14	34.74	22.23	24.82	18.15	22.15	16.14	31.86
ADAPTIVE_PROTON – ADAPTIVE	-15.89	-9.86	-17.59	-20.48	-18.36	-18.95	-18.38	-7.68

Table 6.7 Mean dose to mandible for Adaptive VMAT plans (Gy), Adaptive IMPT plans (Gy/RBE) and the difference between the two techniques (Gy).

6.3.4 Impact of adaptation on OAR mean dose for VMAT compared to IMPT plans

The difference adaptation has on average mean doses for VMAT and IMPT planning is similar, suggesting adaptation as per the PEARL protocol conveys a comparable impact on both. The average mean dose is reduced for all OARs apart from the ipsilateral parotid gland (Table 6.7).

Adaptation has greater impact on mandible sparing when used with VMAT in Cases 1 and 4. In Case 3 the impact on the mean dose was larger for IMPT although the D30 was raised. The converse occurred with VMAT where adaptation resulted in a reduction of the D30 by 10.45Gy. Case 2 did not show improved mandible sparing with adaptation regarding mean dose although the D30 was reduced in the adaptive IMPT plans (Table 6.8).

Dose (Gy)	Oral Cavity	Superior pharyngeal constrictor muscle	Middle pharyngeal constrictor muscle	Inferior pharyngeal constrictor muscle	Supraglottis	Glottis	C/L Parotid gland	I/L Parotid gland	C/L SMG	I/L SMG
Adaptive- Non adaptive VMAT	-0.8	-2.1	-2.2	-3.2	-4	-3.9	-1	1.3	-1	0.2
Adaptive IMPT – Non adaptive IMPT	-3.51	-0.51	-3.52	-0.93	-6.85	-4.2	-0.89	1.25	-1.32	0.33

Table 6.8 Difference in average mean dose (Gy) to each OAR between adaptive and non-adaptive VMAT, and adaptive and non-adaptive IMPT plans.

Dose (Gy)	Mandible							
	Case 1		Case 2		Case 3		Case 4	
	Mean	D30	Mean	D30	Mean	D30	Mean	D30
NON-ADAPTIVE - ADAPTIVE	1.78	2.07	-1	-1.05	1.66	1.69	1.46	3.1
NON-ADAPTIVE_PROTON – ADAPTIVE_PROTON	0.57	1.59	-0.28	13.15	10.45	-6.01	-1.98	-0.31

Table 6.9 Difference in mean dose and D30 to the mandible between adaptive and non-adaptive VMAT, and adaptive and non-adaptive IMPT plans to mandible

Blue shading indicates when mean dose reduction due to adaptation for IMPT plans was greater, red shading for when dose reduction was greater for adaptation of VMAT plans.

6.3.5 NTCP calculations for dysphagia risk in non-adapted and adapted VMAT plans for comparison with non-adapted IMPT plans

The NTCP complication risk of dysphagia as per Christianen (140) was calculated for non-adaptive and adaptive VMAT plans for each case and compared to non-adapted IMPT plans to generate Δ NTCP (Table 6.10). The mean Δ NTCP for non-adaptive VMAT compared to non-adaptive IMPT was 17.1% (range 13.9 – 20.85%). The mean Δ NTCP for adaptive VMAT compared to non-adaptive IMPT was 11.37% (range 9.48 – 12.64%).

Case	Non-adaptive VMAT NTCP complication risk (%)	Adaptive VMAT NTCP complication risk (%)	Non-adaptive protons NTCP complication risk (%)	Non-adaptive VMAT – nonadaptive protons Δ NTCP	Adaptive VMAT – non adaptive protons Δ NTCP
1	37.80	29.59	16.95	20.85	12.64
2	32.64	23.32	13.84	18.8	9.48
3	22.92	18.99	8.02	14.9	10.97
4	19.99	18.48	6.09	13.9	12.39
Mean	28.34	22.6	11.23	17.1	11.37

Table 6.10 NTCP complication risks and Δ NTCP for cases 1 – 4 non-adaptive and adaptive VMAT plans, and non-adaptive IMPT plans.

I produced radar diagrams (Fig. 6.7) to compare data from the pilot cases to radar diagrams from Tambas et al (133) (Fig. 6.2) and visually assess if the pilot cases were likely to have been approved for proton beam therapy in The Netherland.

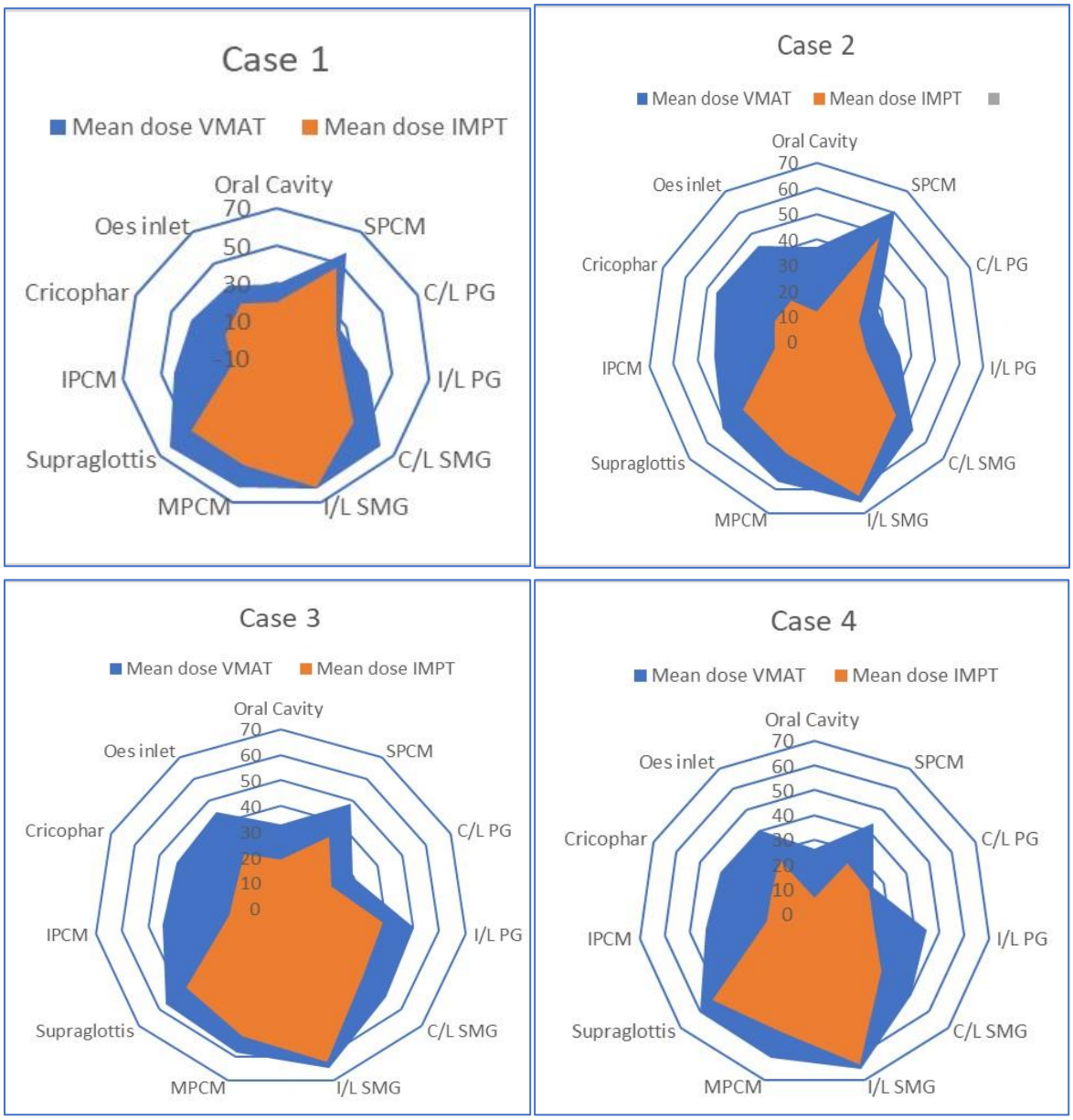

Fig 6.7 Radar diagrams for Cases 1 – 4 in the style of Tambas et al (133) demonstrating the difference in mean dose to OARs in modelled non-adaptive VMAT and IMPT plans

6.3.6 Relative impact of optimisation for SWOARs, adaptation and IMPT planning on total dose to OARs for cases 1 – 4

All cases had a reduction in their total mean dose to OARs when optimised for SWOARs, adapted as per PEARL, and planned with IMPT. The magnitude of impact was ranked in the same order for all cases, with optimisation reducing the total mean dose the least, and adapted IMPT the most. Cases 1 and 2, and Cases 3 and 4, demonstrated similar total mean dose reductions despite having different degrees of biological GTV reduction on the iPET-CT. Adaptation had the greatest impact on Cases 2 and 3 for both VMAT and IMPT plans (Fig. 6.8).

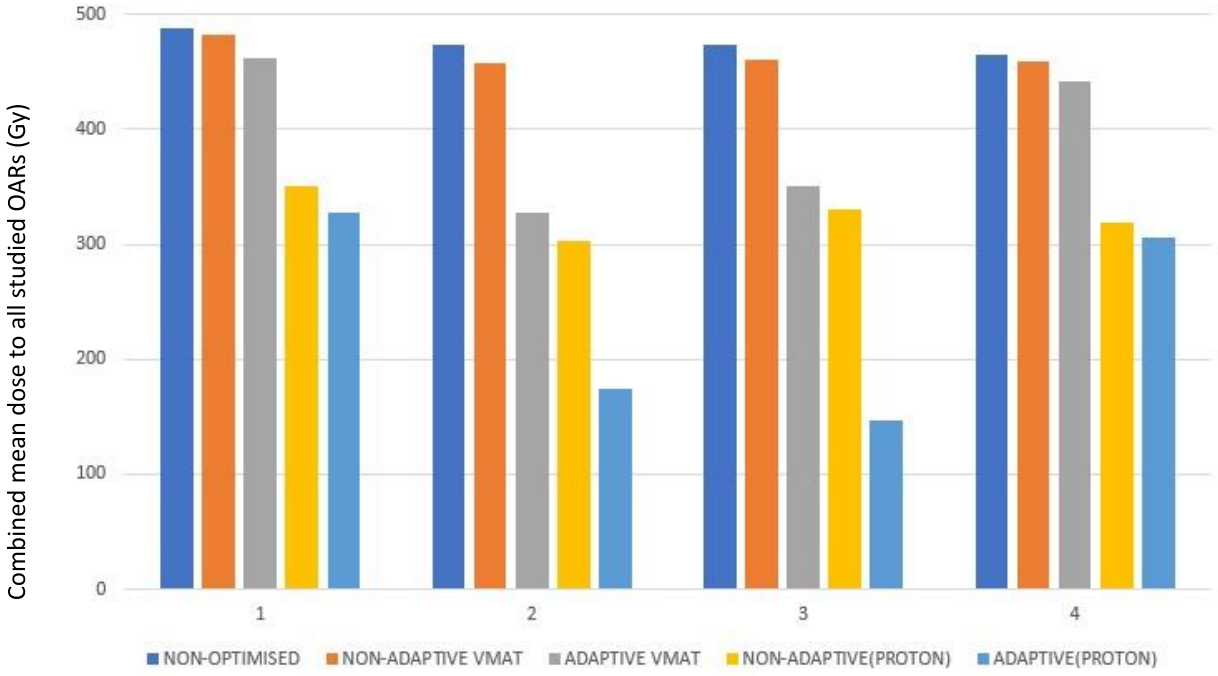

Fig. 6. 8 Combined mean dose to studied OARs for Pilot Study Cases 1 – 4 for non-optimised, non-adaptive VMAT plans and subsequent comparators: Optimised non-adaptive VMAT plans, adaptive VMAT, non-adaptive IMPT and adaptive IMPT plans

6.4 Discussion

This piece of work was a modelling planning study designed to look at the dosimetric differences between VMAT and IMPT plans using the cases from the PEARL pilot study. Specifically, mean dose to OARs was studied, to look for an indication of potential benefits of both standard IMPT, and adaptive IMPT, when compared with the standard of care method, non-adaptive VMAT planning. Finally, the magnitude of impact of PEARL adaptive on an IMPT plan was compared to the impact of PEARL adaptive on the VMAT technique.

6.4.1 NON-ADAPTED VMAT versus NON-ADAPTED IMPT plans

IMPT uniformly reduced the mean dose to OARs across all four cases when non-adaptive VMAT and non-adaptive IMPT were compared, in line with published data. The superior pharyngeal constrictor muscle, glottis, supraglottis, oral cavity, contralateral and ipsilateral parotids and contralateral submandibular gland all demonstrated markedly large reductions in mean dose because of model planning with IMPT.

A notable IMPT-related reduction in mean dose to the superior pharyngeal constrictor muscle between 10.07 – 19.31Gy, and the contralateral submandibular gland and parotid gland by a mean of 13.83Gy and 5.65Gy respectively is likely to result in improved toxicity rates when compared to published modelled NTCP curves. The ipsilateral parotid gland had improved sparing with Cases 2 and 4 achieving optimal dose constraints (mean dose <24Gy) when planned with IMPT. The smaller difference seen for the contralateral parotid compared to the ipsilateral parotid may be a result of the different beam arrangements standardly used in VMAT and IMPT planning. As described by Behrends et al (141), dose to the contralateral parotid can be relatively higher with IMPT plans due to the common use of lateral beams. These are utilized to reduce dose through the oral cavity which is in line with the sparing of the oral cavity seen in the pilot non-adaptive IMPT cases. VMAT on the other hand uses

multiple beams in an arc arrangement, and therefore spreads out the dose distribution more evenly across the axial plane.

The NTCP differences between non-adaptive VMAT plans and non-adaptive IMPT plans were >10% suggesting these cases would be candidates for IMPT funding as as per the NIPP-head and neck cancer criteria in The Netherlands. Both the pilot cases and Tambas data radar diagrams demonstrate the largest predicted differences are seen in the more inferior structures and oral cavity. Visually, there is a larger difference in mean dose to most of the OARs between the VMAT and IMPT plans in my pilot cases compared to the Tambas data. There is improved sparing of the contralateral submandibular gland and parotid glands with IMPT in the pilot cases compared to Tambas.

In Section 6.1, I explain the difficulties in defining osteoradionecrosis, and therefore the challenge of establishing important dosimetric constraints by NTCP modelling for the mandible in IMPT. In the literature the D30 metric has been suggested as an important predictor of osteoradionecrosis. To keep the risk of osteoradionecrosis of any grade to under 5%, suggested the D30 needs to be below 42Gy if teeth extractions have not occurred prior to radiotherapy, and 35Gy if they have. When assessing my results, it is important to appreciate that D30 was not prospectively defined as an optimal dose constraint at the time of planning. Had it been, there may have been greater impact on the D30 by IMPT and adaptation.

Non-adaptive IMPT delivered a lower mean dose and D30 compared to non-adaptive VMAT across the four pilot cases. In Cases 1 and 2, IMPT reduced the D30 to <42Gy and in cases 3 and 4, to <35Gy. I do not have the teeth extraction information for the pilot cases and therefore cannot comment on which was the more important constraint for each case. It is clear, however, that IMPT planning reduced the modelled risk of osteoradionecrosis for all cases when compared to VMAT. As previously mentioned earlier in the chapter, a retrospective study found that patients who developed osteoradionecrosis received an average mean dose of 46.8Gy compared to 39.3Gy in those who did not. With average mean doses of 38.2Gy and 16.86Gy for non-adaptive VMAT and non-adaptive IMPT respectively, our modelled standard

plans could be expected to confer a low risk of osteoradionecrosis had they been used to treat patients.

The global reduction in mean dose to OARs with IMPT is in keeping with consensus in the literature that the greatest dosimetric benefit of IMPT is the reduction of low to middle dose to normal tissues, as opposed to an improved conformality of high dose to the target volume.

6.4.2 The impact of biological response-based adaptation on IMPT plans

Whilst the magnitude of impact of adaptation on mean dose to OARs varied across the IMPT plans, most OARs had reduced mean doses because of IMPT adaptive planning. There was a trend for the largest reductions in the more caudal OARs with consistent reductions of up to 19Gy in the supraglottis, glottis and 8.62Gy in the middle pharyngeal constrictor muscle compared to non-adaptive IMPT plans. There was less reduction for the superior pharyngeal constrictor muscle (range 0.36Gy - - 1.72Gy) which may be due to the fact it is closer to or included within the high dose primary CTV whereas the middle pharyngeal constrictor muscle and more caudal structures benefited from reduced low and middle dose due to adaption. Even where large reductions in mean dose had been made by non-adaptive IMPT, e.g the oral cavity in Case 3, further reduction was seen with adaptation with an additional reduction of 10.98Gy. This suggests that adaptation as per the PEARL protocol may still of benefit regarding organ sparing in IMPT plans.

Many examples where PEARL adaptive increased the mean dose were changes of less than 1Gy. The ipsilateral parotid and submandibular gland received an increased dose with adaptation. These structures are often near the nodal target volumes. Unlike the primary target, the nodes were not adapted. Dose may have been moved from the area of the primary towards the peripheral, nodal volumes during the phase 2 planning, increasing the dose to OARs nearby. In addition, the ipsilateral parotid and submandibular gland are lower down on the list of priorities for OAR sparing and so limited effort may have been made to spare them.

The mean dose and D30 to the mandible for NON-ADAPTIVE_PROTON were already lowered by IMPT compared to NON-ADAPTIVE. This may in part explain why there was limited effect of PEARL adaptive. There was potential for clinical benefit seen in case 3 where the mean dose was reduced by 10.45Gy, and in case 2 where the D30 was reduced by 13.15Gy.

6.4.3 Impact of PEARL adaptation VMAT and IMPT plans

The magnitude of organ sparing by IMPT was far greater than the organ sparing effects of adaptation on VMAT and IMPT plans (Fig. 6.7). The mean doses were consistently lower with non-adaptive IMPT than non-adaptive VMAT, and adaptive IMPT plans had the lowest mean doses overall. Whereas both VMAT and IMPT techniques benefited from adaptation by reducing mean dose to the more cranial dysphagia associated OARs, IMPT was able to also reduce dose to the caudal OARs where VMAT appeared to have pushed dose inferiorly.

Response based adaption of IMPT plans produced more organ sparing than adaptation of VMAT plans. This could be expected given the amount of organ sparing already seen with non-adaptive IMPT. All cases had lower mean doses to the xerostomia and dysphagia associated OARs when planned with adaptive IMPT.

PEARL adaptation had a larger impact on the superior pharyngeal constrictor muscle, middle pharyngeal constrictor muscle, inferior pharyngeal constrictor muscle and ipsilateral parotid gland in the VMAT plans, and on the supraglottis, glottis, and oral cavity in the IMPT plans.

Cases 2 and 3 had the greatest reduction in combined mean dose to OARs with adaptation, both for their VMAT and IMPT plans. This is of interest as Case 3 had very limited reduction in the biological GTV on iPET. Combining mean doses may not reflect meaningful differences resulting from adaptation. For example, Case 1 had the largest bGTV reduction of 66% and

benefited the most from adaptation of the IMPT plans regarding the pharyngeal constrictor muscles which may be more clinically relevant.

That the combination of adaption and IMPT should work synergistically on organ sparing, and should be further explored, was championed in a recent review by Gamez and Ma (142). They noted that deintensification of radical radiotherapy for OPSCC by reduction in dose and or irradiated volume, is complimentary to the radiobiological characteristics of proton beam therapy which already limit normal tissue exposure. They called for future studies to better define which patients will benefit most from the combination of proton beam therapy and deintensification. PET-CT assessed response of the primary during treatment offers a potential option for further investigation.

6.4.4 Limitations

Whilst many papers have suggested aiming for a variety of dosimetry metrics to reduce acute and late toxicity, and NTCP curves calculated and applied, no consensus currently exists regarding what merits a 'significant' change in mean dose to head and neck OARs. It is not possible to determine what true clinical benefit resulting from the improved dosimetry seen in this study with adaptation using IMPT. With the follow up of the PEARL Study, the toxicity data gathered from patients treated on adapted plans will allow us to compare dose delivered to OARs with toxicity experienced by the patient.

As in previous chapters, a major limitation of this work is the low number of cases. Further work involving a much larger cohort of modelled plans is needed to make my data more robust.

The VMAT and IMPT plans were manually planned in different cancer centres and in collaboration with different planners. There is therefore a potential for some of the differences between the VMAT and IMPT plans to be due to human and system factors rather than the planning technique alone. I planned the non-adaptive and adaptive VMAT plans, and non-

adaptive and adaptive IMPT plans alongside the same planner however, so this should be minimised.

The Phase 2 optimisation was performed differently when planning the VMAT and IMPT plans. IMPT planning of Phase 2 took into consideration dose delivered by Phase 1 by deformably fusing it with the iPET-CT, VMAT did not. Whilst this won't affect the marked differences seen when comparing non-adaptive VMAT to non-adaptive IMPT, it could affect the modelled relative impact of adaptation between the 2 different types of radiotherapy delivery.

Finally, in order to facilitate the modelling of the IMPT plans, the pilot study imaging and contoured structures had to be transferred twice between 2 different planning systems. This can lead to distortion of structures which may result in minor differences in the volumes of OARs I have studied. Changes in volumes may have an impact on the dosimetry I have presented although in most cases, I believe the differences to be negligible.

6.5 Conclusion

Whilst primarily limited by the small number of cases, I have demonstrated that IMPT markedly reduces doses to OARs compared to VMAT planning in line with widely published studies. I have also demonstrated that adaptation based on the biological response to the tumour after 2 weeks of chemoradiotherapy can further improve the tissue sparing already achieved with IMPT. This is the first study to demonstrate that OAR sparing by IMPT can be improved with biological response guided adaptive.

My results are in line with published data that IMPT can spare many head and neck OARs to a greater extent than VMAT in the treatment of oropharyngeal cancers. From my data, the impact of IMPT on the mean dose to OARs is greater than the impact of adaptation when compared to standard VMAT planning, but there may be additional benefit to adapting IMPT to tumour response during a course of radiotherapy treatment, especially to the OARs caudal to the middle pharyngeal constrictor muscle. In my small cohort, adaptation on VMAT plans is

unlikely to have affected a decision for IMPT treatment as per the Netherlands NTCP-based algorithm.

Further work with a larger cohort of patients, as well as real-time studies to collect prospective clinical data on xerostomia and dysphagia rates, is required to properly investigate the clinical advantages of adaptive in IMPT.

Chapter 7: A study looking at changes in hyoid position during radiotherapy for oropharyngeal squamous cell carcinoma and potential use in verification and decisions for re-planning

7.1 Introduction

7.1.1 Background

IMRT and VMAT improve the conformality of radiotherapy delivery according to the plan calculated on the initial planning CT. They cannot, however, account for anatomical changes during a course of treatment unless the plan is adapted to these changes throughout the course of treatment with reactive re-planning. The steep dose gradients typical of highly conformal IMRT/VMAT plans make target coverage vulnerable to small changes in position or anatomy which can result in differences between the planned and delivered dose. This is of relevance to OPSCC where the tumour is near large numbers of critical structures and OARs within a small anatomical space. An additional challenge is the movement of normal structures within the neck as part of normal physiological processes e.g., swallowing. The introduction of the '5 + 5' expansion of head and neck GTVs to produce high dose and intermediate dose CTVs as adopted in the PEARL protocol, means the volumes planned to receive the highest dose are smaller than those based upon the historical 1cm GTV to CTV expansion. The further expansion of the CTV to the PTV with a non-edited margin is designed to mitigate for set up error and treatment delivery inaccuracies. For head and neck patients, the PTV margin is standardly defined by departmental assessment of their in-house levels of accuracy for set up and treatment delivery. It is not standardly altered as a result of different subsites of head and neck cancers.

Despite advancements in the quality of imaging and machine accuracy, there is no standardized verification protocol in the UK and no current consensus on the implementation of reactive or prospectively scheduled re-planning in head and neck radiotherapy.

7.1.2 Reactive re-planning

Reactive re-planning is the unscheduled replanning of radiotherapy plans in response to changes in patient anatomy during a course of radiotherapy to further reduce uncertainties around internal organ motion and deformations. The implementation of reactive re-planning to avoid excess dose to OARs and improve coverage of target volumes is routine practice in most UK radiotherapy departments, although the threshold is not standardized. Re-planning generally requires a second planning CT and mitigates for deformations such as tumor regression and weight change. This additional work is an arduous process requiring several hours of involvement by both clinician and physicist/planner. In many over-stretched radiotherapy departments, it can be a challenge to produce a re-plan in a clinically acceptable amount of time. Identifying which patients are likely to need re-planning in a timely way so that treatment can continue the original plan whilst re-planning is carried out is important.

7.1.3 Treatment verification in head and neck radiotherapy

The decision of whether a radiotherapy plan is acceptable to treat a patient on any given day within the course of radiotherapy relies upon the verification process. Verification refers to checks performed to ensure the patient and target volume positions are within an acceptable range for the current plan to be delivered safely and effectively. Maintenance of target volume coverage, and avoidance of breaching dose constraints is paramount.

Once the patient is on the treatment couch, imaging is performed to verify patient position prior to treatment. Imaging is performed with either kilovoltage (kV) or megavoltage (MV) imaging modalities and allows visualisation of the target volume, or its surrogate, in relation to OARs. Either 2D or 3D imaging can be performed. Electronic portal imaging (EPI) devices and KV planar imaging deliver 2D images whereas linear accelerator-based kV cone beam CT (CBCT) or MV CBCT on tomotherapy units deliver 3D imaging.

In ESTRO guidelines for Positioning, Immobilization and Position Verification of Head and Neck Patients for radiation therapists published in 2016 (142) European cancer centres were sent questionnaires designed to investigate their immobilization, set up and verification processes. Out of 32 countries surveyed, 24 responded, a total of 187 centres. Alongside Germany and Greece, the UK was one of the highest responders, providing information from 31 cancer centres. In just over half the centres (51.2%), on treat imaging was performed with CBCT alone, in 15.4% MV EPI was used alone, and for 35.2%, a mixture of both. Some of the centres' different set up and verification protocols were published as part of the introduction to the ESTRO guidelines.

7.1.3.1 Anatomical structures used for set up verification

There are various structures listed in the literature which are used to help radiotherapists optimise a head and neck cancer patient's position for treatment. Common practice is to match the CBCT to the planning CT at the skull base and C1/C2 vertebrae – as this is the most stable bony anatomy when the patient is in the treatment position, immobilised with the beam direction mask. Matching at one position alone, however, can mean other parts of the anatomy are displaced relative to their position on the planning CT.

7.1.3.2 Multiple Regions of Interest for Head and Neck treatment verification

Matching up multiple locations, or regions of interest (ROI), can improve confidence of matching for a larger proportion of the patient anatomy. The need for this is informed by several studies demonstrating different degrees of movement at different points of the anatomy. Ove et al (144) retrospectively reviewed 20 head and neck cancer patient's CBCTs. The daily CBCTs were matched at the C1/C2 vertebrae at the cranial end, and at the most anterior aspect of the clavicles on the most caudal slice displaying both lobes of the thyroid gland, at the caudal end. The group found that the mean systemic shift was 3.08mm in the anterior-posterior direction for the lower part of the neck in relation to the C1/C2 vertebrae,

with random shifts of up to 3.9mm anterior-posterior, 2.6m cranio-caudal and 3.3mm laterally. They concluded that larger PTV margins may be required for plans involving the lower neck with volumes some distance from the C1/C2 fusion.

Giske et al (145) retrospectively reviewed 45 head and neck cancer patient CBCTs to look at the impact of weight loss on patient position. They defined a few local region boxes containing anatomical structures expected to show inter-fractional position changes; the skull base, nose, C1/C2 vertebrae, mandible, larynx, T2 vertebra and the medial aspect of the clavicle. They found the skull base was the least susceptible to changes in weight but that the neck was more affected by weight loss. They suggested that the use of local region boxes specific to the location of the tumour and weighted in importance on an individual patient basis would be more beneficial in verification than the use of general landmarks.

Van Kranen (146) sought to quantify the geometric uncertainties in 8 regions of interest including the mandible and larynx. They defined the local set up accuracy for each region of interest and compared to an overall accuracy of the clinically used larger region of interest. Deformation was distinguished from rigid body movements by measuring movement relative to the C1 – C3 vertebrae. The group showed that systematic deformation ranged from only 0.4mm near the C1 – C3 region of interest, to 3.8mm at the larynx. They concluded that their current PTV margins may be inadequate to account for this degree of uncertainty and proposed the introduction of smaller region of interests, and correction protocols that accounted for movement in all of them, in addition to the implementation of re-planning to reduce the frequency of set up errors.

The findings of these three groups suggest the need for a more tailored approach to verification based upon the location of the target volumes and their distance from the most stable region of head and neck anatomy, the skull base/C1, C2 vertebrae.

7.1.4 Dosimetric impact of set up errors in Head and Neck Radiotherapy

High quality verification is required for radical head and neck radiotherapy as changes in set up and anatomy can lead to dosimetric changes in a treatment plan. Neubauer et al (147) looked at 10 patients who were matched by the neck (C2 – T3 vertebrae) and shoulder position (head of humerus). They demonstrated that a superior couch shift of 5mm could result in loss of target coverage by the 100% isodose of 2 – 24cm^3. A superior shift of 15mm could reduce coverage by the 95% isodose by 40cm^3 and the 100% isodose by 100cm^3. In addition, the group demonstrated that the loss of coverage was not mitigated for by a couch shift in the opposite direction due to the beams passing through a different transverse section of the body. Similarly work by Sieber et al (148) found that 3mm systemic errors had a negative effect on target coverage and that the dose delivered to 98% of the GTV (D98%) was the metric most sensitive to uncertainty in set up position.

These studies support the need for accurate treatment set up and demonstrate the potentially clinically significant impact inaccurate set up can have on the dosimetry of a plan. In line with this, the ESTRO guidelines recommend that the anatomical structures chosen for matching should be surrogates for the target volume and may need to vary between head and neck cancer patients according to the location of their tumour. They also suggest it may be prudent to define primary and secondary matching structures; the primary structures being those closest to the target volumes and therefore prioritized. They would also be the optimal location to place the clipbox in the use of CBCT.

There is very little published on the individualization of verification protocols for individual patients. In this chapter, I explore the use of the hyoid bone as a potential surrogate for oropharyngeal tumour position and consider which patients it may be appropriate for as part of a patient-tailored verification protocol.

7.1.5 Role of the hyoid in OPSCC treatment verification

The complexity of head and neck anatomy and the variety of internal organ movement and external shape change commonly seen in head and neck cancer patients during a course of radical radiotherapy points to the need for a more complex verification of patient position on the treatment couch.

Van Beek et al (149) published their first clinical experience of multiple regions of interest (region of interests) used to verify OPSCC patient set up. In a cohort of 50 patients, 12 – 13 region of interests containing bony structures seen on the planning CT were defined. Each region of interest was individually registered to subsequent daily CBCT and global and local (individual region of interest) set up errors were quantified. Thresholds of either >5mm shift or >5□ rotation were set. In 40% of CBCT there was at least 1 or more region of interest which met the threshold. The majority were seen at the hyoid, 31% demonstrating a rotational error and 14% a translational error. Overall, the set-up errors led to 52 consultations with the treating radiation oncologist. This study demonstrated the labour intensity of head and neck cancer patient treatment verification required for optimal set up and suggested the hyoid bone position is the source of a substantial number of set up errors. The same group outlined their local protocol – based on this work - in the ESTRO guidelines. Their centre used 9 bony structures (Fig 7.1) including the hyoid bone to set up their head and neck cancer patients by rigidly registering them to the planning CT. Average local set up errors then informed the couch shift correction, or the need for re-planning.

Fig. 7.1 Demonstration of the 9 regions of interest for matching head and neck cancer patients. The red box demonstrates the hyoid region of interest. Figure courtesy of Suzanne Van Beek, NKI Cancer Centre, The Netherlands (Published in the ESTRO Guidelines for positioning, immobilization and position verification of Head and Neck Patients for RTTs)

The hyoid bone is an attractive option for oropharyngeal tumour position checks as it is often near the primary cancer (GTV_P) and seen easily on CBCT. In some OPSCC cases, the hyoid bone is directly involved with tumour, in other cases it is indirectly involved. Indirect involvement can be via tumour invasion of hyoid muscle attachments including the middle pharyngeal constrictor muscle and extrinsic tongue muscles (ETMs). Whilst the hyoid bone normally moves with physiological processes such as swallowing, pathological involvement of the hyoid by direct or indirect tumour invasion can fix its position, impairing or preventing its normal movement.

7.1.6 Importance of coverage of the hyoid bone

Locally advanced OPSCCs can involve the extrinsic tongue muscles which attach to the hyoid. Farzal et al (150) found that in P16 positive primaries, the most common muscles invaded were the hyoglossus (57.8% of patients, and genioglossus (56.3%), both of which insert onto the hyoid bone. Coverage of the hyoid by the prescribed dose is therefore important to ensure the primary PTV is adequately covered. Heaton et al (150) retrospectively examined the prognostic influence of hyoid bone involvement by base of tongue cancers treated with chemoradiotherapy in 37 patients. 11 patients had evidence of hyoid bone involvement on pre-treatment imaging. When compared to the 26 patients who did not have hyoid involvement, these 11 patients had a reduction in all measured survival metrics. 2-year locoregional relapse was 63.6% versus 12.5%- and 5-year locoregional relapse was 86.4% versus 36.4%. This demonstrates the poor prognosis of tumours involving the hyoid bone and whilst that is likely to be due to multiple factors including advanced tumour stage, it is possible that unreliable coverage of the hyoid bone during a fractionated course of radiotherapy may have an effect.

A change in hyoid position on CBCT compared to baseline planning CT is a concern as it may reflect a change in the position of the target volume and OARs. It is a common reason for an imaging specialist radiographer referral for Head and Neck patients at Velindre Cancer Centre. If the baseline hyoid position or tumour specific factors were predictive for a future displacement of the hyoid, re-planning could be prospectively factored into a patient's treatment pathway. It may also allow for the reduction of PTV margin in patients whose hyoid position on the planning CT predicts a stable position throughout treatment or signal a need to increase PTV margins in the lower neck to account for hyoid position variability.

7.1.7 Rationale for study

In my clinical practice, I noted a large proportion of OPSCC referrals to the imaging verification meeting were triggered by a change in the position of the hyoid bone on CBCT compared to

the planning CT. Due to the relationship between the position of many oropharyngeal tumours and the hyoid bone, the hyoid position can change as the tumour responds to treatment e.g., it may move inferiorly over the course of radiotherapy as base of tongue tumours respond to radiotherapy and release extrinsic muscles of the tongue, or the hyoid itself. If the hyoid bone is used as a surrogate for the primary GTV position, we may well inaccurately verify treatment during the latter fractions of radiotherapy as the hyoid moves more independently of the primary GTV. Alternatively, if we don't consider the hyoid bone in verification and match to other bony landmarks in patients where the primary tumour moves with the hyoid, we could risk geographical miss, or an unplanned increase in dose to OARs. Finally, hyoid position at baseline or its relationship to the primary GTV may well predict for the need to re-plan midway through treatment in some patients, or the need for an adjusted PTV margin.

There is a paucity of literature addressing the relationship between primary GTV and hyoid movement during radiotherapy. No standard protocols to reduce its prevalence and impact upon verification exist to my knowledge. In this chapter, I explore the use of the hyoid bone as a potential surrogate for oropharyngeal tumour position and consider which patients it may be appropriate to create a patient-tailored verification protocol for.

7.1.8 Objectives

1. Retrospectively investigate the prevalence and magnitude of hyoid position change in radically treated OPSCC patients in our cancer centre referred for image review during 2018 and 2019.
2. Determine how many patients referred for hyoid movement were at risk of geographic miss of the high dose primary clinical target volume (CTV) or primary GTV due to hyoid movement.
3. Investigate potential tumour and patient features that predicted hyoid movement: the presence of cranio-caudal overlap of primary GTV and hyoid; the position of the hyoid

in relation to the mandible as a surrogate for how high the hyoid sits during patient set up; the involvement of extrinsic muscles of the tongue by the tumour.

7.1.9 Hypotheses

1. When the hyoid bone is a surrogate for an OPSCC primary tumour, hyoid bone displacement in some patients may risk the geographical miss of the part of the primary GTV and/or primary CTV.
2. The magnitude of the hyoid bone displacement is larger in patients with larger tumours, and tumours involving structures anatomically attached to the hyoid bone including the epiglottis and floor of mouth muscles i.e., T3 and T4 primaries, and base of tongue tumours.

7.2 Methods

7.2.1 Identification of the 2018 and 2019 patient cohort, their tumour specific features and prevalence of hyoid position change

At Velindre Cancer Centre, radically treated head and neck patients who have persistent onset changes to the hyoid position on CBCT at verification, are referred for review and discussion of potential geographical miss. If clinically indicated, a dosimetric study is performed on the CBCT by the physics team. This involves the deformable registration of the initial treatment plan onto the CBCT. This is used to assess whether PTV coverage is adequate, and whether dose to critical structures e.g., the spinal cord, remain within their mandatory tolerance. If there is concern about either of these issues, the patient has a repeat planning scan performed and a new plan is produced based on up-to-date contouring. Usually, the patient

is treated on the initial plan whilst the new plan is calculated. This urgent re-planning takes 1 – 2 days.

The records of all OPSCC patients treated with radical radiotherapy at Velindre from 01.01.2018 – 31.12.2019 were collected from the electronic patient (Canisc) database. The radiographer database of patients referred for set-up imaging review during the same time period was screened. The reasons for referral were concern over target coverage and/or excess dose to OARs, occurring as a result of factors including weight loss, tumour regression, random set up errors, and a change in hyoid position. All patients who were referred on account of hyoid movement during 2018 and 2019 were identified. The date of referral was recorded as the date of the on-set CBCT demonstrating hyoid displacement compared to the planning CT scan which triggered referral to the imaging team. T stage and subsite of primary tumour was also recorded. To assess whether more T4 and base of tongue tumours were referred for hyoid displacement than expected from the total number treated, Chi squared tests were performed.

7.2.2. Measurement of magnitude of hyoid bone displacement

7.2.2.1 Importing of CBCT from X-ray Volumetric Imaging (XVI) software and fusion with planning CT

I imported the CBCT for each patient that had been referred to the imaging team from the treatment linear accelerator XVI software to the Prosoma treatment planning system. I fused the CBCT fused by automatic rigid registration with the planning CT on Prosoma (Fig. 7.2a). When necessary, I made manual adjustments to the fusion. The priority areas for match were those standardly used at Velindre Cancer Centre; the skull base and C1/C2 vertebra. These are immobile structures in the neck and have high levels of positional reproducibility.

7.2.2.2 Contouring of the hyoid bone

I contoured the baseline hyoid bone position in its entirety (cornua and body) on the axial slices of the planning CT (Fig. 7.2b), and the interim hyoid position on the on-treatment CBCT (Fig. 7.2c).

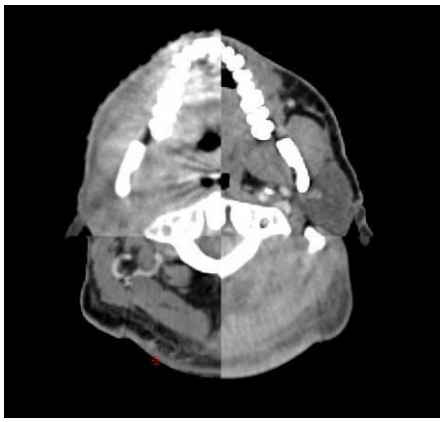

Fig. 7.2a

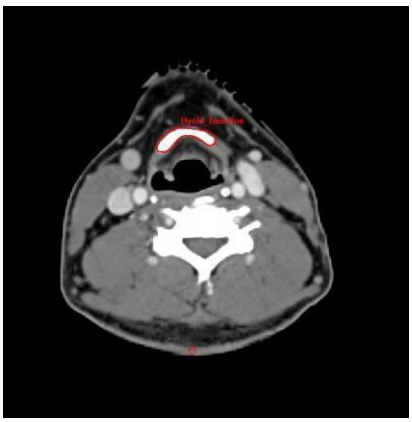

Fig. 7.2b

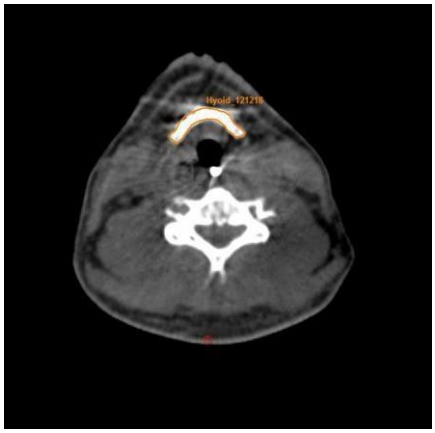

Fig. 7.2c

Fig. 7.2a - c: An example of axial CT slices showing the fusion of the planning CT and on-treatment CBCT, and the contouring of the interim hyoid (orange) and baseline hyoid (red) position.

7.2.2.3 Measurement of hyoid movement

Using the CT slice numbers obtained from Prosoma, the position of the primary GTV, baseline hyoid position and interim hyoid position at the time of referral were recorded. The most

cranial axial CT slice with any part of the hyoid visible on it was recorded as the cranial extent of hyoid, and the most caudal axial CT slice was recorded as the caudal extent. In addition to the body of hyoid, the cornua were also included so that rotational shifts in hyoid position could be better accounted for.

7.2.2.4 Primary GTV/hyoid overlap

The amount of cranial/caudal overlap between the primary GTV and baseline hyoid position was also recorded by recording the axial CT slices on the planning CT they were visible on, multiplying by 2mm for the thickness of the CT slice, and deriving, if any, the degree of overlap. Fig. 7.3a + b shows the fused planning CT and CBCT from the case in Fig. 7.2, in the sagittal plane. The planning CT slices demonstrate the position of the hyoid bone contoured on the planning CT scan (red) compared to the position of the hyoid bone contoured on the on-treatment CBCT scan (orange). The fusion of the CBCT hyoid onto the planning CT scan shows the difference in position of the hyoid.

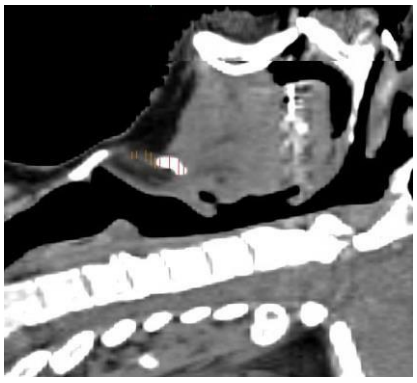

Fig. 7.3a

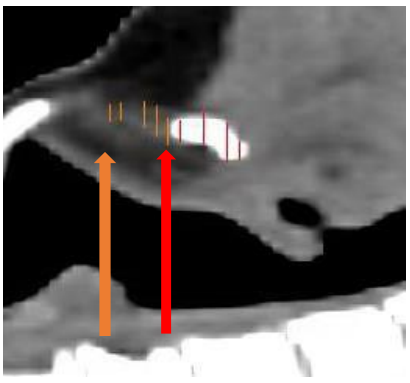

Fig. 7.3b

Fig. 7.3a: An example of a sagittal CT slice showing the interim hyoid (orange) displacement from the baseline hyoid (red) position. Fig 7.3b is a zoomed in image of the hyoid contours. The red arrow points to the caudal extent of the hyoid bone on the planning scan. The orange arrow points to the caudal extent of the hyoid bone on the CBCT.

To create a standard high dose PTV from the GTV, a 5-6mmto form the high dose CTV, then a further a 3-5mm margin for PTV, is added circumferentially, caudally and cranially to account

for microscopic spread and internal movement/set up error respectively. At Velindre Cancer Centre, we use 5mm. The total margin added onto the primary GTV is therefore 8-11mm depending on the treating centre specific margin protocols.

I studied the magnitude of hyoid displacement in head and neck patients at our centre to identify those whose hyoid moved superiorly or inferiorly by 8mm or more and so were at risk of geographical miss of the primary GTV by the high dose coverage by the 95% isodose if the PTV margin was 3mm, the minimal margin used standardly in the UK for head and neck VMAT with daily imaging. By measuring deviation of both the cranial and caudal extent of the hyoid bone I also captured any rotational movement that may have occurred with the deviation.

Displacement of the hyoid was measured by recording the most superior and inferior axial CT slice any part of the body or cornua of the hyoid was visible on the planning CT and CBCT and comparing the planning CT and CBCT measurements.

7.2.3 Determining the position of hyoid bone in relation to mandible

If the hyoid lies more cranially on the planning CT, it may suggest fixation by the oropharyngeal tumour and potential for the hyoid to drop caudally as the tumour responds. To investigate this, I designed a novel method to measure how high the hyoid was positioned relative to the fixed position of the cervical spine. Whilst this is a single time point regarding the position of the hyoid, I have assumed that the impact of swallowing and respiration is minimal given how short a period of time these functions occur for, within a 10 – 15 minute treatment. In addition, these were only referred after systemic set up errors occurred over 3 consecutive days therefore unlikely to be due to transient physiological changes in hyoid position. I used the sagittal slice of the planning CT corresponding to the midline of the axial slice the caudal extent of the hyoid was visible on (Fig. 7.4). On the sagittal slice, I drew a red line from the caudal border of the mandible to the postero-caudal edge of the C2 vertebra. I then drew a

yellow line perpendicularly from the red line to caudal extent of the hyoid body. This distance was recorded as a measure of how cranial the hyoid was positioned on the planning CT.

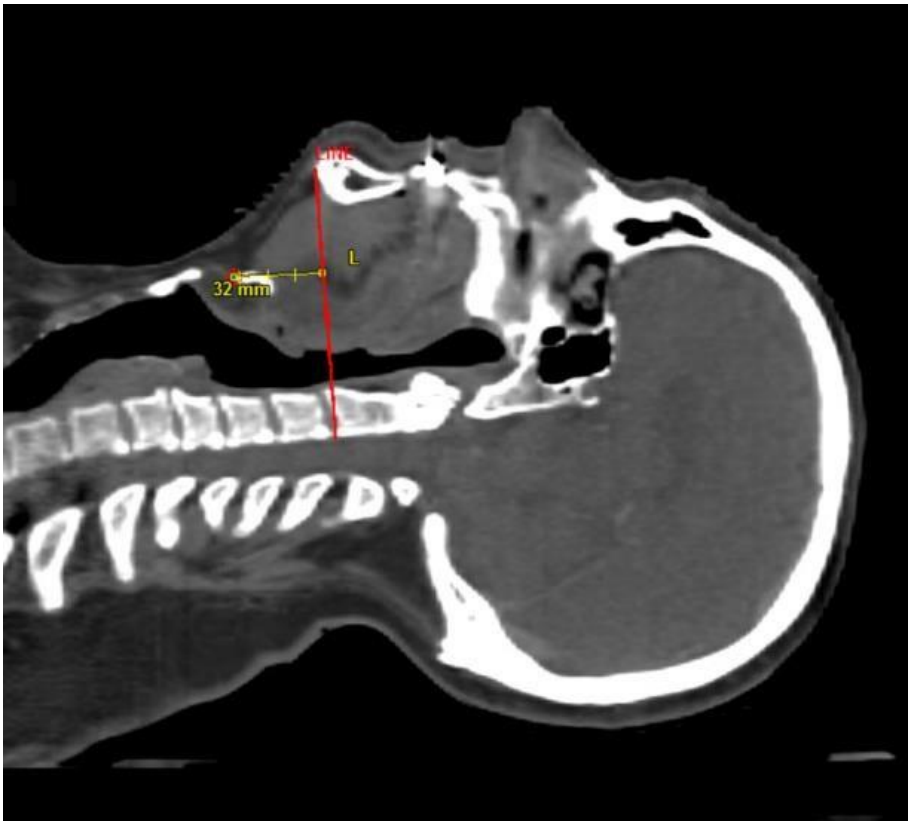

Fig. 7.4 Measurement of hyoid position in relation to the mandible to measure how high the hyoid sits. In this example, the distance from the most caudal extent of the hyoid, to the line drawn between most caudal extent of the mandible and posterior edge of the C2 vertebra, is 32mm.

7.2.4 Measuring the extent of tumour infiltration into the floor of mouth

Radiology reports of the diagnostic MRI and CT scans were reviewed for evidence of floor of mouth or extrinsic tongue muscle involvement by the primary. The involvement of the following extrinsic muscles of tongue was recorded:

- Hyoglossus
- Genioglossus
- Styloglossus

- Mylohyloid

In patients with radiological evidence of extrinsic tongue muscle involvement, the maximum anterior-posterior extent of the primary GTV was measured on the CT slice at the level of the lingual septum with reference to complementary MRI imaging. This measurement was used as a surrogate measure of extrinsic tongue muscle involvement. The level of the lingual septum was chosen as it corresponds with a level where hyoglossus, genioglossus and mylohyoid muscles are visible (Fig. 7.5a+b).

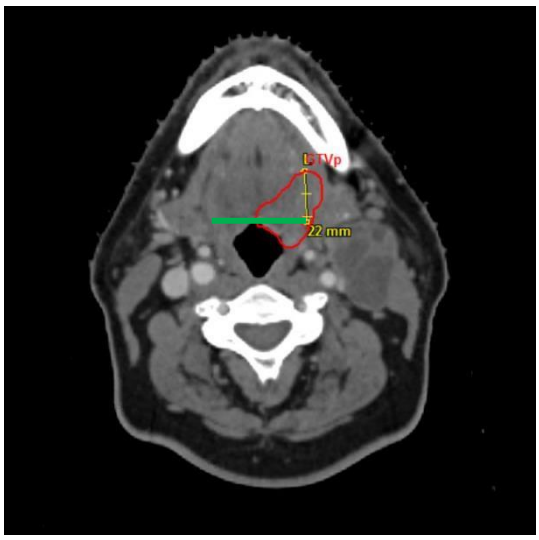

Fig. 7.5a

Fig. 7.5b

Fig 7.5a Maximum Anterior – Posterior dimension measured perpendicularly from the anterior pharyngeal air lumen (green line) to anterior extent of primary GTV (red contour) at the level of the lingual septum.

Fig 7.5b Marked extrinsic muscles of tongue at level of the lingual septum (red arrow): Green = Mylohyoid, Pink = Genioglossus, Yellow = Hyoglossus, Purple = Submandibular Glands. Courtesy of Eneva, M et al from their poster 'MDCT of the floor of the mouth' exhibited at the European Congress of Radiology 2019.

I looked at the proportion of patients who had tumour involvement of any extrinsic tongue muscle, and then specifically at whether the hyoglossus was involved, either in addition to the other extrinsic tongue muscles, or alone. The hyoglossus muscle directly connects the base of tongue to the hyoid body, and entire length of the greater cornua, and so could be expected to be the muscle with the greatest impact on hyoid position.

7.2.5 Statistics

I performed Chi squared tests to look for over representation of tumours with associated features in those referred for hyoid displacement, compared to those not referred. I calculated the Chi squared test taking into account the multiple data points on an excel spreadsheet. The raw data is not included in this thesis.

7.3 Results

7.3.1 Number and staging of OPSCC patients referred with hyoid displacement in 2018 - 2019

A total of 232 patients with OPSCC were referred for definitive radiotherapy from 01.01.2018 – 31.12.2019 through the Southeast Wales network and treated with definitive radiotherapy or chemo-radiotherapy (Fig. 7.6). 47 (20.3%) patients were referred for hyoid bone displacement, 29 in 2018 and 18 in 2019. Of these, 13 (27.7%) were T3 and 29 (61.7%) T4, compared to 41.4% T3 and 40.9% T4 of the total number of patients. The chi squared test for T4, base of tongue tumours, and involvement of extrinsic tongue muscles was statistically significant at <0.001, 0.048 and 0.002 respectively. I had complete CBCT imaging histories (planning CT and CBCT referred for hyoid displacement) on 38 referred patients.

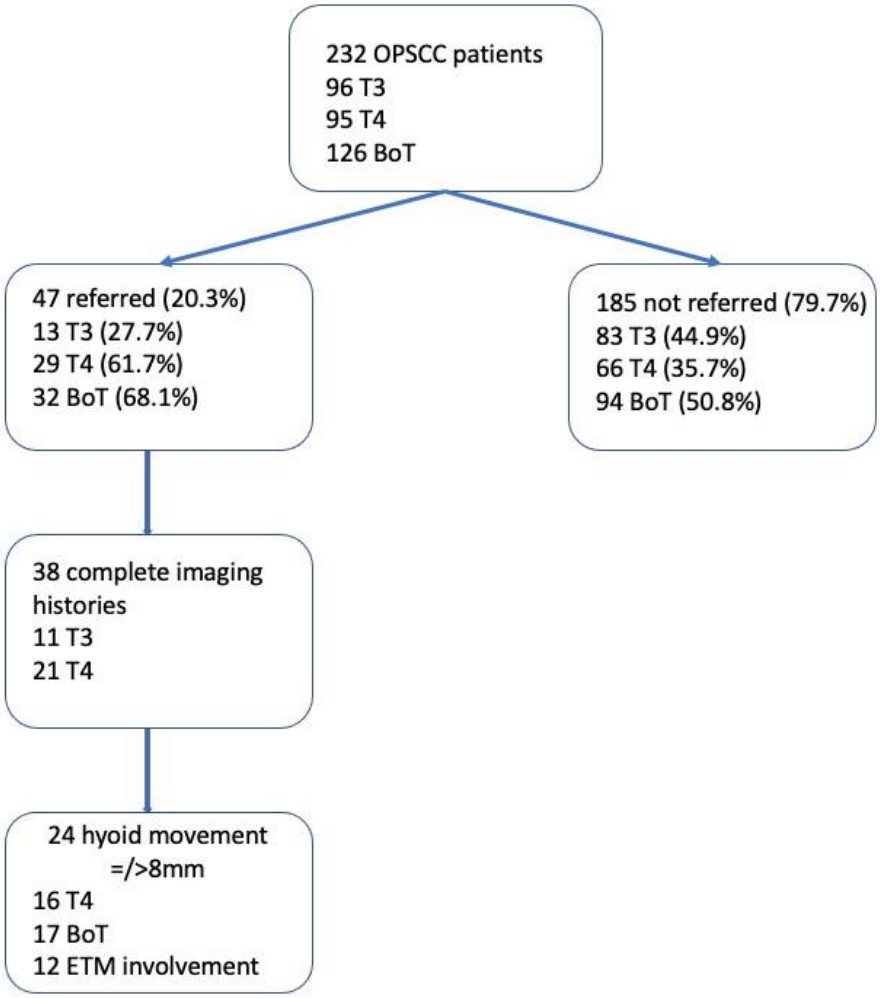

Fig. 7.6 OPSCC patients treated with radiotherapy 2018 – 2019: Those referred because of hyoid displacement during radiotherapy versus those not referred. Percentages do not add up to 100% in each arm due to some tumours being both a T3, or a T4, and a base of tongue primary.

BoT = Base of Tongue

ETM = Extrinsic Tongue Muscle

7.3.2 Comparison of radiological features in the OPSCC patients referred to imaging team for hyoid displacement vs those not referred.

The pre-defined radiological features of the tumours referred to the imaging team were compared to those in the non-referred group (Table 7.1).

	Referred	Non referred	Chi Squared Test
Total number of patients	47 (20.3%)	185 (79.7%)	N/A
% With overlap of primary GTV and hyoid Mean overlap	45 (95.7%) 9.4mm	123 (66.5%) 6.4mm	0.012
Mean distance mandible to hyoid at baseline	10.2mm	16.4mm	N/A
Radiological evidence of extrinsic tongue muscle involvement	21 (44.7%)	56 (30.3%)	0.002
% With radiological evidence of any hyoglossus involvement	16 (34%)	28 (15.1%)	<0.001
% With radiological evidence of hyoglossus involvement and no other extrinsic tongue muscle	7 (14.9%)	11 (5.9%)	<0.001

Table 7.1 Characteristics of patients receiving radical radiotherapy for OPSCC during 2018 -2019

7.3.2.1 Magnitude of hyoid displacement

26 of the 38 referred patients with complete imaging histories had displacement of either the cranial, caudal, or both borders of the hyoid of 8mm or more (reaching the red lines on Fig 7.7). They represent 11.2% of the total number of OPSCC radically irradiated during 2018 and 2019 and 55% of patients referred for hyoid displacement. The mean displacement of the cranial hyoid border was a caudal displacement of 7.8mm, and caudal hyoid border was a caudal displacement of 6.5mm.

For all patient studied, the cranial and caudal borders of the hyoid bone move in the same direction. In 2 cases there was cranial displacement of the hyoid, all others were referred for caudal displacement. In 30 cases, the cranial and caudal hyoid borders moved to differing extents in the same patient. The largest displacements were seen for the superior border of the hyoid moving caudally.

With the adoption of the '5+5' geometric expansion of the GTV in many UK cancer centres, the margin of primary GTV to PTV in many departments is a minimum of 8mm (5mm for high dose CTV and 3mm for HD PTV). Patients with a hyoid deviation of 8mm or more are therefore at risk of geographical miss of the primary GTV if we assume the hyoid movement is representative of tumour movement. I classified patients with hyoid drop of 8mm or more as having a 'significant' hyoid drop. Of those with a significant hyoid drop, 16 (67%) are staged as T4 and 17 (70.8%) were base of tongue primaries which suggests the primary tumour is near the hyoid bone.

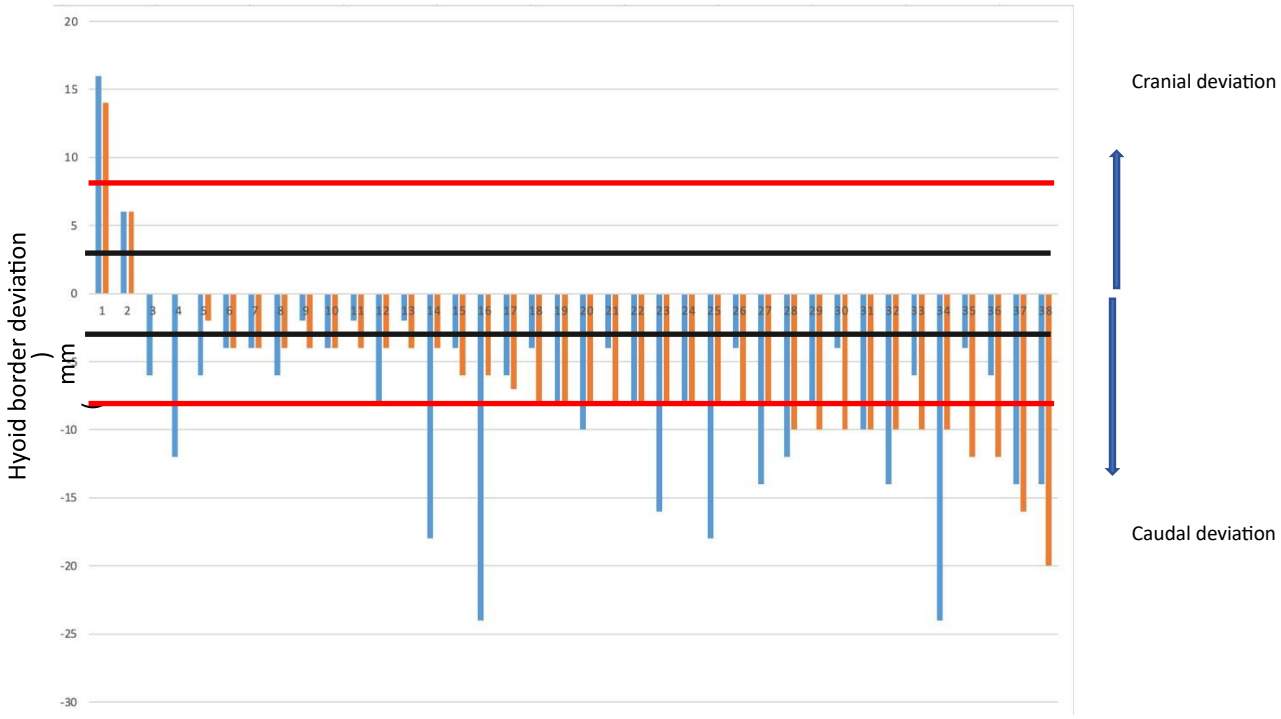

Black horizontal line = +/- 3mm (risk of TV miss) Red horizontal line = +/- 8mm (risk of GTV miss)

Fig 7.7 Deviation of the hyoid's superior (blue) and inferior border (orange) on the imaging team referral CBCT compared to planning CT for each referred patient with complete imaging histories (n=38).

7.3.2.3 Anatomical features: GTV_P and hyoid cranio-caudal overlap

The primary GTV overlapped with the hyoid bone on the planning CT in 95.7% of referred patients versus 66.5% of patients not referred with a significant Chi squared test of 0.012. (Table 7.1). The mean extent of primary GTV and hyoid overlap was 9.4mm versus 6.4mm.

7.3.2.4 Extent of tumour infiltration into the floor of mouth

21 (46.7%) of patients referred to the imaging team had radiological evidence of floor of mouth / extrinsic tongue muscle invasion. Maximum anteroposterior dimension of tumour

invasion into the floor of mouth was used as a surrogate for extent of extrinsic tongue muscle invasion.

16 out of 47 (35.5%) of patients referred to the imaging team had radiological evidence of hyoglossus involvement compared to 22.8% not referred, and 7 (15.6%) patients had radiological evidence of hyoglossus involvement alone, with no other extrinsic tongue muscle invaded, compared to 8.9% in the non-referred group.

There was a significant difference in the involvement of extrinsic tongue muscles, and hyoglossus involvement, between those referred for hyoid displacement, and those who were not.

7.3.2.5 Relationship of height of hyoid on planning CT and hyoid displacement

The mean distance between the hyoid bone and the mandible was 10.2 mm in referred patients (range 4 – 14mm) and 16.4mm in non-referred patients (range 4 – 25mm).

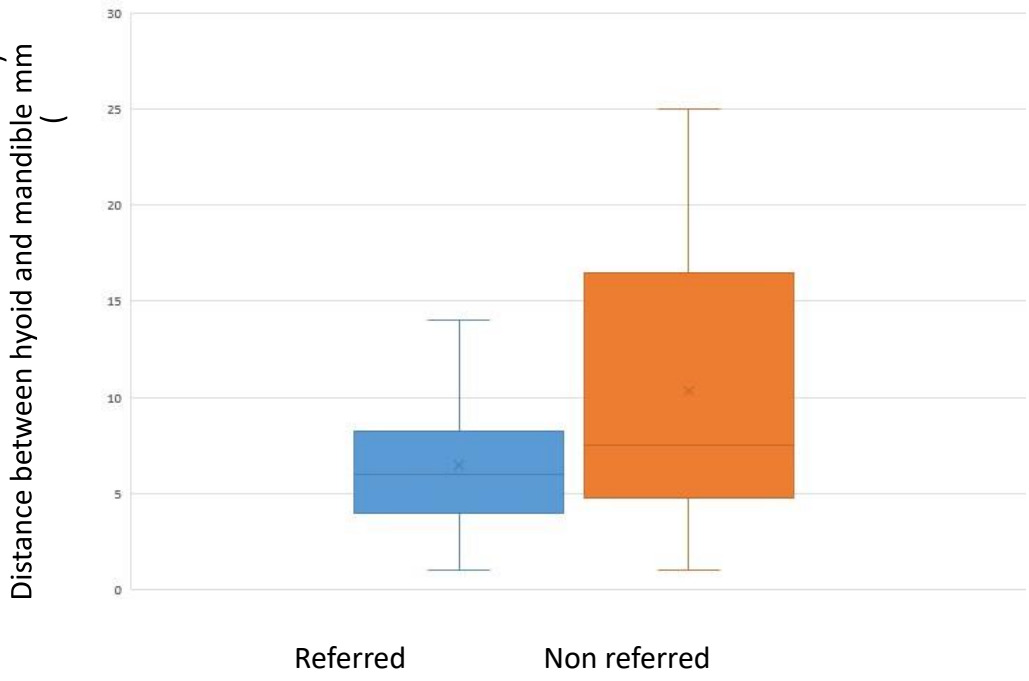

Fig. 7.8 Box and whisker plot of distance (mm) between hyoid and mandible.

7.3.2.6 The use of hyoid position as a surrogate for position of the primary GTV

3 patients referred for hyoid deviation were re-scanned with a kV planning CT which was used to generate a second mid-treatment plan. I looked at these cases and assessed if the primary GTV moved with, or independently of, the hyoid. If the hyoid drop is a result of tumour response and the subsequent release of extrinsic tongue muscles, it would be rational to expect the primary GTV to remain in its original position after the hyoid drop. Out of the 3 patients re-planned, 2 had a caudal shift of the primary GTV to correspond with the change in position of the hyoid bone. Below is an example of a patient in whom the hyoid drop is associated with a caudal shift in the primary GTV (Patient A, Fig. 7.9), and a patient in whom the hyoid drop is independent of the primary GTV position (Patient B, Fig. 7.10).

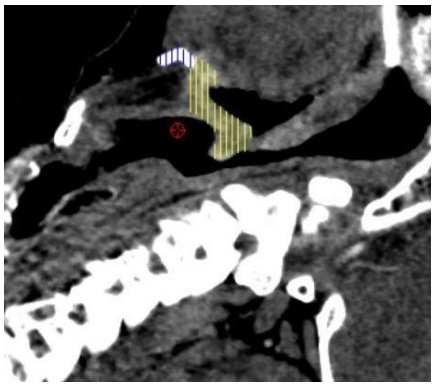

Fig. 7.9a Patient A: planning CT.
GTV outlined in yellow, hyoid in blue

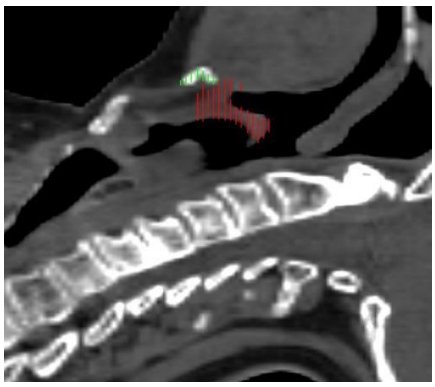

Fig. 7.9b Patient A: Re-scan CT.
GTV outlined in red, hyoid in green

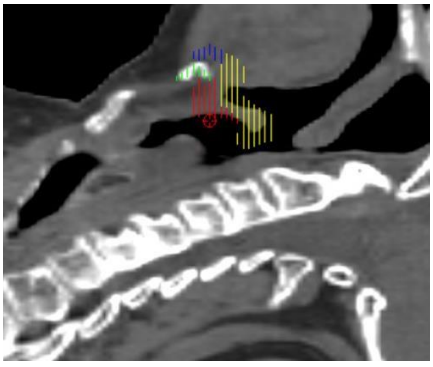

Fig. 7.9c Patient A: planning CT structures added to the re-scan. The GTV and hyoid remain near each other on both scans but on the re-scan, the hyoid (green) and GTV (red) have both dropped from their original position.

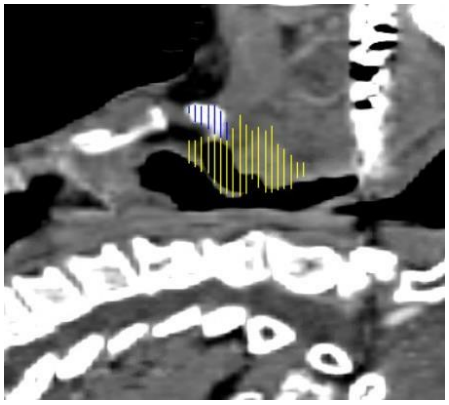

Fig. 7.10a Patient B: planning CT.
GTV outlined in yellow, hyoid in blue

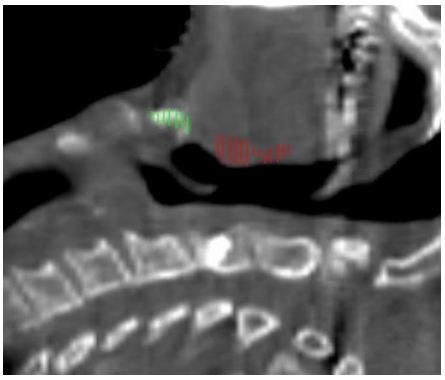

Fig. 7.10b Patient B: Re-scan CT
GTV outlined in red, hyoid in green

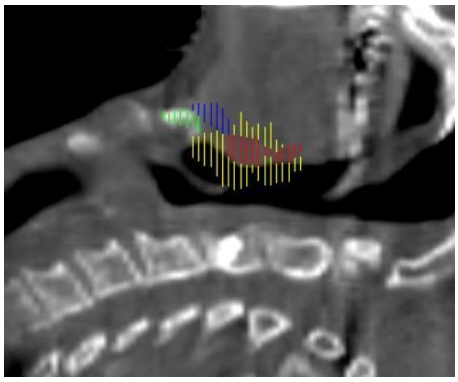

Fig. 7.10c Baseline structures added to the mid-treatment scan. On the re-scan, the hyoid has dropped but the GTV has retained its original position.

7.4 Discussion

The full benefit of adaptive radiotherapy for OPSCC can only be delivered when treatment verification is optimised. Patient set up uncertainty is a regular challenge to the head and neck radiotherapy team in every day clinical practice. There is a growing amount of published literature defining deviations in the planning CT anatomy seen on CBCT, calling for a more nuanced consideration of PTV margins with an altered ITV to mitigate for this.

In this chapter I set out to investigate a specific set up issue commonly referred for imaging review; displacement of the hyoid bone compared to its position on the planning CT. This is a

particular concern in OPSCC patients as the primary tumour is often near, or involving, the hyoid bone. As primary tumours have the density of soft tissue, their position can be difficult to determine on a CBCT; the hyoid bone may offer a potential surrogate for tumour location.

As per my objectives, I determined the prevalence of referrals to the imaging team for hyoid displacement in OPSCC patients, and the degree of displacement that triggered referral. I calculated that out of the patients with full imaging available, 63% may have been at risk of geographical miss of the CTV and GTV if the hyoid is a true surrogate for the primary GTV position as per my first hypothesis.

7.4.1 Prevalence of hyoid displacement triggering referral to imaging team

During 2018 and 2019, 20.3% (47/232) of the OPSCC patients treated with radical radiotherapy in our cancer centre were referred for movement of the hyoid during a course of radical radiotherapy. This proportion of patients has important consequences for treatment timelines and radiotherapy department resources, particularly if a change in hyoid position triggers a re-plan. On average, a radical head and neck plan can take up to 2 – 3 hours to contour, and up to 6 – 8 hours to produce an optimised plan.

7.4.2 Magnitude of hyoid displacement triggering referral to imaging team

I have shown that the hyoid bone can move considerably throughout a course of radiotherapy for OPSCC, particularly in patients with T3/T4 staged primaries, and involving the base of tongue. As expected, in the majority of patients the hyoid displacement was in a caudal direction – a 'hyoid drop' – reflecting the release of the hyoid from direct or indirect tumour involvement as it responds to the radiotherapy. In two patients, the hyoid bone moved cranially. In one of these cases, the tumour extensively involved the lateral pharyngeal walls

so may have fixed the hyoid bone in a different way that resulted in it originally being pulled down from its natural position.

There was often a difference in the extent of displacement between the superior and inferior border of the hyoid bone. I recorded both to capture any antero-posterior tilting of the hyoid bone. The difference in superior and inferior border displacements suggests that the hyoid moves in more than one plane with tumour response, both moving cranio-caudally and pitching antero-posteriorly.

If the hyoid bone is a surrogate for tumour position, part of the CTV or GTV may lie outside of the 95% isodose leading to a risk of undertreatment. Limitations of kV CBCT imaging and the poor image resolution meant I could not assess with meaningful accuracy the position of the GTV_P on the CBCTs in most patients. As a result, I have been unable to prove that this is the case for all patients with a hyoid displacement at or over the 5mm and 8mm threshold, but I have demonstrated that it was the case in 2 of the 3 patients who were re-planned, and therefore underwent a planning CT scan with enough resolution to see the primary tumour. Further work is needed to determine the true impact of hyoid movement on CTV coverage, done using better resolution verification imaging (e.g., MRI Linac).

7.4.3 Predictive features

7.4.3.1 Primary stage of tumour

T3 and T4 oropharyngeal tumours are either larger (>4cm) or have grown into adjacent structures including the epiglottis/extrinsic tongue muscles/larynx, or both. In addition, they would also be expected to reduce the most with radiotherapy, in relation to their pre-treatment volume. I therefore hypothesized that they would make up most of the referrals for hyoid movement and my results supported this hypothesis.

A significantly higher proportion of patients who were referred for hyoid movement had T4 tumours and base of tongue primaries compared to the patients not referred; 61.7% versus 35.7% (Chi Squared <0.001), and 68.1% versus 50.8% (Chi Squared 0.048). In these patients, a mid-treatment repeat planning CT could be factored into the initial patient appointment schedule to help workforce planning for a worse-case scenario. This would have to be a clinical decision as a proportion of T4 and base of tongue patients will not be referred and therefore would be exposed to extra radiation unnecessarily.

7.4.3.2 Indirect hyoid involvement by tumour

There is a suggestion from my data, that patients who have tumours invading the hyoglossus muscle, but no other extrinsic tongue muscle, are more likely to be referred for hyoid displacement. This may be explained because it removes the possible influence of the other extrinsic tongue muscles which could indirectly displace the hyoid in an opposing direction to the hyoglossus if also involved by tumour. Dedicated radiological reviews reporting on the specific extent of extrinsic tongue muscle involvement of large tumours, or those in the base of tongue, could highlight patients at increased risk of hyoid displacement throughout a course of treatment.

7.4.3.4 Height of hyoid on planning CT relative to the mandible

The average distance between the mandible and the hyoid was smaller in the patients referred compared to those patients who were not. These results are in keeping with my hypothesis that a hyoid bone fixed by tumour in a more cranial position at set up – demonstrated by a smaller mandible to hyoid distance – is likely to demonstrate a larger displacement once released during tumour response. Like those with T4 and base of tongue tumours, patients

who have a higher hyoid on planning scan could also have a re-scan scheduled into their pathway for a predicted hyoid displacement later in the treatment course.

7.4.4 Reduced referrals in 2019

Fewer patients were diagnosed with OPSCC and referred for radical radiotherapy in 2019 compared to 2018. This may be due to a natural fluctuation in patient numbers year on year. A lower percentage of the 2019 cohort were referred for imaging review. This may be due to natural variation in patients but could indicate changes in radiographer experience, or an improved confidence in the visualisation of the GTV_P and subsequent reassurance of target volume coverage despite hyoid movement. The low numbers of patients referred with hyoid displacement and ultimately re-planned during 2018 may have also informed a reduced rate of referral during 2019.

7.4.5 Relationship of hyoid to the primary tumour mid-treatment

The question of whether the change in hyoid position acts as a surrogate for the position change of the primary GTV cannot be resolved by my study. It was very difficult to assess the primary GTV on the vast majority of the CBCT with any accuracy due to the poor resolution of the CBCT despite looking through them with an experienced image guidance radiographer. There were three patients who had repeat planning CTs performed, and I could compare primary tumour and hyoid bone position on the repeat planning CT, to the initial one. All three patients had base of tongue tumours. In two of these patients, the primary tumour moved with the hyoid bone. The patient whose hyoid bone moved independently of the tumour had radiological evidence of hyoglossus and genioglossus involvement. It is reasonable to suggest that tumour response resulted in the freeing of hyoglossus and indirect release of the hyoid bone. Of the two patients where the hyoid bone and primary tumour remained in the same relative positions, neither patient was reported as having radiological evidence of direct hyoid bone involvement. One patient had radiological evidence of hyoglossus and genioglossus involvement, but the re-plan was performed after 8 fractions, and it is possible that not

enough radiotherapy had been received at this point to elicit enough tumour response for release of the hyoid.

It is unexpected, given the high percentage (63%) of patients referred for hyoid displacement who demonstrated a displacement of 8mm or more, that only 3 patients were formally replanned. It is possible that many of these patients presented at a late stage in their course of treatment and it was decided by clinicians that there would only be minimal benefit to replanning and delivering only a small number of fractions on the second plan. Another reason may be that the dosimetric analysis was reassuring, that OARs remained within tolerance and there was adequate coverage of the PTV, or the CTV. Finally, it is also possible that some patients would have benefited from a re-plan, but it was decided against for external reasons including patient frailty or a high number of random set up errors.

7.4.6 Predicting the need for re-planning

My work suggests patients with T3/T4 and base of tongue primary cancers, particularly those tumours which have a larger length of overlap between the primary GTV and the hyoid bone on the planning CT, involve the external tongue muscles, or where the hyoid is closer to the mandible on planning CT, are more likely to be referred to the imaging team for hyoid displacement during treatment. These are the patients where re-planning could be prospectively built into their treatment schedules, then removed should the need not arise. I did not look at the impact of large nodal disease in this study. It is feasible that large volume nodes particularly with extranodal extension, in addition to primary tumours, could involve extrinsic tongue muscles and influence hyoid position and mobility.

7.4.7 Tailored PTV margins

My findings regarding the magnitude of hyoid displacement are in keeping with published studies discussed at the beginning of this chapter. When considering PTV margins for OPSCC

primaries, the location of the primary and its involvement of adjacent structures with the propensity to move e.g., the hyoid bone, should be considered as the ITV. As per the findings of other groups, I have shown that the hyoid bone is a region of interest that moves enough to be clinically significant in patients with locally advanced OPSCC and moves to the extent that it can result in unfavourable dosimetric consequences.

The requirement for re-planning could be reduced if the inferior PTV margin is increased and the risk of geographical miss minimised. On the other hand, an expanded PTV margin will increase the volume of normal tissue irradiated at a high dose and consequently increase the likelihood of toxicity. On balance, prospectively planned re-planning is a more appealing strategy.

If a group of tumours could be demonstrated to have a more stable position throughout a course of treatment, it may be reasonable to explore a reduction in PTV margins. Whilst the need for PTV margins is in part due to the degree of uncertainty around treatment delivery by the treatment machines, the internal target movement (ITV) is also a factor. My work suggests that T1 and T2 tumours are very rarely referred for hyoid movement and the inferior PTV margin for these may be safely reduced. Further work specifically looking at the position of T1/T2 OPSCC tumours throughout a course of radiotherapy is required, alongside the improvement in imaging quality, so that treatment radiographers can deliver treatment to a smaller target with confidence.

7.4.8 Limitations

I acknowledge several limitations to my study.

I did not account for large nodal disease. In retrospect, including large volume nodes and any nodes with substantial extranodal extension would have been an informative addition to my study.

My definition of external tongue muscle involvement relied upon historical radiological reports to discern which patients had tumours with extrinsic tongue muscle involvement.

Whilst extrinsic tongue muscle involvement is a feature of describing the staging of a primary OPSCC cancer, the reporting radiologist was not specifically asked to report on this at the time. If tumours were T4 for other reasons, extrinsic tongue muscle involvement may not have been specifically mentioned even if present. When extrinsic tongue muscles were mentioned in some reports, often the detail did not include individual muscles and so my subdivision of patients based on which extrinsic tongue muscles were involved may be inaccurate as I used reports to record them. In addition to whether the extrinsic tongue muscles were involved at all, my method for measuring the extent of involvement was novel and un-validated. A blind radiology review of the non-referred and referred patients to specifically assess their involvement would be a more accurate method to investigate any relationship between extrinsic tongue muscle involvement and displacement of the hyoid during a course of radiotherapy treatment.

The inability to visualise the primary on CBCT with any degree of certainty in this piece of work was disappointing. A key question I planned to address is whether the hyoid bone remains an accurate surrogate for an OPSCC primary throughout a course of radiotherapy; I have not been able to answer this so far. Further work involving better verification imaging e.g., improved CBCT resolution, or the use of an MRI linear accelerator, would improve visualisation of the primary tumour and ascertain its relationship with the hyoid throughout 6 – 7 weeks of radiotherapy. An opportunity to study this relationship further presents itself with the repeat imaging after 2 weeks of chemoradiotherapy within the PEARL Study. While not all PEARL patients may be referred to the imaging team for hyoid displacement, using the interim PET-CT (iPET-CT) to visualise the hyoid and primary after 2 weeks of treatment will provide an improved imaging method with which to look at any change in their respective positions.

7.5 Conclusion

Hyoid movement is commonly seen in OPSCC patients during radical courses of radiotherapy. This movement cannot be corrected by treatment couch shifts and often involves significant

use of radiotherapy department resources in the review of verification images and in some cases, the generation of a new plan. Further work needs to be done to better elucidate the relationship of the hyoid and primary GTV, and whether tumour or radiological features may offer a way to predict which patients are most likely to have a significant hyoid drop during treatment, and which of them may require a subsequent re-plan. Prospective identification of these patients could help streamline patient treatment pathways by factoring in replanning time and improving the efficiency of a radiotherapy department's resources.

Chapter 8: Summary of thesis and future directions

8.1 Hypothesis 1: Adaptive radiotherapy based on biological response to treatment on interim FDG-PET-CT scan during chemoradiotherapy treatment can be used to reduce the dose received to the Swallowing Related Organs at Risk (SWOARS) and major salivary glands in patients with HPV positive OPSCC

8.1.1 Feasibility of recruitment to the PEARL Study

My thesis is based upon work I led on writing the study protocol for PEARL, a Phase 2 study of de-intensification of radical radiotherapy for HPV positive oropharyngeal squamous cell carcinoma. The PEARL study introduces a novel method of deintensification for this good prognosis group of patients where survival rates are high and survivorship issues paramount. By adapting the primary GTV to the avid volume visible on PET-CT after 2 weeks of chemoradiotherapy, the aim is to demonstrate a reduction in delivered dose to organs at risk, specifically those involved in toxicities known to impact on patient quality of life.

PEARL opened to recruitment in January 2020 and whilst initially a single centre study, recruited the first 4 eligible patients within the first 2 months.

Like many other clinic studies, the PEARL study recruitment was severely affected by the impact of the COVID-19 pandemic. PEARL closed to recruitment within 3 months of opening, and other centres in set up suspended the process. Now open again, with a total of 4 centres currently recruiting, there remain challenges to attaining the target number of participants. Examples include the difficulties in NHS service provision and staffing levels exacerbated by the pandemic, in addition to patients presenting with more advanced tumours and thus ineligible for deintensification studies.

Changes to the planning method were explored to improve simplicity of planning PEARL patients, specifically Phase 2, and my thesis lays out the design of a new adaptive planning method, ADAPTIVE_B which was conceived to simplify planning whilst increasing the minimal dose per fraction to the prophylactic nodal volume. In my thesis I have demonstrated that this change to the planning method is unlikely to impact on the results of the PEARL study, with

no significant difference in the mean dose to the OARs under study between the original planning method and ADAPTIVE B. ADAPTIVE B is now the planning method used for all patients recruited to the study.

8.1.2 Impact of adaptation on mean dose to OARs

To inform the PEARL protocol, I developed a pilot study modelling the adaptive PEARL planning protocol on datasets from an external centre. In work presented in this thesis, I have demonstrated the feasibility of adapting the primary GTV as mandated in PEARL, and using modelled plans, have demonstrated dosimetric benefits to this method of adaptation. The pilot study results show a reduction in mean dose to swallowing associated OARs and major salivary glands of up to 7Gy, and the achievement of multiple optimal dose constraints suggesting a clinically evident reduction in toxicity could be expected from this deintensification.

I performed another dosimetric study on the first 4 patients recruited to PEARL to look for differences compared to non-adaptive plans. I was able to demonstrate biological response adaptation was feasible in real world patients recruited to a clinical study.

Due to the constraints and working conditions in the pandemic, I was unable to build on my experience of planning VMAT head and neck plans and produce high quality non-adaptive plans to compare to the patient's adaptive plans they were treated with. This was a major limitation to my original research plan. In response to this, I changed my research plan to collaborate with Dr Philip Wheeler's team at Velindre Cancer Centre. I worked with them on their automated planning software, EdgeVCC, to refine the process for head and neck patients. Once validated (data not yet published), we used EdgeVCC to produce automated non-adaptive plans to compare with the adaptive PEARL plans

The comparison of the manually planned adaptive plans the first 4 PEARL patients were treated on, with the modelled automated non-adaptive plans produced by EdgeVCC showed a less uniform benefit of adaptation. Whilst the mean dose to various OARs was reduced,

there was no significant difference between the 2 plans in any of the 4 patients. In some cases, the mean dose to OARs was increased by up to 3Gy.

I adjusted my research plan a second time, to include work that explored the impact of automated planning and if it could be a confounding factor in the reduced benefit seen in the first 4 PEARL patients. The dosimetric benefits of automated planning are well published, and it is a rapidly growing area of research. I performed a second modelling study, producing automated adaptive plans to compare to manual adaptive plans. In Chapter 3 I show automated planning results in a global reduction in mean dose compared to the manually planned equivalent. Whilst not significant, the often-superior dose distribution of automated planning is likely to explain in part why the comparison of manual plan to automated nonadaptive plans was diminished compared to the pilot study, which had manual plans for comparators.

Current ongoing work led by Dr Phillip Wheeler's team involves taking a closer look at the whole dose volume histogram data to further explore the dosimetric impact of PEARL. By focusing on Phase 2, they are producing non-adaptive comparators by fusing the Phase 1 plan onto the interim PET-CT to generate a more accurate model of the dose distribution to the patient in the second half of chemoradiotherapy (38.7Gy in 18 fractions over 3 weeks), had they not had adaptation. Results so far suggest that the impact of PEARL significantly reduces the amount of high dose received by the supraglottis, middle and superior pharyngeal constrictor muscles with reductions in the volume receiving 38.7Gy (V38.7) of up to 50%.

An additional benefit of automated planning is the speed with which high quality plans can be produced. The development of the head and neck automated planning that I was involved with has since been validated for clinical use and has become a standard planning method for head and neck cancer patients treated at Velindre both within and outside the PEARL study.

Once PEARL has completed recruitment and follow up, the dosimetric advantages modelled can be compared to real world toxicity data and conclusions drawn as to whether organ sparing by PEARL adaption provides meaningful benefit to our patients.

8.2 Hypothesis 2: Adaptive radiotherapy based on biological response to treatment on interim FDG-PET-CT scan during chemoradiotherapy treatment will be superior using Proton Beam Therapy compared to VMAT in terms of sparing dose to the Swallowing Related Organs at Risk (SWOARS) and major salivary glands in patients with HPV positive OPSCC

8.2.1 Impact of non-adaptive IMPT planning

I collaborated with the only proton facility in Wales, The Rutherford Cancer Centre, to model IMPT plans based on the pilot study cases.

The sizeable difference in mean dose to OARs, and the achievement of nearly all optimal dose constraints in all 4 cases is in line with current literature on the superior organ sparing capability of IMPT compared to photon based VMAT for head and neck cancers. Mean dose to the supraglottis was reduced by up to 25Gy, and to the inferior pharyngeal constrictor muscle by 30Gy.

I applied a validated Normal Tissue Complication Probability (NTCP) model to my pilot cases and demonstrate that they would likely reach the criteria for proton therapy funding in The Netherlands. Whilst adaptation reduced the NTCP by up to 50%, reflecting the biological response volume reduction, it did not appear to reduce the NTCP by enough to change the eligibility status for proton funding.

The Torpedo Study is currently open and recruiting in the UK. Results from Torpedo will provide objective data on what benefits proton beam therapy provides OPSCC patients in a UK setting. Should the results be positive, further collaboration with private proton centres like The Rutherford Cancer Centre will be vital in order to improve access to NHS proton treatment to a wider population of patients across the UK and ensure the appropriate selection of patients for IMPT.

8.2.2 Impact of adaptive IMPT planning

Whilst the substantial potential for organ sparing by IMPT is undisputed, I have demonstrated for the first time, that it can be improved by biological response based adaptive radiotherapy.

Furthermore, the degree of dose reduction adaptation conveys appears to be of a similar scale to the benefits of adaptation in VMAT planning. Adaptive IMPT plans were able to drive down dose further by up to another 7Gy in the glottis and 10Gy in the oral cavity. The impact of adaptation on average mean dose to OARs on IMPT plans reached significance.

8.3 Hypothesis 3: Hyoid bone movement can play a part in radiotherapy treatment verification, and better understanding of hyoid movement may allow a reduction in CTV-PTV margins

8.3.1 Hyoid displacement in real world head and neck cancer patients undergoing radical radiotherapy

The improved conformality of radiotherapy techniques including VMAT and IMPT, and the reduction in CTV margins standardly used in OPSCC radiotherapy plans emphasizes the requirement for high quality treatment position and delivery verification. In clinical practice, reviewing the on-set imaging is a common scenario but there is a paucity of data regarding which patients are most at risk of set up errors.

In my thesis I present work I performed on 2 years of head and neck patients referred for on set imaging review due to hyoid displacement. I have shown that over 60% of patients referred are at risk of under treatment of the primary GTV, should the hyoid position be an accurate surrogate for tumour position.

8.3.2 Predictive features for hyoid displacement

Larger tumours and those involving extrinsic tongue muscles (e.g., T4 and base of tongue primaries), are overrepresented in the cohort referred and it is reasonable to suggest they are more likely to have anatomical connection to the hyoid either directly or via muscle infiltration. These patients may be considered for prospectively scheduled re-planning, especially if they also display additional predictive factors e.g., a reduced mandible to hyoid

distance. Likewise, patients without these features may be considered for reduced PTV margins thus reducing the high dose volume receiving the prescription dose.

A limitation to my work in Chapter 7 is the lack of visibility of primary tumours on the CBCTs. As such I am unable to definitively report if the hyoid movement is independent of the primary tumour. I will be using the PEARL patients interim PET-CT to further explore the relationship between the hyoid and the OPSCC primary tumour during a course of radical radiotherapy. T4 tumours are not eligible for PEARL so this next piece of work will provide me with a difference cohort and allow me to explore if non-T4 tumours could have reduced ITV/PTV margins.

8.3 Conclusion

The better prognosis and younger, healthier cohort of patients with locally advanced HPV positive oropharyngeal squamous cell cancer offers potential for reducing the intensity of treatment and minimizing the risk of long term, disabling and life quality reducing toxicity. In my work presented in this thesis, I have explored 3 different methods of radiotherapy deintensification: biological response-based adaptation, IMPT planning, and towards a more tailored verification protocol and PTV margins. I have demonstrated significant dosimetric advantage to adaptation and the use of IMPT. The toxicity data from the PEARL study and ongoing additional dosimetric modelling projects will provide additional insight into how clinically relevant these deintensification methods could be.

References

1. Cancer Research UK website (cancerresearchuk.org)
2. Mehanna H, Robinson M, Hartley A, Kong A, Foran B, Fulton-Lieuw T, Dalby M, Mistry P, Sen M, O'Toole L, Al Booz H, Dyker K, Moleron R, Whitaker S, Brennan S, Cook A, Griffin M, Aynsley E, Rolles M, De Winton E, Chan A, Srinivasan D, Nixon I, Grumett J, Leemans CR, Buter J, Henderson J, Harrington K, McConkey C, Gray A, Dunn J; De-ESCALaTE HPV Trial Group. Radiotherapy plus cisplatin or cetuximab in low-risk human papillomavirus-positive oropharyngeal cancer (De-ESCALaTE HPV): an open-label randomised controlled phase 3 trial. Lancet. 2019 Jan 5;393(10166):51-60.
3. Maura L. Gillison, Wayne M. Koch, Randolph B. Capone, Michael Spafford, William H. Westra, Li Wu, Marianna L. Zahurak, Richard W. Daniel, Michael Viglione, David E. Symer, Keerti V. Shah, David Sidransky, Evidence for a Causal Association Between Human Papillomavirus and a Subset of Head and Neck Cancers, *JNCI: Journal of the National Cancer Institute*, Volume 92, Issue 9, 3 May 2000, Pages 709–720,
4. Ang KK, Harris J, Wheeler R, Weber R, Rosenthal DI, Nguyen-Tân PF, Westra WH, Chung CH, Jordan RC, Lu C, Kim H, Axelrod R, Silverman CC, Redmond KP, Gillison ML. Human papillomavirus and survival of patients with oropharyngeal cancer. N Engl J Med. 2010 Jul 1;363(1):24-35.
5. Schache, AG, Powell, NG, Cuschieri, KS, Leary, SD, Mehanna, H, Rapozo, D, Cubie, H, Junor, E, Monaghan, H, Harrington, KJ, Nutting, CM, Schick, U, Lau, AS, Upile, N, Sheard, J, Brougham, K, West, CML, Oguejiofor, K, Thomas, S, Ness, AR, Pring, M, King, EV, McCance, D, James, JA, Moran, M, Sloan, P, Evans, M & Jones, TM 2016, 'HPV-related oropharyngeal cancer in the United Kingdom: an evolution in understanding of disease etiology', *Cancer Research*, vol. 76, no. 22, pp. 6598-6606.
6. McBride AA, Warburton A (2017) The role of integration in oncogenic progression of HPV-associated cancers. PLoS Pathog 13(4): e1006211
7. Linton OR, Moore MG, Brigance JS, Gordon CA, Summerlin D, McDonald MW. Prognostic Significance of Basaloid Squamous Cell Carcinoma in Head and Neck Cancer. *JAMA Otolaryngol Head Neck Surg.* 2013;139(12):1306–1311
8. Maura L. Gillison, Gypsyamber D'Souza, William Westra, Elizabeth Sugar, Weihong Xiao, Shahnaz Begum, Raphael Viscidi, Distinct Risk Factor Profiles for Human Papillomavirus Type 16–Positive and Human Papillomavirus Type 16–Negative Head and Neck Cancers, *JNCI: Journal of the National Cancer Institute*, Volume 100, Issue 6, 19 March 2008, Pages 407–420
9. Tornesello ML, Annunziata C, Tornesello AL, Buonaguro L, Buonaguro FM. Human Oncoviruses and p53 Tumor Suppressor Pathway Deregulation at the Origin of Human Cancers. Cancers (Basel). 2018 Jun 22;10(7):213.
10. Grønhøj Larsen, C., Gyldenløve, M., Jensen, D. et al. Correlation between human papillomavirus and p16 overexpression in oropharyngeal tumours: a systematic review. Br J Cancer 110, 1587–1594 (2014)
11. Ang KK, Harris J, Wheeler R, Weber R, Rosenthal DI, Nguyen-Tân PF, Westra WH, Chung CH, Jordan RC, Lu C, Kim H, Axelrod R, Silverman CC, Redmond KP, Gillison ML. Human papillomavirus and survival of patients with oropharyngeal cancer. N Engl J Med. 2010 Jul 1;363(1):24-35.
12. Adelstein DJ, Li Y, Adams GL, Wagner H Jr, Kish JA, Ensley JF, Schuller DE, Forastiere AA. An intergroup phase III comparison of standard radiation therapy and two schedules of concurrent chemoradiotherapy in patients with unresectable squamous cell head and neck cancer. J Clin Oncol. 2003 Jan 1;21(1):92-8.
13. Nørregaard C, Grønhøj C, Jensen D, Friborg J, Andersen E, von Buchwald C. Cause-specific mortality in HPV+ and HPV- oropharyngeal cancer patients: insights from a population-based cohort. Cancer Med. 2018 Jan;7(1):87-94.
14. Zhang Y, Fakhry C, D'Souza G. Projected Association of Human Papillomavirus Vaccination with Oropharynx Cancer Incidence in the US, 2020-2045. *JAMA Oncol.* 2021;7(10):e212907.
15. Johnson, D.E., Burtness, B., Leemans, C.R. et al. Head and neck squamous cell carcinoma. Nat Rev Dis Primers 6, 92 (2020)

16. Amin MB, Edge S, Greene F, Byrd DR, Brookland RK, Washington MK, Gershenwald JE, Compton CC, Hess KR, et al. (Eds.). AJCC Cancer Staging Manual (8th edition). Springer International Publishing: American Joint Commission on Cancer; 2017 [cited 2016 Dec 28].
17. Mehanna H, Evans M, Beasley M, Chatterjee S, Dilkes M, Homer J, O'Hara J, Robinson M, Shaw R, Sloan P. Oropharyngeal cancer: United Kingdom National Multidisciplinary Guidelines. J Laryngol Otol. 2016 May;130(S2):S90-S96.
18. de Almeida JR, Byrd JK, Wu R, Stucken CL, Duvvuri U, Goldstein DP, Miles BA, Teng MS, Gupta V, Genden EM. A systematic review of transoral robotic surgery and radiotherapy for early oropharynx cancer: a systematic review. Laryngoscope. 2014 Sep;124(9):2096-102.
19. Park S, Cho Y, Lee J, Koh YW, Kim SH, Choi EC, Kim HR, Keum KC, Park KR, Lee CG. Survival and Functional Outcome after Treatment for Primary Base of Tongue Cancer: A Comparison of Definitive Chemoradiotherapy versus Surgery Followed by Adjuvant Radiotherapy. Cancer Res Treat. 2018 Oct;50(4):1214-1225.
20. Pignon JP, le Maitre A, Maillard E, Bourhis J, Group M-NC. Meta-analysis of chemotherapy in head and neck cancer (MACH-NC): an update on 93 randomised trials and 17,346 patients. Radiother Oncol 2009;92:4–14
21. Tabrizi R, Garajei A, Shafie E, Jamshidi S. Outcome of Neoadjuvant Chemotherapy on Local Recurrence and Distant Metastasis of Oral Squamous Cell Carcinoma: A Retrospective Study. J Dent (Shiraz). 2016 Sep;17(3):207-12.
22. Tupchong L, Scott CB, Blitzer PH, Marcial VA, Lowry LD, Jacobs JR, Stetz J, Davis LW, Snow JB, Chandler R, et al. Randomized study of preoperative versus postoperative radiation therapy in advanced head and neck carcinoma: long-term follow-up of RTOG study 73-03. Int J Radiat Oncol Biol Phys. 1991 Jan;20(1):21-8.
23. Peters L, Goepfert H, Ang K, Byers R, Maor M, Guillamondegui O, Morrison W, Weber R, Garden A, Frankenthaler R, Oswald M, Brown B. Evaluation of the dose for postoperative radiation therapy of head and neck cancer: First report of a prospective randomised trial. Int J Radiat Oncol Biol Phys. 1993 April;26(1):3-11
24. Radiotherapy dose fractionation, third edition. Online at www.rcr.ac.uk/publication
25. Bernier J, Domenge C, Ozsahin M, Matuszewska K, Lefebvre J, Greiner R et al Post operative irradiation with or without concomitant chemotherapy for locally advanced head and neck cancer N Engl J Med 2004; 350:1945-1952
26. Cooper JS, Zhang Q, Pajak TF, Forastiere AA, Jacobs J, Saxman SB, Kish JA, Kim HE, Cmelak AJ, Rotman M, Lustig R, Ensley JF, Thorstad W, Schultz CJ, Yom SS, Ang KK. Long-term follow-up of the RTOG 9501/intergroup phase III trial: postoperative concurrent radiation therapy and chemotherapy in highrisk squamous cell carcinoma of the head and neck. Int J Radiat Oncol Biol Phys. 2012 Dec 1;84(5):1198205.
27. Owadally, W., Hurt, C., Timmins, H. et al. PATHOS: a phase II/III trial of risk-stratified, reduced intensity adjuvant treatment in patients undergoing transoral surgery for Human papillomavirus (HPV) positive oropharyngeal cancer. BMC Cancer 15, 602 (2015).
28. Bentzen S. Radiobioloigcal considerations in the design of clinical trials Radiotherapy and Oncology 1994 32(1): 1 – 11
29. Jadon, R., Higgins, E., Hanna, L. et al. A systematic review of dose-volume predictors and constraints for late bowel toxicity following pelvic radiotherapy. Radiat Oncol 14, 57 (2019)
30. Nutting CM, Morden JP, Harrington KJ, Urbano TG, Bhide SA, Clark C, Miles EA, Miah AB, Newbold K, Tanay M, Adab F, Jefferies SJ, Scrase C, Yap BK, A'Hern RP, Sydenham MA, Emson M, Hall E; PARSPORT trial management group. Parotid-sparing intensity modulated versus conventional radiotherapy in head and neck cancer (PARSPORT): a phase 3 multicentre randomised controlled trial. Lancet Oncol. 2011 Feb;12(2):127-36. d
31. Han, P., Lakshminarayanan, P., Jiang, W. *et al.* Dose/Volume histogram patterns in Salivary Gland subvolumes influence xerostomia injury and recovery. *Sci Rep* 9, 3616 (2019).
32. Marks LB, Yorke ED, Jackson A, Ten Haken RK, Constine LS, Eisbruch A, Bentzen SM, Nam J, Deasy JO. Use of normal tissue complication probability models in the clinic. Int J Radiat Oncol Biol Phys. 2010 Mar 1;76(3 Suppl):S10-9.

33. Emami B, Lyman J, Brown A, Coia L, Goitein M, Munzenrider JE, Shank B, Solin LJ, Wesson M. Tolerance of normal tissue to therapeutic irradiation. Int J Radiat Oncol Biol Phys. 1991 May 15;21(1):109-22.
34. Brodin NP, Tomé WA. Revisiting the dose constraints for head and neck OARs in the current era of IMRT. Oral Oncol. 2018 Nov;86:8-18.
35. Bjordal K, Hammerlid E, Ahlner-Elmqvist M, de Graeff A, Boysen M, Evensen JF, Biörklund A, de Leeuw JR, Fayers PM, Jannert M, Westin T, Kaasa S. Quality of life in head and neck cancer patients: validation of the European Organization for Research and Treatment of Cancer Quality of Life QuestionnaireH&N35. J Clin Oncol. 1999 Mar;17(3):1008-19.
36. Chen AY, Frankowski R, Bishop-Leone J, Hebert T, Leyk S, Lewin J, Goepfert H. The development and validation of a dysphagia-specific quality-of-life questionnaire for patients with head and neck cancer: the M. D. Anderson dysphagia inventory. Arch Otolaryngol Head Neck Surg. 2001 Jul;127(7):870-6.
37. Wilson JA, Carding PN, Patterson JM. Dysphagia after nonsurgical head and neck cancer treatment: patients' perspectives. Otolaryngol Head Neck Surg. 2011 Nov;145(5):767-71.
38. Eisbruch A, Kim HM, Feng FY, Lyden TH, Haxer MJ, Feng M, Worden FP, Bradford CR, Prince ME, Moyer JS, Wolf GT, Chepeha DB, Ten Haken RK. Chemo-IMRT of oropharyngeal cancer aiming to reduce dysphagia: swallowing organs late complication probabilities and dosimetric correlates. Int J Radiat Oncol Biol Phys. 2011 Nov 1;81(3):e93-9.
39. Schwartz DL, Hutcheson K, Barringer D, Tucker SL, Kies M, Holsinger FC, Ang KK, Morrison WH, Rosenthal DI, Garden AS, Dong L, Lewin JS. Candidate dosimetric predictors of long-term swallowing dysfunction after oropharyngeal intensity-modulated radiotherapy. Int J Radiat Oncol Biol Phys. 2010 Dec 1;78(5):1356-65.
40. Christopher Nutting, Keith Rooney, Bernadette Foran, Laura Pettit, Matthew Beasley, Laura Finneran, Justin Roe, Justine Tyler, Tom Roques, Audrey Cook, Imran Petkar, Shree Bhide, Devraj Srinivasan, Cheng Boon, Emma De Winton, Robert Frogley, Kathrin Mertens, Marie Emson, Emma Hall, and on behalf of the DARS Investigators Results of a randomized phase III study of dysphagia-optimized intensity modulated radiotherapy (Do-IMRT) versus standard IMRT (S-IMRT) in head and neck cancer. Journal of Clinical Oncology 2020 38:15_suppl, 6508-6508
41. Caudell JJ, Schaner PE, Meredith RF, Locher JL, Nabell LM, Carroll WR, Magnuson JS, Spencer SA, Bonner JA. Factors associated with long-term dysphagia after definitive radiotherapy for locally advanced headand-neck cancer. Int J Radiat Oncol Biol Phys. 2009 Feb 1;73(2):410-5.
42. Mogadas S, Busch CJ, Pflug C, Hanken H, Krüll A, Petersen C, Tribius S. Influence of radiation dose to pharyngeal constrictor muscles on late dysphagia and quality of life in patients with locally advanced oropharyngeal carcinoma. Strahlenther Onkol. 2020 Jun;196(6):522-529.
43. Baijal G, Kar R, Agarwal JP Radiartion induced xerostomia IJHNS 2012; 3(2):82-86
44. Deasy JO, Moiseenko V, Marks L, Chao KS, Nam J, Eisbruch A. Radiotherapy dose-volume effects on salivary gland function. Int J Radiat Oncol Biol Phys. 2010 Mar 1;76(3 Suppl):S58-63.
45. Tasaka S, Jingu K, Takahashi N, Umezawa R, Yamamoto T, Ishikawa Y, Takeda K, Suzuki Y, Kadoya N. The Long-Term Recovery of Parotid Glands in Nasopharyngeal Carcinoma Treated by Intensity-Modulated Radiotherapy. Front Oncol. 2021 May 7;11:665837.
46. van Luijk P, Pringle S, Deasy JO, Moiseenko VV, Faber H, Hovan A, Baanstra M, van der Laan HP, Kierkels RG, van der Schaaf A, Witjes MJ, Schippers JM, Brandenburg S, Langendijk JA, Wu J, Coppes RP. Sparing the region of the salivary gland containing stem cells preserves saliva production after radiotherapy for head and neck cancer. Sci Transl Med. 2015 Sep 16;7(305):305
47. Steenbakkers RJHM, van Rijn-Dekker MI, Stokman MA, Kierkels RGJ, van der Schaaf A, van den Hoek JGM, Bijl HP, Kramer MCA, Coppes RP, Langendijk JA, van Luijk P. Parotid Gland Stem Cell Sparing Radiation Therapy for Patients With Head and Neck Cancer: A Double-Blind Randomized Controlled Trial. Int J Radiat Oncol Biol Phys. 2022 Feb 1;112(2):306-316.
48. Murdoch-Kinch CA, Kim HM, Vineberg KA, Ship JA, Eisbruch A. Dose-effect relationships for the submandibular salivary glands and implications for their sparing by intensity modulated radiotherapy. Int J Radiat Oncol Biol Phys. 2008 Oct 1;72(2):373-82.
49. Al-Rudayni AHM, Gopinath D, Maharajan MK, Menon RK. Impact of oral mucositis on quality of life in patients undergoing oncological treatment: a systematic review. Transl Cancer Res. 2020 Apr;9(4):3126-3134.

50. Zhang, Z., Xu, J., Zhou, T. *et al.* Risk factors of radiation-induced acute esophagitis in non-small cell lung cancer patients treated with concomitant chemoradiotherapy. *Radiat Oncol* 9, 54 (2014)
51. Dankers F, Wijsman R, Troost EG, Monshouwer R, Bussink J, Hoffmann AL. Esophageal wall dose-surface maps do not improve the predictive performance of a multivariable NTCP model for acute esophageal toxicity in advanced stage NSCLC patients treated with intensity-modulated (chemo-)radiotherapy. Phys Med Biol. 2017 May 7;62(9):3668-3681.
52. Notani K, Yamazaki Y, Kitada H, Sakakibara N, Fukuda H, Omori K, Nakamura M. Management of mandibular osteoradionecrosis corresponding to the severity of osteoradionecrosis and the method of radiotherapy. Head Neck. 2003 Mar;25(3):181-6.
53. Shokri T, Wang W, Vincent A, Cohn JE, Kadakia S, Ducic Y. Osteoradionecrosis of the Maxilla: Conservative Management and Reconstructive Considerations. Semin Plast Surg. 2020 May;34(2):106113.
54. Lajolo C, Rupe C, Gioco G, Troiano G, Patini R, Petruzzi M, Micciche' F, Giuliani M. Osteoradionecrosis of the Jaws Due to Teeth Extractions during and after Radiotherapy: A Systematic Review. Cancers (Basel). 2021 Nov 18;13(22):5798.
55. Ludwig R, Hoffmann JM, Pouymayou B, Däppen MB, Morand G, Guckenberger M, Grégoire V, Balermpas P, Unkelbach J. Detailed patient-individual reporting of lymph node involvement in oropharyngeal squamous cell carcinoma with an online interface. Radiother Oncol. 2022 Apr; 169: p1-7.
56. Vincent Grégoire, Mererid Evans, Quynh-Thu Le, Jean Bourhis, Volker Budach, Amy Chen, Abraham Eisbruch, Mei Feng, Jordi Giralt et al. Delineation of the primary tumour Clinical Target Volumes (CTVP) in laryngeal, hypopharyngeal, oropharyngeal and oral cavity squamous cell carcinoma: AIRO, CACA, DAHANCA, EORTC, GEORCC, GORTEC, HKNPCSG, head and neck cancerIG, IAG-KHT, LPRHHT, NCIC CTG, NCRI, NRG Oncology, PHNS, SBradiotherapy, SOMERA, SRO, SSHNO, TROG consensus guidelines. Radiotherapy and Oncology, Volume 126, Issue 1, 2018, Pages 3-24
57. Overgaard J, Hansen HS, Specht L, Overgaard M, Grau C, Andersen E, Bentzen J, Bastholt L, Hansen O, Johansen J, Andersen L, Evensen JF. Five compared with six fractions per week of conventional radiotherapy of squamous-cell carcinoma of head and neck: DAHANCA 6 and 7 randomised controlled trial. Lancet. 2003 Sep 20;362(9388):933-40. Erratum in: Lancet. 2003 Nov 8;362(9395):1588
58. ASTRO Guideline on Radiation Therapy for Oropharyngeal Squamous Cell Carcinoma. Available at www.ASTRO.org/Patient-Care-and-researc/Clinical-Practice-Statements
59. Machiels JP, René Leemans C, Golusinski W, Grau C, Licitra L, Gregoire V; EHNS Executive Board. Electronic address: secretariat@ehns.org; ESMO Guidelines Committee. Electronic address: clinicalguidelines@esmo.org; ESTRO Executive Board. Electronic address: info@estro.org. Squamous cell carcinoma of the oral cavity, larynx, oropharynx and hypopharynx: EHNS-ESMO-ESTRO Clinical Practice Guidelines for diagnosis, treatment and follow-up. Ann Oncol. 2020 Nov;31(11):1462-1475.
60. Yom SS, Torres-Saavedra P, Caudell JJ, Waldron JN, Gillison ML, Xia P, Truong MT, Kong C, Jordan R, Subramaniam RM, Yao M, Chung CH, Geiger JL, Chan JW, O'Sullivan B, Blakaj DM, Mell LK, Thorstad WL, Jones CU, Banerjee RN, Lominska C, Le QT. Reduced-Dose Radiation Therapy for HPV-Associated Oropharyngeal Carcinoma (NRG Oncology HN002). J Clin Oncol. 2021 Mar 20;39(9):956-965.
61. Chera, B., et al., Phase 2 trial of de-intensified chemoradiotherapy for favourable-risk HPV- associated oropharyngeal squamous cell carcinoma. International Journal of Radiation Oncology, Biology, Physics 2015, 93(5): p. 976 – 985
62. Haddad R, O'Neill A, Rabinowits G, Tishler R, Khuri F, Adkins D, Clark J, Sarlis N, Lorch J, Beitler JJ, Limaye S, Riley S, Posner M. Induction chemotherapy followed by concurrent chemoradiotherapy (sequential chemoradiotherapy) versus concurrent chemoradiotherapy alone in locally advanced head and neck cancer (PARADIGM): a randomised phase 3 trial. Lancet Oncol. 2013 Mar;14(3):257-64.
63. Chen AM, Felix C, Wang PC, Hsu S, Basehart V, Garst J, Beron P, Wong D, Rosove MH, Rao S, Melanson H, Kim E, Palmer D, Qi L, Kelly K, Steinberg ML, Kupelian PA, Daly ME. Reduced-dose radiotherapy for human papillomavirus-associated squamous-cell carcinoma of the oropharynx: a single-arm, phase 2 study. Lancet Oncol. 2017 Jun;18(6):803-811.
64. Marur, S., et al., E1308: A phase 2 trial or induction chemotherapy followed by reduced dose radiotherapy and weekly cetuximab in patients with HPV-associated resectable squamous cell

carcinoma of the oropharynx – ECOG-AGRIN Cancer Research Group. Journal of Clinical Oncology 2017 35(5): p. 492 – 497

65. Seiwert TY, Foster CC, Blair EA, Karrison TG, Agrawal N, Melotek JM, Portugal L, Brisson RJ, Dekker A, Kochanny S, Gooi Z, Lingen MW, Villaflor VM, Ginat DT, Haraf DJ, Vokes EE. OPTIMA: a phase II dose and volume de-escalation trial for human papillomavirus-positive oropharyngeal cancer. Ann Oncol. 2019 Oct 1;30(10):1673. Erratum for: Ann Oncol. 2019 Feb 1;30(2):297-302.
66. Burr AR, Harari PM, Ko HC, Bruce JY, Kimple RJ, Witek ME. Reducing radiotherapy target volume expansion for patients with HPV-associated oropharyngeal cancer. Oral Oncol. 2019 May;92:52-56.
67. Michaelidou A, Adjogatse D, Suh Y, Pike L, Thomas C, Woodley O, Rackely T, Palaniappan N, Jayaprakasam V, Sanchez-Nieto B, Evans M, Barrington S, Lei M, Guerrero Urbano T. 18F-FDG-PET in guided dose-painting with intensity modulated radiotherapy in oropharyngeal tumours: A phase I study (FiGaRO). Radiother Oncol. 2021 Feb;155:261-268.
68. Berwouts D, Madani I, Duprez F, Olteanu AL, Vercauteren T, Boterberg T, Deron P, Bonte K, Huvenne W, De Neve W, Goethals I. Long-term outcome of ^{18} F-fluorodeoxyglucose-positron emission tomography-guided dose painting for head and neck cancer: Matched case-control study. Head Neck. 2017 Nov;39(11):2264-2275.
69. Wood, K., et al., Positron Emission Tomography in oncology: A review. Clinical Oncology (R Coll Rad) 2007,, 19(4): p. 237 – 255
70. Due, A.K., et al., Recurrence after intensity modulated radiotherapy for head and neck squamous cell carcinoma more likely to originate from regions with high baseline FDG uptake. Radiation Oncology 2014, 111 (3): p. 360 – 365
71. Daisne, J., et al., Tumour volume in pharyngolaryngeal squamous cell carcinoma: Comparison of CT, MRI and FDG PET and validation with surgical specimens. Radiology, 2004, 233 (1): p.93 – 100
72. Heukelom J, Hamming O, Bartelink H, Hoebers F, Giralt J, Herlestam T, Verheij M, van den Brekel M, Vogel W, Slevin N, Deutsch E, Sonke JJ, Lambin P, Rasch C. Adaptive and innovative Radiation Treatment FOR improving Cancer treatment outcomE (adaptiveFORCE); a randomized controlled phase II trial for individualized treatment of head and neck cancer. BMC Cancer. 2013 Feb 22;13:84.
73. Geets, X., et al., Adaptive biological image-guided IMRT with anatomical and functional imaging in pharyngo-laryngeal tumours: Impact on target volume delineation and dose distribution using helical tomography. Radiotherapy and Oncology, 2007, 85: p. 105 – 115
74. Subesinghe, M., et al., Alterations in anatomical and functional imaging parameters with repeated FDG PET and MRI during radiotherapy for head and neck cancer: A pilot study. BMC Cancer, 2015, 15: 137 p. 1 -11
75. Cliffe H, Patel C, Prestwich R, Scarsbrook A. Radiotherapy response evaluation using FDG PET-CTestablished and emerging applications. Br J Radiol. 2017 Mar;90(1071):20160764.
76. Geets, X., et al., Impact of the type of imaging modality on target volume delineation and dose distribution in pharyngo-laryngeal squamous cell carcinoma. Comparison between pre-and pertreatment studies. Radiotherapy and Oncology, 2006, 78: p. 291 – 297
77. Garibaldi, C et al., Interim FDG PET/CT during chemoradiation therapy in the management of head and neck cancer patients: A systematic review. IJROBP 2017, 98; 3: p. 555 - 573
78. Castaldi P, Rufini V, Bussu F, Miccichè F, Dinapoli N, Autorino R, Lago M, De Corso E, Almadori G, Galli J, Paludetti G, Giordano A, Valentini V. Can "early" and "late"18F-FDG PET-CT be used as prognostic factors for the clinical outcome of patients with locally advanced head and neck cancer treated with radio-chemotherapy? Radiother Oncol. 2012 Apr;103(1):63-8.
79. Brun, E., et al., FDG PET studies during treatment: Prediction of therapeutic outcome in head and neck squamous cell carcinoma. Head and Neck 2002: p. 127 - 135
80. Hentschel, M., et al., Early FDG PET at 10 or 20Gy during chemoradiotherapy is prognostic for locoregional control and overall survival. European Journal of Nuclear medicine and molecular imaging, 2011 38: p. 1203 – 1211
81. Ceulemans G, Voordeckers M, Farrag A, Verdries D, Storme G, Everaert H. Can 18-FDG-PET during radiotherapy replace post-therapy scanning for detection/demonstration of tumor response in headand-neck cancer? Int J Radiat Oncol Biol Phys. 2011 Nov 15;81(4):938-42.

82. Marcus, C., et al., Head and neck PET/CT: Therapy response interpretation criteria (Hopkins Criteria) – Inter-reader reliability, accuracy and survival outcomes. The Journal of Nuclear Medicine, 2014, 55(9): p. 1411 – 1416
83. Min, M., et al., Prognostic value of 2 – [18] Fluoro-2-deoxy-D-glucose positron emission therapycomputerised tomography scans carried out during and after radiation therapy for head and neck cancer using visual therapy response interpretation criteria. Clinical Oncology (R Coll Rad) 2016, 28: p. 393 – 401
84. Dibble, EH., et al., F-18-FDG Metabolic Tumor Volume and Total Glycolytic Activity of Oral Cavity and Oropharyngeal Squamous Cell Cancer: Adding Value to Clinical Staging Journal of Nuclear Medicine 2012; 53; p. 709 - 715
85. Kao, CH., et al., Use of pretreatment metabolic tumour volumes to predict the outcome of pharyngeal cancer treated by definitive radiotherapy European Journal of Nuclear Medicine and Molecular Imaging 2012; 39: p. 1297 - 1305
86. Lim, R. et al., FDG PET CT metabolic tumour volume and total lesion glycolysis predict outcome in oropharyngeal squamous cell cancer. Journal of Nuclear Medicine 2012; 53: p. 1506 - 1513
87. Abgral, R. et al., Prognostic value of volume parameters measured by FDG PET CT in patients with head and neck squamous cell cancer. European Journal of Nuclear Medicine and Molecular Imaging 2014; 41: p. 659 - 667
88. Foley KG, Hills RK, Berthon B, et al. Development and validation of a prognostic model incorporating texture analysis derived from standardised segmentation of PET in patients with oesophageal cancer. *Eur Radiol*. 2018;28(1):428-436.
89. Rhee DJ, Jhingran A, Kisling K, Cardenas C, Simonds H, Court L. Automated Radiation Treatment Planning for Cervical Cancer. Semin Radiat Oncol. 2020 Oct;30(4):340-347.
90. Lucido JJ, Shiraishi S, Seetamsetty S, Ellerbusch DC, Antolak JA, Moseley DJ. Automated testing platform for radiotherapy treatment planning scripts. J Appl Clin Med Phys. 2022 Nov 21:e13845
91. Kevin L. Moore, Automated Radiotherapy Treatment Planning, Seminars in Radiation Oncology, Volume 29, Issue 3, 2019,
92. Wheeler PA, Chu M, Holmes R, Woodley OW, Jones CS, Maggs R, Staffurth J, Palaniappan N, Spezi E, Lewis DG, Campbell S, Fitzgibbon J, Millin AE. Evaluating the application of Pareto navigation guided automated radiotherapy treatment planning to prostate cancer. Radiother Oncol. 2019 Dec;141:220226.
93. Michalski JM, Moughan J, Purdy J, Bosch W, Bruner DW, Bahary JP, Lau H, Duclos M, Parliament M, Morton G, Hamstra D, Seider M, Lock MI, Patel M, Gay H, Vigneault E, Winter K, Sandler H. Effect of Standard vs Dose-Escalated Radiation Therapy for Patients With Intermediate-Risk Prostate Cancer: The NRG Oncology RTOG 0126 Randomized Clinical Trial. JAMA Oncol. 2018 Jun 14;4(6):e180039.
94. Tol JP, Dahele M, Gregoire V, Overgaard J, Slotman BJ, Verbakel WFAR. Analysis of EORTC-1219DAHANCA-29 trial plans demonstrates the potential of knowledge-based planning to provide patientspecific treatment plan quality assurance. Radiother Oncol. 2019 Jan;130:75-81.
95. Lundkvist J, Ekman M, Ericsson SR, Isacsson U, Jönsson B, Glimelius B. Economic evaluation of proton radiation therapy in the treatment of breast cancer. Radiother Oncol. 2005 May;75(2):179-85.
96. Langendijk JA, Hoebers FJP, de Jong MA, Doornaert P, Terhaard CHJ, Steenbakkers RJHM, HammingVrieze O, van de Kamer JB, Verbakel WFAR, Keskin-Cambay F, Reitsma JB, van der Schaaf A, Boersma LJ, Schuit E. National Protocol for Model-Based Selection for Proton Therapy in Head and Neck Cancer. Int J Part Ther. 2021 Jun 25;8(1):354-365.
97. Arts T, Breedveld S, de Jong MA, Astreinidou E, Tans L, Keskin-Cambay F, Krol ADG, van de Water S, Bijman RG, Hoogeman MS. The impact of treatment accuracy on proton therapy patient selection for oropharyngeal cancer patients. Radiother Oncol. 2017 Dec;125(3):520-525.
98. Slater JD, Yonemoto LT, Mantik DW, Bush DA, Preston W, Grove RI, Miller DW, Slater JM. Proton radiation for treatment of cancer of the oropharynx: early experience at Loma Linda University Medical Center using a concomitant boost technique. Int J Radiat Oncol Biol Phys. 2005 Jun 1;62(2):494-500.
99. Blanchard P, Garden AS, Gunn GB, Rosenthal DI, Morrison WH, Hernandez M, Crutison J, Lee JJ, Ye R, Fuller CD, Mohamed AS, Hutcheson KA, Holliday EB, Thaker NG, Sturgis EM, Kies MS, Zhu XR, Mohan R,

Frank SJ. Intensity-modulated proton beam therapy (IMPT) versus intensity-modulated photon therapy (IMRT) for patients with oropharynx cancer - A case matched analysis. Radiother Oncol. 2016 Jul;120(1):48-55.

100. Sio TT, Lin HK, Shi Q, Gunn GB, Cleeland CS, Lee JJ, Hernandez M, Blanchard P, Thaker NG, Phan J, Rosenthal DI, Garden AS, Morrison WH, Fuller CD, Mendoza TR, Mohan R, Wang XS, Frank SJ. Intensity Modulated Proton Therapy Versus Intensity Modulated Photon Radiation Therapy for Oropharyngeal Cancer: First Comparative Results of Patient-Reported Outcomes. Int J Radiat Oncol Biol Phys. 2016 Jul 15;95(4):1107-14

101. Zhang W, Zhang X, Yang P, Blanchard P, Garden AS, Gunn B, Fuller CD, Chambers M, Hutcheson KA, Ye R, Lai SY, Radwan MAS, Zhu XR, Frank SJ. Intensity-modulated proton therapy and osteoradionecrosis in oropharyngeal cancer. Radiother Oncol. 2017 Jun;123(3):401-405.

102. Price J, Hall E, West C, Thomson D. TORPEdO - A Phase III Trial of Intensity-modulated Proton Beam Therapy Versus Intensity-modulated Radiotherapy for Multi-toxicity Reduction in Oropharyngeal Cancer. Clin Oncol (R Coll Radiol). 2020 Feb;32(2):84-88

103. https://clinicaltrials.gov/ct2/show/NCT01893307

104. https://www.rcr.ac.uk/system/files/publication/field_publication_files/bfco191_radiotherapytreatment-interruptions.pdf

105. Groh BA, Siewerdsen JH, Drake DG, Wong JW, Jaffray DA. A performance comparison of flat-panel imager-based MV and kV cone-beam CT. Med Phys. 2002 Jun;29(6):967-75.

106. Kanakavelu N, Samuel EJ. Accuracy in automatic image registration between MV cone beam computed tomography and planning kV computed tomography in image guided radiotherapy. Rep Pract Oncol Radiother. 2016 Sep-Oct;21(5):487-94

107. Navran A, Heemsbergen W, Janssen T, Hamming-Vrieze O, Jonker M, Zuur C, Verheij M, Remeijer P, Sonke JJ, van den Brekel M, Al-Mamgani A. The impact of margin reduction on outcome and toxicity in head and neck cancer patients treated with image-guided volumetric modulated arc therapy (VMAT). Radiother Oncol. 2019 Jan;130:25-31.

108. Yip C, Thomas C, Michaelidou A, James D, Lynn R, Lei M, Guerrero Urbano T. Co-registration of cone beam CT and planning CT in head and neck IMRT dose estimation: a feasible adaptive radiotherapy strategy. Br J Radiol. 2014 Feb;87(1034):20130532

109. Jiao SX, Wang ML, Chen LX, Liu XW. Evaluation of dose-volume histogram prediction for organ-at risk and planning target volume based on machine learning. Sci Rep. 2021 Feb 4;11(1):3117

110. Fiorentino A, Caivano R, Metallo V, Chiumento C, Cozzolino M, Califano G, Clemente S, Pedicini P, Fusco V. Parotid gland volumetric changes during intensity-modulated radiotherapy in head and neck cancer. Br J Radiol. 2012 Oct;85(1018):1415-9

111. Wu VWC, Leung KY. A Review on the Assessment of Radiation Induced Salivary Gland Damage After Radiotherapy. Front Oncol. 2019 Oct 17;9:1090.

112. van Kranen S, van Beek S, Mencarelli A, Rasch C, van Herk M, Sonke JJ. Correction strategies to manage deformations in head-and-neck radiotherapy. Radiother Oncol. 2010 Feb;94(2):199-205.

113. Noble DJ, Yeap PL, Seah SYK, Harrison K, Shelley LEA, Romanchikova M, Bates AM, Zheng Y, Barnett GC, Benson RJ, Jefferies SJ, Thomas SJ, Jena R, Burnet NG. Anatomical change during radiotherapy for head and neck cancer, and its effect on delivered dose to the spinal cord. Radiother Oncol. 2019 Jan;130:3238.

114. Hunter KU, Fernandes LL, Vineberg KA, McShan D, Antonuk AE, Cornwall C, Feng M, Schipper MJ, Balter JM, Eisbruch A. Parotid glands dose-effect relationships based on their actually delivered doses: implications for adaptive replanning in radiation therapy of head-and-neck cancer. Int J Radiat Oncol Biol Phys. 2013 Nov 15;87(4):676-82

115. van Beek S, Jonker M, Hamming-Vrieze O, Al-Mamgani A, Navran A, Remeijer P, van de Kamer JB. Protocolised way to cope with anatomical changes in head & neck cancer during the course of radiotherapy. Tech Innov Patient Support Radiat Oncol. 2019 Dec 16;12:34-40.

116. Mehanna H, Robinson M, Hartley A, Kong A, Foran B, Fulton-Lieuw T, Dalby M, Mistry P, Sen M, O'Toole L, Al Booz H, Dyker K, Moleron R, Whitaker S, Brennan S, Cook A, Griffin M, Aynsley E, Rolles M, De Winton E, Chan A, Srinivasan D, Nixon I, Grumett J, Leemans CR, Buter J, Henderson J, Harrington K, McConkey C, Gray A, Dunn J; De-ESCALaTE HPV Trial Group. Radiotherapy plus cisplatin or cetuximab in

low-risk human papillomavirus-positive oropharyngeal cancer (De-ESCALaTE HPV): an open-label randomised controlled phase 3 trial. Lancet. 2019 Jan 5;393(10166):51-60.

117. Gillison ML, Trotti AM, Harris J, Eisbruch A, Harari PM, Adelstein DJ, Jordan RCK, Zhao W, Sturgis EM, Burtness B, Ridge JA, Ringash J, Galvin J, Yao M, Koyfman SA, Blakaj DM, Razaq MA, Colevas AD, Beitler JJ, Jones CU, Dunlap NE, Seaward SA, Spencer S, Galloway TJ, Phan J, Dignam JJ, Le QT. Radiotherapy plus cetuximab or cisplatin in human papillomavirus-positive oropharyngeal cancer (NRG Oncology RTOG 1016): a randomised, multicentre, non-inferiority trial. Lancet. 2019 Jan 5;393(10166):40-50.
118. Zhong H, Men K, Wang J, van Soest J, Rosenthal D, Dekker A, Zhang Z, Xiao Y. The Impact of Clinical Trial Quality Assurance on Outcome in Head and Neck Radiotherapy Treatment. Front Oncol. 2019 Aug 21;9:792.
119. Soret M, Bacharach SL, Buvat I. Partial-Volume Effect in PET tumour imaging. J Nuc Med. 2007, 48(6) 932-945
120. van Beek S, Jonker M, Hamming-Vrieze O, Al-Mamgani A, Navran A, Remeijer P, van de Kamer JB. Protocolised way to cope with anatomical changes in head & neck cancer during the course of radiotherapy. Tech Innov Patient Support Radiat Oncol. 2019 Dec 16;12:34-40.
121. Takao S, Tadano S, Taguchi H, Yasuda K, Onimaru R, Ishikawa M, Bengua G, Suzuki R, Shirato H. Accurate analysis of the change in volume, location, and shape of metastatic cervical lymph nodes during radiotherapy. Int J Radiat Oncol Biol Phys. 2011 Nov 1;81(3):871-9.
122. Yock A. Forecasting longitudinal changes in oropharyngeal tumour volume, position and morphology during image-guided radiation therapy. The Univeristy of Texas MD Anderson Cancer Center (Open Access 438)
123. Allal AS, Dulguerov P, Allaoua M, Haenggeli CA, El-Ghazi el A, Lehmann W, Slosman DO. Standardized uptake value of 2-[(18)F] fluoro-2-deoxy-D-glucose in predicting outcome in head and neck carcinomas treated by radiotherapy with or without chemotherapy. J Clin Oncol. 2002 Mar 1;20(5):1398-404.
124. Barker JL Jr, Garden AS, Ang KK, O'Daniel JC, Wang H, Court LE, Morrison WH, Rosenthal DI, Chao KS, Tucker SL, Mohan R, Dong L. Quantification of volumetric and geometric changes occurring during fractionated radiotherapy for head-and-neck cancer using an integrated CT/linear accelerator system. Int J Radiat Oncol Biol Phys. 2004 Jul 15;59(4):960-70.
125. Castelli, J., Simon, A., Rigaud, B. *et al.* A Nomogram to predict parotid gland overdose in head and neck IMRT. *Radiat Oncol* **11**, 79 (2016)
126. Brouwer CL, Steenbakkers RJ, Langendijk JA, Sijtsema NM. Identifying patients who may benefit from adaptive radiotherapy: Does the literature on anatomic and dosimetric changes in head and neck organs at risk during radiotherapy provide information to help? Radiother Oncol. 2015 Jun;115(3):28594.
127. Ricchetti F, Wu B, McNutt T, Wong J, Forastiere A, Marur S, Starmer H, Sanguineti G. Volumetric change of selected organs at risk during IMRT for oropharyngeal cancer. Int J Radiat Oncol Biol Phys. 2011 May 1;80(1):161-8.
128. Sanguineti G, Ricchetti F, Wu B, McNutt T, Fiorino C. Parotid gland shrinkage during IMRT predicts the time to Xerostomia resolution. Radiat Oncol. 2015 Jan 17;10:19.
129. Wang ZH, Yan C, Zhang ZY, Zhang CP, Hu HS, Kirwan J, Mendenhall WM. Radiation-induced volume changes in parotid and submandibular glands in patients with head and neck cancer receiving postoperative radiotherapy: a longitudinal study. Laryngoscope. 2009 Oct;119(10):1966-74.
130. Mohan R, Wu Q, Manning M, Schmidt-Ullrich R. Radiobiological considerations in the design of fractionation strategies for intensity-modulated radiation therapy of head and neck cancers. Int J Radiat Oncol Biol Phys. 2000 Feb 1;46(3):619-30
131. Stieb S, Lee A, van Dijk LV, Frank S, Fuller CD, Blanchard P. NTCP Modeling of Late Effects for Head and Neck Cancer: A Systematic Review. Int J Part Ther. 2021 Jun 25;8(1):95-107
132. Rwigema JM, Langendijk JA, Paul van der Laan H, Lukens JN, Swisher-McClure SD, Lin A. A Model-Based Approach to Predict Short-Term Toxicity Benefits with Proton Therapy for Oropharyngeal Cancer. Int J Radiat Oncol Biol Phys. 2019 Jul 1;104(3):553-562.
133. Tambas M, Steenbakkers RJHM, van der Laan HP, Wolters AM, Kierkels RGJ, Scandurra D, Korevaar EW, Oldehinkel E, van Zon-Meijer TWH, Both S, van den Hoek JGM, Langendijk JA. First experience with model-based selection of head and neck cancer patients for proton therapy. Radiother Oncol. 2020 Oct;151:206-213.

134. MD Anderson Head and Neck Cancer Symptom Working Group. Dose-volume correlates of mandibular osteoradionecrosis in Oropharynx cancer patients receiving intensity-modulated radiotherapy: Results from a case-matched comparison. Radiother Oncol. 2017 Aug;124(2):232-239
135. Singh A, Huryn J, Kronstadt K, et al., Osteoradionecrosis of the jaw: a mini review. Frontiers in Oral Health 28 July 2022
136. van Dijk LV, Abusaif AA, Rigert J, Naser MA, Hutcheson KA, Lai SY, Fuller CD, Mohamed ASR; on behalf on the MD Anderson Symptom Working Group. Normal Tissue Complication Probability (NTCP) Prediction Model for Osteoradionecrosis of the Mandible in Patients With Head and Neck Cancer After Radiation Therapy: Large-Scale Observational Cohort. Int J Radiat Oncol Biol Phys. 2021 Oct 1;111(2):549-558.
137. Tsai CJ, Hofstede TM, Sturgis EM, Garden AS, Lindberg ME, Wei Q, Tucker SL, Dong L. Osteoradionecrosis and radiation dose to the mandible in patients with oropharyngeal cancer. Int J Radiat Oncol Biol Phys. 2013 Feb 1;85(2):415-20.
138. Lalonde A, Bobić M, Winey B, Verburg J, Sharp GC, Paganetti H. Anatomic changes in head and neck intensity-modulated proton therapy: Comparison between robust optimization and online adaptation. Radiother Oncol. 2021 Jun;159:39-47
139. Bobić M, Lalonde A, Sharp GC, Grassberger C, Verburg JM, Winey BA, Lomax AJ, Paganetti H. Comparison of weekly and daily online adaptation for head and neck intensity-modulated proton therapy. Phys Med Biol. 2021 Feb 25;66(5):10.
140. Christianen ME, van der Schaaf A, van der Laan HP, Verdonck-de Leeuw IM, Doornaert P, Chouvalova O, Steenbakkers RJ, Leemans CR, Oosting SF, van der Laan BF, Roodenburg JL, Slotman BJ, Bijl HP, Langendijk JA. Swallowing sparing intensity modulated radiotherapy (SW-IMRT) in head and neck cancer: Clinical validation according to the model-based approach. Radiother Oncol. 2016 Feb;118(2):298-303.
141. Behrends, C., Haussmann, J., Kramer, P-H., Langendijk, J. A., Gottschlag, H., Geismar, D., Budach, W., & Timmermann, B. (2021). Model-based comparison of organ at risk protection between VMAT and robustly optimised IMPT plans. Zeitschrift fur medizinische Physik, 31(1), 5-15.
142. Gamez M and Ma D. Deintnsification strategies using proton beam therapy for HPV-related oropharyngeal cancer Int J Part Ther(2021) 8 (1):223 – 233
143. https://www.estro.org/ESTRO/media/ESTRO/About/Committees/RTT/guidelines-for-positioningimmobilisation-and-position-verification-of-head-and-neck-patients-for-rtts.pdf
144. Ove R, Cavalieri R, Noble D and Russo SM. Variation of neck position with Image-guided radiotherapy for head and neck cancer. Am J Clin Oncol. 2012. 35 (1): 1-5.
145. Giske K, Stoiber EM, Schwarz M, Stoll A, Muenter MW, Timke C, Roeder F, Debus J, Huber PE, Thieke C, Bendl R. Local setup errors in image-guided radiotherapy for head and neck cancer patients immobilized with a custom-made device. Int J Radiat Oncol Biol Phys. 2011 Jun 1;80(2):582-9.
146. van Kranen S, van Beek S, Rasch C, van Herk M, Sonke JJ. Setup uncertainties of anatomical sub-regions in head-and-neck cancer patients after offline CBCT guidance. Int J Radiat Oncol Biol Phys. 2009 Apr 1;73(5):1566-73.
147. Neubauer E, Dong L, Followill DS, Garden AS, Court LE, White RA, Kry SF. Assessment of shoulder position variation and its impact on IMRT and VMAT doses for head and neck cancer. Radiat Oncol. 2012 Feb 8;7:19.
148. Siebers JV, Keall PJ, Wu Q, Williamson JF and Schmidt-Ullrich RK. Effect of patient set-up errors on simultaneously integrated boost head and neck IMRT treatment plans. Int. J. Radiation Oncol Biol Phys. 2005. 63 (2): 422-433.
149. van Beek S, van Kranen S, Mencarelli A, Remeijer P, Rasch C, van Herk M, Sonke JJ. First clinical experience with a multiple region of interest registration and correction method in radiotherapy of head-and-neck cancer patients. Radiother Oncol. 2010 Feb;94(2):213-7.
150. Farzal Z, Du E, Yim E, Mazul A, Zevallos JP, Huang BY, Hackman TG. Radiographic muscle invasion not a recurrence predictor in HPV-associated oropharyngeal squamous cell carcinoma. Laryngoscope. 2019 Apr;129(4):871-876.
151. Heaton CM, Al-Shwaiheen F, Liu CS, Yom SS, Ryan WR. Prognostic significance of hyoid bone invasion in advanced base of tongue carcinoma treated by chemoradiation. Clin Otolaryngol. 2015 Jun;40(3):260-5.

152. Kunder S, Chatterjee A, Manna S, Mahimkar M, Patil A, Rangarajan V, Budrukkar A, Ghosh-Laskar S, Agarwal JP, Gupta T. Correlation between imaging and tissue biomarkers of hypoxia in squamous cell cancer of the head and neck. World J Nucl Med. 2021 Aug 20;20(3): p228-236

153. Wiedenmann N, Bunea H, Rischke HC, Bunea A, Majerus L, Bielak L, Protopopov A, Ludwig U, Büchert M, Stoykow C, Nicolay NH, Weber WA, Mix M, Meyer PT, Hennig J, Bock M, Grosu AL. Effect of radiochemotherapy on T2* MRI in HNSCC and its relation to FMISO PET derived hypoxia and FDG PET. Radiat Oncol. 2018 Aug 29;13(1): p159. Erroratum in: Radiat Oncol. 2018 Sep 21;13(1): p183.